Geoarchäologische Untersuchungen zum Abfall- und Ressourcen-Management in der jüngerlatènezeitlichen Siedlung Basel-Gasfabrik

Inauguraldissertation
zur
Erlangung der Würde eines Doktors der Philosophie
vorgelegt der
Philosophisch-Naturwissenschaftlichen Fakultät
der Universität Basel

von

David Simon Brönnimann

aus Gurzelen (BE), Schweiz

Basel, 2020

Originaldokument gespeichert auf dem Dokumentenserver der Universität Basel
edoc.unibas.ch

Genehmigt von der Philisophisch-Naturwissenschaftlichen Fakultät auf Antrag von

Prof. Dr. Jörg Schibler, Dr. habil. Philippe Rentzel, Prof. Dr. Brigitte Röder

Basel, den 16.10.2018

Prof. Dr. Martin Spiess, Dekan

Inhalt

Danksagung 5

Kapitel 1 Einleitung 7
- 1.1 Die Fundstelle Basel-Gasfabrik
- 1.2 Geologie und Geomorphologie
- 1.3 Kurzer Abriss der Forschungsgeschichte
- 1.4 Theoretische Konzepte und Terminologie
- 1.5 Fragestellungen
- 1.6 Material, Methoden und neue Ansätze

Kapitel 2 The Lay of Land 16

Strontium isotope variability in the dietary catchment of the Late Iron Age proto-urban settlement of Basel-Gasfabrik, Switzerland. David Brönnimann, Corina Knipper, Sandra L. Pichler, Brigitte Röder, Hannele Rissanen, Barbara Stopp, Martin Rosner, Malou Blank, Ole Warnberg, Kurt W. Alt, Guido Lassau, Philippe Rentzel. Journal of Archaeological Science: Reports 17 (2018) 279-292.

Kapitel 3 The Hidden Midden 40

Geoarchaeological investigation of sedimentation processes, waste disposal practices and resource management at the Latène settlement Basel-Gasfabrik (Switzerland). David Brönnimann, Philippe Rentzel, Brigitte Röder, Norbert Spichtig, Hannele Rissanen, Guido Lassau. Geoarchaeology: An International Journal 35 (2020) 522-544.

Kapitel 4 Contextualising the Dead 71

Combining geoarchaeology and osteo-anthropology in a new multi-focus approach in bone histotaphonomy. David Brönnimann, Cordula Portmann, Sandra L. Pichler, Tom J. Booth, Brigitte Röder, Jörg Schibler, Philippe Rentzel. Journal of Archaeological Science 98 (2018) 45-58.

Kapitel 5 Zusammenfassung und Synthese 100
- 5.1 The Lay of Land
- 5.2 The Hidden Midden
- 5.3 Contextualising the Dead

Kapitel 6 Ausblick 117

Kapitel 7 (Persönliches) Fazit 118

Literaturverzeichnis 120

Supplements

Danksagung

An erster Stelle möchte ich mich ganz herzlich bei meinen Betreuern Philippe Rentzel und Brigitte Röder für die intensive, sehr spannende und angenehme Zeit bedanken. Philippe Rentzel im Speziellen für die unermüdliche Unterstützung, für die sehr angenehme und konstruktive Zusammenarbeit und für die Chance, im geoarchäologischen Labor arbeiten und mich mit diesen spannenden Projekten beschäftigten zu dürfen. Ein ebenso grosses Dankeschön möchte ich an Brigitte Röder richten für ihr schier unerschöpfliches Wissen zu allen möglichen archäologischen Themen, das sie während Besprechungen und gemeinsamen Lehrveranstaltungen mit viel Wohlwollen mit mir teilte, und das mich stets einen Schritt weitergebracht hat.

Wer sich einmal mit einer der vielen tiefen Gruben von Basel-Gasfabrik befasst hat, der kommt da so schnell nicht wieder heraus. Zu steil die Wände, und zu freundlich das Forschungsteam. Viele meiner Dissertations-Fragestellungen sind das Resultat zahlreicher spannender Diskussionsrunden, wofür ich mich bei Kurt Alt, Ole Warnberg und Jörg Schibler herzlich bedanken möchte. Einen ganz besonderen Dank möchte ich Corina Knipper aussprechen, die mich in die Thematik der Isotopie eingeführt und unterstützt hat. Ein herzliches Dankeschön geht auch an Sandra Pichler für ihre zahlreichen sprachlichen und fachlichen Inputs.

Meine Dissertation ist Teil des interdisziplinären Forschungsprojektes „Über den Grubenrand geschaut - Integrative Forschung zu *site formation* und Siedlungsdynamik innerhalb der jüngerlatènezeitlichen Grosssiedlung Basel-Gasfabrik“. Während unserer regelmässigen Mittags-Treffen sind zwischen Sandwich und Teigwarensalat viele Ideen geboren und herangewachsen. Dafür und für die angenehme Zusammenarbeit möchte ich mich herzlich bei Norbert Spichtig, Barbara Stopp, Milena Müller-Kissing, Marlu Kühn und Johannes Wimmer bedanken – und ganz besonders bei Hannele Rissanen für ihre grossartige Unterstützung sowie bei Guido Lassau für das Vertrauen, das ich seitens der Archäologischen Bodenforschung Basel-Stadt entgegennehmen durfte.

Ein sehr herzliches Dankeschön geht an unser Geoarchäologie-Team, in dem man sich einfach nur wohlfühlen und jedes (geo-) archäologische Problem besprechen kann: Kristin Ismail-Meyer, Christine Pümpin und Philippe Rentzel, sowie Sarah Lo Russo und Mathias Lutz. Ausserdem bedanke ich mich bei Thomas Beckmann sowie bei Willy und Pascal Tschudin für die sorgfältige Dünnschliffherstellung.

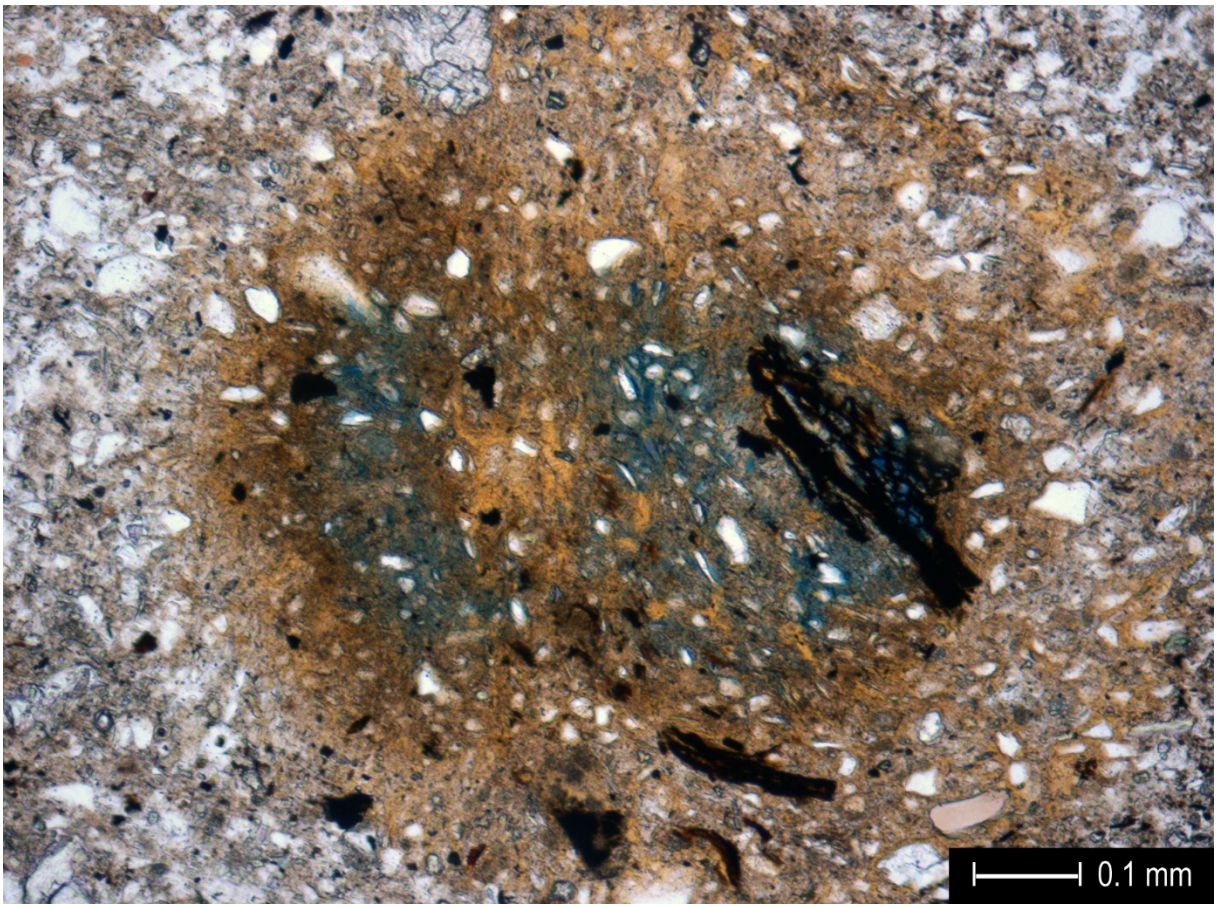
Die grosse Stärke unseres Instituts ist die Kaffeepause, während der sich tagtäglich ein interdisziplinäres Stelldichein mit ungezwungenen Gesprächen einstellt. Einen herzlichen Dank geht deshalb an alle ArbeitskollegInnen, insbesondere an Brigitte Heitz, Viviane Kolter und Ruth Sahli für ihre wunderbare Hilfe. Ganz besonders möchte ich mich bei Cordula Portmann für die tolle Zusammenarbeit bedanken. Ohne sie wäre unsere histotaphonomische Forschung, in der wir uns perfekt ergänzt haben, nie möglich gewesen.

Man findet nur das, was man kennt. Das gilt insbesondere für die Mikromorphologie, weshalb ein Austausch mit KollegInnen sehr wichtig ist. Ein grosses Dankeschön geht deshalb an Christiano Nicosia, Hans Huisman, Barbora Wouters, Yannick Devos, Richard Macphail, Carolina Mallol, Karen Milek und an Luc Vrydaghs.

Ein grosses Dankeschön möchte ich an Tom Booth und Richard Madgwick sowie an Kirsten Mandl und Estella Weiss-Krejci für ihre grossartige Zusammenarbeit und Gastfreundschaft in London und Wien richten. Ausserdem möchte ich mich bei Willem B. Stern für die Tipps zum Glashandwerk und bei Sabine Fiedler und Kristina Reetz für die Sterol-Analysen bedanken.

Ich danke ausserdem allen Editoren und anonymen Reviewern für ihre konstruktive Arbeit, für die zahlreichen Tipps und Vorschläge, die unsere Texte einen grossen Schritt vorwärts gebracht haben.

Ganz zum Schluss und trotzdem an erster Stelle danke ich von Herzen Sophia. Für alles.



Mikroskop-Foto (parallelen Polarisatoren) einer Phosphat (gelblich)- und Vivianit-Ausfällung (blau). Diese hat sich in einer Grubenverfüllung in einem stark siltig-sandigem, holzkohlehaltigem Lehm gebildet, die als „Kulturschichtmaterial" umschrieben wurde.

Kapitel 1

Einleitung

1.1 Die Fundstelle Basel-Gasfabrik

Die jüngerlatènezeitliche Fundstelle Basel-Gasfabrik befindet sich in der Nordwestschweiz im Norden der Stadt Basel, rund 100 m von der Grenze zu Frankreich entfernt. Mit ihrer Lage direkt am linken Rheinufer und an der historischen Verkehrsachse Basel-Strasbourg (IVS BS 4) (Doswald, 2004), liegt die Siedlung verkehrstechnisch überaus günstig. Bis zum heutigen Zeitpunkt konnte keine architektonische Begrenzung der latènezeitlichen Siedlung festgestellt werden, weshalb ihre genaue Ausdehnung nicht abschliessend geklärt ist. Es wird eine Grösse von etwa 15 Hektar angenommen (z. B. Hecht und Niederhäuser, 2011). Nördlich der Siedlung liegen zwei dazugehörige Gräberfelder mit insgesamt 193 Körper- und 2 Brandbestattungen. Während der über 100-jährigen Forschungsgeschichte wurden hunderte Pfostenstellungen, zahlreiche Gräben, Öfen, Feuerstellen, Keramikbrennöfen und über 500 Gruben ausgegraben und dokumentiert (z. B. Jud, 2008). Letztere sind meist 2-3 m breit sowie bis zu 3 m tief erhalten und bilden die bisher am besten untersuchte Befundgattung. Dies geht unter anderem darauf zurück, dass ein Grossteil der über 700'000 Keramikscherben und 1.6 Millionen Tierknochenfragmente aus ebensolchen Gruben stammt.

Die bisherigen Forschungsergebnisse zeigen nicht nur, dass Basel-Gasfabrik mit Metall- und Glashandwerk sowie mit lokaler Keramikproduktion in Verbindung zu setzen ist (Hecht et al., 2007; Jud, 2008; Hecht und Niederhäuser, 2011), sondern auch, dass die Siedlung in regem Kontakt mit dem näheren und weiteren Umland stand (Blöck et al., 2012). Fernimporte wie zum Beispiel Amphoren und lokaler Handel (Oberrheingraben, Schwarzwald, Jura) zeichnen sich anhand der Keramik, aber auch anhand anderer Fund- und Materialgattungen wie zum Beispiel den Mühlsteinen ab (Joos, 1975; Fischer, 2012). Ausserdem zeigen archäobotanische und archäozoologische Untersuchungen, dass auch Tiere und Agrarprodukte importiert und transportiert wurden (Stopp et al., 1999; Kühn und Iseli, 2008; Stopp, 2008). Folgerichtig wird Basel-Gasfabrik als Zentralsiedlung angesprochen. Die präzise Datierung der jüngerlatènezeitlichen Siedlung birgt einige Probleme – nicht zuletzt deshalb, weil bis heute eine typochronologische Aufarbeitung der Keramik fehlt, was im Rahmen einer laufenden Dissertation durch Johannes Wimmer erarbeitet werden soll. Während für den Zeitpunkt der Auflassung der Siedlung (um 80 v. Chr.) Konsens herrscht, ist insbesondere der Beginn unklar und wird momentan um 200/150 v. Chr. angesetzt.

1.2 Geologie und Geomorphologie

Die Region Basel ist nicht nur kulturell, sondern auch aus geologisch-geomorphologischer Sicht sehr vielseitig: Die Stadt liegt am südlichen Ende des Oberrheingrabens, der durch pleistozäne Ablagerungen (Rheinschotter, Löss und Überflutungssedimente) und einer sanften Topografie geprägt ist (Leser, 1982; Bitterli-Brunner et al., 1984; Bitterli-Brunner, 1987; Brönnimann und Rentzel, 2014). Direkt südlich schliesst das Sundgauer Hügelland an, dessen weiche Hügel und Kuppen von einer teils mehrere Meter mächtigen Lössablagerung überdeckt sind und heute (und wohl auch in der Vergangenheit) landwirtschaftlich intensiv genutzt werden. Im Nordosten erhebt sich mit dem Schwarzwald das Grundgebirge, das vorwiegend aus geologisch alten metamorphen Gesteinen besteht (Granit, Porphyr, Gneis, Schiefer etc.) und deutlich über 1‘000 m ü. M. reicht. Dazu gehört unter

anderem die Rotliegend Brekzie, die während der Latènezeit im Wiesental bei Schopfheim abgebaut und zu Mühlsteinen verarbeitet wurde (Joos, 1975; Fischer, 2012). Wenige Kilometer südlich von Basel schliesst der Tafeljura (südöstlich) respektive der Faltenjura (südwestlich) an. Beide sind aus Kalken und Mergeln des Jura aufgebaut. Im Tafeljura finden sich auf den Plateaus Löss- und Verwitterungslehme, die für Ackerbau und Viehhaltung gut geeignet sind. Die bisher bekannten latènezeitlichen Siedlungen befinden sich vor allem in den Tälern (Blöck et al., 2012).

Die Fundstelle Basel-Gasfabrik selber liegt auf der tiefsten Stufe (B3) der pleistozänen Niederterrasse des Rheins (Kock et al., 2009; Rentzel et al., 2015). Dabei handelt es sich um kalkhaltige, grobgeschichtete, sandig-kiesige Schotter, die währen der letzten Eiszeit abgelagert und während dem Atlantikum von einem feinkörnigen Hochflutsand überdeckt wurden (Rentzel, 1994, 1997). Der kalkhaltige, siltig-feinsandige Hochflutsand ist in Muldenzonen bis zu 2 m mächtig erhalten. Auf dem Hochflutsand und dem Rheinschotter hat sich ein Luvisol mit charakteristischem Ah-Al-Bt-Cv-C-Profil ausgebildet (Rentzel, 1997). In Analogie zu anderen Bodenprofilen in vergleichbarer Lage (Rentzel, 1997) ist von einem einst 60-80 cm tiefgründigen Boden und einem wohl rund 40 cm mächtigen B-Horizont auszugehen. Von diesem war bereits während der latènezeitlichen Besiedelung oftmals nichts oder nur noch ein Teil vorhanden (Brönnimann et al., accepted). Im Siedlungsgebiet waren folglich verschiedene Substrattypen mit unterschiedlichen Eigenschaften anstehend.

1.3 Kurzer Abriss der Forschungsgeschichte

Die jüngerlatènezeitliche Siedlung Basel-Gasfabrik wurde im Jahr 1911 beim Bau eines weiteren Gaskessels der damaligen Gasfabrik von Karl Stehlin entdeckt. Der Fokus lag schon damals auf den mit hunderten von Keramikscherben und Tierknochen verfüllten Gruben, die von Stehlin als Wohngruben interpretiert wurden (Hecht und Niederhäuser, 2011). Mit dem Wissen, dass es sich um eine "keltische" Siedlung und dem damaligen Zeitgeist entsprechend um eine „Ur-Schweizer“- Siedlung handelte, war das (Forschungs-) Interesse entsprechend gross. Während den nächsten Jahrzehnten folgten zahlreiche archäologische Ausgrabungen. Die Zusammenarbeit mit dem Labor für Ur- und Frühgeschichte der Universität Basel (damals unter der Leitung von Elisabeth Schmid) ist es zu verdanken, dass die Fundstelle nun schon seit über 40 Jahren interdisziplinär erforscht wird. Bereits in den 1970er Jahren erfolgten die ersten geoarchäologischen, malakologischen, archäobotanischen und archäozoologischen Untersuchungen mit einer interdisziplinären Synthese zu den damals schon als unterschiedlich wahrgenommenen Schichtbildungsprozessen innerhalb und ausserhalb von Gruben (Imhof et al., 1977). Diese interdisziplinare Zusammenarbeit intensivierte sich insbesondere ab den 1990er Jahren. Gleichzeitig wurde die Methode der Mikromorphologie durch Philippe Rentzel am Labor für Ur- und Frühgeschichte eingeführt und weiterentwickelt. Die Anwendung mikromorphologischer Analysen erlaubte neue Interpretationen zu Schichtbildungsprozessen und zu menschlichen Aktivitäten. Dadurch konnten neue Erkenntnisse zur einstigen Topografie und den pedologischen Verhältnissen (Rentzel, 1994, 1997), zu Grubensedimenten und der Verfüllung von Gruben sowie zu Schichtbildungsprozessen gewonnen werden (Rentzel, 1998).

Nebst der interdisziplinären Auswertung eines Siedlungsareals durch Peter Jud (Jud, 2008) stellt vor allem das von 2011 bis 2014 durchgeführte SNF-Forschungsprojekt „Über die Toten zu den Lebenden: Menschliche Überreste vom spätlatènezeitlichen Fundplatz Basel-Gasfabrik und ihre kulturgeschichtlichen Deutungen“ (Nr.

133052) einen Meilenstein in der (interdisziplinären) Forschung zu Basel-Gasfabrik dar (Pichler et al., 2017). Der Fokus des acht Disziplinen umfassenden Forschungsprojektes lag auf der Rekonstruktion der Totenbehandlung und der Erforschung des damaligen Lebens. Hierfür wurden unter anderem zwei Gruben geoarchäologisch untersucht und deren Verfüllungsgeschichte nachgezeichnet (Brönnimann und Rissanen, 2017; Brönnimann und Rentzel, in Vorb.). Dabei stellte sich heraus, dass beide Gruben rasch verfüllt wurden, wobei die Mehrheit der Funde mit einem dunklen, stark holzkohlehaltigen Sediment assoziiert war. Dieses als „Kulturschichtmaterial" bezeichnete Sediment – so die damalige Hypothese – weist eine andere Biografie auf, als die darin eingebetteten Keramikscherben und Knochenfragmente. Es wurden verschiedene Abfallhaufen postuliert, die beim Verfüllen der Gruben zusammen mit holzkohlehaltigem Sediment als Füllmaterial gedient haben könnten (Brönnimann und Rissanen, 2017; Brönnimann und Rentzel, in Vorb.). Im Zuge des SNF-Forschungsprojekts wurden ausserdem zur Untersuchung der Mobilität menschlicher (und tierischer) Individuen Strontium- und Sauerstoffisotopen-Analyse durchgeführt. Die dafür notwendige Strontiumisotopen-Kartierung sowie die Interpretation der entsprechenden Resultate ist Teil dieser Dissertation (Brönnimann et al., 2018). Ebenfalls aus dem SNF-Forschungsprojekt hervorgegangen ist das an der IPNA neu eröffnete Forschungsfeld der Histotaphonomie, das im Nachgang der histologischen Untersuchungen von Cordula Portmann (Portmann, 2015) etabliert wurde.

1.4 Theoretische Konzepte und Terminologie

Spätestens mit der *New Archaeology* wird die Frage nach der Entstehung dessen, was wir heute als archäologischen Befund vorfinden, intensiv diskutiert. Dabei spielen die Arbeiten von Michael Schiffer (Schiffer, 1972, 1975, 1983) eine wichtige Rolle. Schiffer versuchte, Prozesse zu fassen, die zur Bildung archäologischer Hinterlassenschaften führten (*site formation processes*). Dazu zeichnete er den „Lebenszyklus" (*life cycle*) von beständigen (*durable elements*) und von konsumierbaren Objekten (*consumable elements*) nach (Schiffer, 1972) (Abb. 1), die den Weg von Objekten oder Materialien von deren Entstehung bis hin zur Entsorgung beschreiben. Auf diesem Weg werden die Objekte von unterschiedlichen Prozessen „verformt", die Schiffer in natürliche (*n-transforms*) und kulturelle (*c-transforms*) „Verformungsprozesse" unterteilte. Letztere entstehen durch menschliches Handeln, während erstere unter anderem postsedimentäre Prozesse umfassen. Die Entstehung archäologischer Befunde wird laut Schiffer also vom Handlungsmuster einer Gruppe (*behavioral archaeology*) geprägt (Schiffer, 1975, 1987). Ganz ähnlich argumentierte auch Lewis Binford, auch wenn er sich zunächst als Gegner von Schiffers Ideen verstand. Tatsächlich aber ergänzen sich die beiden Ansichten. Binford argumentiert, dass sich mit der Archäologie fast nie individuelle Handlungen (Pompeji-Prämisse), sondern vor allem Handlungsmuster feststellen lassen (Binford, 1981), dass der archäologische Befund also von regelhaften, (alltäglichen) Aktivitäten und somit von übergeordneten (gesellschaftlichen) Organisationsprinzipien geprägt wird. Dieser Grundsatz, dass archäologische Befunde das Resultat gesellschaftlicher Handlungsmuster sind und somit zu einem gewissen Grad ein Abbild des „Kosmos" einer Gruppen darstellt, bildet die theoretische Basis der vorliegenden Dissertation. Ausserdem wird die von Schiffer vorgeschlagene Terminologie zu den verschiedenen Abfall-Kategorien übernommen. Dazu gehört der Begriff des Defacto-Abfalls („Pompeji-Prämisse"; Ablagerung des Objektes / Materials am Ort der Nutzung), des Primärabfalls („Ausscheiden" des Objektes / Materials aus dem Zyklus) und des Sekundär-Abfalls (verlagerter Abfall).

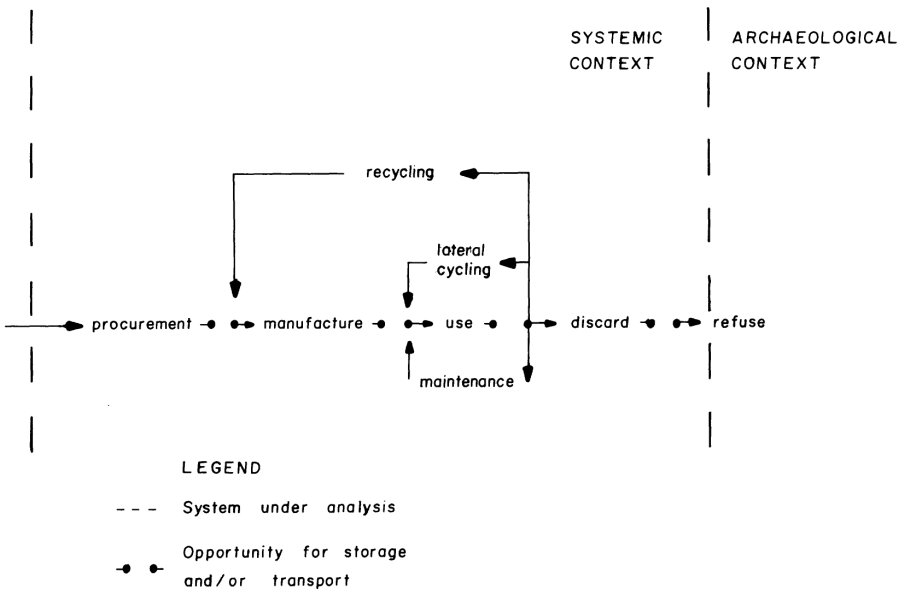


Abb. 1: Flussmodell eines life cycle von beständigen Objekten nach Michael Schiffer (1972, Fig. 1).

Bei der Rekonstruktion, Quantifizierung und Evaluation von kulturellen und natürlichen Prozessen kann die Mikromorphologie einen wesentlichen Beitrag leisten (Goldberg und Aldeias, 2016; Shahack-Gross, 2017). Mit ihr können Schichtbildungsprozesse nachgezeichnet und gesellschaftlich geprägte Handlungsmuster rekonstruiert werden. Zu letzteren gehört unter anderem das Abfallverhalten, das die Fundverteilung und somit die Interpretationsmöglichkeiten massgeblich beeinflusst (z. B. Wolfram, 2003; Sommer, 2012). Damit eng verbunden ist das Ressourcen-Management – die Frage also, wie mit Rohstoffen und Gegenständen umgegangen wird (Recycling, Umnutzung etc.). Bei diesen Themen fällt häufig der Begriff der Objektbiografie, der von Igor Kopytoff geprägt wurde (Kopytoff, 1986). Im Gegensatz zur von André Leroi-Gourhan eingeführten *Chaîne Opératoire*, die ihren Ursprung in der paläolithischen Forschung hat und vor allem den Herstellungszyklus thematisiert (Sommer, 2012), liegt der Fokus bei Kopytoff auf der kulturellen Biografie einer ganzen Objektkategorie (*cultural biography of objects*). Kopytoff's Ziel war es, den Umgang einer Objektgruppe als Folge regelhafter Verhaltensmuster einer Gesellschaft nachzuzeichnen (Kopytoff, 1986). In der Archäologie und Ethnologie gewann der Begriff in den letzten Jahren stark an Bedeutung, wird allerdings häufig für die „Geschichte" eines Einzelobjektes verwendet, was nicht dem ursprünglichen Sinn entspricht. Der Begriff der Objektbiografie wurde jüngst mehrfach kritisiert, insbesondere von Hans Peter Hahn (Hahn, 2015), der den Begriff der Biographie und den damit verbundenen linearen Verlauf des Objektwerdegangs, die Bezeichnung als lebendiges Objekt und das dadurch implizierte aktive Handeln des Untersuchungsgegenstandes kritisiert. Hahns Vorschlag, nicht von Objektbiographien, sondern von „*Itineraries*" – von Reiserouten also – zu sprechen, ist meiner Ansicht nach keine grundlegende Verbesserung: Das Objekt wird auch hier als Entscheidungsträger[1] dargestellt, und auch die Linearität bleibt unverändert bestehen. Eine Linearität darf meines Erachtens aber nicht zwingend angenommen werden. Ein Kochtopf zum Beispiel kann in Dutzende Scherben zerbrechen. Während die grossen Scherben vielleicht als Unterlage zum

[1] Mit meiner Kritik an Hahns Vorschlag möchte ich keinesfalls das postprozessuale Konzept der *agency* in Frage stellen und Objekten eine Handlungskraft gegenüber den Menschen absprechen. Trotzdem erscheint mir die Metapher einer Reiseroute nicht optimal, zumal die Entscheidungskraft hierbei primär beim Reisenden liegt.

Töpfern Verwendung finden, werden die kleineren für die Schamott-Magerung zerstossen. Es handelt sich hier partiell um einen Zyklus und gleichzeitig um einen Weg, der sich mehrfach teilt. Eine lineare Entwicklung ist es aber keinesfalls. In der vorliegenden Dissertation wird deshalb der Begriff der Objektbiografie beibehalten, allerdings mit dessen ursprünglichen Hintergrund einer *cultural biography of objects*.

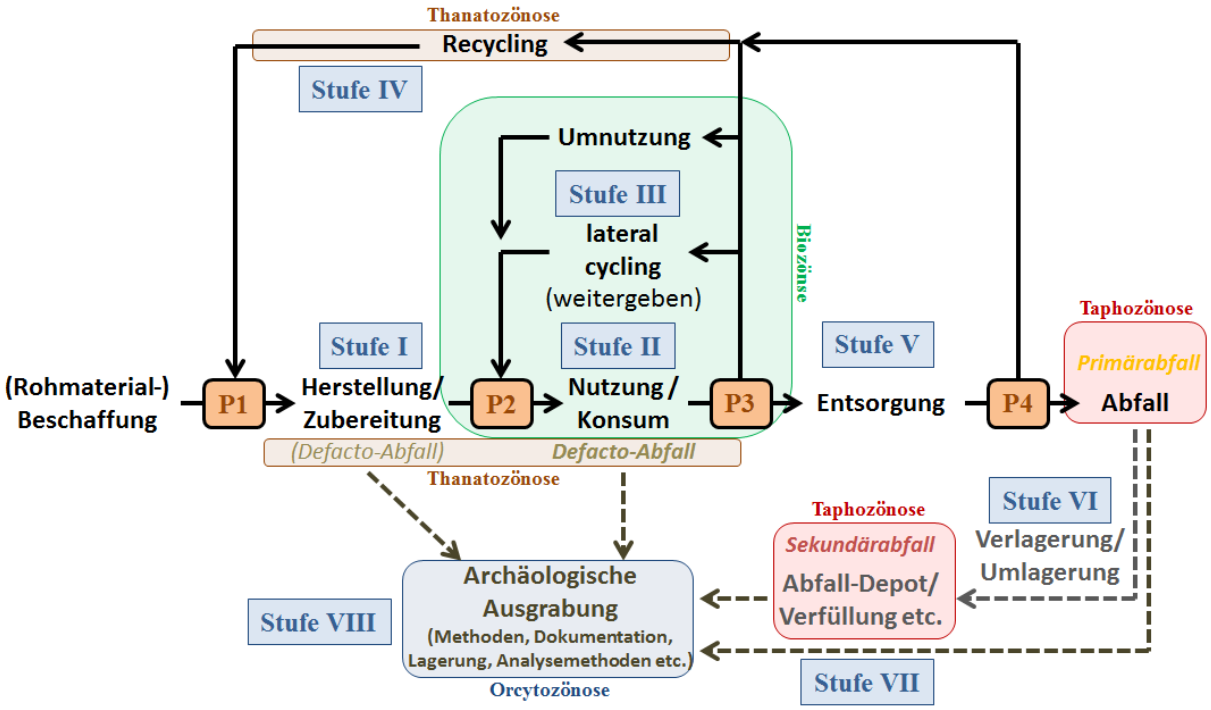


Abb. 2: *Schematisches Flussdiagram einer Objektbiografie (im Sinne der cultural biography of objects) auf Basis des von Schiffer vorgestellten, hier mit weiteren Stufen ergänzten „life cycle" (Schiffer, 1972, Fig. 1 und 2) und mit den von Schiffer (1972) definierten Abfall-Begriffen. Ausserdem sind auf Vorlage von Sommer (1991) die taphonomischen Stufen der Bio-, Thanato-, Tapho- und Orcytozönose (= Ausgrabung und Erforschung) eingefügt. Dabei zeigt sich, dass sich dieses paläontologische Konzept nicht in das Flussdiagram einpassen lässt. Mit P1-4 werden mögliche „passive" Phasen (Lagerung etc.) visualisiert, während die verschiedenen Stufen „aktive" oder „aktivierte" Phasen darstellen.*

Das Miteinbeziehen und Berücksichtigen taphonomischer Prozesse, von Schiffer als „Verformungen" (*n- und c-transforms*) umschrieben, stammt ursprünglich aus der Paläontologie. So sind auch die Ursprünge der Histotaphonomie ebenda zu finden und gehen ins 19. Jahrhundert zurück (Kölliker, 1854; Wedl, 1865). Auch Ulrike Sommer bedient sich bei ihrem Vorschlag zur Gliederung der taphonomischen Prozesse bei der Paläontologie und teilt die verschiedenen „Lebensphasen" eines Objektes der Bio-, Tanatho- und Taphozönose (Sommer, 1991) zu, wobei sie mit der archäologischen Ausgrabung zusätzlich die Orcytozönose einführt. Meines Erachtens ist das kein geeigneter Ansatz, da dieses System zur Beschreibung der Fossilbildung ausgearbeitet wurde, das keinen menschlichen Einfluss kennt. Dieses Problem zeigt sich darin, dass die verschiedenen paläontologischen Stufen nicht immer eindeutig einem Ereignis oder Zustand zuzuordnen sind (Abb. 2). Ich schlage deshalb eine Adaption von Schiffers System vor, das mit weiteren Stufen (Abfall-Verlagerung, archäologische Ausgrabung) und mit den von Schiffer definierten Begriffen des Defacto-, Primär- und Sekundärabfalls ergänzt wurde (Abb. 2), und das für die weiteren Ausführungen als Grundlage dient. Ausserdem rege ich an, die verschiedenen Phasen nicht mit aus der Paläontologie entlehnten Begriffen zu benennen, sondern von neutralen Begriffen (z. B. von Stufen oder «aktivierten» Phasen) zu sprechen. Ausserdem gilt zu beachten, dass auch mögliche „passive" Phasen (P1–4) wie zum Beispiel eine Lagerung mitberücksichtig werden müssen, wie dies bereits Schiffer in seinen

Fluss-Diagrammen aufgeführt hat (Abb. 1). Dabei darf gerne an das Sprichwort „wer rastet, der rostet“ gedacht werden: Auch wenn ein Objekt rastet, können (natürliche) Prozesse einwirken – z. B. Korrosionsprozesse, um beim Sprichwort zu bleiben.

Natürlich können in der Archäologie niemals alle Phasen, die eine Objektgruppe durchlebt haben, vollständig rekonstruiert werden. Trotzdem ist es wichtig darüber nachzudenken, wie die *cultural biography* einer Objektgruppe ausgesehen haben könnte, und welche „Verformungen“ die Reste vergangener Gesellschaften zu dem gemacht haben, wie wir sie heute vorfinden. Dabei kann die Hypothese formuliert werden, dass die Wahrscheinlichkeit einer „Verformung“ eines Objektes / Materials mit jeder Phase und mit der Dauer derselben ansteigt.

1.5 Fragestellungen

Die der vorliegenden Dissertation zugrundeliegenden Fragestellungen umfassen verschiedene Ebenen und Blickwinkel, die – ähnlich wie bei der Mikroskopie – als unterschiedliche „Vergrösserungen“ umschrieben werden können. Die kleinste Vergrösserung befasst sich mit dem Siedlungsraum von Basel-Gasfabrik und den Landschaftsräumen in dessen Umfeld (Kap. 2). Dabei liegt der Fokus auf der Charakterisierung und einer Evaluation bezüglich der möglichen landwirtschaftlichen Nutzung der verschiedenen Landschaftsräume, um in einem zweiten Schritt den Einfluss jener Regionen auf die Subsistenz der in Basel-Gasfabrik lebenden Menschen (und Tieren) zu schliessen. Der Einbezug der Landschaft geschieht auch vor dem Hintergrund, dass die diese zwar vom Menschen (mit-)geprägt wird, umgekehrt aber auch das Empfinden und Handeln von Gruppen gleichfalls beeinflusst (z. B. Turner et al., 2018).

Die zweite Ebene arbeitet mit einer sehr viel stärkeren Vergrösserung und fokussiert auf spezifische Befunde und Schichten innerhalb der Siedlung Basel-Gasfabrik (Kap. 3). Dabei spielt die Rekonstruktion von Schichtbildungsprozessen innerhalb unterschiedlicher Befundtypen eine zentrale Rolle. Ausserdem soll ein Beitrag zur Befundinterpretation geleistet und die räumliche Gliederung innerhalb der untersuchten Siedlungszone beurteilt werden. Darauf aufbauend können Erkenntnisse zu regelhaften Handlungsmustern wie zum Beispiel dem Abfallverhalten und dem Ressourcen-Management gewonnen werden. Das übergeordnete Ziel ist ein Erkenntnisgewinn zur Entstehung archäologischer Hinterlassenschaften, wobei hierfür die kulturellen und natürlichen „Verformungen“ so gut wie möglich nachvollzogen werden sollen.

Die dritte Ebene schliesslich benötigt die stärkste Vergrösserung. Dabei wird auf eine einzelne Materialgattung fokussiert – auf diejenige des Knochens (Kap. 4). Knochen sind aufgrund ihrer biogenen Entstehung und ihrer ausgeprägten Mikrostruktur wichtige Informationsträger und können eine ganze Reihe unterschiedlicher taphonomischer Prozesse sichtbar machen. Somit kann die Untersuchung dieser taphonomischen Phänomene wichtige Hinweise zu Schichtbildungsprozessen, aber auch zu den Todesumständen einzelner Individuen beitragen. Hierfür wird eine Kontextualisierung der Knochenproben mittels der Kombination von geoarchäologischen und histologischen Methoden angewandt. Auf diese Weise soll geklärt werden, ob Zusammenhänge zwischen den einzelnen taphonomischen Phänomen und den verschiedenen Befund- und Sedimenttypen bestehen, und wie diese erklärt werden können.

1.6 Material, Methoden und neue Ansätze

Für die verschiedenen Fragestellungen wurden ganz unterschiedliche Daten und Proben benötigt (Tab. 1). Diese wurden mit vielfältigen geoarchäologische Methoden untersucht, die in den jeweiligen Papers (Kap. 3, 4 und 5) im Detail erläutert sind. Dabei wurden die etablierten Standards der jeweiligen Methoden berücksichtigt, aber auch neue methodische Aspekte ausgearbeitet.

Probenart	Anzahl	Methode / Analyse
Moderne Vegetationsproben	102	Strontium-Isotopie
Moderne Wasserproben	9	Strontium-Isotopie
Milchzähne Mensch (archäologisch)	28	Strontium-Isotopie
Zähne Schwein (archäologisch)	6	Strontium-Isotopie
Zähne Hund (archäologisch)	5	Strontium-Isotopie
Blockproben	48	Mikromorphologie
Bodendünnschliffe	89	Mikromorphologie
Sedimentproben	19	Granulometrie, Geochemie
Knochendünnschnitte (Mensch; archäologisch)	124	Histotaphonomie
Knochenfragmente in Dünnschliffen (Tier; archäologisch)	183	Histotaphonomie

Tab. 1: *Probenarten und Probenzahl, die im Rahmen der Dissertation untersucht wurden.*

Strontiumisotopen-Kartierung (Brönnimann et al., 2018a) (Kap. 2)

Der Einbezug moderner Pflanzen- und Wasserproben zur Erstellung einer Strontium-Isotopen-Karte ist eine etablierte Methode. Die Evaluation der für die Subsistenz essentiellen Landschaftsformen ist ein neuer Ansatz in der Strontium-Isotopie, der für Basel-Gasfabrik ausgearbeitet wurde. Hintergrund ist die Überlegung, dass nicht alle Probenstandorte oder Landschaftsformen aufgrund ihrer Topografie und Bodenqualität zur Subsistenz der zu untersuchenden Gesellschaft beigetragen haben.

Mikromorphologische Analyse (Brönnimann et al., accepted) (Kap. 3)

Die mikromorphologische Analyse archäologischer Schichten ist eine Methode mit jahrzehntelanger Tradition, entsprechend umfangreich und etabliert sind die Richtlinien und Protokolle (z. B. Courty et al., 1989; Stoops, 2003; Goldberg und Macphail, 2006). Sehr unterschiedlich allerdings ist die Erhebung und Darstellung der Daten, zumal die Mikromorphologie lange nur deskriptiv angewandt wurde. Im Rahmen der vorliegenden Dissertation wurde deshalb eine Datenbank entwickelt, die 54 quantitative (v. a. Mikrokomponenten und texturelle Phänomene) sowie 38 qualitative Kriterien (Überprägungen etc.) umfasst. Für die Datenauswertung wurde eine schematische Darstellungsweise konzipiert, die das untersuchte Profil und die wichtigsten mikromorphologischen Kriterien visualisiert (Abb. 3).

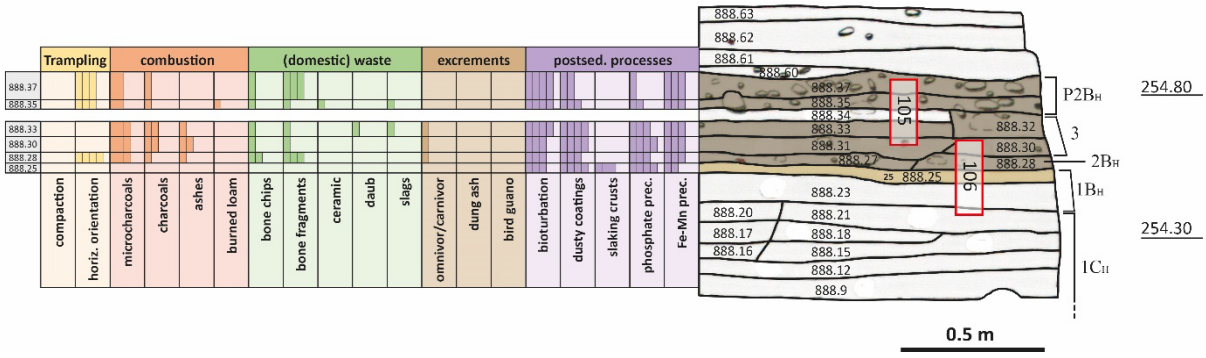


Abb. 3: *Beispiel einer schematischen Darstellung der geoarchäologischen Resultate (Profil 888, 2002/13). Die farbig dargestellten Schichten wurden mikromorphologisch untersucht. Links ist eine Auswahl der halbquantitativen Daten grafisch dargestellt, wobei die Balken die 6-teilige Skala (0-5) widergeben. Ganz rechts sind die Mikrofazies-Typen ausgewiesen.*

Histotaphonomische Analyse (Brönnimann et al., 2018b) (Kap. 4)

In der Histotaphonomie hat sich der *Oxford Histological Index* (OHI) etabliert, der die Gesamtheit der Bioerosion in einer 6-teiligen Skala wiedergibt (Hedges und Millard, 1995). Die histotaphonomischen Analysen an Knochen von Basel-Gasfabrik mit unterschiedlich dicken Präparaten haben aber gezeigt, dass eine Differenzierung der bioerosiven Phänomene nur mit 30 µm dünnen Dünnschnitten möglich ist und dass diese Phänomene unterschiedliche Ursachen haben. Deshalb wurden verschiedene Indizes ausgearbeitet, die jeweils nur einen taphonomischen Prozess umschreiben. Diese methodische Weiterentwicklung ist eine grundlegende Neuerung in der Histotaphonomie und wird die zukünftige Forschung hoffentlich entscheidend weiterbringen.



Entnahme von Wasserproben des Rheins in Basel für die Sauerstoff- und Strontium-Isotopenproben unter strenger Beobachtung einer lokalen Stadttaube. Diese Proben wurden benötigt, um das lokal verfügbare Strontium für die Siedlung Basel-Gasfabrik zu eruieren, um auf diese Weise „Lokale“ und „Fremde“ zu identifizieren.

Kapitel 2

The lay of land: Strontium isotope variability in the dietary catchment of the Late Iron Age proto-urban settlement of Basel-Gasfabrik, Switzerland

David Brönnimann, Corina Knipper, Sandra L. Pichler, Brigitte Röder, Hannele Rissanen, Barbara Stopp, Martin Rosner, Malou Blank, Ole Warnberg, Kurt W. Alt, Guido Lassau, Philippe Rentzel

Journal of Archaeological Science: Reports 17 (2018) 279-292.
DOI: 10.1016/j.jasrep.2017.11.009

Keywords: strontium isotopes, environmental samples, isotope mapping, biologically available strontium, land use patterns, Iron Age

Abstract

Basel-Gasfabrik (Switzerland) comprises an extensive La Tène (chiefly Lt D, 150–80 BCE) settlement and two associated cemeteries at which strontium ($^{87}Sr/^{86}Sr$) isotope analysis of human and animal teeth investigated regional and supra-regional contacts. The interpretation of the analytic data, however, requires information on the isotopic baseline values around the site. Using 102 modern vegetation and 9 water samples from 51 localities, this study characterizes the isotopic ratios of the biologically available strontium of geological units and watercourses around Basel and compares these to 28 human infant, 6 pig, and 5 dog teeth from the site. Furthermore, pedological criteria evaluate the suitability of landforms for crop and pasturelands. The $^{87}Sr/^{86}Sr$ ratios of the environmental samples from geological units in up to 50 km distance varied between 0.70776 and 0.71794. Human infant teeth exhibited much more homogeneous $^{87}Sr/^{86}Sr$ ratios (0.70847–0.70950), which coincided largely with those of potential arable soils around Basel and indicate targeted exploitation of landscapes for agriculture. The more variable values of the faunal teeth suggest more widely ranging habitats or imports from the site's hinterlands. Two local isotope ranges were defined based on archaeological enamel samples and modern vegetation data from a confined radius around Basel. The study documents the complexity of distinguishing local and non-local individuals in a geologically heterogeneous region as well as the potential of isotope analyses to explore prehistoric land-use patterns.

Introduction

Strontium isotope ratios ($^{87}Sr/^{86}Sr$) are widely used to investigate mobility and migration in (pre-) historic communities (e.g. Chenery et al., 2010; Knipper et al., 2012; Neil et al., 2016; Nehlich et al., 2009), the origin of single human individuals and animals (e.g. Alt et al., 2013; Müller et al., 2003; Lamb et al., 2014; Tütken et al., 2004) or animal husbandry and land-use around settlements (e.g. Knipper, 2011; Stephan et al., 2012; van der Jagt et al., 2012). Strontium is a trace element, which commonly occurs in rocks (Bentley, 2006). It has four stable isotopes, of which the radiogenic isotope ^{87}Sr results from β- decay of ^{87}Rb (rubidium). Depending on the original rubidium content and the age of bedrock formations, the relative amount of ^{87}Sr varies among geological units, which is expressed as $^{87}Sr/^{86}Sr$ ratios. Due to weathering, strontium is released into the soil and ground water. From there it is biologically available, meaning that it can be taken up by plants and transported along food chains with very little isotopic fractionation. In humans and animals, strontium substitutes for calcium in the biogenic hard tissues of teeth and bones. While bones are constantly remodelled and also fairly prone to postdepositional alteration of the chemical composition (e.g. Budd et al., 2000; Trickett et al., 2003), the isotopic composition of tooth enamel goes back to the age of dental formation. Provided that humans or animals lived on local resources, the $^{87}Sr/^{86}Sr$ ratios of their tooth enamel reflect the habitat in which they grew up, and are thus a key to the identification of non-local individuals. This, however, requires a profound characterisation of the isotope composition of the biologically available strontium at the site where their remains were found.

The strontium isotope study was carried out on human teeth from the Late Iron Age settlement of Basel-Gasfabrik and its cemeteries (Knipper et al., 2018). Basel-Gasfabrik is situated in north-western Switzerland on the left bank of the Rhine River (Figs. 1 and 2). Since 1911, numerous excavations revealed an unfortified settlement with domestic and economic structures covering an area of about 150,000 m2 (Hecht and Niederhäuser, 2011) as well as two associated cemeteries with about 170 inhumation burials. Additionally, complete skeletons in settlement features such as pits and wells along with hundreds of isolated human bones scattered throughout the settlement reflect a highly diverse and complex treatment of the dead (Pichler et al., 2013; Pichler et al., 2015; Rissanen et al., 2013). Settlement and cemeteries were in use during the La Tène period (200/150–80 BCE). Millstone fragments of Rotliegend breccia and certain ceramic wares can be linked with neighbouring areas (Black Forest, Swiss Jura Mountains), whereas amphorae, Campana and other imports document Mediterranean contacts (Blöck et al., 2014). Furthermore, bioarchaeological data suggest imports of cereals, meat or animals on the hoof from the hinterland (Knipper et al., 2017; Kühn and Iseli, 2008; Stopp, 2008) and thus show close contacts to the surrounding countryside (Swiss Jura Mountains, Sundgau, Upper Rhine Valley, Vosges and Black Forest).

Strontium and oxygen isotope analyses on enamel of burials in the cemeteries and human remains from settlement features aimed at disclosing whether these (bio-) archaeologically indicated contacts of the Basel-Gasfabrik community were also reflected in residential moves (Knipper et al., 2018). However, the interpretation of the analytic data requires the characterisation of the isotopic baseline values of the investigated elements in the potentially exploited habitats. This study, therefore, presents strontium isotope data of modern vegetation and water samples from the prevailing geological units in up to 50 km distance from the site. Moreover, we discuss the suitability of strontium isotope ratios of archaeological pig and dog teeth, and the early forming teeth of

children for the definition of local isotope ranges. The investigation aims at characterizing the biologically available strontium in relation to soil and bedrock conditions. Moreover, using pedological criteria, suitability for crop and pasturelands of different environments was evaluated.

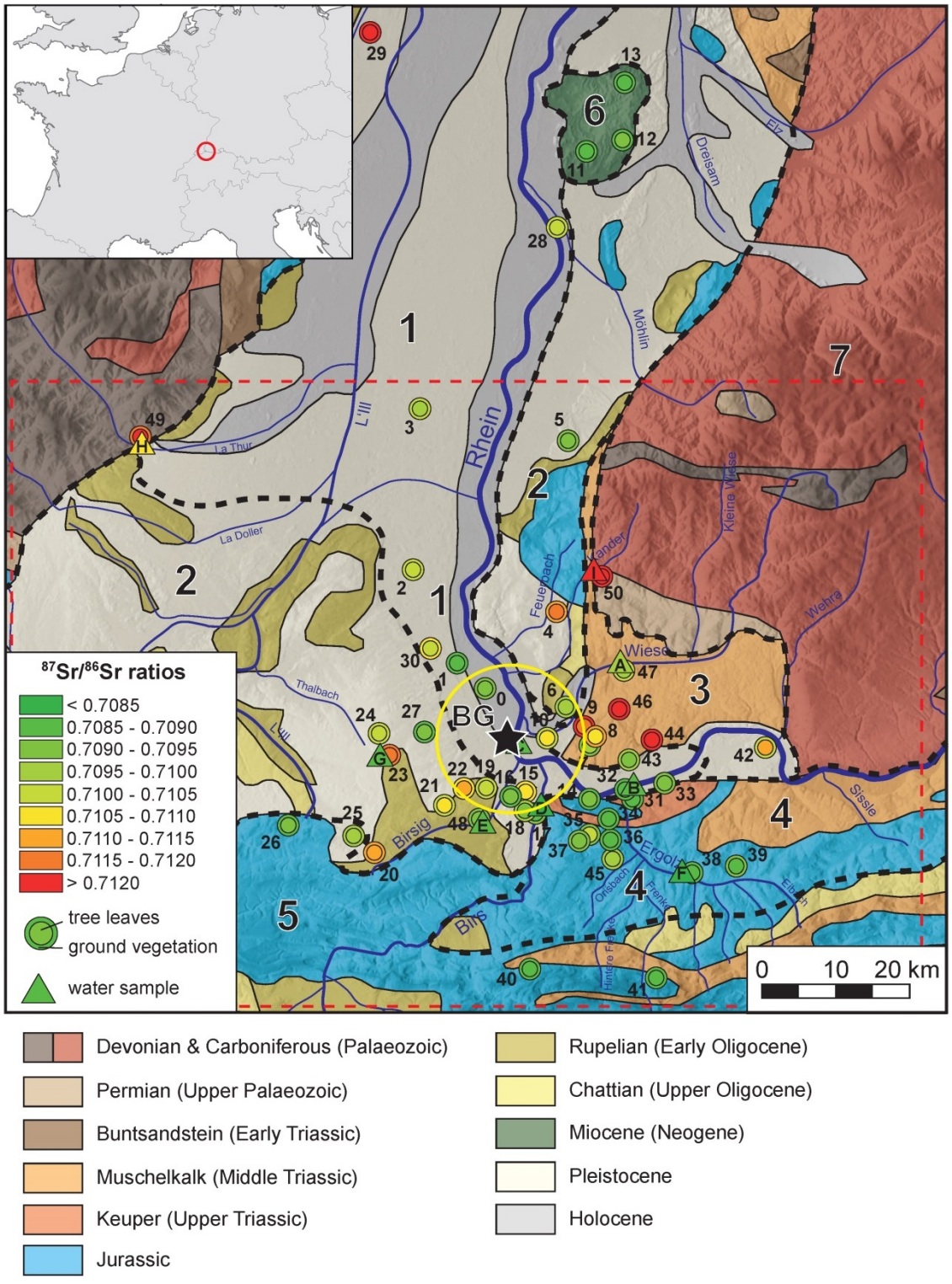


Fig. 1: *General map of the geology of the Upper Rhine Valley with landscapes: 1) Upper Rhine Valley; 2) Sundgau hill country; 3) Table and hill country; 4) Table Jura; 5) Folded Jura; 6) Kaiserstuhl (KS); 7) Low mountain ranges (Vosges and Black Forest; LMR). 87Sr/86Sr ratios of the modern vegetation and water samples are indicated by the symbol colour. The red bordered box indicates the map section enlarged in Fig. 2. Yellow circle: 7 km radius around the site. Geological map after Röhr, 2006 (modified).*

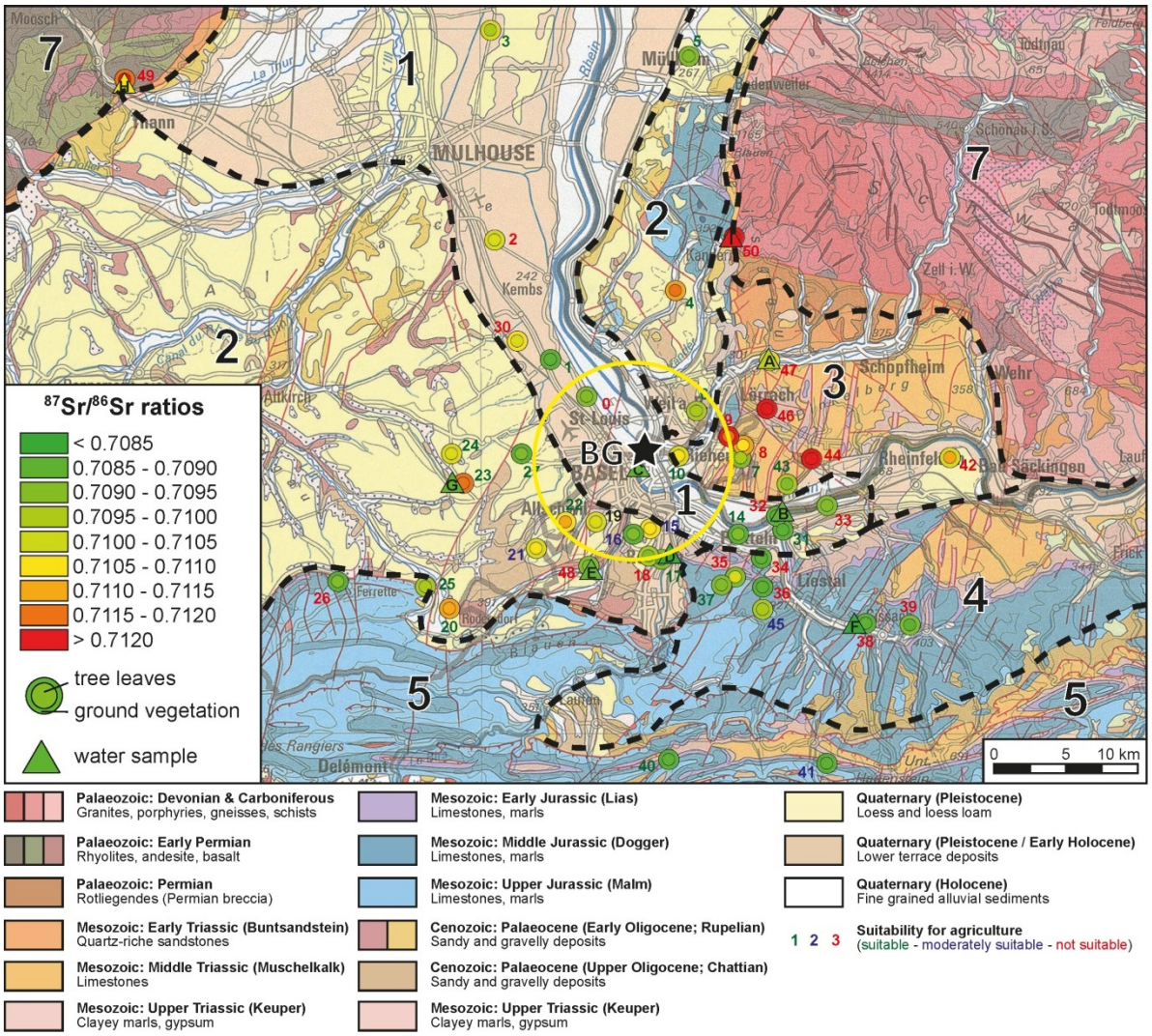


Fig. 2: *Detail of the geological map of Switzerland (1:500'000) around Basel-Gasfabrik (BG) with landscapes (see Fig. 1). The colour of the sampling site number indicates suitability for agriculture. Yellow circle: 7 km radius around the site. Reproduced by permission of swisstopo (BA17070).*

Principles and challenges of defining strontium isotope baselines

The advantages of various sampling strategies for defining local ranges of the isotope ratios of the biologically available strontium have already been discussed intensely (e.g. Bentley, 2006; Brandt et al., 2010; Maurer et al., 2012; Price et al., 2002). Comparison with the isotope ratios of bedrock is the first and most obvious approach. However, this may not be entirely conclusive because $^{87}Sr/^{86}Sr$ ratios of rocks, sediments and soil leachates do not necessarily represent the biologically available fraction (e.g. Maurer et al., 2012; Warham, 2011). $^{87}Sr/^{86}Sr$ ratios can differ among soil horizons with varying clay and carbonate contents (Bullen and Bailey, 2005; Dambrine et al., 1997; Drouet et al., 2007), and the detected isotope ratios may also vary depending on sample preparation techniques, such as whole rock analysis, water or weak acid extractions (Hodell et al., 2004).

Water $^{87}Sr/^{86}Sr$ isotope ratios depend on the complexity of the fluvial system and average the soluble strontium of their catchment area (Probst et al., 2000; Warham, 2011). Especially large rivers, such as the Rhine, transport strontium from different geological units and their isotope composition may therefore not be representative for a specific sampling location. Modern anthropogenic influence can also change the natural baseline strontium

isotope ratios of surface waters. At the base of food webs, plants are the first representatives of the biologically available strontium, which is primarily soil-derived, but also includes contributions from the atmosphere (rain, dust) and groundwater (Pett-Ridge et al., 2009). A major shortcoming is possible modern anthropogenic alteration due to fertilizers (Maurer et al., 2012; Vitòria et al., 2004), which can be minimized by sample collection in forests. However, trees and herbaceous plants from the same location may exhibit different strontium isotope ratios depending on rooting depth (Bélanger et al., 2012; Poszwa et al., 2004). In highly acidic soils and because of acidic rain, plants increasingly incorporate atmospheric Sr, which may alter the $^{87}Sr/^{86}Sr$ ratios significantly. In contrast, soils developed on calcareous substratum, which also prevail around Basel, show no clear response to acidic rain (Drouet et al., 2005b, 2007).

Modern snail shells and bones from small mammals were also considered valuable baseline samples, as the animals have a limited activity radius and sample preparation is very straightforward (Price et al., 2002). However, snail shells repeatedly produced lower $^{87}Sr/^{86}Sr$ ratios than plants (Evans et al., 2010; Frei and Frei, 2011; Oelze et al., 2012) which points to an influence of rainwater or a bias towards the isotopic composition of the calcareous component of the soil.

In sum, the major advantages of modern samples are the exact determination of their origin using handheld GPS devices and the specific selection of sampling locations. While plants are easily available, collecting samples of modern small mammals can be logistically challenging, as it requires trapping and rapid processing. The major disadvantage of modern samples, however, is a possible change in the biologically available strontium over time. These factors must be considered in evaluating reference data for archaeological settings.

Archaeological animal teeth and bones are also widely used comparative samples. Domestic and wild animal bones, for instance, formed the basis of an isotope-mapping project in southern Germany and the Alps (Toncala et al., 2017). Earlier comparative analysis of bone and enamel pairs, however, often revealed higher strontium concentrations and less isotopic variation in bones than in enamel (e. g. Price et al., 2004; Schweissing and Grupe, 2003), pointing to greater diagenetic alteration of the former. Nevertheless, two standard deviations from the average of bone samples were often used to determine local isotopic ranges in archaeological contexts (e.g. Bentley et al., 2004; Price and Bentley, 2005; Turck et al., 2012). If, however, strontium from the direct burial environment dominates due to diagenetic alteration, bone data may underestimate the isotopic variability within the human or animal habitat.

Because enamel is less susceptible to postdepositional changes of the $^{87}Sr/^{86}Sr$ ratios, domestic or small wild animal teeth are valuable samples for isotopic baseline examinations (Bentley, 2006; Kootker et al., 2016). The advantage of archaeological enamel samples is to represent strontium that was incorporated before substantial modern anthropogenic influence on the environment. However, humans have always determined the home ranges of their domestic animals, so that their isotope ratios do not necessarily represent the near surrounding of the sites where these were found. Therefore, working with archaeological faunal samples also requires archaeozoological knowledge as well as consideration of other lines of evidence for mobile husbandry strategies (e.g. transhumance, animal import etc.).

Geological setting and landscapes

The area around Basel comprises various bedrock formations (Figs. 1 and 2). The oldest geological unit are the Palaeozoic crystalline rocks (mainly granite and gneiss) of the Vosges and Black Forest (Geyer and Gwinner, 2011). While Buntsandstein (Early Triassic; non-calcareous sandstone) is relatively scarce (Fischer, 1969; Hauber, 1978), Middle Triassic deposits (Muschelkalk; limestone) appear east and northeast of Basel. The Upper Triassic Keuper comprises numerous, small-scale geological units, such as gypsum, clayey marls and sandstones. South of Basel, the Swiss Jura Mountains rise, which mainly consist of Jurassic marine limestone and marl deposits of the Middle (Dogger) and Upper Jurassic (Malm) (Bitterli-Brunner, 1987; Fischer et al., 1971). During the Paleogene (Oligocene), clayey and sandy lacustrine sediments (Alsace Molasse) and freshwater limestone (Tüllingen Freshwater Limestone) were deposited (Hauber, 1993; Sissingh, 1998), but are often covered by Pleistocene sediments. In the Neogene (Miocene), volcanic activity occurred in the Upper Rhine Valley (Kaiserstuhl, mainly tephrite and phonolite) (Geyer and Gwinner, 2011; Mäckel and Seidel, 2003). Large areas of those volcanic rocks are, however, covered with loess. The latter is a widely spread Pleistocene deposit in the Sundgau area (Rentzel et al., 2009) and around Basel. The settlement of Basel-Gasfabrik itself is situated on the Pleistocene Lower Terrace of the Rhine River (Kock et al., 2009; Wittmann, 1961). Those terraces consist of sandy-gravelly, originally calcareous deposits. During the Holocene, a decalcified Luvisol developed there (Rentzel, 1997, 1998). The Holocene flood basin is covered with fine-grained floodplain sediments.

The country around Basel is made up of diverse landforms (Leser, 1982, 1986) (Figs. 1 and 2), which largely agree with specific geological units. A wide alluvial plain and partly loess-covered river terraces dominate the Upper Rhine Valley (1). Loess sediments also prevail in the gentle hills of the Sundgau with its fertile soils (2) (Mosimann, 2015). The hilly country on the southern flank of the Black Forest (Dinkelberg) (3) shows high plateaus with Keuper and Pleistocene covering. The Table Jura (4) encompasses some relatively wide valleys (e. g. Birs and Ergolz valley) and high plateaus with thin loam covers and rather fertile soils. Clayey deposits on steep, forested hill slopes and anticlines dominate the Folded Jura (5), which is nowadays preferred as pastureland. In contrast, the loess covered hillslopes of the Kaiserstuhl (6) provide good arable soils. Vosges and Black Forest (7) are characterized by narrow valleys and steep hillslopes, where topography and acidic bedrock do not offer suitable agricultural land.

Material and methods

Sample locations and collection

As summarized above, rock and sediment samples, soil leachates, and soil water do not necessarily reflect the biologically available strontium, and the isotope ratios of snail shells may be biased towards calcareous soil components or rainwater. These materials were thus not included in our research. For logistical reasons, we also decided against trapping or collecting modern mice or other small mammals. We instead used modern vegetation and water and archaeological animal teeth to characterize the isotopic composition of the biologically available strontium. Moreover, we considered human infants' deciduous teeth and first permanent molars from the settlement and cemeteries of Basel-Gasfabrik (Tables 1–3).

The archaeological samples comprise enamel of 28 teeth from 18 human infants, of six pigs, and five dogs. Their selection is based on the assumption that old female pigs (as determined on mandibular teeth and likely being breeding animals) and dogs ranged in the near environs of the settlement. Other animal teeth were not sampled, because archaeozoological investigations indicated that domestic animals from Basel-Gasfabrik may have ranged more widely or may have been traded among sites (Stopp, 2008). For the children, burial in Basel-Gasfabrik is perceived as a likely indication of local birth.

The modern samples included vegetation from 51 locations (BG 0–50; n =102) and 9 water samples (BG A-I) from 8 water courses (Tables 1 and 2) from within a radius of ca. 20 km and single sites in the Vosges and Kaiserstuhl beyond this (Figs. 1 and 2). Although the strontium incorporated in plants may comprise strontium from modern anthropogenic sources, we reduced the risk of alteration by fertilizers by a careful selection of sampling spots in unaffected, old forests. Because the site of Basel-Gasfabrik lies within the modern city limits, we did not include vegetation samples from the site itself and its immediate environs (< 3 km distance). Using geological maps (https://map.geo. admin.ch, http://maps.geopotenziale.eu, http://infoterre.brgm.fr), we selected at least two representative locations under forest cover for each geological unit. From these, two vegetation samples were gathered including leaves from individual trees (deep rooting plants) and ground vegetation (shallow rooting plants) from several plants of the same species (Suppl. 1). River water was collected from the major watercourses. Samples were taken with a syringe and stored in acid-cleaned Teflon tubes. All locations were recorded with a handheld GPS. Geological and pedological settings as well as potential contaminations were noted. Additionally, each sampling location was evaluated for its suitability for crop and (woodland) pastureland (Table 2). For this, five quality levels (well suitable – suitable – moderately suitable – unsuitable – not possible) were defined on the basis of topographic settings and soil properties. For the latter, soil depth, substratum type, available water and nutrient capacity were assessed by modern soil data (Mosimann, 2015) and information from web platforms (https://maps. geo.admin.ch,http://geoview.bl.ch).

Sample preparation and analysis

Modern vegetation samples were rinsed with deionized water, dried at 50 °C overnight, and ashed in quartz glass crucibles at 500 °C for 12 h. Strontium separation and isotope analyses were conducted by IsoAnalysis UG, Berlin. Plant ashes were digested using concentrated HNO_3 in PFA beakers on a hot plate at 160 °C. The Sr-Spec resin (250 µl) was used for Sr-matrix separation. Sample loading and the removal of the matrix were carried out with 3 N HNO_3. Finally, Sr was eluted with H_2O. The Sr isotope compositions were measured with TIMS (VG Sector 54) and the raw data were corrected for a potential rubidium contribution on mass 87 and mass fractionation using an $^{86}Sr/88Sr$ isotope ratio of 0.1194. The $^{87}Sr/^{86}Sr$ isotope ratios were normalised to the widely accepted isotope ratio of 0.71025 for NIST SRM 987. In the course of the analytical campaign the accuracy of the used method was demonstrated by determined $^{87}Sr/^{86}Sr$ isotope ratios of fully processed seawater standard IAPSO of 0.70918 ± 0.00008 (n =5). The expanded analytical uncertainty of the $^{87}Sr/^{86}Sr$ isotope ratios of 0.000080 was exemplarily calculated using the IAPSO seawater standard. Based on a second Sr-Spec separation step necessary of six samples (BG 36b, 44b, 46a, 46b, 49b, 50b), however, the expanded analytical uncertainty for these samples were estimated to 0.00020.

Enamel from archaeological human and faunal teeth was separated using a diamond-coated cutting disc attached to a dental drill, and all surfaces and adhering dentine were removed with a diamond-coated burr. Enamel powder was then pre-cleaned in an ultrasonic bath with de-ionised H_2O and 0.1 M acetic acid buffered with Li-acetate (pH 4.5) and afterwards ashed (3 h, 850 °C). Strontium separation of the enamel and of the water samples using Eichrom Sr-Spec resin was done under clean-lab conditions following the procedures described in Knipper et al., 2012. Strontium concentrations were determined by Quadrupole- Inductively Coupled Plasma-Mass Spectrometry (Q-ICP-MS) and $^{87}Sr/^{86}Sr$ ratios by High-Resolution Multi Collector-ICP-MS (VG Axiom) at the Curt-Engelhorn-Centre for Archaeometry in Mannheim, Germany. Raw data were corrected according to the exponential mass fractionation law to $^{86}Sr/^{88}Sr = 0.1194$. Blank values were lower than 10 pg Sr during the whole clean lab procedure. The Eimer & Amend (E & A) standard run during the course of the analyses yielded $^{87}Sr/^{86}Sr$ ratios of 0.70798 ± 0.00006 (n = 96). The NBS 987 standard yielded an average $^{87}Sr/^{86}Sr$ ratio of 0.71018 ± 0.00003.

Results

Data from archaeological samples from Basel-Gasfabrik

The $^{87}Sr/^{86}Sr$ isotope ratios of 28 samples of deciduous teeth and first permanent molars from 18 children varied between 0.70847 and 0.70950 (Table 3). Two standard deviations from their average gave a range of between 0.70832 and 0.70928 (Figs. 4 and 5). The $^{87}Sr/^{86}Sr$ isotope values of 6 pig teeth varied between 0.70929 and 0.71152 (average ± 2 SD =0.70860–0.71166), and those of 5 dog teeth between 0.70884 and 0.71024 (average ± 2 SD = 0.70863–0.71058). Despite partial overlap, the difference between the animal and the human infants' teeth is statistically significant (Student's t-test $t(37) = -7.05141$, $p \leq 0.00001$).

No.	River	Site	GPS coordinates (WGS84)		Altidue [m]	Date	Sr isotope ratios	
			Latitude [°]	Longitude [°]			$^{87}Sr/^{86}Sr$	± 2 SD
BG A	**Wiese**	Brombach	47.63775	7.70873	315	05.07.2011	0.70996	0.00002
BG B	**Rhine**	Kaiseraugst	47.54095	7.72115	260	01.07.2011	0.70857	0.00008
BG C	**Rhine**	**Basel**	**47.56933**	**7.58608**	**252**	**04.07.2011**	**0.70860**	**0.00008**
BG D	**Birs**	**Reinach**	**47.51432**	**7.61552**	**280**	**30.06.2011**	**0.70835**	**0.00002**
BG E	**Birsig**	Therwil	47.50443	7.54217	310	30.06.2011	0.70852	0.00004
BG F	**Ergolz**	Ittingen	47.46975	7.78802	355	08.07.2011	0.70830	0.00006
BG G	**Thalbach**	Knoeringue	47.55937	7.41177	410	08.07.2011	0.70889	0.00001
BG H	**Thur**	Thann	47.81210	7.10342	340	03.07.2011	0.71025	0.00002
BG I	**Kander**	Kandern	47.71523	7.67387	365	05.07.2011	0.71240	0.00002

Table: *$^{87}Sr/^{86}Sr$ ratios of modern water samples. Samples within a 7 km radius are indicated in bold.*

Water data

The $^{87}Sr/^{86}Sr$ isotope ratios of the water samples ranged from 0.70830 to 0.71240 (average ± 1 SD = 0.70932 ± 0.00135) (Table 1) and are normally distributed (Kolmogorov-Smirnov-test, p =0.4351). The $^{87}Sr/^{86}Sr$ isotope ratios of the Rhine River coincide with other data of the High and Upper Rhine Valley (0.70844–0.70874) (Buhl et al., 1991; Eikenberg et al., 2001) (Suppl. 2) and mainly reflect the calcareous unconsolidated rock of this region (Rhine gravel and loess) (Eikenberg et al., 2001). Further downstream, the isotope values increased due to the confluence of rivers from the Black Forest and the Vosges. Rivers which originate in the Swiss Jura Mountains (Ergolz and Birs) exhibited slightly lower values (0.70830–0.70835) and reflect the underlying Jurassic limestone

bedrock. The $^{87}Sr/^{86}Sr$ isotope ratios of the Birsig and the Thalbach, both flowing through loess-dominated landscapes, are slightly higher (0.70852–0.70889). Other published water $^{87}Sr/^{86}Sr$ isotope ratios of small rivers in the Sundgau and the Upper Rhine Valley show similar ranges, and geochemical criteria suggest that fertilizers do not have a clear impact on their strontium isotope composition (Kloppmann, 2003; Kloppmann et al., 2013). The $^{87}Sr/^{86}Sr$ isotope values of the Wiese (0.70996), Thur (0.71025), and Kander (0.71240) are remarkably higher and reflect the influence of more radiogenic crystalline and metamorphic bedrock in the Black Forest and Vosges.

Locality		Geology and sediment cover		Ground veg.		Tree leaves		Diff.	Suitability		
No.	Site	System	Serie	$^{87}Sr/^{86}Sr$	± 2 SD	$^{87}Sr/^{86}Sr$	± 2 SD		AC	PA	WP
BG0	**Rosenau**	**Quarternary**	**Holocene**	**0.70859**	**0.00001**	**0.70852**	**0.00001**	**0.00008**	**--**	**--**	**++**
BG1	Bartenheim	Quarternary	Late Pleistocene	0.70830	0.00001	0.70831	0.00001	-0.00001	+	++	+
BG2	Habsheim	Quarternary	Late Pleistocene	0.70967	0.00001	0.70965	0.00001	0.00002	--	--	++
BG3	Munchhouse	Quarternary	Late Pleistocene	0.70962	0.00001	0.70935	0.00001	0.00027	++	++	+
BG4	Maugenhard	Paleogene	Oligocene	0.71096	0.00001	0.71145	0.00001	-0.00049	++	++	+
BG5	Hügelheim	Quarternary	Late Pleistocene	0.70865	0.00001	0.70874	0.00001	-0.00009	-	o	+
BG6	**Tüllingen**	**Paleogene**	**Oligocene**	**0.70941**	**0.00001**	**0.70907**	**0.00001**	**0.00034**	**+**	**++**	**+**
BG7	Bettingen	Triassic	Keuper (Midd. Triassic)	0.70872	0.00001	0.70905	0.00001	-0.00033	--	--	+
BG8	Inzlingen	Triassic	Muschelkalk (Upp. Triassic)	0.71053	0.00001	0.71004	0.00001	0.00049	++	++	+
BG9	Riehen	Triassic	Upper Buntsandstein	0.71234	0.00001	0.71126	0.00001	0.00108	+	++	+
BG10	**Basel**	**Quarternary**	**Holocene**	**0.70958**	**0.00001**	**0.71029**	**0.00001**	**-0.00072**	**--**	**--**	**+**
BG11	Bickensohl	Neogene	Miocene	0.70827	0.00001	0.70837	0.00001	-0.00009	++	++	+
BG12	Bötzingen	Neogene	Miocene	0.70848	0.00001	0.70864	0.00001	-0.00016	+	++	+
BG13	Amoltern	Neogene	Miocene	0.70782	0.00001	0.70795	0.00001	-0.00013	--	--	+
BG14	Pratteln	Quarternary	Late Pleistocene	0.70847	0.00001	0.70886	0.00002	-0.00040	++	++	+
BG15	**Basel**	**Quarternary**	**Early Pleistocene**	**0.71012**	**0.00001**	**0.71035**	**0.00001**	**-0.00022**	**o**	**+**	**+**
BG16	**Basel**	**Quarternary**	**Late Pleistocene**	**0.70847**	**0.00001**	**0.70892**	**0.00001**	**-0.00045**	**o**	**+**	**+**
BG17	Reinach	Quarternary	Late Pleistocene	0.70851	0.00001	0.70814	0.00001	0.00036	++	++	+
BG18	**Reinach**	**Quarternary**	**Middle Pleistocene**	**0.70928**	**0.00001**	**0.70878**	**0.00001**	**0.00050**	**--**	**--**	**+**
BG19	**Allschwil**	**Quarternary**	**Late Pleistocene**	**0.70966**	**0.00001**	**0.70970**	**0.00001**	**-0.00005**	**--**	**--**	**+**
BG20	Oltingue	Paleogene	Oligocene	0.71085	0.00001	0.71091	0.00001	-0.00006	++	++	+
BG21	Hagenthal-le-Bas	Quarternary	Late Pleistocene	0.70999	0.00001	0.71035	0.00001	-0.00036	--	--	++
BG22	**Schönenbuch**	**Quarternary**	**Early Pleistocene**	**0.71041**	**0.00001**	**0.71093**	**0.00001**	**-0.00052**	**++**	**++**	**+**
BG23	Knoeringue	Neogene	Pliocene	0.71107	0.00001	0.71144	0.00001	-0.00037	+	++	+
BG24	Ranspach-le-Haut	Quarternary	Late Pleistocene	0.70985	0.00001	0.70969	0.00001	0.00016	+	++	+
BG25	Oltingue	Paleogene	Oligocene	0.70903	0.00001	0.70906	0.00001	-0.00003	+	++	+
BG26	Ferrette	Jurassic	Dogger (Mid. Jurassic)	0.70839	0.00001	0.70878	0.00001	-0.00039	-	-	++
BG27	Hésingue	Quarternary	Late Pleistocene	0.70842	0.00001	0.70892	0.00001	-0.00050	+	++	+
BG28	Hochstetten	Quarternary	Holocene	0.70964	0.00001	0.71000	0.00001	-0.00035	--	--	o
BG29	Ostheim	Quarternary	Late Pleistocene	0.71300	0.00001	0.71423	0.00001	-0.00124	--	--	o
BG30	Sierentz	Quarternary	Late Pleistocene	0.71002	0.00001	0.70997	0.00001	0.00005	--	--	o
BG31	Augst	Quarternary	Late Pleistocene	0.70817	0.00001	0.70820	0.00001	-0.00003	+	++	+
BG32	Kaiseraugst	Quarternary	Late Pleistocene	0.70842	0.00001	0.70843	0.00001	-0.00001	-	-	++
BG33	Rheinfelden	Quarternary	Late Pleistocene	0.70890	0.00001	0.70865	0.00001	0.00026	--	--	o
BG34	Pratteln	Jurassic	Dogger (Mid. Jurassic)	0.70809	0.00001	0.70827	0.00001	-0.00018	--	--	+
BG35	Frenkendorf	Jurassic	Malm (Upp. Jurassic)	0.70854	0.00001	0.70960	0.00001	-0.00106	--	--	+
BG36	Liestal	Jurassic	Dogger (Mid. Jurassic)	0.70788	0.00001	0.70781	0.00001	0.00006	--	--	+
BG37	Gempen	Quarternary	Holocene	0.70859	0.00001	0.70850	0.00001	0.00008	++	++	+
BG38	Sissach	Quarternary	Late Pleistocene	0.70830	0.00001	0.70832	0.00001	-0.00002	--	--	+
BG39	Böckten	Jurassic	Dogger (Mid. Jurassic)	0.70864	0.00001	0.70841	0.00001	0.00023	--	--	o
BG40	Nunningen	Jurassic	Dogger (Mid. Jurassic)	0.70788	0.00001	0.70801	0.00001	-0.00013	+	++	+
BG41	Waldenburg	Jurassic	Dogger (Mid. Jurassic)	0.70780	0.00001	0.70776	0.00001	0.00004	-	o	+
BG42	Möhlin	Quarternary	Early Pleistocene	0.70989	0.00001	0.71062	0.00001	-0.00073	--	--	+
BG43	Herten	Triassic	Muschelkalk (Upp. Triassic)	0.70910	0.00001	0.70877	0.00001	0.00033	++	++	+
BG44	Degerfelden	Triassic	Middle Buntsandstein	0.71538	0.00001	0.71638	0.00002	-0.00099	--	-	+
BG45	Liestal	Quarternary	Holocene	0.70940	0.00001	0.70942	0.00002	-0.00002	o	o	+
BG46	Inzlingen	Triassic	Keuper (Middle Triassic)	0.71412	0.00001	0.71409	0.00001	0.00003	--	++	+
BG47	Brombach	Triassic	Muschelkalk (Upp. Triassic)	0.70987	0.00001	0.70906	0.00001	0.00082	-	o	+
BG48	Oberwil	Quarternary	Late Pleistocene	0.70874	0.00001	0.70888	0.00001	-0.00014	-	o	+
BG49	Thann	Devon / Carbonif.		0.71146	0.00001	0.71210	0.00001	-0.00063	--	--	+
BG50	Kandern	Devon / Carbonif.		0.71662	0.00001	0.71794	0.00001	-0.00131	--	--	+

Table 2: *$^{87}Sr/^{86}Sr$ ratios of modern vegetation samples and classification of the suitability for agriculture (AC), pasture (PA) and woodland pasture (WP) according to five categories: ++ well suitable; + suitable; o moderately suitable; - unsuitable; – not possible. Samples within a 7 km radius are indicated in bold.*

Vegetation data

The $^{87}Sr/^{86}Sr$ isotope values of vegetation samples ranged from 0.70776 (BG 41, Jurassic limestone) to 0.71794 (BG 50, granite) (Table 2, Figs. 3, 4 and 5). Both $^{87}Sr/^{86}Sr$ isotope values of ground vegetation and tree leaves show a normal distribution (Kolmogorov- Smirnov-test, p = 0.0613 [ground vegetation] and p= 0.0627 [tree], average ± 1 SD = 0.70965 ± 0.00186). The differences of the $^{87}Sr/^{86}Sr$ ratios of ground vegetation and tree leaves from the same location (ground vegetation minus tree leaves) varied between −0.00131 and 0.00108 (average ± 1 SD = −0.00014 ± 0.00046). Where samples of the ground vegetation exhibited more radiogenic $^{87}Sr/^{86}Sr$ ratios than those of the tree leaves, the difference is statistically significant (Student's t-test: t (48) =−2.11824, p < 0.05). Nevertheless, only in twelve of the 51 sample pairs, the differences exceeded 0.0005 (Fig. 6). In general, samples from more radiogenic geological units exhibited larger differences between deep and shallow rooting plants than those from less radiogenic units.

Lab code		sample	$^{87}Sr/^{86}Sr$	± 2 SD	sample	$^{87}Sr/^{86}Sr$	± 2 SD
BGA 2	Humans (infants)	62 (dec. tooth)	0.70885	0.00005			
BGA 7		65 (dec. tooth)	0.70867	0.00003	64 (dec. tooth)	0.70862	0.00004
BGA 11		85 (dec. tooth)	0.70873	0.00001			
BGA 12		74 (dec. tooth)	0.70867	0.00001	16 (M1)	0.70913	0.00001
BGA 14		84 (dec. tooth)	0.70855	0.00001	85 (dec. tooth)	0.70864	0.00001
BGA 15		52 (dec. tooth)	0.70921	0.00003			
BGA 16		65 (dec. tooth)	0.70866	0.00003	64 (dec. tooth)	0.70860	0.00003
BGB 5		73 (dec. tooth)	0.70908	0.00003			
BGB 7		84 (dec. tooth)	0.70908	0.00003			
BGB 15		46 (dec. tooth)	0.70855	0.00003	64 (M1)	0.70879	0.00002
BGB 17		85 (dec. tooth)	0.70888	0.00005			
BGB 21		64 (dec. tooth)	0.70853	0.00002	51 (dec. tooth)	0.70847	0.00003
BGB 22		81 (dec. tooth)	0.70881	0.00003	dec. tooth indet.	0.70870	0.00003
BGB 24		61 (dec. tooth)	0.70876	0.00002			
BGB 25		74 (dec. tooth)	0.70896	0.00006			
BGS 3		85 (dec. tooth)	0.70871	0.00002	46 (M1)	0.70872	0.00004
BGS 19		63 (dec. tooth)	0.70878	0.00001	75 (M1)	0.70867	0.00003
BGS 31		85 (dec. tooth)	0.70950	0.00003	46 (M1)	0.70907	0.00002
BGT 17.1	*Sus domesticus*	lower left P4	0.70947	0.00001			
BGT 18.1		upper left M3	0.71008	0.00001			
BGT 19.1		lower left M3	0.70975	0.00003			
BGT 20.1		lower left P3	0.71067	0.00005			
BGT 21.1		lower left P4	0.71152	0.00002			
BGT 22.1		lower right M3	0.70929	0.00005			
BGT 23.1	*Canis familiaris*	lower right M1	0.70935	0.00001			
BGT 26.1		upper right M1	0.71024	0.00003			
BGT 28.1		lower right M1	0.70884	0.00003			
BGT 34.1		lower left M1	0.70998	0.00007			
BGT 36.1		upper right P4	0.70961	0.00001			

Table 3: $^{87}Sr/^{86}Sr$ ratios of archaeological tooth enamel from human infants, Sus domesticus and Canis familiaris; human teeth numbered according to FDI (Alt and Türp, 1998).

The **Holocene floodplain of the Rhine River** (n= 2 locations [loc], 4 samples [spl]) showed a wide range of plant $^{87}Sr/^{86}Sr$ ratios (0.70852–0.71000). The difference may be due to varying compositions of the underlying Rhine gravel and groundwater influence. The **Holocene floodplain of the Wiese** (n = 1 loc, 2 spl) is consistent with water sample BG A (0.70958–0.71029).

The lower **terrace deposits of the Rhine River** (n= 6 loc, 12 spl) comprise a large area along the watercourse and their $^{87}Sr/^{86}Sr$ isotope ratios varied remarkably (0.70830–0.71002). They may reflect smallscale differences in the composition of the Rhine gravel. Because most of the samples were collected in an old forest without agricultural overprint (Hardtwald), impact by chemical fertilizers is unlikely, even though other contamination, such as liming (Drouet et al., 2005a) cannot be wholly excluded. **Terrace and moraine deposits of older glacial stages** (n= 3 loc, 6 spl) showed higher values (0.70989–0.71093), which probably reflect advanced soil formation processes during interglacial periods. Plants growing on the **alluvial fan of the Fecht** (BG 29, n =1 loc, 2 spl), which originates in the Vosges, exhibited elevated $^{87}Sr/^{86}Sr$ isotope values (0.71300 and 0.71423) which correlate with water samples (Eikenberg et al., 2001) and reflect the crystalline basement of its catchment. In contrast, **lower terrace deposits of rivers from the Swiss Jura Mountains** (n =4 loc, 8 spl) had low values (0.70817–0.70851) and mirror the limestone gravel. Older calcareous terrace deposits (n = 1 loc, 2 spl) gave slightly higher values (0.7087 and 0.70928).

Pleistocene loess soils in the surrounding of Basel are today largely cultivated. Nevertheless, several locations under forest cover could be sampled (n =7 loc, 14 spl). Their range was rather large (0.70842–0.70985, excluding sample location BG 21 because of underlying sandstones), but compares well with vegetation data from central Germany (0.70825–0.70973) (Knipper et al., 2012). The large variability of the ratios is probably the result of erosional processes, which led to truncated Ap-C soil profiles, and modern anthropogenic influence may have affected the soils.

The $^{87}Sr/^{86}Sr$ isotope ratios for the **volcanic Kaiserstuhl** region (n = 3 loc, 6 spl) (0.70782–0.70864) were consistent with data from other volcanic regions (Bentley and Knipper, 2005; Willmes et al., 2014), including the Hegau near Lake Constance (Oelze et al., 2012) (0.70435–0.70822). The relatively high values of BG 11 and BG 12 (0.70827–0.70864) probably reflect a mixture of strontium of volcanic origin and from the overlying loess loam.

Paleogene (Oligocene) deposits in the Upper Rhine Valley are characterized by mainly **sandy sediments** (n =2 loc, 4 spl) with high values (0.71085–0.71145), which are slightly higher than vegetation data from locations with comparable conditions in France (Willmes et al., 2014) (0.70968–0.71026). **Freshwater limestone** of the same age (n= 2 loc, 4 spl) is rare (e.g. Tüllingen Freshwater Limestone) and showed low $^{87}Sr/^{86}Sr$ isotope ratios (0.70903–070941).

Jurassic limestone (n = 7 loc, 14 spl) (Middle and Upper Jurassic) consistently exhibited low $^{87}Sr/^{86}Sr$ isotope values (0.70780–0.70864), which are congruent with vegetation samples from around Singen, Baden-Württemberg, Germany (Oelze et al., 2012). Higher values probably go back to overlying loamy sediments, as it was observed for BG 37 and BG 45 (0.70850–0.70942).

The same is probably true for the vegetation samples on **Upper Triassic limestone (Muschelkalk)** (n =3 loc, 6 spl), whose $^{87}Sr/^{86}Sr$ isotope ratios varied widely (0.70877–0.71053). Vegetation data from central Germany (Knipper et al., 2012) showed persistently low values (0.70819–0.70875), whereas such from around Singen (Oelze et al., 2012) were similar to our samples (0.70890–0.71005). Conditions at the sample locations suggest that plants growing directly on Triassic limestone have low values (0.708–0.709), whereas loam cover leads to a wider range

including values of above 0.709. **Middle Triassic deposits (Keuper)** show highly variable small-scale geological units, leading to a wide range of $^{87}Sr/^{86}Sr$ ratios from 0.70872 (probable gypsum) to 0.71409 (probable marl), which was also observed in other regions (Knipper, 2011; Oelze et al., 2012). $^{87}Sr/^{86}Sr$ isotope ratios of **Upper Triassic sandstone (Buntsandstein)** (n =2 loc, 4 spl) were clearly above 0.71000 (0.71126–0.71638).

Devonian and Carboniferous rocks (n =2 loc, 4 spl) (granites, gneisses, psephites, schists etc.) appear in the Vosges and Black Forest. Their strontium isotope range (0.71146–0.71794) was consistent with other vegetation and archaeological data from the Black Forest (Bentley and Knipper, 2005; Oelze et al., 2012) and the Vosges (Willmes et al., 2014), which show generally high values above 0.71000.

Overall, water and vegetation samples from the area around Basel exhibited a wide range of $^{87}Sr/^{86}Sr$ isotope values, which reflects the diverse, small-scale character of the geologic setting. The isotopic compositions of the bio-available strontium from many geological units ranged widely and overlapped (Table 4). Especially $^{87}Sr/^{86}Sr$ isotope ratios of between 0.70850 and 0.7100 were frequent and occurred on floodplain sediments and lower terrace deposits of the Rhine River, on loess and other loam covers in the Sundgau and the Table Jura, on Triassic limestone (Muschelkalk), and on some Keuper and Miocene units (gypsum, freshwater limestone). Lower values (0.7077–0.7086) only appeared on Jurassic limestone and in the Kaiserstuhl volcanic region. High values (0.711–712) in turn were found on Triassic sandstone (Buntsandstein), on some Keuper units (clayey marl) and on the crystalline bedrock of the Vosges and Black Forest, whereas the latter may exceed 0.712.

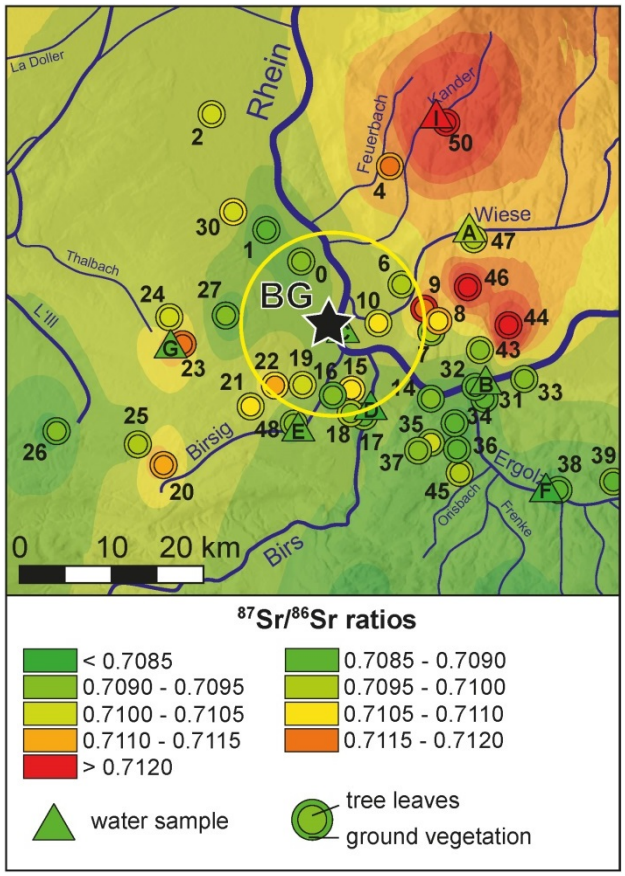


Fig. 3: *Interpolation surface of the 87Sr/86Sr ratios isotope ratios in the surrounding of Basel (Inverse Distance Weighting with ArcGis 10.1.). Interpolation based on shallow rooting plants. Yellow circle: 7 km radius around the site.*

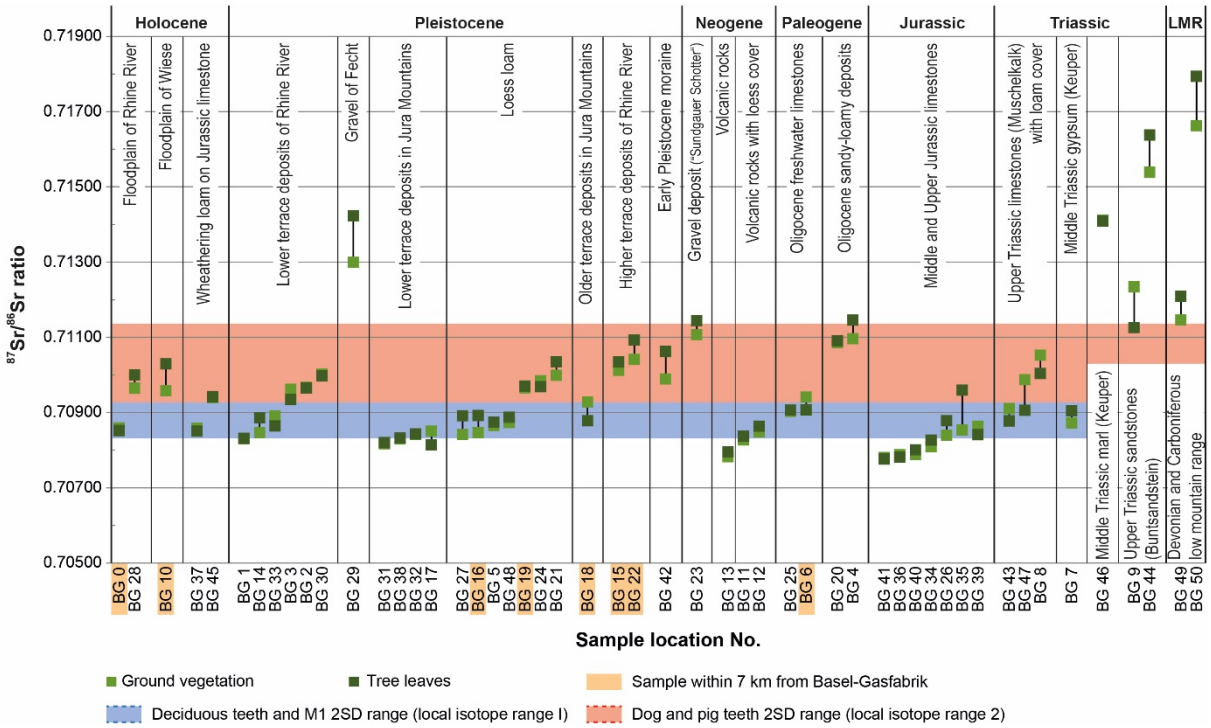


Fig. 4: Strontium isotope ratios of modern vegetation (shallow rooting plants; light green) and tree samples (deep rooting plants; dark green), arranged after geological units. Local isotope range I (blue) and local isotope range II (red) are indicated (see paragraph 6.3). Sampling sites within a radius of 7 km to Basel-Gasfabrik are marked orange.

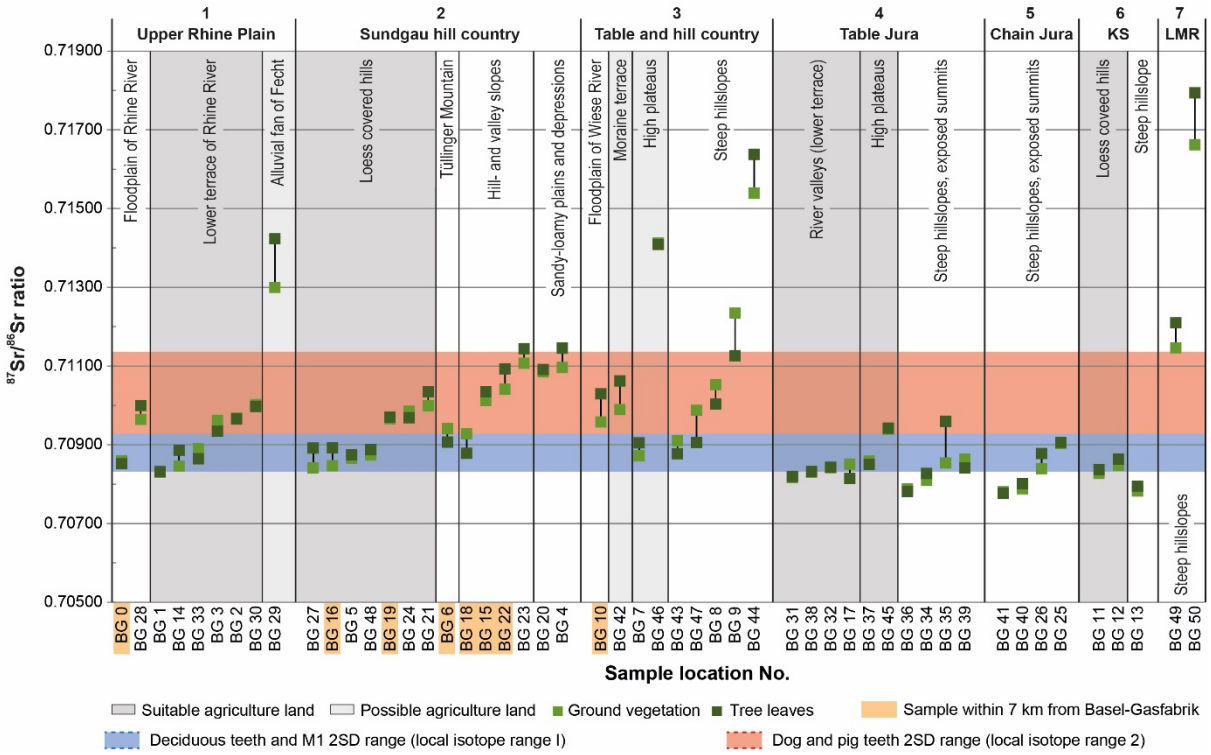


Fig. 5: Strontium isotope ratios of modern vegetation (shallow rooting plants; light green) and tree samples (deep rooting plants; dark green), arranged after landscapes. Local isotope range I (blue) and local isotope range II (red) are indicated (see paragraph 6.3). Sampling sites within a radius of 7 km to Basel-Gasfabrik are marked orange.

Discussion

Differences of tree leaves and ground vegetation $^{87}Sr/^{86}Sr$ isotope ratios

Even though tree leaves and ground vegetation from the same location had significantly different $^{87}Sr/^{86}Sr$ ratios (Fig. 6), only at the minority of the sampling locations can the offsets be considered meaningful for the interpretation of archaeological data. We suggest those differences of $^{87}Sr/^{86}Sr$ ratios of ground vegetation and tree leaves depend on the kind and thickness of the sediment cover of the bedrock. At the locations BG 6, 8, 17, 18, 43 and 47, a thin layer of clayey loam covers the calcareous, weakly radiogenic bedrock (Jurassic limestone or calcareous gravel). All of them exhibited higher $^{87}Sr/^{86}Sr$ ratios in the shallow rooting vegetation. It is thus probable that these plants reflect the loam cover, while tree leaves mirror the underlying calcareous bedrock. On the other hand, sample locations with thick loam cover (BG 0, 5, 11, 12, 19, 24, 37, 45, 48), on thick gravel deposits (BG 30, 31, 32, 36, 38) or on bedrock without sediment cover (BG 13, 25, 40, 41, 46) showed similar $^{87}Sr/^{86}Sr$ isotope ratios in tree leaves and ground vegetation.

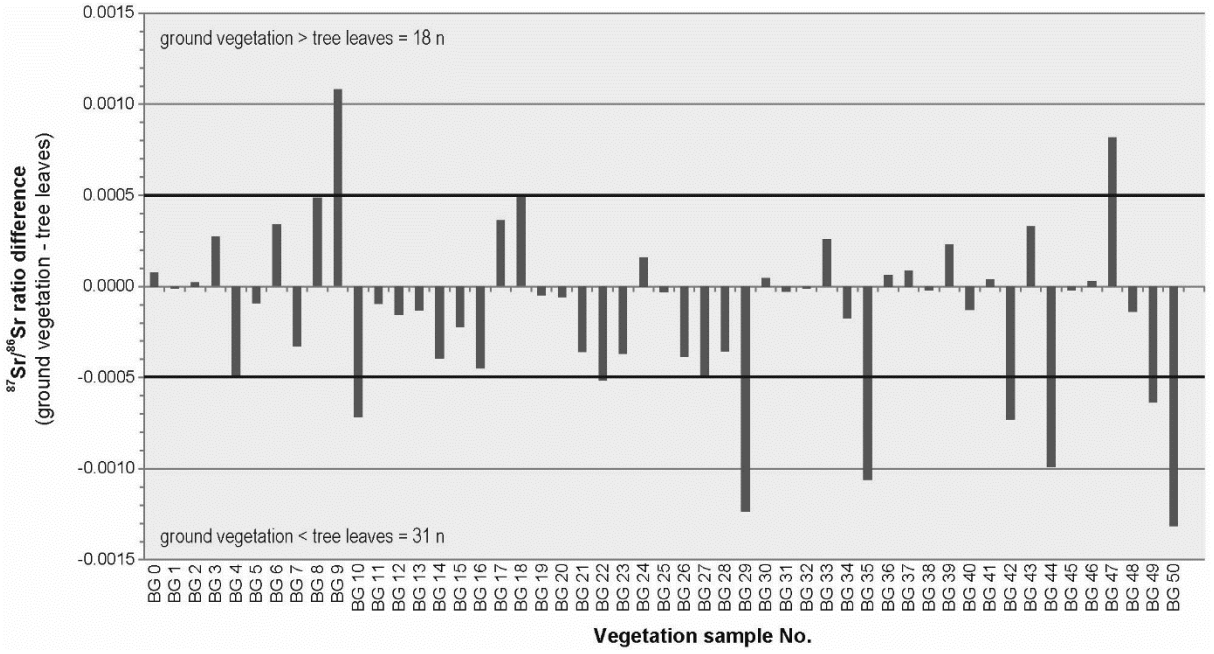


Fig. 6: *Differences of the $^{87}Sr/^{86}Sr$ isotope ratios of the ground vegetation and the tree leaves from the same location. In 31 cases, tree leaves values are higher than ground vegetation $^{87}Sr/^{86}Sr$ ratios (negative difference), while the opposite is true for 18 cases, yet difference rarely exceeds 0.0005 (11 cases).*

In general, more systematic research into the bio-availability of strontium in connection with pedological and hydrological properties of different landscapes is needed. The results of this study, however, demonstrate that the differences between the $^{87}Sr/^{86}Sr$ isotope ratios of tree leaves and ground vegetation not only depend on the bedrock, but also on the character and thickness of the overlying sediments. Thus, local characteristics of topography, hydrology, and soil conditions are likely causes for a frequently observed variation of $^{87}Sr/^{86}Sr$ isotope ratios in plants from similar bedrock settings. In most cases the differences between tree leaves and ground-covering vegetation are small in relation to the variation among different sample locations of the same geological unit and even more so in comparison to the variation among different geological units present in the study area. Therefore, we consider both ground vegetation and tree leaves representative of the specific locations.

Nevertheless, sampling both is advisable and ensures the representativeness of both sample types in the given study area and exposes unusual isotope ratios.

Characterization of the biologically available strontium at Basel-Gasfabrik and spatially structured land use

The $^{87}Sr/^{86}Sr$ data of the modern vegetation and water samples reflect the diversity of the geological settings in the southern Upper Rhine Valley and the adjacent low mountain ranges. The sampling locations are situated up to about 50 km away from Basel-Gasfabrik and include the wider hinterlands as well as landforms whose properties may not offer prime conditions for cultivation (see paragraph 6.3). We therefore discuss a more representative characterization of the strontium, which entered the food web of the Basel-Gasfabrik population and define isotopic cut-off values for the identification of non-local individuals (Knipper et al., 2018). These approaches include animal and human children's teeth (Fig. 7) and the examination of modern vegetation data from a confined radius. We regarded seven kilometres around Basel-Gasfabrik an appropriate radius for closer examination of the modern vegetation data. This is similar to the six-kilometre radius that was used for habitat evaluations at Early Iron Age central sites in nearby southwest Germany (Fischer et al., 2010), and included a potential agricultural area with far-off fields in up to 1.5 h walking distance. This confined dataset comprises eight localities, most of them between 5 and 7 km away (Fig. 2). The archaeological site itself and its nearest environs are not covered with sampling due to its location within a modern city. However, the tested flood plain, low terrace of the Rhine River, and loess hills also dominate the potential farmland in< 5 km from Basel-Gasfabrik as well as extending beyond the considered area. Thus one can assume the local values to be well covered. The $^{87}Sr/^{86}Sr$ ratios of the tree leaves and ground vegetation within this radius varied between 0.70847 and 0.71093 (average ± 1 SD = 0.70951 ± 0.00073). Spatial differentiation of specific isotope packages is, however, not possible because the $^{87}Sr/^{86}Sr$ ratios of the represented geological units, landscapes, and groups of agricultural suitability exhibited considerable internal variation at low sample sizes (Figs. 4 and 5).

The archaeological pig and dog teeth overlapped widely with the modern vegetation data from the seven-kilometre radius. Their combined average isotope ratios± 2 SD gave a range of between 0.70841 and 0.71137. The difference between the modern vegetation and the animal teeth was not statistically significant (Student's t-test $t(25) = -1.570$, $p= 0.129$). However, all animal samples exhibit $^{87}Sr/^{86}Sr$ ratios above 0.709, while only one dog sample (BGT 28.1) fell below (Fig. 7).

With a two-sigma-range of between 0.70832 and 0.70928, the strontium isotope ratios of deciduous teeth and the first permanent molars of the human infants from Basel-Gasfabrik were remarkably restricted to the lower half of the data spectrum of the modern vegetation within the seven-kilometre radius from the site and of the animal teeth. Notably, the difference between the isotope ratios of the children's and the animal teeth was statistically significant (Student's t-test animals: $t(37) = -7.05141$, $p \leq 0.00001$), even though both could be expected to mirror the local biologically available strontium. Because both archaeological datasets match the modern vegetation values, we interpret this outcome as resulting from differential land use of the inhabitants of Basel-Gasfabrik. We argue that the homogenous isotope ratios of the infants' teeth point to a deliberate selection of land for crop and other plant food production. Plant foods dominate the strontium that is incorporated into human teeth and bones because they usually have higher strontium concentrations than animal-derived

foodstuffs and water (Burton and Hahn, 2016; Knipper, 2011). In deciduous teeth, enamel starts forming in utero and mineralization continues after birth. In the portion that is laid down before weaning, the strontium originates at least partly from breastmilk. It therefore primarily reflects the mothers' diet, which however also largely goes back to the plant component. Both the generally high proportions of plant-derived foodstuffs in the human diet and the breastfeeding of infants are well documented in carbon and nitrogen isotope data of bone collagen from the site (Knipper et al., 2017). Moreover, the characteristic strontium isotope range occurred among children from both cemeteries and the settlement and thus precludes the possibility of describing a spatial or social subset of the children only. The homogenous isotope ratios of the infants' teeth also argue against any non-local females who arrived pregnant at the site only shortly before giving birth. A precise assignment of the former agricultural fields to certain portions of the landscape is, however, not possible. Loess-covered hills (e.g. BG 16) as well as Lower Rhine Terrace sediments (e.g. BG 17) yielded modern vegetation samples with $^{87}Sr/^{86}Sr$ ratios in the isotope range of the children's teeth. Both geological units are well suitable for agriculture according to soil quality criteria (Table 2, Figs. 4 and 5) and widely distributed around the site.

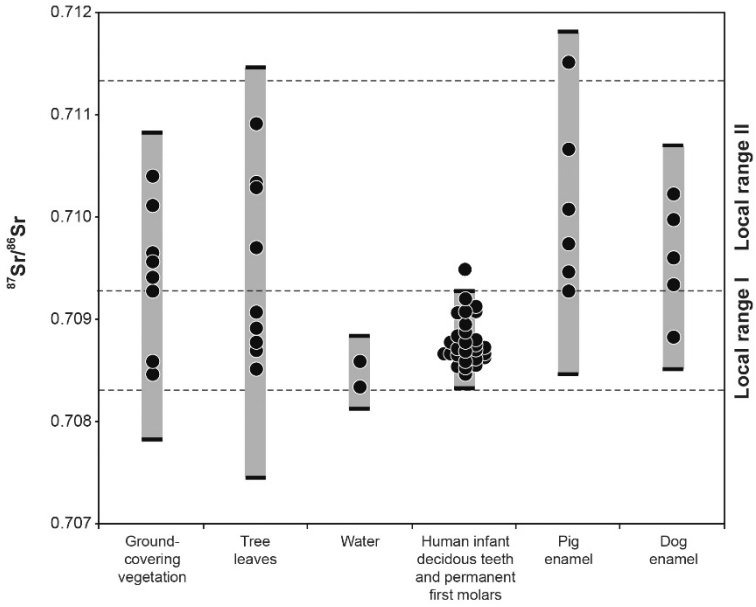


Fig. 7: *Strontium isotope ratios of modern shallow and deeprooting plants and water from a seven-kilometre radius around the Basel-Gasfabrik site, infants' deciduous teeth and first permanent molars from Basel-Gasfabrik. The grey shading marks two standard deviations from the average of each dataset. The hatched lines indicate two standard deviations of the infants' teeth (local range I) and the upper limit of the combined two standard deviation range of the pig and dog teeth. The portion above the upper limit of range I is assigned as "local range II".*

The more variable and often more radiogenic strontium isotope ratios of the pig and dog teeth point to the animals feeding of different, spatially less restricted areas. Stable carbon and nitrogen isotope analyses showed that pigs were mostly fed on vegetable food, while dogs had a more omnivorous diet (Knipper et al., 2017). In the light of contemporaneous smaller settlements and farmsteads around Basel- Gasfabrik (Blöck et al., 2014), it also seems plausible that some of the animals reflect supply of the proto-urban center from its regional network. Thus trade or exchange of animals needs to be considered as well. Moreover, dogs may have travelled together with their owners, which may have contributed to heterogeneous $^{87}Sr/^{86}Sr$ ratios. Again, precise isotopic identification of the portions of the landscape that provided the animals' feed is not possible because of the repeated occurrence of the respective isotope ratios among the modern plant samples.

Overall, both the selection of portions of land for agriculture and the spatially more flexible provision of the animals seems to have gone beyond utilitarian aspects, such as soil fertility or geological conditions. Instead, the isotope ratios of the human infants' and domestic animals' teeth point to deliberate choices, but also restriction,

possibly due to differential ownership, use rights ("land laws"), trade relations, kinship or conceivably even taboos or other culturally determined behaviour. The respective geological units and strontium isotope ranges also extend beyond our confined seven-kilometre radius, so that provision of the proto-urban centre with crops and animal products from the wider hinterland can hardly be distinguished.

Localities (BG-Numbers)	Geological system	Geological unit	n	$^{87}Sr/^{86}Sr$ Range
BG 0, 28	Holocene	Holocene floodplain of Rhine	2 (4)	0.70852-0.71000
BG 10	Holocene	Holocene floodplain of Wiese	1 (2)	0.70958-0.71029
BG 37, 45	Holocene	Holocene wheathering loam upon Jurassic limestone	2 (4)	0.70850-0.70942
BG 1, 2, 3, 13, 30, 33	Pleistocene	Late Pleistocene lower terrace deposits of Upper Rhine Valley	6 (12)	0.70830-0.71002
BG 29	Pleistocene	Late Pleistocene fluvial fan of Fecht	1 (2)	0.71300-0.71423
BG 17, 31, 32, 38	Pleistocene	Late Pleistocene lower terrace deposits of river plains in Jura Mountains	4(8)	0.70817-0.70851
BG 5, 16, 19, 21, 24, 27, 48	Pleistocene	Late Pleistocene loess loam	7 (14)	0.70842-0.70985*
BG 18	Pleistocene	Higher terrace deposits in Jura Mountains	1 (2)	0.70878-0.70928
BG 15, 22	Pleistocene	Early Pleistocene terrace deposits of Rhine	2 (4)	0.71012-0.71093
BG 42	Pleistocene	Early Pleistocene moraine	1 (2)	0.70989-0.71062
BG 23	Neogene	Neogene gravel deposits	1 (2)	0.71107-0.71144
BG 11, 12, 13	Neogene	Neogene volcanic sediments with loess cover	3 (6)	0.70782-0.70864
BG 6, 25	Paleogene	Paleogene (Oligocene) freshwater limestone	2 (4)	0.70903-0.70941
BG 4, 20	Paleogene	Paleogene (Oligocene) sandy-loamy deposits	2 (4)	0.71085-0.71145
BG 26, 34, 35, 36, 39, 40, 41	Jurassic	Middle and Upper Jurassic limestones	7 (14)	0.70776-0.70864
BG 8, 43, 47	Triassic	Upper Triassic limestones (Muschelkalk) with (loess) loam cover	3 (6)	0.70877-0.71053
BG 7	Triassic	Middle Triassic gypsum (Keuper)	1 (2)	0.70872-0.70905
BG 46	Triassic	Middle Triassic marl (Keuper)	1 (2)	0.71412-0.71409
BG 9, 44	Triassic	Early Triassic sandstones (Buntsandstein)	2 (4)	0.71126-0.71638
BG 49, 50	Devonian, Carbonife-rous	Granitic-gneissig low mountain range	2 (4)	0.71146-0.71794

Table 4: *Summary of the 87Sr/86Sr ratios of the sampled geological units. N= number of sampling locations and number of samples (in brackets). * without BG 21.*

In addition to these reflections regarding Late Iron Age land use, we consider the distinct isotope ratios of the human infant and animal teeth meaningful for defining cut-off values for the identification of non-local individuals among the human remains in both cemeteries and settlement features at the Basel-Gasfabrik site (Knipper et al., 2018). We perceive the narrow isotope range of deciduous teeth and permanent first molars of the children as an indication for local births and, at the same time, as an estimate of the isotopic composition of the strontium that entered the food web at Basel-Gasfabrik via local food production. The two-standard-deviation range of the enamel values of the children (0.70832–0.70928) is therefore regarded as "local isotope range I". Enamel of human individuals from Basel with $^{87}Sr/^{86}Sr$ ratios within this range likely reflects provision from the same economic area as that of the sampled children. These values will be regarded as "local" to Basel, even though an origin from another area with similar biologically available strontium cannot be excluded.

The modern vegetation within the seven-kilometre radius around Basel also backs up the strontium isotope ratios of the animal teeth, even though they range wider than "local isotope range I". We therefore define "local isotope range II" (0.70928–0.71137) as the portion of the two-standard-deviation range of the pigs and dogs teeth that is more radiogenic than the infants' teeth (Fig. 7). Enamel with strontium isotope ratios within this range reflects exploitation of arable land that differed from that which provided the children from Basel-Gasfabrik. However, because these isotope ratios occurred among the supposedly local domestic animals and in the modern vegetation in the near environs of the site, burials with enamel isotope ratios within this range may also be considered "local". Biologically available strontium with $^{87}Sr/^{86}Sr$ ratios in both ranges is dispersed within

the seven-kilometre radius around the site without spatial distinction and is also not restricted to it. In the evaluation of the complete human dataset (Knipper et al., 2018), we apply the ranges as defined in this study. We consider individuals with more or less radiogenic $^{87}Sr/^{86}Sr$ ratios than both ranges as "non-local" or coming from beyond the seven-kilometre radius. Their places of origin may include landforms in the hinterlands of Basel-Gasfabrik or from a farther distance. For human individuals with enamel strontium isotope ratios within both "local" ranges, origins from other areas with similar geologic conditions will, however, remain unrecognized.

Characterization of the biologically available strontium of different landforms in the hinterlands of the Basel-Gasfabrik settlement

Sample collection of modern vegetation aimed at covering all relevant geological units in the surroundings of Basel and was restricted to locations with the smallest possible anthropogenic overprint (forests). It therefore also included locations on unproductive soils and steep outcrops unlikely to have been used as arable land. Each sampling location therefore was evaluated for its suitability as crop or pastures land on the basis of topography, geology and soil fertility (Table 2). This revealed the $^{87}Sr/^{86}Sr$ isotope ratios of landforms and territories for which agriculture and pastoral activities are probable (Fig. 5). The higher the suitability of a specific landform for agriculture and pasture, the more likely it contributed to the strontium that entered the human and animal food chain. In contrast, the contribution of parts of the landscape with less favourable conditions to the human strontium budget was likely limited, even though the biologically available strontium at these locations needs to be recognized. Around Basel, such landscapes include Keuper and Buntsandstein sediments in the Black Forest, the Table and Hill Country, and the Vosges with radiogenic $^{87}Sr/^{86}Sr$ ratios above 0.711 as well as bare Jurassic limestone of the Table Jura and Folded Jura with $^{87}Sr/^{86}Sr$ ratios below about 0.708. Such values were not found among the investigated human and animal teeth. This underlines the limited importance of foodstuffs originating from these areas for the local population at Basel. Furthermore, the respective geological units prevail beyond a distance of 10 km from the site, and therefore probably beyond the area that the settlement community exploited directly.

Combining the observations regarding the biologically available strontium, the suitability of soils for agriculture, and the archaeological record from the southern Upper Rhine Graben (Blöck et al., 2014), animal husbandry seems possible in all major landscapes around the Basel-Gasfabrik site. According to the modern vegetation data at locations that are considered suitable or well suitable for pasture, regionally herded animals may have had highly diverse $^{87}Sr/^{86}Sr$ isotope values of between 0.70814 and 0.71794 (Table 2). Plant isotope ratios at locations that are more suitable as agricultural land are more restricted. They include the partly loess covered Lower Terrace of the Rhine River (0.70830–0.71002) and the loess soils of the nearby Sundgau (0.70842–0.70985). These formations are part of the landscape in the direct neighbourhood of Basel-Gasfabrik, but also extend beyond it. Moreover, potentially good arable soils also occur in some river valleys (0.70814 and 0.70851) and on high plateaus (0.70850–0.70942) of the Swiss Jura Mountains (Fig. 2). The overall patchy distribution of biologically available strontium with different isotope ratios and soil conditions with varying agricultural potential hinder the differentiation of human and animal individuals who originated directly from the Basel-Gasfabrik settlement from those coming from its hinterland in the southern Upper Rhine Graben and adjacent landscapes.

Conclusion

$^{87}Sr/^{86}Sr$ ratios of modern tree leaves, ground-covering vegetation and water samples from forested locations around Basel (chiefly within a 20-km-radius) as well as archaeological pig and dog teeth, human infant deciduous teeth and first permanent molars from the La Tène site of Basel-Gasfabrik document the complexity of characterizing strontium isotope baseline values in a geologically varied environment.

In general, most of the differences between the ground vegetation and tree leave $^{87}Sr/^{86}Sr$ isotope ratios from the same location were so small (< 0.0005) as not be considered meaningful for the interpretation regarding archaeological human mobility. The extent of the differences, and whether higher values occur in shallow or deep-rooting plants, depends on the specific character of the sampling spots including thickness of soil horizons and the type of sediments overlying bedrock. Taking multiple samples from each geological unit, sampling plants of different rooting depths and careful documentation of the geomorphological settings, soil types, and indication of possible anthropogenic alteration are highly advisable. Water samples average the labile strontium from the catchment of the water bodies and are a useful addition for the characterization of $^{87}Sr/^{86}Sr$ ratios of a region.

The $^{87}Sr/^{86}Sr$ isotope ratios of modern water and vegetation samples from the near environs of the Basel-Gasfabrik settlement (7 km radius) varied between 0.70847 and 0.71093 and reflect the small-scale geological variability of the area. The prevailing geological units of loess and Lower Terrace sediments of the Rhine River exhibited similar and widely varying $^{87}Sr/^{86}Sr$ isotope ratios. Strontium isotope ratios of between 0.70850 and 0.7100 were frequently found on floodplain sediments and Lower Terrace deposits of the Rhine River, loess deposits in the Sundgau, loam covered plateaus of the Swiss Jura Mountains, Triassic limestone (Muschelkalk) and some Keuper and Miocene units (gypsum, freshwater limestone) and extend beyond the immediate environs of the site. Lower $^{87}Sr/^{86}Sr$ isotope ratios of 0.7077 to 0.7085 only appeared on bare Jurassic limestones in the Swiss Jura Mountains and in the volcanic Kaiserstuhl region. Higher $^{87}Sr/^{86}Sr$ isotope values of above 0.7110 were found for Triassic sandstone (Buntsandstein), clayey Keuper deposits and for the crystalline bedrock of Vosges and Black Forest.

An evaluation of the sampling spots regarding their agricultural potential helped distinguishing strontium isotope ratios that likely entered the human food chain. Presumably arable landforms around Basel included loess soils in the Sundgau, Lower Terraces of the Upper Rhine Valley and loam covered plateaus of the Table Jura, which all revealed $^{87}Sr/^{86}Sr$ isotope ratios of between 0.70830 and 0.71000. Many of the sampling spots in the mountainous areas that yielded either comparatively high or comparatively low $^{87}Sr/^{86}Sr$ ratios were not well suited for farming and thus probably contributed little to the human dietary strontium.

Human infants' deciduous teeth and first permanent molars revealed a restricted $^{87}Sr/^{86}Sr$ isotope range while enamel samples of dogs and pigs varied more widely. Both kinds of archaeological samples agreed with the modern vegetation data in the near surroundings of the site. We use them to define two local isotope ranges (I and II) that form the basis for distinguishing local and non-local individuals among human remains in the Basel-Gasfabrik settlement itself and its two cemeteries (Knipper et al., 2018). The different isotope ranges of human infant (local isotope range I) and animal enamel (local isotope range II) suggest differentiated land-use for grow-

ing crops and animal husbandry. Moreover, the modern plant data indicate that the variable isotope ratios of the animal teeth in particular may also have resulted from contacts into the hinterlands including the exchange of animals or provision. Based on pedological criteria, the selection of plots for growing human staples went beyond agricultural potential, and was largely culturally determined and a matter of choice or possibly also restriction by use rights, trade relations, kinship or land ownership.

The combined evaluation of isotopic baseline values and factors such as soil fertility and geomorphology provides important impulses for further research. Both modern and archaeological data argue against a uniform exploitation of the catchment area of the proto-urban centre of Basel-Gasfabrik. Reconstruction of subsistence and (commercial) relationships therefore require going beyond purely utilitarian approaches, taking into account local preferences, customs and the social interrelations of the archaeological communities.

Acknowledgments

This work was financially supported by the Swiss National Foundation (grant number 133052), the Freiwillige Akademische Gesellschaft Basel and the Archäologische Bodenforschung Basel Stadt. The authors thank Sigrid Klaus and Bernd Höppner (Curt-Engelhorn Center of Archaeometry, Mannheim) for preparing the water samples for strontium isotope analysis and for mass spectrometry, Sophia Joray for assistance during the sample collection, and Nicola Silber for technical help with ashing of vegetation samples for Sr isotope analysis.

References (chapter 2)

Alt, K.W., Türp, J.C., 1998. Roll call: thirty-two white horses on a red field: the advantages of the FDI two-digit system of designating teeth. In: Alt, K.W., Rösing, F.W., Teschler-Nicola, M. (Eds.), Dental Anthropology. Fundamentals, Limits, and Prospects. Springer, Wien, New York.

Alt, K.W., Knipper, C., Held, P., Nicklisch, N., Fecher, M., Roth, C., Enzmann, F., Tuckermann, J., Seitz, H., Polzin, C., Klopsch, V., Brauns, M., Pike, A.W.G., 2013. Königin Editha – ein Indizienbeweis zur Identifikation einer historischen Persönlichkeit aus dem Magdeburger Dom. Archäologie in Sachsen-Anhalt 2012. Sonderband 17, 9–60.

Bélanger, N., Holmden, C., Courchesne, F., Côté, B., Hendershot, W.H., 2012. Constraining soil mineral weathering $^{87}Sr/^{86}Sr$ for calcium apportionment studies of a deciduous forest growing on soils developed from granitoid igneous rocks. Geoderma 185–186, 84–96.

Bentley, A.R., 2006. Strontium isotopes from the earth to the archaeological skeleton: a review. J. Archaeol. Method Theory 13 (3), 135–187.

Bentley, A.R., Knipper, C., 2005. Geographical patterns in biologically available strontium, carbon and oxygen isotope signatures in prehistoric SW Germany. Archaeometry 47 (3), 629–644.

Bentley, A.R., Price, T.D., Stephan, E., 2004. Determining the "local" $^{87}Sr/^{86}Sr$ range for archaeological skeletons: a case study from Neolithic Europe. J. Archaeol. Sci. 31 (4), 365–375.

Bitterli-Brunner, P., 1987. Geologischer Führer der Region Basel. Mit 24 Exkursionen. 19 Veröffentlichungen aus dem Naturhistorischen Museum Basel Birkhäuser, Basel, Boston.

Blöck, L., Bräuning, A., Deschler-Erb, E., Fischer, A., Hecht, Y., Knipper, C., Marti, R., Nick, M., Rissanen, H., Spichtig, N., Roth-Zehner, M., 2014. Interdisciplinary and trinational research into the Late La Tène settlement landscape uf the Upper Rhine. In: Fernández-Götz, M., Wendling, H., Winger, K. (Eds.), Paths to Complexity. Centralisation and urbanisation in Iron Age Europe. Oxbow Books, Oxford, pp. 179–190.

Brandt, G., Knipper, C., Roth, C., Siebert, A., Alt, K.W., 2010. Beprobungsstrategien für aDNA und Isotopenanalysen an historischem und prähistorischem Skelettmaterial, in: Anthropologie, Isotopie und DNA. 2. Mitteldeutscher Archäologentag vom 8. bis 10. Oktober 2009 in Halle. 2. Mitteldeutscher Archäologentag vom 8. bis 10. Oktober 2009 in Halle, Halle. 8.-10.10.2009. Landesamt für Denkmalpflege und Archäologie Sachsen-Anhalt. Landesmuseum für Vorgeschichte, Halle (Saale), pp. 17–32.

Budd, P., Montgomery, J., Barreiro, B., Thomas, R.G., 2000. Differential diagenesis of strontium in archaeological human dental tissues. Appl. Geochem. 15, 687–694.

Buhl, D., Neuser, R.D., Richter, D.K., Riedel, D., Roberts, B., Strauss, H., Veizer, J., 1991. Nature and nurture: environmental isotope story of the River Rhine. Naturwissenschaften 78, 337–346.

Bullen, T.D., Bailey, S.W., 2005. Identifying calcium sources at an

acid deposition-impacted spruce forest: a strontium isotope, alkaline earth element multi-tracer approach. Biogeochemistry 74 (1), 63–99.

Burton, J.H., Hahn, R., 2016. Assessing the "local" $^{87}Sr/^{86}Sr$ ratio for humans. In: Isotopic Landscapes in Bioarchaeology. Proceedings of the International Workshop "a Critical Look at the Concept of Isotopic Landscapes and its Application in Future Bioarchaeological Research", Munich, October 13–15, 2014. A Critical Look at the Concept of Isotopic, München. 13.–15. Oktober. vol. 2014. Springer, Berlin, pp. 113–121.

Chenery, C., Müldner, G., Evans, J., Eckardt, H., Lewis, M., 2010. Strontium and stable isotope evidence for diet and mobility in Roman Gloucester, UK. J. Archaeol. Sci. 37 (1), 150–163.

Dambrine, E., Loubet, M., Vega, J.A., Lissarague, A., 1997. Localisation of mineral uptake by roots using Sr isotopes. Plant Soil 192 (1), 129–132.

Drouet, T., Herbauts, J., Demaiffe, D., 2005a. Long-term records of strontium isotopic composition in tree rings suggest changes in forest calcium sources in the early 20th century. Glob. Chang. Biol. 11, 1926–1940.

Drouet, T., Herbauts, J., Gruber, W., Demaiffe, D., 2005b. Strontium isotope composition as a tracer of calcium sources in two forest ecosystems in Belgium. Geoderma 126, 203–223.

Drouet, T., Herbauts, J., Gruber, W., Demaiffe, D., 2007. Natural strontium isotope composition as a tracer of weathering patterns and of exchangeable calcium sources in acid leached soils developed on loess of central Belgium. Eur. J. Soil Sci. 58 (1), 302–319.

Eikenberg, J., Tricca, A., Vezzu, G., Stille, P., Bajo, S., Ruethi, M., 2001. 228Ra/226Ra/224Ra and $^{87}Sr/^{86}Sr$ isotope relationships for determining interactions between ground and river water in the upper Rhine valley. J. Environ. Radioact. 54 (1), 133–162.

Evans, J.A., Montgomery, J., Wildman, G., Boulton, N., 2010. Spatial variations in biosphere $^{87}Sr/^{86}Sr$ in Britain. J. Geol. Soc. 167 (1), 1–4.

Fischer, H., 1969. Geologischer Überblick über den südlichen Oberrheingraben und seine weitere Umgebung. Regio Basiliensis 10 (1), 57–84.

Fischer, H., Hauber, L., Wittmann, O., 1971. Geologischer Atlas der Schweiz 1:25'000: Blatt 1047 Basel. In: Erläuterungen Atlasblatt 59. Wabern, Bundesamt für Landestopografie swisstopo.

Fischer, E., Rösch, M., Sillmann, M., Ehrmann, O., Liese-Kleiber, H., Vogt, R., Stobbe, A., Stephan, E., Schatz, K., Posluschny, A.G., 2010. Landnutzung im Umkreis der Zentralorte Hohenasperg, Heuneburg und Ipf: Archäobotanische und archäozoologische Untersuchungen und Modellberechnungen zum Ertragspotential von Ackerbau und Viehhaltung. In: Krausse, D. (Ed.), "Fürstensitze" und Zentralorte der frühen Kelten. Abschlusskolloquium des DFG-Schwerpunktprogramms 1171 in Stuttgart, 12.–15. Oktober 2009. Forschungen und Berichte zur Vor- und Frühgeschichte in Baden-Württemberg. vol. 120. Thesis, Stuttgart, pp. 195–266.

Frei, K.M., Frei, R., 2011. The geographic distribution of strontium isotopes in Danish surface waters — a base for provenance studies in archaeology, hydrology and agriculture. Appl. Geochem. 26 (3), 326–340.

Geyer, O.F., Gwinner, M.P., 2011. Geologie von Baden-Württemberg. In: 5. völlig neu bearbeitete Auflage von Matthias Geyer, Edgar Nitsch, Theo Simon ed. Schweizerbart, Stuttgart, (627 pp).

Hauber, L., 1978. Wenn Steine reden: Geologie von Basel und Umgebung. Buchverlag Basler Zeitung, Basel (66 pp).

Hauber, L., 1993. Der südliche Rheingraben und seine geothermische Situation. Bulletin der Vereinigung Schweizerischer Petroleum-Geologen und -Ingenieure 137, 53–69.

Hecht, Y., Niederhäuser, A., 2011. The everyday culture and funerary rituals of the Celts. In: A Central Settlement on the Upper Rhine around 100 BCE. Merian, Basel (113 pp).

Hodell, D.A., Quinn, R.L., Brenner, M., Kamenov, G., 2004. Spatial variation of strontium isotopes ($^{87}Sr/^{86}Sr$) in the Maya region: a tool for tracking ancient human migration. J. Archaeol. Sci. 31 (5), 585–601.

Van der Jagt, I., Kootker, L.M., van Kolfschoten, T., Kars, H., Davies, G.R., 2012. An insight into animal exchange in Early Medieval Oegstgeest: a combined archaeozoological and isotopic approach. In: Raemaekers, Daan, C.M., Esser, E., Lauwerier, Roel, C.G.M., Zeiler, J.T. (Eds.), A Bouquet of Archaeozoological Studies. Essays in Honour of Wietske Prummel. Groningen archaeological studies 21. Barkhuis, Eelde, pp. 132–149.

Kloppmann, W., 2003. Etude isotopique de la pollution azotée de la nappe d'Alsace entre Sierentz et Ottmarsheim: Kelten am Rhein. (Kelten am Rhein. BRGM – Géosciences pour une terre durable).

Kloppmann, W., Urban, S., Gourcy, L., 2013. Etude isotopique de la pollution azotée des captages Kabis et St. Louis, Haut-Rhin: Rapport final BRGM/RP-62777-FR. BRGM - Géosciences pour une terre durable. 62 pp. (Accessed 29 January 2016).

Knipper, C., 2011. Die räumliche Organisation der linearbandkeramischen Rinderhaltung: Naturwissenschaftliche und archäologische Untersuchungen. In: BAR International Series 2305. Archaeopress, Oxford (485 pp).

Knipper, C., Mauer, A.-F., Peters, D., Meyer, C., Brauns, M., Galer, S.J.G., Freeden, U., von Schöne, B., Meller, H., Alt, K.W., 2012. Mobility in Thuringia or mobile Thuringians: a strontium isotope study from early medieval Central Germany. In: Kaiser, E., Burger, J., Schier, W. (Eds.), Population Dynamics in pre- and Early History. New

Approaches by Using Stable Isotopes and Genetics. Topoi. Berlin Studies of the Ancient World. De Gruyter, Boston, pp. 287–310.

Knipper, C., Pichler, S.L., Rissanen, H., Stopp, B., Kühn, M., Spichtig, N., Röder, B., Schibler, J., Lassau, G., Alt, K.W., 2017. What is on the menu in a Celtic town? Iron Age diet reconstructed at Basel-Gasfabrik, Switzerland. Archaeol. Anthropol. Sci. 9, 1307–1326.

Knipper, C., Pichler, S.L., Brönnimann, D., Rissanen, H., Rosner, M., Spichtig, N., Stopp, B., Rentzel, P., Röder, B., Schibler, J., Lassau, G., Alt, K.W., 2018. A knot in a network: Residential

mobility at the Late Iron Age proto-urban centre of Basel-Gasfabrik (Switzerland) revealed by isotope analyses. Journal of Archaeological Science: Reports 17, 735–753.

Kock, S., Huggenberger, P., Preusser, F., Rentzel, P., Wetzel, A., 2009. Formation and evolution of the Lower Terrace of the Rhine River in the area of Basel. Swiss J. Geosci. 102 (2), 307–321.

Kootker, L.M., van Lanen, R.J., Kars, H., Davies, G.R., 2016. Strontium isoscapes in The Netherlands. Spatial variations in $^{87}Sr/^{86}Sr$ as a proxy for palaeomobility. J. Archaeol. Sci. Rep. 6, 1–13.

Kühn, M., Iseli, M., 2008. Botanische Makroreste aus der spätlatènezeitlichen Siedlung Basel-Gasfasbrik, Grabung 1989/5. In: Jud, P. (Ed.), Die Töpferin und der Schmied. Basel-Gasfabrik, Grabung 1989/5. Dissertation 2004, Teil I: Text. Materialhefte zur Archäologie in Basel 20:1. Archäologische Bodenforschung des Kantons Basel-Stadt, Basel, pp. 293–324.

Lamb, A.L., Evans, J.E., Buckley, R., Appleby, J., 2014. Multi-isotope analysis demonstrates significant lifestyle changes in King Richard III. J. Archaeol. Sci. 50, 559–565.

Leser, H., 1982. Die Landschaft der Basler Region und ihre naturräumliche Gliederungsprobleme. Regio Basiliensis 23 (1–2), 2–23.

Leser, H., 1986. Die GMK 100 Blatt Freiburg-Süd — Bemerkungen zur Kartenbeilage. Regio Basiliensis 27 (3), 221–231.

Mäckel, R., Seidel, J., 2003. Der Kaiserstuhl – ein Vulkan im Oberrheingraben. In: Liedtke, H., Mäusbacher, R., Schmidt, K.-H. (Eds.), Relief, Boden und Wasser. Nationalatlas Bundesrepublik Deutschland 2. Spektrum, Heidelberg, pp. 64–65.

Maurer, A.-F., Galer, S.J.G., Knipper, C., Beierlein, L., Nunn, E.V., Peters, D., Tütken, T., Alt, K.W., Schöne, B.R., 2012. Bioavailable $^{87}Sr/^{86}Sr$ in different environmental samples—effects of anthropogenic contamination and implications for isoscapes in past migration studies. Sci. Total Environ. 433, 216–229.

Mosimann, T., 2015. Erd-reich: Eine Reise durch die Böden des Kantons Basel-Landschaft und seiner Nachbargebiete. In: Quellen und Forschungen zur Geschichte und Landeskunde des Kantons Basel-Landschaft 95. Verlag des Kantons Basel-Landschaft, Liestal (415 pp).

Müller, W., Fricke, H., Halliday, A.N., McCulloch, Malcolm T., Wartho, J.-A., 2003. Origin and migration of the Alpine Iceman. Science 302 (5646), 862–866.

Nehlich, O., Montgomery, J., Evans, J., Schade-Lindig, S., Pichler, S.L., Richards, M.P., Alt, K.W., 2009. Mobility or migration: a case study from the Neolithic settlement of Nieder-Mörlen (Hessen, Germany). J. Archaeol. Sci. 36 (8), 1791–1799.

Neil, S., Evans, J., Montgomery, J., Scarre, C., 2016. Isotopic evidence for residential mobility of farming communities during the transition to agriculture in Britain. Royal Society Open Science 3 (1), 150522.

Oelze, V.M., Nehlich, O., Richards, M.P., 2012. "There's no place like home" — no isotopic evidence for mobility at the Early Bronze Age cemetery of Singen, Germany. Archaeometry 54 (4), 752–778.

Pett-Ridge, J.C., Derry, L.A., Barrows, J.K., 2009. Ca/Sr and $^{87}Sr/^{86}Sr$ ratios as tracers of Ca and Sr cycling in the Rio Icacos watershed, Luquillo Mountains, Puerto Rico. Chem. Geol. 267 (1–2), 32–45.

Pichler, S.L., Rissanen, H., Spichtig, N., Alt, K.W., Röder, B., Schibler, J., Lassau, G., 2013. Die Regelmäßigkeit des Irregulären: Menschliche Skelettreste vom spätlatènezeitlichen Fundplatz Basel-Gasfabrik. In: Irreguläre' Bestattungen in der Urgeschichte: Norm, Ritual, Strafe …? Akten der Internationalen Tagung in Frankfurt a. M. vom 3. bis 5. Februar 2012, Frankfurt. 3.-5.2.2012. Dr. Rudolf Habelt GmbH, Bonn, pp. 471–484.

Pichler, S.L., Rissanen, H., Spichtig, N., 2015. Ein Platz unter den Lebenden, ein Platz unter den Toten – Kinderbestattungen des latènezeitlichen Fundplatzes Basel-Gasfabrik. In: Kory, R.W. (Ed.), Lebenswelten von Kindern und Frauen in der Vormoderne. Archäologische und anthropologische Forschungen in memoriam Brigitte Lohrke. Paläowissenschaftliche Studien 4. curach bhán publications, Berlin, pp. 257–273.

Poszwa, A., Ferry, B., Dambrine, E., Pollier, B., Wickman, T., Loubet, M., Bishop, K., 2004. Variations of bioavailable Sr concentration and $^{87}Sr/^{86}Sr$ ratio in boreal forest ecosystems: role of biocycling, mineral weathering and depth of root uptake. Biogeochemistry 67, 1–20.

Price, T.D., Bentley, A.R., 2005. Human mobility in the Linearbandkeramik: an archaeometric approach. In: Die Bandkeramik im 21. Jahrhundert. Symposium in der Abtei Brauweiler bei Köln vom 16.9.-19.9.2002. Verlag Marie Leidorf, Rahden Westfahlen, pp. 203–215.

Price, T.D., Burton, J.H., Bentley, A.R., 2002. The characterization of biologically available strontium isotope ratios for the study of prehistoric migration. Archaeometry 44 (1), 117–135.

Price, T.D., Knipper, C., Grupe, G., Smrcka, V., 2004. Strontium isotopes and prehistoric human migration: the bell beaker period in Central Europe. Eur. J. Archaeol. 7 (1), 9–40.

Probst, A., El Gh'mari, A., Aubert, D., Fritz, B., McNutt, R., 2000. Strontium as a tracer of weathering processes in a silicate catchment polluted by acid atmospheric inputs, Strengbach, France. Chem. Geol. 170, 203–219.

Rentzel, P., 1997. Geologisch-bodenkundliche Untersuchungen an den Niederterrassenfeldern bei Basel unter besonderer Berücksichtigung der spätlatènezeitlichen Fundstelle Basel-Gasfabrik. Jahresbericht der Archäologischen Bodenforschung des Kantons Basel-Stadt 1994, 31–52.

Rentzel, P., 1998. Ausgewählte Grubenstrukturen aus der spätlatènezeitlichen Fundstelle Basel-Gasfabrik. Jahresbericht der Archäologischen Bodenforschung des Kantons Basel-Stadt 1995, 35–79.

Rentzel, P., Preusser, F., Pümpin, C., Wolf, J.-J., 2009. Loess and palaeosols on the High Terrace at Sierentz (France), and implications for the chronology of terrace formation in the Upper Rhine Graben. Swiss J. Geosci. 102 (3), 387–401.

Rissanen, H., Pichler, S.L., Spichtig, N., Alt, K.W., Brönnimann, D., Knipper, C., Kühn, M., Rentzel, P., Röder, B., Schibler, J., Stopp, B., Vach, W., Warnberg, O., Lassau, G., 2013. "Wenn

Kinder sterben…" – Säuglinge und Kleinkinder vom latènezeitlichen Fundplatz Basel-Gasfabrik (Kanton Basel-Stadt, Schweiz). In: Wefers, S., Fries, J.E., Fries-Knoblach, J., Later, C., Rambuscheck, U., Trebsche, P., Wiethold, J. (Eds.), Bilder - Räume - Rollen. Beiträge zur gemeinsamen Sitzung der AG Eisenzeit und der AG Geschlechterforschung während des 7. Deutschen Archäologenkongresses in Bremen 2011. Beiträge zur Ur- und Frühgeschichte Mitteleuropas 72. Beier & Beran, Langenweißbach, pp. 127–142.

Röhr, C., 2006. Geologische Karte des Oberrheingrabens. Schweissing, M.M., Grupe, G., 2003. Stable strontium isotopes in human teeth and bone: a key to migration events of the late Roman period in Bavaria. J. Archaeol. Sci. 30, 1373–1383.

Sissingh, W., 1998. Comparative Tertiary stratigraphy of the Rhine Graben, Bresse Graben and Molasse Basin: correlation of Alpine foreland events. Tectonophysics 300 (1–4), 249–284.

Stephan, E., Knipper, C., Schatz, K., Price, T.D., Hegner, E., 2012. Strontium isotopes in faunal remains: evidence of the strategies for land use at the Iron Age site Eberdingen-Hochdorf (Baden-Württemberg, Germany). In: Kaiser, E., Burger, J., Schier, W. (Eds.), Population Dynamics in pre- and Early History. New approaches by Using Stable Isotopes and Genetics. Topoi. Berlin Studies of the Ancient World. De Gruyter, Boston, pp. 265–286.

Stopp, B., 2008. Archäozoologische Untersuchung der Tierknochen aus Gruben der spätlatènezeitlichen Siedlung Basel-Gasfabrik, Grabung 1989/5. In: Jud, P. (Ed.), Die Töpferin und der Schmied. Basel-Gasfabrik, Grabung 1989/5. Dissertation 2004, Teil I: Text. Materialhefte zur Archäologie in Basel 20:1. Archäologische Bodenforschung des Kantons Basel-Stadt, Basel, pp. 249–292.

Toncala, A., Söllner, F., Mayr, C., Hölzl, S., Heck, K., Wycisk, D., Grupe, G., 2017. Isotopic map of the Inn-Eisack-Adige-Brenner passage and its application to prehistoric human cremations. In: Grupe, G., Grigat, A., McGlynn, G.C. (Eds.), Across the Alps in Prehistory. Isotopic Mapping of the Brenner Passage by Bioarchaeology. Springer International Publishing, Heidelberg, pp. 127–227.

Trickett, M.A., Budd, P., Montgomery, J., Evans, J., 2003. An assessment of solubility profiling as a decontamination procedure for the $^{87}Sr/^{86}Sr$ analysis of archaeological human skeletal tissue. Appl. Geochem. 18 (5), 653–658.

Turck, R., Kober, B., Kontny, J., Haack, F., Zeeb-Lanz, A., 2012. "Widely travelled people" at Herxheim: Sr isotopes as indicators of mobility. In: Kaiser, E., Burger, J., Schier, W. (Eds.), Population Dynamics in pre- and Early History. New Approaches by Using Stable Isotopes and Genetics. Topoi. Berlin Studies of the Ancient World. De Gruyter, Boston, pp. 149–163.

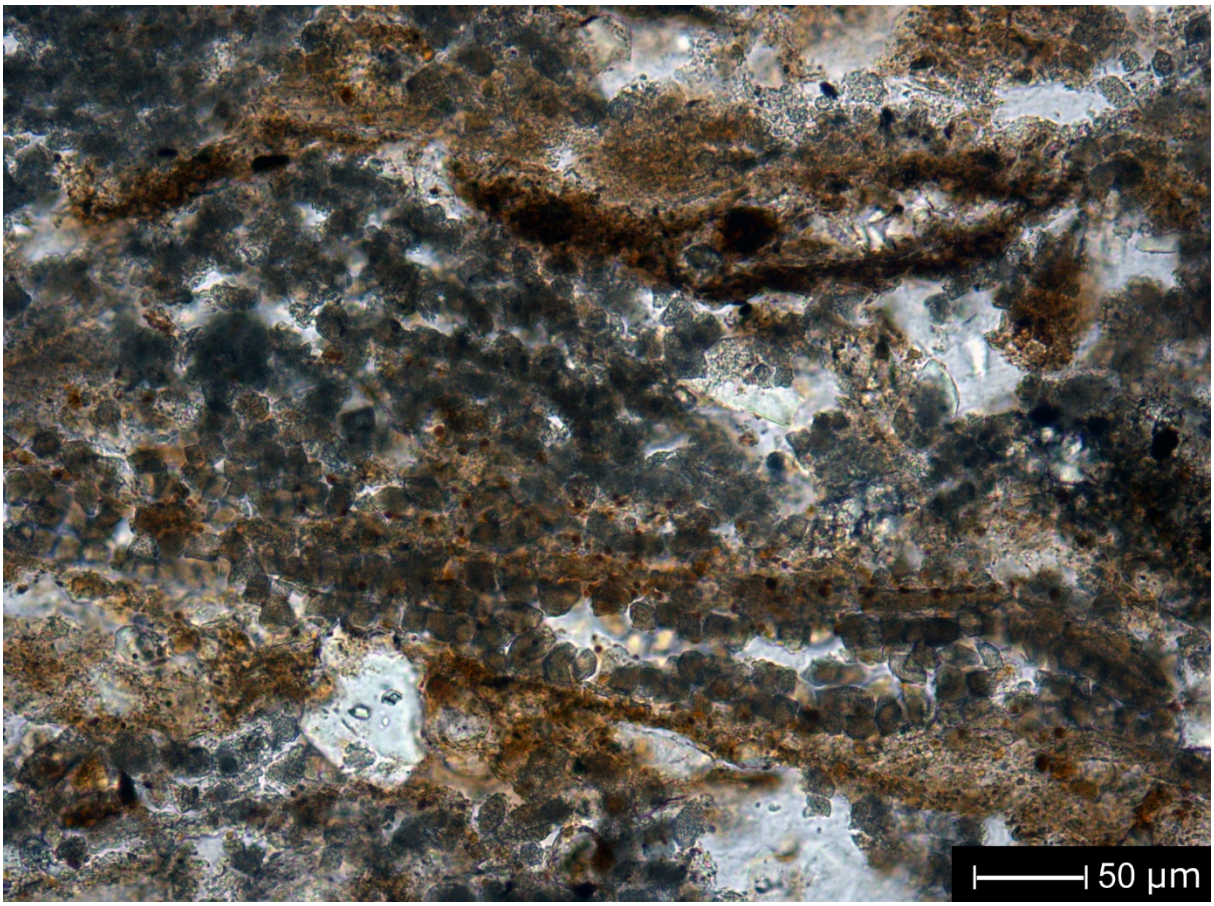
Tütken, T., Vennemann, T.W., Pfretzschner, H.-U., 2004. Analyse stabiler und radiogener Isotope in archäologischem Skelettmaterial: Herkunftsbestimmung des karolingischen Maultiers von Frankenthal und Vergleich mit spätpleistozänen Großsäugerknochen aus den Rheinablagerungen. Prähistorische Zeitschrift 79, 89–110.

Vitòria, L., Otero, N., Soler, A., Canals, À., 2004. Fertilizer characterization: isotopic data (N, S, O, C, and Sr). Environ. Sci. Technol. 38 (12), 3254–3262.

Warham, J.O., 2011. Mapping Biosphere Strontium Isotope Ratios across Major Lithological Boundaries: A Systematic Investigation of the Major Influences on Geographic Variation in the $^{87}Sr/^{86}Sr$ Composition of Bioavailable Strontium above the Cretaceous and Jurassic Rocks of England. Submitted for the degree of Doctor of Philosophy, Bradford.

Willmes, M., McMorrow, L., Kinsley, L., Armstrong, R., Aubert, M., Eggins, S., Falguères, C., Maureille, B., Moffat, I., Grün, R., 2014. The IRHUM (isotopic reconstruction of human migration) database — bioavailable strontium isotope ratios for geochemical fingerprinting in France. Earth System Science Data 6 (1), 117–122.

Wittmann, O., 1961. Die Niederterrassenfelder im Umkreis von Basel und ihre kartographische Darstellung. Regio Basiliensis 3, 7–46.



Mikroskop-Foto (parallele Polarisatoren) einer feingeschichteten, in situ ausgebildeten Grubenverfüllung. Es handelt sich um feingeschichtete pflanzliche Asche mit sehr gut erhaltenen, grauen Asche-Rhomboedern, die die einstige Zellstruktur der Pflanze noch erahnen lassen.

Kapitel 3

The hidden midden – Geoarchaeological investigation of sedimentation processes, waste disposal practices and resource management at the La Tène settlement Basel-Gasfabrik (Switzerland)

David Brönnimann, Brigitte Röder, Norbert Spichtig, Hannele Rissanen, Guido Lassau, Philippe Rentzel

Geoarchaeology: An International Journal 35 (2020) 522-544.
DOI: 10.1002/gea.21787

Keywords: Geoarchaeology, Iron Age, Micromorphology, Prehistoric settlement, Resource management, Site formation processes, Taphonomy, Waste management

Abstract

In order to interpret artefact assemblages it is necessary to understand the processes that have formed and influenced them: layer formation processes, cultural practices and the way resources were used. In this study, we present our results of micromorphologically analysed pits, ditches, house floors and occupation layers found within the younger Iron Age settlement of Basel-Gasfabrik. We defined eleven microfacies types and put them into a spatial and stratigraphic context. In addition, we quantify waste categories according to the archaeological features and microfacies types.

Our results suggest that some ditches played a role in the spatial organisation of the settlement, others were used as water canals. Several pits show a secondary use as roofed construction in the context of handicrafts. Additionally, mapping the microfacies types reveals a differentiated use of space. Finally, differences between waste categories are visible. Dung was used as fuel and probably as fertiliser, whereas animal bone fragments and ceramic sherds have been stored on rubbish dumps, where they were available as raw material.

These new insights into the use of pits, ditches and settlement areas as well as the handling of resources provide an important basis for understanding everyday life in the settlement of Basel-Gasfabrik.

Introduction

As argued by Michael Schiffer over 40 years ago, objects (and sediments) are subject to various “natural” and "cultural" transformation processes (Schiffer, 1972). The latter is termed “anthropogenic formation processes” in this paper. Within dense settlements such as the Basel-Gasfabrik, these transformation processes are mainly characterized by everyday activities. The formation of archaeological features is thus determined by the behaviour of a group (Schiffer, 1972, 1983, 1987; Binford, 1981) and is therefore the consequence of overall organisational principles. These include waste disposal practices and resource management, both of which involve the handling of objects and materials and have a significant influence on the distribution of finds within a settlement

(Wolfram, 2003; Schmidt, 2005; Müller-Scheessel et al., 2010; Shillito et al., 2011; Shillito and Matthews, 2013; Jones, 2015; Karkanas et al., 2015).

Waste is defined as objects or materials that are actively or passively removed temporarily or irretrievably from the activities of everyday life. In most cases these objects are worthless, no longer usable, forgotten or tabooed. The objects or materials can be deposited or dropped (unnoticed) on site (defacto refuse), collected and disposed of (primary refuse) and relocated several times (secondary refuse) (Schiffer 1972).

However, it is known from various ethnological studies that waste is not necessarily a quantity that is clearly defined by social rules and that it is often viewed as a raw material (Beck et al., 2004; Gifford-Gonzalez, 2014; Friesem, 2016). Consequently, "waste" and "resource" are often closely related, with one sometimes be a temporary state of the other. It is therefore not always possible to clearly label a specific group of objects or materials as "waste" or "resource". For this reason, different categories of waste have been defined for the present work:

- Animal bone and pottery fragments
- Combustion residues (charcoal fragments, ash, burned loam)
- Faeces (omnivore and/or carnivore), guano and herbivore dung
- Excavation material resulting from the digging of the numerous pits and trenches, consisting of sandy gravel and calcareous or decalcified and clayey loam

Geoarchaeology and especially micromorphology can make a substantial contribution to the reconstruction, quantification, and evaluation of layer formation processes (Goldberg, 1980; Bullock et al., 1985; Shahack-Gross, 2017). Accordingly, such analyses form the core of this study. By means of micrormophology layer formation processes were reconstructed and the above-mentioned waste categories were identified and quantified within various features (pits, ditches, house floors, occupation surfaces, post holes; table 3). On the basis of this information, eleven microfacies types were defined (MFT I–XI) and were put in a spatial and stratigraphic (relative-chronological) context.

For this study, a well-preserved area of the site Basel-Gasfabrik (figure 1), an extensively studied settlement from the younger La Tène period (chiefly 200/150-80 BC) with hundreds of geoarchaeological samples, was selected.

The site Basel-Gasfabrik

Basel-Gasfabrik is a site from the younger La Tène period in the North-West of Switzerland in today's city of Basel (Hecht and Niederhäuser, 2011). The unfortified central site is situated directly beside the Rhine and encompasses an area of roughly 150,000 square metres (figure 1).

The average annual precipitation in Basel is 842 mm; the average temperature is around 11.5°C (data 1981–2010; www.meteoschweiz.admin.ch). The settlement of Basel-Gasfabrik is located on the lower terrace, which is composed of calcareous sandy gravel deposited by the Rhine during the last glaciation (Kock et al., 2009; Rentzel et al., 2015). The Rhine gravel is covered by a silty-sandy overbank deposit that accumulated during the Atlantic period (Rentzel, 1997). This overbank deposit reaches a thickness of up to 2 metres and is mainly found in topographic depressions (Rentzel, 1994, 1997). A luvisol (IUSS Working Group WRB, 2006) developed during the

middle and late Holocene forms the substrate of the Iron Age settlement (Rentzel, 1997). The settlement area investigated in this study is situated in a topographic depression, where the stratigraphy is well preserved and allows a differentiation of at least three settlement phases.

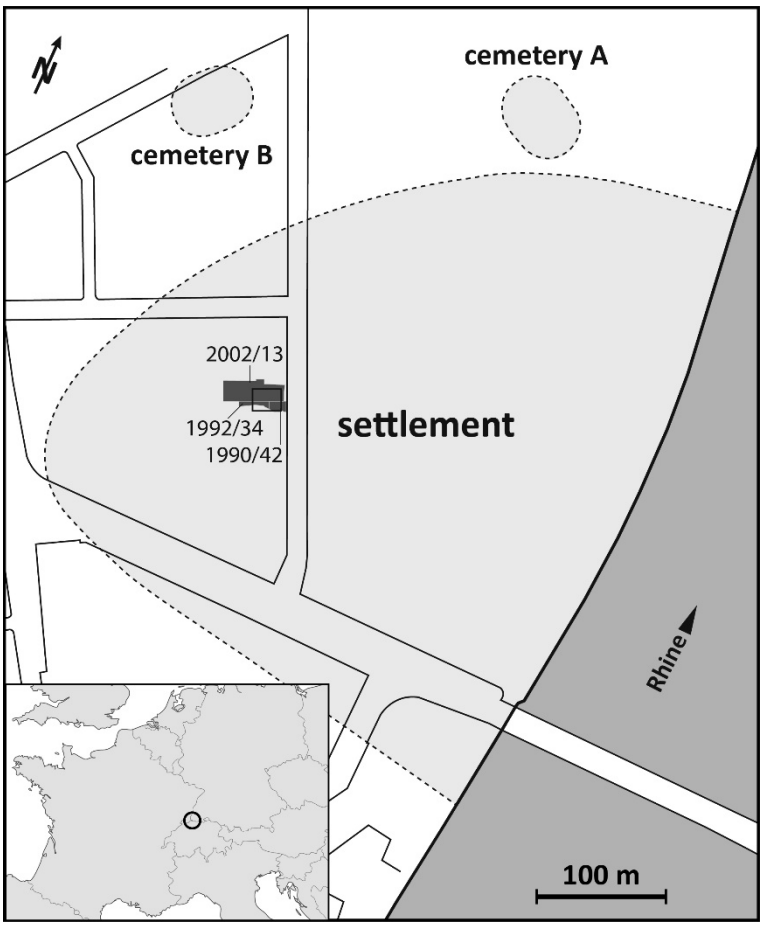


Fig. 1: *Location of the site Basel-Gasfabrik in the north-west of Switzerland (inset). Expansion of the settlement (grey area) with the three excavation areas (dark grey) in which the investigated settlement zone lies (square).*

Current state of research and objectives

The modern interdisciplinary study of the site has been ongoing for more than 40 years while excavations began as early as 1911. Thus far the excavations have revealed more than 500 settlement pits (usually preserved 2–3 m in diameter and 1–3 m in depth, most of them interpreted as cellar pits), hundreds of post holes and large numbers of ditches (0.5-2 wide, up to 0.8 deep and several dozen meters long). The site also includes two burial sites with 193 inhumation burials and two cremation burials (Pichler et al., 2013; Pichler et al., 2015).

The geoarchaeological investigations in the 1990s were mainly concerned with pedological questions, the investigation of pits, and assessing formation processes (Rentzel, 1997, 1998; Rentzel et al., 2017). Between 2011 and 2015, within the framework of an interdisciplinary research project, the focus was on how the dead at Basel-Gasfabrik were treated and on how these treatments differed from one another (Pichler et al., 2015; Pichler et al., 2017). During the same project two settlement pits were analysed micromorphologically (Pichler et al., 2014; Brönnimann and Rissanen, 2018). It was noted that (bio-) archaeological finds from pits often co-occur with a dark sediment rich in charcoal fragments and that the pits were filled in within a short time (Brönnimann and

Rissanen, 2018). Thus, the question arose as to where and how these charcoal-rich sediments were formed before they found their way into the pits. This question has been addressed micromorphologically within the scope of a PhD thesis (Brönnimann, 2019), which analysed different feature types (pits, house floors, trampled surfaces, occupation layers, ditches) within a well-preserved settlement area. An important aspect was to include supposedly "unspectacular" and – at least for this site – neglected archaeological features such as ditches. Our specific research questions were as follows:

1. Layer formation processes within all feature types:
    - Can anthropogenic, natural and postdepositional processes be identified?
    - Are there sediment types that are characteristic for certain archaeological features?
2. Interpretation of archaeological features and spatial organisation:
    - What activities, functions and changes can be identified in the different feature types?
    - Is there a spatial and/or stratigraphic connection between different sediment types (activity zones, spatial organisation)?
3. Reconstructing waste disposal practices and resource management:
    - Are some of the waste categories (see above) characteristic for certain types of archaeological features?
    - Are there any patterns in regards to how those waste categories are distributed?

Material and methodology

Material

For this geoarchaeological investigation a zone with an area of 17 x 26 m within the settlement of Basel-Gasfabrik was chosen (figure 1 and 2). The archaeological features and stratigraphy within this zone are well-preserved as it is located in a depression. It is part of a well-researched area excavated during three excavation campaigns between 1990 and 2002 (excavation area 1990/42, 1992/34 and 2002/13). The micromorphological analysis is based on 89 thin sections from 50 block samples taken from 25 profiles. The investigation included in total 124 stratigraphic units from three settlement pits (pit 287, 302 and 400), four ditches (ditch 4, 7, 9 and one ditch from another settlement area), three house floors and one posthole as well as 16 profiles with archaeological layers (and with the natural soil horizons in some parts) (figure 2).

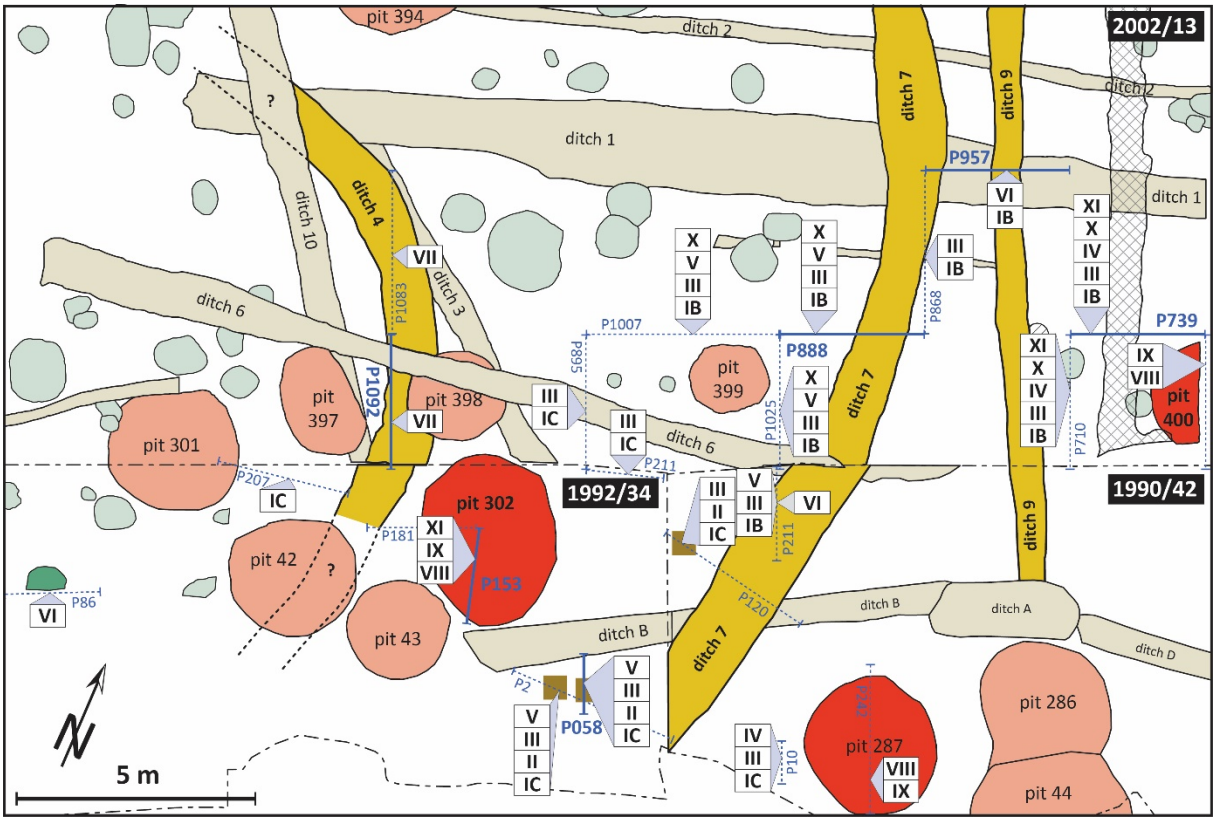


Fig. 2: Map of the investigated settlement zone. The dark red (pits), dark yellow (ditches) and dark green (post hole) structures were analysed micromorphologically. The blue lines indicate geoarchaeologically examined profiles. The lines for profiles that are discussed in the text are shown in bold. The microfacies types (MFT) are given next to every profile as roman numeral. Their order corresponds to their stratigraphic position. The brown squares give the locations of the rammed earth floors.

Methodology

The block samples were taken from the profiles using plaster bandages, dried, solidified using epoxy resin (Laromin C260, Araldite DY 026 SP, Aceton), and cut into polished sections using a diamond saw. The covered thin sections (4.5 x 4.5 cm) of 30 µm thickness were made in Braunschweig (Germany), Caen (France) and Basel (Switzerland). For the analysis, we used an optical microscope (Leica DM-RXP) with a polarisation filter of 16-630x magnification. The 124 stratigraphic units (SU) were analysed regarding their texture, fabric and their composition in accordance with the guidelines for micromorphological examination of archaeological sediments (Bullock et al., 1985; Stoops, 2003). The natural (e.g. terrestrial gastropod shells) and anthropogenic (micro-) components (e.g. bone chips, ashes) were recorded in a semiquantitative (absent [0%] – single [<2%] – few [2–10%] – frequent [10–25%] – numerous [25-50%] – dominant [>50%]) and in a qualitative fashion. Structural phenomena (e.g. compaction, horizontal orientation), indicators of bioturbation (e.g. earthworm granules) and postdepositional processes (e.g. dusty clay coatings, phosphate precipitations) were treated in the same way (see supplementary information).

Close attention was paid to taphonomic alterations in bone fragments embedded in soil samples and visible in thin sections, since the extent of bioerosion and the collagen preservation may be indicators of surface exposure of a bone (and of the corresponding stratigraphic unit) (Brönnimann et al., 2018). Fire impact on bones on the other hand could be due to the use of bones as fuel. Every fragment (> 2 mm) was analysed regarding bioerosion

(fungal and bacterial attack), collagen content and fire impact. For this, a semiquantitative approach was applied using the Wedl-Tunnel-Index (WTI) for fungal attack, the Bacterial-Attack-Index (BAI) for bacterial attack and the Collagen-Index (COI) according to Brönnimann et al., 2018. WTI and BAI describe the destruction of the bone microstructure by fungi and bacteria respectively on a scale of 0 to 5 based on the Oxford Histological Index (OHI, after Hollund et al., 2012). The collagen preservation was likewise graded on a scale of 1 to 5, with 1 being no birefringence and 5 strong birefringence when using crossed polarisers (Brönnimann et al., 2018).

Every stratigraphic unit was evaluated with respect to 136 attributes and recorded in a database that provided the basis for defining eleven microfacies types (MFT I–XI) (Courty, 2001; Goldberg and Macphail, 2006). These were defined according to the micro-artefacts embedded in the sediment, sediment structure, the natural (e. g. washed in sediments in a ditch) and anthropogenic sedimentation processes (e. g. intentional infill of a pit), and the taphonomic processes. Results from experimental studies on trampling effects conducted indoors and outdoors were also taken into consideration (Rentzel et al., 2017).

Results

As it is impossible to introduce every single stratigraphic unit and each profile individually, section 3.1 will focus on six representative profiles (profile P058, P153, P739, P888, P957 and P1092) (table 1, figure 3–8), which are selected because of their good preservation and the high number of samples. With these profiles, a characteristic stratigraphic sequence can be outlined for every feature type. Section 3.2 will characterise the eleven microfacies types (MFT I–XI), whose spatial and stratigraphic allocation is given in figure 2 (for all results see supplementary information).

The stratigraphic sequence of selected profiles

Profile P058 – rammed earth floors

Profile P058 (figure 3) is situated in the south of the investigated area. The archaeological layers are directly above the calcareous C horizon of the overbank deposit (SU 58.2a). The top 10 mm of the C horizon (SU 58.2b) are conspicuously compact (figure 9A; porosity < 2% with a gradual transition to SU 58.2a), discoloured reddish-brown due to iron oxides, and with a sharp boundary between SU 58.2b and SU 58.3. The latter contains several horizontally oriented gravels, ceramic fragments and bone fragments showing pronounced fungal attack. While SU 58.4 includes fewer gravels and ceramic fragments, it does contain charred organic matter and some charcoal fragments. Furthermore, the stratigraphic unit shows dusty coatings containing some micro-charcoal and there are numerous phosphate precipitates (infillings in pores and impregnation of the micromass, rarely crystal intergrowth; figure 3). SU 58.4 is covered by a thick gravel and pebble layer consisting of size selected coarse gravel (Rentzel, 1997) and cobbles, which can be up to 40 cm and were intentionally dumped using Rhine gravel material (same petrographic spectrum).

Profile P739 – occupation layer in the western area

In contrast to profile P058, around 20 cm of the Bt horizon of the luvisol (figure 4) is still preserved in profile P739 (SU 739.6). The above following SU 739.7–739.9 include several horizontally oriented gravels (often red-

dened due to firing), bone fragments (at times burnt, frequently showing fungal attack), charcoal fragments, charred seeds and sclerotia, and frequent dusty clay coatings. This sediment is covered by a loamy layer of gravel and debris (SU 739.11) of 6–8 cm thickness. The topmost part of the analysed sequence is a loamy decalcified sediment full of gravel (SU 739.15 and 739.16). It exhibits strong weathering (decalcification) and bioturbation. As the sediment contains fragments of modern pottery, it can be assumed that the layer was reworked in the more recent past.

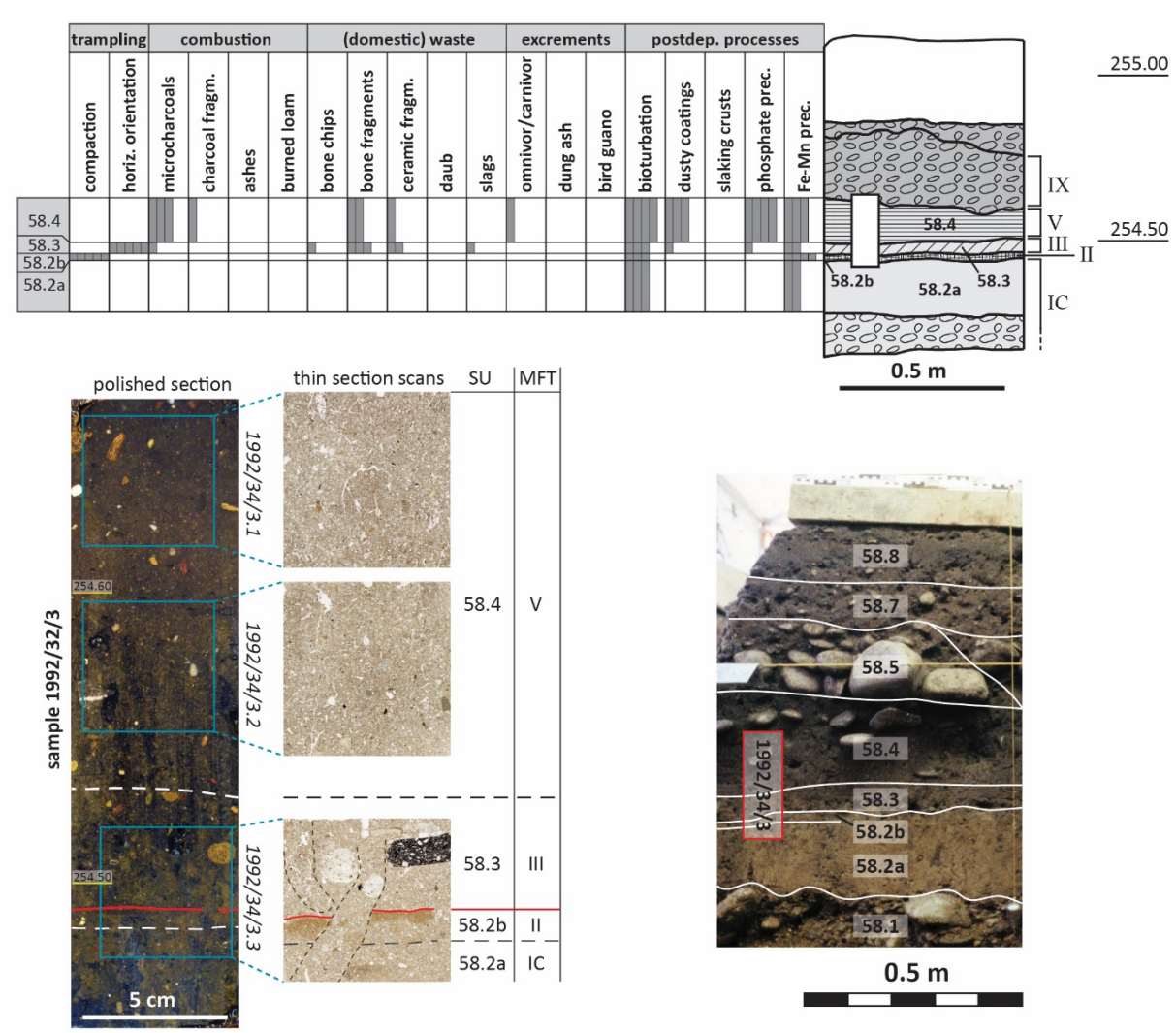


Fig. 3: *Top: Schematic drawing of* ***profile P058*** *(reference profiles for house floors; MFT II) with block sample No. 3 and the different microfacies types (MFT, given as roman numerals). Left: Selection of micromorphological results regarding trampling, combustion material, waste material, excrements and postdepositional processes given in a semi-quantitative scale: No bar = absent; one bar = single (< 2%); two bars = few (2–10%); three bars = frequent (10–25%); four bars = numerous (25–50%); five bars = dominant (>50%). Below: Photograph of profile P058 (right) and polished section with thin section scans (left).*

SU	microstructure	sediment characteristics	MFT	formation processes
58.2a	CCS	greyish-brown, homogeneous, calcareous, silty-sandy loam	1C	natural overbank deposit; C-horizon
58.2b	MA	reddish-brown, homogeneous, calcareous, silty-sandy, very dense loam	2	compaction, probably due to intense trampling in a roofed area (probable house floor)
58.3	CCS; PO	brown, calcareous, silty-sandy loam with gravels	3	Accumulation due to trampling on a loamy, unsheltered surface
58.4	CCS; PO	brown, homogeneous, calcareous, silty-sandy loam	5	Brought-in loam (calcareous overbank deposit); mixed with micro-charcoals, probably due to tillage / manuring

Tab. 1.1: *Brief description of the stratigraphic units (SU), assignment to microfacies type (MFT) and interpretation of the micromorphologically analysed layers of* ***profile P058****. Microstructure: FL = finely layered; MA = massive; CCS = channel and chamber structure; PO = parallel orientation; UO = un-oriented; SGS = single-grain-structure.*

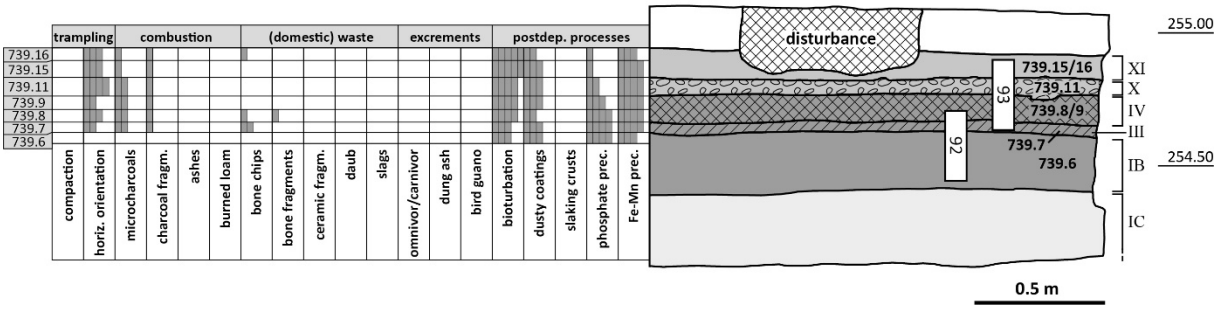


Fig. 4: *Schematic drawing of* ***profile P739*** *(reference profile for MFT IV) with block sample No. 92 and 93, the different microfacies types (MFT, given as roman numerals) and a selection of semi-quantitative results. For the profile photo and polished section / thin section scans see supplementary information.*

SU	microstructure	sediment characteristics	MFT	formation processes
739.6	CCS	light-brown, homogeneous, decalcified, silty-sandy loam	1B	Natural overbank deposit; B-horizon
739.7	CCS; PO	brown, homogeneous, decalcified, silty-sandy loam with gravels	3	Accumulation due to trampling on a loamy, unsheltered surface
739.8	CCS; PO	brown, homogeneous, decalcified, silty-sandy loam with few gravels	4	Accumulation due to trampling on a loamy, unsheltered surface
739.9	CCS; PO	brown, homogeneous decalcified, silty-sandy loam with few gravels	4	Accumulation due to trampling on a loamy, unsheltered surface
739.1	CCS; PO	brown, slightly layered, silty-sandy loam (decalcified) with gravel and pebbles (rhine gravel)	10	Brought-in loam and rhine gravel; probable trampling on a loamy, paved, unsheltered surface
739.2	CCS; UO	brown, slightly layered, silty-sandy loam (decalcified) with fine to coarse gravel	11	Heavily weathered and disturbed Iron Age occupation layer
739.2	CCS; PO	brown, slightly layered, silty-sandy loam (decalcified) with middle to coarse gravel	11	Heavily weathered and disturbed Iron Age occupation layer

Tab. 1.2: *Brief description of the stratigraphic units (SU), assignment to microfacies type (MFT) and interpretation of the micromorpho-logically analysed layers of* ***profile P739****. Shortcuts for microstructure see table 1.1.*

Profile P888 – occupation layer in the eastern area

The stratigraphic sequence of profile P888 (figure 5) seems, at first glance, to resemble the one of profile P739, which is located 5 m to the east. The 10 cm thick Bt horizon of the overbank deposit (SU 888.25) is covered by a gravelly layer (SU 888.28) of roughly 5 cm thickness containing horizontally oriented pebbles, gravels, and bone fragments (frequently showing fungal attack). However, in contrast to profile P739, the gravel layer of profile P888 comprises a small amount of ash. The same applies for the subsequent SU 888.30 and SU 888.33, which additionally contain some bone chips (figure 9B) and coprolite fragments (< 1 mm). These components are strikingly uniform in size (usually 0.5–2 mm). Furthermore, several dusty clay coatings with micro-charcoal have been recorded. The top part of profile P888 is a loamy-gravelly layer (SU 888.35/37) of 10–15 cm thickness, which strongly resembles SU 739.15/16 in profile P739.

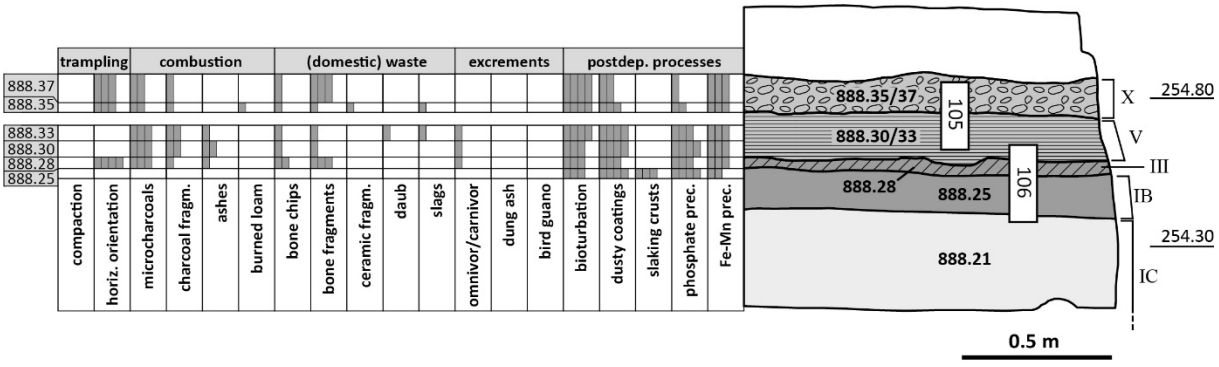


*Fig. 5: Schematic drawing of **profile P888** (reference profile for MFT V) with block sample No. 105 and 106, the different micro-facies types (MFT, given as roman numerals) and a selection of semi-quantitative results. For the profile photo and polished section / thin section scans see supplementary information.*

SU	microstructure	sediment characteristics	MFT	formation processes
888.3	CCS	light-brown, homogeneous, decalcified, silty-sandy loam	1B	Natural overbank deposit; B-horizon
888.3	CCS; PO	brown, homogeneous, weakly calcareous, silty-sandy loam with gravels	3	Accumulation due to trampling on a loamy, unsheltered surface
888.30	CCS; UO	brown, homogeneous, weakly calcareous, silty-sandy loam	5	Brought-in loam (decalcified overbank deposit); mixed with micro-charcoals and some ashes, probably due to tillage / manuring
888.33	CCS; UO	brown, homogeneous, weakly calcareous, silty-sandy loam	5	Brought-in loam (decalcified overbank deposit); mixed with micro-charcoals and some ashes, probably due to tillage / manuring
888.35	CCS; PO	brown, slightly layered, silty-sandy loam (decalcified) with gravel and pebbles (rhine gravel)	10	Brought-in loam and rhine gravel; probable trampling on a loamy, paved, unsheltered surface
888.37	CCS; PO	brown, slightly layered, silty-sandy loam (decalcified) with gravel and pebbles (rhine gravel)	10	Brought-in loam and rhine gravel; probable trampling on a loamy, paved, unsheltered surface

*Tab. 1.3: Brief description of the stratigraphic units (SU), assignment to microfacies type (MFT) and interpretation of the micromorpho-logically analysed layers of profile **P888**. Shortcuts for microstructure see table 1.1.*

Profile P957 – ditch 9

Ditch 9 (profile P957, figure 6) was preserved to about 40 cm depth and 50–60 cm width. The silty-sandy ditch filling (SU 957.39/40) is layered (figure 9C) and contains a calcareous silt fraction and some lumps of ash. The ditch filling also contains large amounts of charred organic material, several burnt bone chips (figure 10A), small pieces of guano (figure 10B), slag fragments, and one glass drop. All these micro-artefacts have a size of about 0.5–1 mm. It is striking to see that in this layer several gastropod shells and numerous sclerotia have been preserved entirely. The fine layering of SU 957.39/40 is due to thin silty crusts (figure 9C). Pronounced dusty clay coatings are to be found in the overbank deposit at the ditch bottom (SU 957.17).

SU	microstructure	sediment characteristics	MFT	formation processes
957.17	CCS	light-brown, homogeneous, decalcified, silty-sandy loam	1B	Natural overbank deposit; B-horizon
957.39	CCS; PO; FL	brown, layered, calcareous, silty-sandy loam with few gravel	6	Washed-in, fine-grained material and components (from the nearby loamy surface)
957.40	CCS; PO; FL	brown, slightly layered, calcareous, silty-sandy loam	6	Washed-in, fine-grained material and components (from the nearby loamy surface)

*Tab. 1.4: Brief description of the stratigraphic units (SU), assignment to microfacies type (MFT) and interpretation of the micromorpho-logically analysed layers of profile **P957**. Shortcuts for microstructure see table 1.1.*

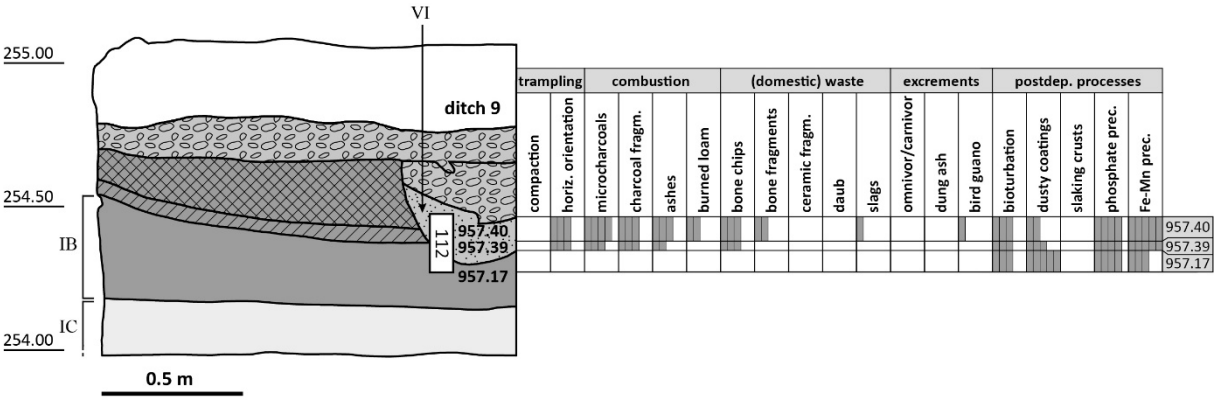


*Fig. 6: Schematic drawing of **profile P957** (reference profile for ditch filling MFT VI; ditch 9) with block sample No. 112, the different microfacies types (MFT, given as roman numerals) and a selection of semi-quantitative results. For the profile photo and polished section / thin section scans see supplementary information.*

Profile P1092 – ditch 4

Ditch 4 (figure 7) runs in an arc from north to south (figure 2). With a depth of 80 cm, ditch 4 is preserved to a greater depth than ditch 9 and is about twice as wide (100 cm). There were several large cobbles and some stone slabs in certain areas at the ditch bottom. The most striking difference between ditch 4 and 9 is that the filling layers of the former (SU 1092.5/11/12/14) consist of calcareous, moderately to well-sorted, layered sands (fine to medium sand) (figure 9D) and do not contain any anthropogenic components – except for some charcoal fragments and bone chips of about 1–2 mm size.

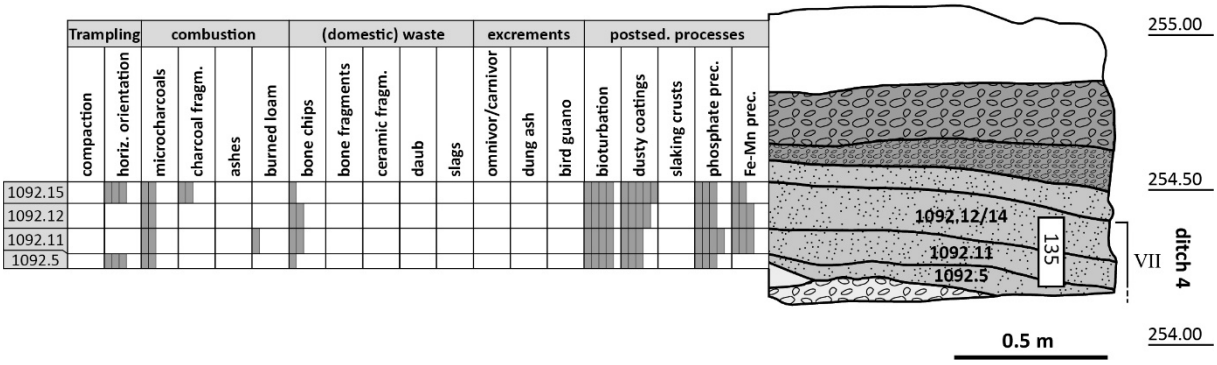


*Fig. 7: Schematic drawing of **profile P1092** (reference profile for pit filling MFT VII; pit 4) with block sample No. 135, the different microfacies types (MFT, given as roman numerals) and a selection of semi-quantitative results. For the profile photo and polished section / thin section scans see supplementary information.*

SU	microstructure	sediment characteristics	MFT	formation processes
1092.5	CCS; FL; SGS	(light-) brown, homogeneous, calcareous, well-sorted sand (fine- to middle-sand)	7	Accumulation by flowing water (20-50 cm/s) within a ditch (river water)
1092.11	CCS; PO; FL; SGS	(light-) brown, layered, calcareous, well-sorted sand (fine- to middle-sand)	7	Accumulation by flowing water (20-50 cm/s) within a ditch (river water)
1092.12	CCS; FL; SGS	(light-) brown, layered, calcareous, well-sorted sand (fine- to middle-sand)	7	Accumulation by flowing water (20-50 cm/s) within a ditch (river water)
1092.14	CCS; PO; FL; SGS	(light-) brown, homogeneous, calcareous, well-sorted sand (fine- to middle-sand)	7	Accumulation by flowing water (20-50 cm/s) within a ditch (river water)

*Tab. 1.5: Brief description of the stratigraphic units (SU), assignment to microfacies type (MFT) and interpretation of the micromorpho-logically analysed layers of **profile P1092**. Shortcuts for microstructure see table 1.1.*

Profile P153 – pit 302

Pit 302 (profile P153, figure 8) has an elongated oval shape (3.4 x 2.8 m), which was preserved to roughly 2.5 m depth (volume of 17 m3) (Jud and Spichtig, 1995). The pit reaches far into the calcareous Rhine gravel. Thus, it is likely that the walls of the pit were supported by some kind of installation (Rentzel, 1998) – probably a lining made out of wood or wattle – as is known to have been the case on other sites (Passard et al., 1991; Passard and Urlacher, 1997; Amoroso and Schenk, 2018). However, no such evidence was found for pit 302.

The pit filling can be divided into a lower finely layered part (SU 153.10/26/29/30) and an upper part concave layer geometry with distinct gravelly layers (SU 153.36/39/41/45/50). This division into two parts can also be seen on a micromorphological level. The lower finely layered sequence is composed of dung and wood ash (figure 9E) with some charcoal fragments, burnt bone chips and burnt soil aggregates. The fact that some of those soil aggregates were vitrified indicates that they were exposed to temperatures between 1000 and 1200°C (Röpke and Dietl, 2017), whereby the presence of fluxing agents such as sodium or potassium may have lowered the melting point (Canti and Brochier, 2017a). The presence of arbuscular mycorrhizal fungi (figure 10C) (Rodríguez-Morelos et al., 2014), which only occur in combination with dung ash, is also noteworthy. In addition, phosphate precipitations and some vivianite crystals are regularly present (figure 10D). The upper part of the pit filling consists of a brown, calcareous, silty-sandy loam that is rather homogenous (figure 9F). It contains burnt and thus reddened gravels, charred organic matter, some remains of ash, mostly isolated phytoliths as well as several pottery and bone fragments. Unlike the lower pit filling, the upper part is not finely layered. The bone fragments do not show any signs of fungal attack and the collagen is well preserved (Brönnimann et al., 2018). The top layers (SU 153.56) run horizontally over the edge of the pit and consist of a sandy-gravelly, non-calcareous loam, which suffered severe weathering and has been altered through modern agricultural activities.

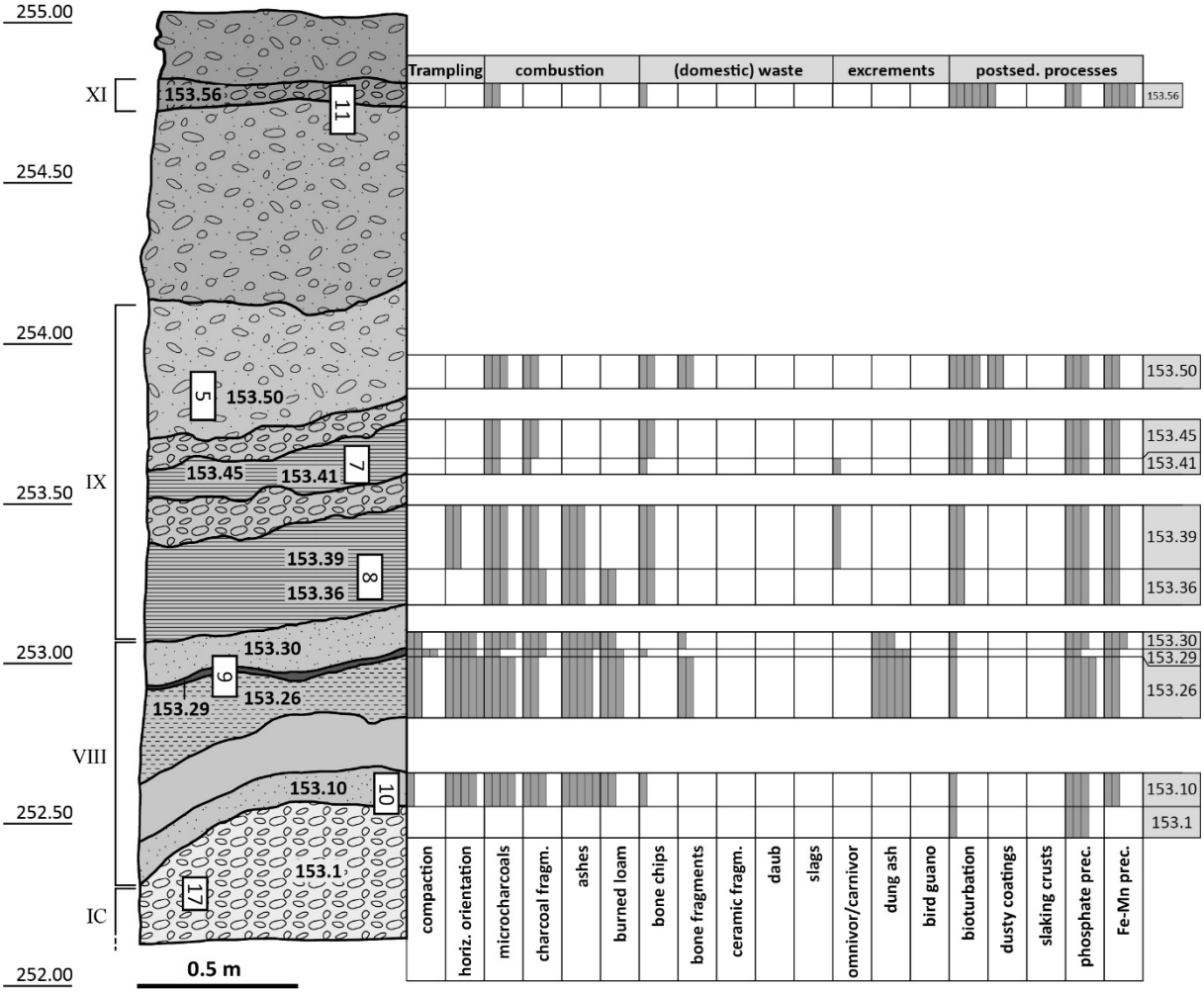


*Fig. 8: Schematic drawing of **profile P153** (reference profile for pit filling MFT VIII and MFT IX; pit 302) with block sample No. 5, 7-11 and 17, the different microfacies types (MFT, given as roman numerals) and a selection of semi-quantitative results. For the profile photo and polished section / thin section scans see supplementary information.*

SU	microstructure	sediment characteristics	MFT	formation processes
153.1	SGS	grey, calcareous, sandy gravel	1C	Natural rhine gravel; C-horizon
153.10	FL; MA; PO	dark-brown, finely layered, calcareous, silty loam	8	In situ accumulated, trampled wood-ashes (oven rake-out)
153.26	FL; MA; PO	brown, slightly layered, calcareous, silty loam	8	in situ accumulated, trampled dung-ashes (oven rake-out)
153.29	FL; MA; PO	blackish, finely layered, calcareous, silty to sandy loam	8	in situ accumulated, trampled dung- and wood-ashes and charcoal (oven rake-out)
153.30	FL; MA; PO	dark-brown, calcareous, silty loam	8	In situ accumulated, trampled wood- (and dung-) ashes (oven rake-out)
153.36	UO	dark-brown, quite homogeneous, calcareous, silty-sandy loam with some gravels	9	Quickly brought-in, ashy loam (and garbage)
153.39	UO	dark-brown, quite homogeneous, calcareous, silty-sandy, gravelly loam	9	Quickly brought-in, ashy loam (and garbage)
153.41	UO; SGS	brown, quite homogeneous, calcareous, silty-sandy, gravelly loam	9	Quickly brought-in, slightly weathered loam (and garbage)
153.45	UO; SGS	brown, quite homogeneous, calcareous, silty-sandy, gravelly loam	9	Quickly brought-in, slightly weathered loam (and garbage)
153.50	UO; SGS	dark-brown, quite homogeneous, calcareous, silty-sandy, gravelly loam	9	Quickly brought-in, slightly weathered loam (and garbage)
153.56	UO; SGS	dark-brown, quite homogeneous, decalcified, sandy-gravelly loam with some pebbles	11	Brought-in, heavily reworked and weathered loam

*Tab. 1.6: Brief description of the stratigraphic units (SU), assignment to microfacies type (MFT) and interpretation of the micromorpho-logically analysed layers of **profile P153**. Shortcuts for microstructure see table 1.1.*

Characterising the microfacies types (MFT 1–11)

Based on the micromorphological results, eleven microfacies types were defined (MFT I–XI). They differ in regards to their composition and micro-artefacts they contain (figure 11), their structure, the identified sedimentation processes and taphonomic indications (table 2 and 3) and their spatial extent and occurrence (Figure 2).

Microfacies type I (MFT I) comprises the overbank deposit. A distinction is made between the calcareous C horizon (MFT IC) and the clayey Bt horizon which has been decalcified through Holocene soil formation processes (MFT IB). The Bt horizon turns out to be missing in the southern part of the analysed area (figure 2). Its maximum thickness is 15 cm (northern part).

Microfacies type II (MFT II) includes an extremely compact (porosity <2%) and sterile loam layer (figure 9A). It is roughly 1–2 cm thick and has turned brown due to iron oxides, probably because of temporary stagnant water. MFT II is the top layer of the levelled, loamy surface and has been compacted because of intense trampling. It is only found in three profiles, all of which are centred only a few metres apart in the south of the area (figure 2).

Microfacies type III (MFT III) is found in all soil profiles except in areas with lowered features. MFT III is a gravelly layer of about 4–6 cm thickness (figure 9G) that runs horizontally directly above the levelled loamy surface. It can contain large bone and pottery fragments. The bones tend to show clear fungal attack (figure 9G and 10E) while the pottery fragments are horizontally oriented.

Microfacies type IV (MFT IV) (10–15 cm thickness) lies above MFT III in some of the profiles (figure 2). It consists of a silty-sandy loam, which can be slightly layered (figure 9H). It also comprises several diffuse layers of fine gravel. Unlike MFT III, MFT IV has a greater proportion of charred organic matter and of bone fragments (figure 11).

Microfacies type V (MFT V) has a thickness of 15–20 cm, is remarkably homogenous and not layered. It includes a small amount of ash, burned bone chips (figure 9B) and some faecal remains (< 1 mm). Both MFT IV and V consist largely of reworked overbank deposit. The matrix tends to be non-calcareous and clayey (MFT IVB and VB) in areas where the decalcified Bt horizon in the underground is still preserved, and vice versa. While MFT IV is only found in the east of the examined area, MFT V exists solely in the west with ditch 7 forming the boundary between them (figure 2).

Microfacies type VI (MFT VI) (up to 25 cm thickness) consists of a silty, partly finely layered loam (figure 9C) and is characterised by its high proportion of micro-charcoal, bone chips (figure 10A), small faecal remains (figure 10B) and ash (figure 11). Those micro-components are usually the size of silt or sand grains. MFT VI has been recorded only in ditches and postholes (figure 2). The bones embedded in this MFT tend to show fungal attack, although less frequently than bones from MFT III.

Microfacies type VII (MFT VII) (up to 50 cm thick) is only present in ditch 4 and can be described as a layered, moderately to well-sorted fine to medium sand (figure 9D). Unlike in MFT VI, anthropogenic components are rare in MFT VII (figure 11).

Microfacies type VIII (MFT VIII) (up to 1 m thick) has the highest concentration of (micro-) charcoal (figure 11). MFT VIII tends to be finely layered and shows a clear horizontal orientation of all components (figure 9E). The

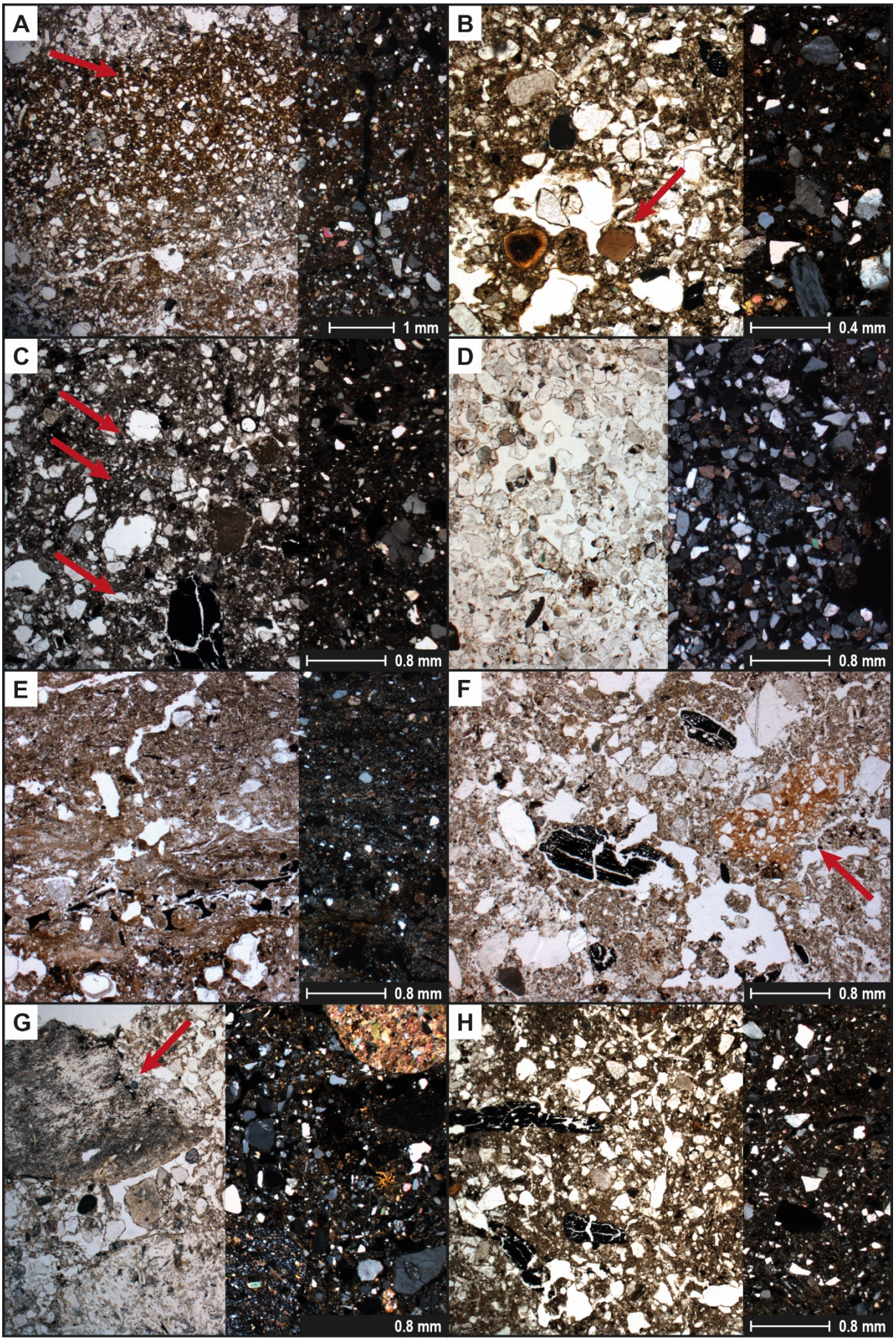
sediments are usually rich in charcoal fragments, wood and dung ashes (figure 10F). MFT VIII also contains some flattened soil aggregates, all of which are burnt or vitrified. The embedded bone chips are burnt and/or calcined. Larger bone fragments show an extraordinary well-preserved collagen and microstructure with no or only minimal fungal attack. MFT VIII is only found in the lower half of pit fillings (figure 2).

Microfacies type IX (MFT IX) (up to 1.5 m thick) is also particular to pits. While MFT IX also features a high amount of (micro-) charcoal, unlike MFT VIII, it is neither finely layered nor is there a uniform orientation of components (figure 9F). Instead, MFT IX has a rather heterogeneous appearance and its characteristics resemble the ones of MFT IV, V and VI.

Microfacies type X (MFT X) has been analysed micromorphologically in only four profiles. It is a layer of gravels, pebbles and cobbles, which is rather thick in the southern part of the study area (20–30 cm) but grows thinner northwards (15–20 cm). MFT X covers the most features from the Iron Age.

Microfacies type XI (MFT XI) – a homogenous gravelly, 20–30 cm thick loam – lies on top of MFT X. It comprises numerous modern finds and will therefore be disregarded when interpreting the results.

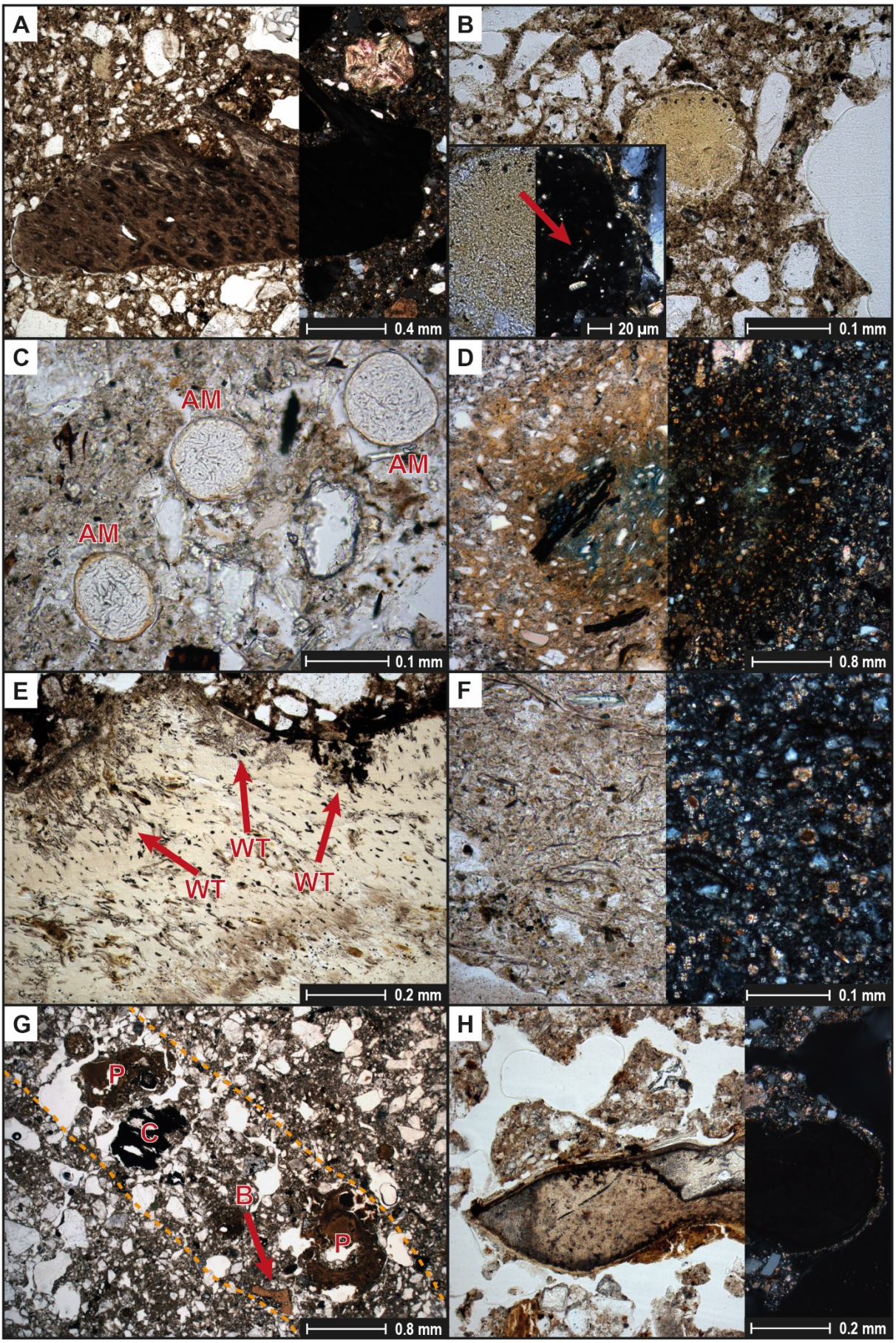
Fig. 9: *Microscope photographs of the microfacies types MFT II–IX. All left image sections in plane polarized light (PPL) and right image sections in crossed polarized light (XPL) (except figure 9F).* ***A) Profile P058, MFT II*** *(SU 58.2b): extremely condensed, supposed rammed earth floor (arrow) (16x magnification).* ***B) Profile P888, MFT V*** *(SU 888.33): homogenous, calcareous, silty-sandy loam with micro charcoals, a reworked phosphate nodule (yellowish-brown) and a rounded, burned bone chip (arrow) (50x magnification).* ***C) Profile P957, MFT VI*** *(SU 957.39, ditch 9): finely layered, silty-sandy loam with some micro-charcoal and some silty crusts (25x magnification).* ***D) Profile P1083, MFT VII*** *(SU 1083.19, ditch 4): well-sorted medium sand (25x magnification).* ***E) Profile P153, MFT VIII*** *(SU 153.29, pit 302): finely layered, heavily trampled sequence of ashes, charred organic material and phytolith layers. (25x magnification).* ***F) Profile P153, MFT IX*** *(SU 153.36, pit 302): heterogeneous, silty-sandy loam with several non-uniformly oriented charcoal fragments and one burned loam fragment (arrow) (25x magnification).* ***G) Profile P1007, MFT III*** *(SU 1007.6): calcareous, unweathered fine gravel and a small bone fragment (arrow) with intense fungal attack (Wedl tunnels) (25x magnification).* ***H) Profile P957, MFT IV*** *(SU 957.22): slightly calcareous, silty-sandy loam with a diffuse layering and horizontally oriented charcoal fragments. Strongly bioturbated and some dusty intercalations (25x magnification).*


A
1 mm
B
0.4 mm
C
0.8 mm
D
0.8 mm
E
0.8 mm
F
0.8 mm
G
0.8 mm
H
0.8 mm

MFT	structure types	sedimentation processes	human activities	Interpretation
1	natural sediments			natural loam; 1C = C horizon; 1B = Bt horizon
2	house floors	compaction	trampling inside in a roofed area	house floor (rammed earth floor)
3	open areas; occupation surface	successive accumulation of gravel and loam (due to trampling), exposure	trampling on an exposed, loamy surface	initial trampling horizon
4	open areas; occupation surface	successive accumulation (due to trampling), incorporation of (micro-) charcoal and few micro-artefacts; exposure	trampling on an exposed, loamy surface, domestic and economic activities	finely layered occupation layer
5	open areas; occupation surface	homogenisation, incorporation of ashes, micro-charcoal, few dung and faeces and micro-artefacts	probable garden cultivation and manuring	garden cultivation (?)
6	ditches	successive accumulation of washed in surface material		natural ditch filling
7	ditches	repeated sedimentation of well-sorted sand by flowing water		water canal
8	pits	repeated accumulation and compaction (due to trampling) of ashes, charcoal fragments and burned loam	trampling inside a covered pit, economic activities (glassmaking, metal handicraft)	Roofed workshop (handicraft)
9	pits	quick infilling	quick and intentional filling of a pit with sediments and waste material (bones, ceramics)	pit infilling
10	open areas	depositing	depositing of selected gravels and pebbles	intentional gravel deposit
11	overall	weathering due to exposure and bioturbation	modern tillage	heavily weathered and disturbed upper part

Tab. 2: *Overview of the microfacies types (MFT I–XI) with regards to what archaeological features they occur, what sedimentation processes and human activities have influenced them and their general interpretation.*

Fig. 10: *Microscope photographs of some special features and components. All left image sections in plane polarized light (PPL) and right sections of figure 10A, 10B (inset), 10D, 10F and 10H in crossed polarized light (XPL).* ***A) P957, MFT VI*** *(SU 957.39): burned bone chip with greyish colour and initial destruction of the bone microstructure; washed in by surface water (50x magnification).* ***B) Profile P957, MFT VI*** *(SU 957.40): rounded guano fragment with phosphatic matrix and some badly preserved avian uric acid spheres with their characteristic shape (arrow) (200x and 630x magnification).* ***C) Profile P153, MFT VIII*** *(SU 153.10, pit 302): finely layered ashes and phytoliths with several arbuscular mycorrhizal fungi (AM), which are often found on roots of (symbiotic) plants (200x magnification).* ***D) Profile P181, MFT VIII*** *(SU 181.27, pit 302): dung ashes (dung spherulites not visible due to insufficient magnification) with impregnating phosphate precipitation and vivianite crystals (25x magnification).* ***E) Profile P957, MFT III*** *(SU 957.21): horizontally oriented bone fragment with clear fungal attack (Wedl tunnels; WT), partly filled with iron oxide precipitations (brownish) (100x magnification).* ***F) Profile P153, MFT VIII*** *(SU 153.26, pit 302): numerous dung spherulites and phytoliths as remains from burnt dung (200x magnification).* ***G) Profile P957, MFT IB*** *(SU 957.18): substrate (decalcified overbank deposit); intense bioturbation with vertically displaced charcoal fragments (C), phosphate nodules (P) and bone chips (B) (25x magnification).* ***H) Profile P1101, MFT VIII*** *(SU 1101.59, pit 400): glass droplet, horizontally embedded in ash-rich sediment (100x magnification).*


A
0.4 mm
B
20 µm
0.1 mm
C
AM
AM
AM
0.1 mm
D
0.8 mm
E
WT
WT
WT
0.2 mm
F
0.1 mm
G
P
C
B
P
0.8 mm
H
0.2 mm

Discussion

General observations about the layer preservation

The micromorphologically analysed stratigraphic units are in general heavily bioturbated (figure 10G), mainly by earthworms and plant roots. The closer to the surface the stratigraphic units are, the greater the bioturbation tends to be (figure 3, 4 and 5). Only stratigraphic units from features that are more than 1.5 m below the surface – thus only large settlement pits – show weak signs of bioturbation (figure 8). Dusty clay coatings in pores, which are often considered to be indicators for exposed surfaces or tillage (e.g. Bresson and Valentin, 1994; Gebhardt, 1995; Adderley et al., 2010; Deák et al., 2017), are found in almost all examined stratigraphic units. For example, all stratigraphic units in profile P739 exhibit roughly the same frequency and intensity of dusty clay coatings. Beside this, the intensity of dusty clay coatings and bioturbation is quite uniform (figure 8). Thus, it seems that dusty clay coatings at Basel-Gasfabrik are a result of bioturbation and modern agricultural activities. Hence, they are indicators of more modern events and will therefore not be used as a diagnostic characteristic for this study. The same applies to slaking crusts as it can be hard to distinguish them from pronounced dusty clay coatings because of the bioturbation.

Reconstructing layer formation processes and human activities

Open areas

The substrate in the examined area is an overbank deposit several decimetres' thick, on which Holocene soil formation processes have developed a roughly 60 cm thick luvisol (Rentzel, 1997, 1998). This soil profile was intentionally levelled out to the Bt horizon (MFT IB, northern area) or to the C horizon respectively (MFT IC, southern area) (figure 2 and 12) with a remarkable regularity and precision in height: in the west of ditch 7 the truncated level lies at 254.50 m a.s.l. (± 2 cm), in the east at 254.60 m a.s.l. It seems that soil was removed and the area levelled out into different "sectors" before the settlement was built. More such levelled "sectors" can be found north and west of the investigated settlement area, which are also separated from their neighbouring "sectors" through ditches and are of different heights. This spatial structure defined by ditches and an intentional levelling also correlates with the extent of MFT IV and V and thus with a different use of space (see below). The question therefore arises as to whether those "sectors" could be some kind of parcelling. Such a parcelling through the use of ditches is a common phenomenon for settlement from the La Tène period (Roth-Zehner, 2005; Georges-Leroy et al., 2007; Giles, 2007; Wendling, 2010; Brestel, 2015) and could be a hint of a planned spatial organisation.

In areas without deepened features, the truncated soil is covered with a gravel layer (MFT III). The horizontal orientation of gravels, charcoal fragments and bone chips and the presence of flattened soil aggregates indicate that this gravelly layer was successively accumulated by trampling. Accumulation due to trampling was observed in various trampling experiments (Banerjea et al., 2015a; Rentzel et al., 2017) and analyses of exposed loam surfaces (Gebhardt and Langohr, 1999; Matthews, 2003b; Miller et al., 2010; Shillito and Ryan, 2013; Wouters et al., 2017). The embedded bone fragments exhibit intense fungal attack, which implies that they lay exposed over a long period of time (Brönnimann et al., 2018). Thus, we assume that MFT III is to be interpreted as an initial

trampling horizon, which successively accumulated due to trampling during or shortly after the terrain was truncated, possibly as the result of construction and excavation activities.

As MFT IV is similar to MFT III (diffuse layering, horizontal orientation of micro-components), it can be assumed that MFT IV has also been repeatedly trampled. The embedding of (micro-) charcoals, bone chips and fragments, and coprolite pieces from omnivores/carnivores suggests domestic and economic activities. Thus, for MFT IV it is assumed that sediment with embedded micro-components accumulated over a longer period of daily activities as has been observed in various other occupation layers (Matthews et al., 1996; Gebhardt and Langohr, 1999; Macphail, 2000; Matthews, 2003a; Shillito and Matthews, 2013; Borderie et al., 2014; Wouters et al., 2017). A glance at the map shows that MFT IV is only to be found to the east of ditch 7 (figure 2).

In the west of ditch 7, MFT III is followed by MFT V – an occupation layer different to MFT IV. As MFT V has a homogenous appearance and is considerably thicker (15–20 cm), it can be postulated that it was either filled in with material from the local overbank deposit or that the sediment accumulated very quickly. However, MFT V is interspersed with micro-charcoal, ash remains, and coprolite pieces as well as some residues of herbivore dung and bird guano. The distribution of the micro-components is strikingly homogenous and with a grain size within the coarse silt and sand spectrum (< 1 mm). This could be seen as a sign that the soil was tilled (Lewis, 2002, 2012; Macphail, 2010; Sageidet, 2013; Devos et al., 2017). We therefore assume that the homogeneous character of MFT V and the uniform size and distribution of the micro-components could be the consequence of intensive gardening within the settlement. The coprolite and dung residues as well as perhaps the ash components could therefore have been used to fertilise the soil. Whether this is the case or not, the botanical analyses and the stable isotopes also suggest that there was intensive garden cultivation within the settlement Basel-Gasfabrik (Knipper et al., 2017).

MFT X, which follows MFT IV or V, consists of large, selected Rhine gravel, pebbles and cobbles as well as of (large) pottery and bone fragments. MFT X covers all features with no regard for the previous spatial organisation of the settlement and apparently breaks the latter. MFT X is therefore seen as the end of a settlement phase. The horizontal orientation of (micro-) charcoal and bone chips suggests the gravelly surface was trampled. As the subsequent Iron Age layers above MFT X have been altered by modern activities, it remains unclear whether MFT X was the start of a new settlement phase with a different spatial organisation, whether the area was repurposed (for example as an open space), or whether the area was abandoned afterwards.

Inside the house

Three profiles with only a few metres distance between them show a dense and compact loam layer directly on top of the natural overbank deposit (MFT II). This compact loam layer is likely to represent a rammed earth floor inside a roofed structure (house). If it was an outdoor area, the sediment would be more homogenous and micro-artefacts would be embedded in it (Matthews, 2003b; Shillito and Ryan, 2013; Rentzel et al., 2017; Wouters et al., 2017). However, there are no traces of domestic activities such as in situ micro-artefacts (de-facto waste according to Schiffer, 1972) or occupation layers rich in charcoal fragments and ash – as would be typical for indoor areas – to be found (Gé et al., 1993; Matthews, 2003b, 2012; Banerjea et al., 2015b; Rentzel et al., 2017). Regular cleaning of the floors or the use of mats or the like to cover the floor might explain this. Several geoar-

chaeological (Karkanas and Efstratiou, 2009; Shillito, 2011; Couture et al., 2017) and ethnological examples from other regions (Milek, 2012; Friesem, 2016; Friesem et al., 2016) show that the cleaning of house or loam floors is likely to have been common. There was, however, no sign of phytolith layers, which could have been interpreted as remains of mats (Karkanas and Efstratiou, 2009).

Ditches

In the examined ditches, two different kinds of sedimentation processes were identified, without them ever co-occurring in the same ditch. Ditch 7 and 9 are filled with MFT VI. The diffuse fine layering of this MFT, the embedded sclerotia, seeds, spores and gastropod fragments, as well as the fact that the micro-components are well sorted suggests that sediment from the surface was continuously washed into the ditch and accumulated (Lisá et al., 2015). The heavy precipitation of iron oxide and phosphate (infillings in pores, impregnation of the micromass, dendritic) are signs of repeated stagnant water. It is therefore safe to assume that the ditches not only divided the settlement into a spatial organisation but were also used to drain surface water. This is hardly surprising as the surfaces of the settlement were loamy, compacted and therefore poorly drained. Some ditches (e.g. ditch 7) have several phases, which might indicate that they were consciously maintained.

Ditch 4, which is filled with MFT VII, did not have the same function. Its well-sorted, layered sands can be interpreted as the residue of flowing water. Ditch 4 seems to have been a canal that was at least temporarily flooded – either by a diverted stream or pumped-up water from a well. The water definitely did not come from the Rhine as the Rhine was flowing at a deeper level (roughly 10 m deeper).

Pits

It is likely that the settlement pits in Basel-Gasfabrik were lined since the sandy and loose Rhine gravel would collapse (Rentzel, 1998). The polygonal shapes suggest that the supports were made of pieces of wood that were wedged against one another. Little is known about the primary use of the pits. While it can be assumed that they were used as cellar and storage areas, the appropriate occupation layers are missing (Brönnimann and Rissanen, 2018; Rentzel, 1998). Some pits show clear signs of secondary use. For example, pit 287, 302 and 400 contain finely layered deposits that are rich in charcoal fragments and ash (MFT VIII). The fact that the components are horizontally oriented and the presence of flattened soil aggregates suggests that, while the pit was sheltered from weathering, the bottom of the pit was trampled intensely (Macphail et al., 2004; Miller et al., 2010; Matthews, 2012; Banerjea et al., 2015a; Couture et al., 2017; Rentzel et al., 2017). Moreover, vitrified soil aggregates and phytolith slags are indicative of temperatures between 1000 and 1200 degree Celsius (Röpke and Dietl, 2017). Lower temperatures are, however, also possible if fluxing agents were present (Canti and Brochier, 2017a). The most likely explanation for those finely layered ashes (MFT VIII) is a successive accumulated and trampled ash rakeout of a nearby oven. Thus, a secondary use of pits as roofed constructions in the context of handicrafts (maybe as part of a workshop) can be assumed. This is demonstrated in pit 400, which contained numerous glass droplets (0.3–2 mm) (figure 10H). Wood as well as herbivore dung was used as fuel, as finely layered dung ash from pit 302 shows (figure 10D and 10G).

Once the pits were no longer needed they were quickly filled in with charcoal-rich loam (MFT IX), which in its

characteristics recalls MFT IV and V (pit 287 and 302) and MFT VI (pit 400). It appears that sediments from settlement activities were used to fill the pits. Fresh Rhine gravel or overbank deposits from recently excavated pits or ditches on the other hand were not used. The finds from pit fillings are better preserved and contain greater quantities than finds from MFT IV–VI, which is particularly notable for bones (Brönnimann et al., 2018). It is therefore likely that waste, which was stored elsewhere, was also used when filling in pits.

archaeological structure	MFT	sedimentation processes	human activities	interpretation
house floors	2	compaction	trampling in a roofed area	house floor (rammed earth floor)
open areas; occupation surface	3, 4, 5, 10	successive accumulation of gravel and loam (due to trampling); incorporation of charcoal fragments, micro-artefacts etc.; homogenisation; exposure; depositing (gravel)	trampling on an exposed, loamy surface; domestic and economic activities; probable garden cultivation and manuring; depositing of selected gravels and pebbles	initial trampling horizon; successively accumulated occupation layer; various domestic and economic activities; garden cultivation (?); intentional gravel deposit
ditches	6, 7	successive accumulation of washed in surface material; repeated sedimentation of well-sorted sand by flowing water		natural ditch filling; water canal
pits	8, 9, 10	repeated accumulation and compaction (due to trampling) of (dung) ashes, charcoal fragments and burned loam; quick infilling; depositing (gravel)	trampling inside a covered pit and economic activities; quick and intentional filling with sediments and waste material; depositing of selected gravels and pebbles	roofed workshop (handicraft); pit infilling; intentional gravel deposit
post holes	6	successive accumulation of washed in surface material; quick infilling	quick and intentional filling with burned daub	natural post hole filling; intentional infilling / deposit of burned daub
house floors	2	compaction	trampling in a roofed area	house floor (rammed earth floor)
open areas; occupation surface	3, 4, 5, 10	successive accumulation of gravel and loam (due to trampling); incorporation of charcoal fragments, micro-artefacts etc.; homogenisation; exposure; depositing (gravel)	trampling on an exposed, loamy surface; domestic and economic activities; probable garden cultivation and manuring; depositing of selected gravels and pebbles	initial trampling horizon; successively accumulated occupation layer; various domestic and economic activities; garden cultivation (?); intentional gravel deposit
ditches	6, 7	successive accumulation of washed in surface material; repeated sedimentation of well-sorted sand by flowing water		natural ditch filling; water canal
pits	8, 9, 10	repeated accumulation and compaction (due to trampling) of (dung) ashes, charcoal fragments and burned loam; quick infilling; depositing (gravel)	trampling inside a covered pit and economic activities; quick and intentional filling with sediments and waste material; depositing of selected gravels and pebbles	roofed workshop (handicraft); pit infilling; intentional gravel deposit
post holes	6	successive accumulation of washed in surface material; quick infilling	quick and intentional filling with burned daub	natural post hole filling; intentional infilling / deposit of burned daub
house floors	2	compaction	trampling in a roofed area	house floor (rammed earth floor)

Tab. 3: *Overview of the archaeological structures with regards to the microfacies types, sedimentation processes and human activities and their general interpretation.*

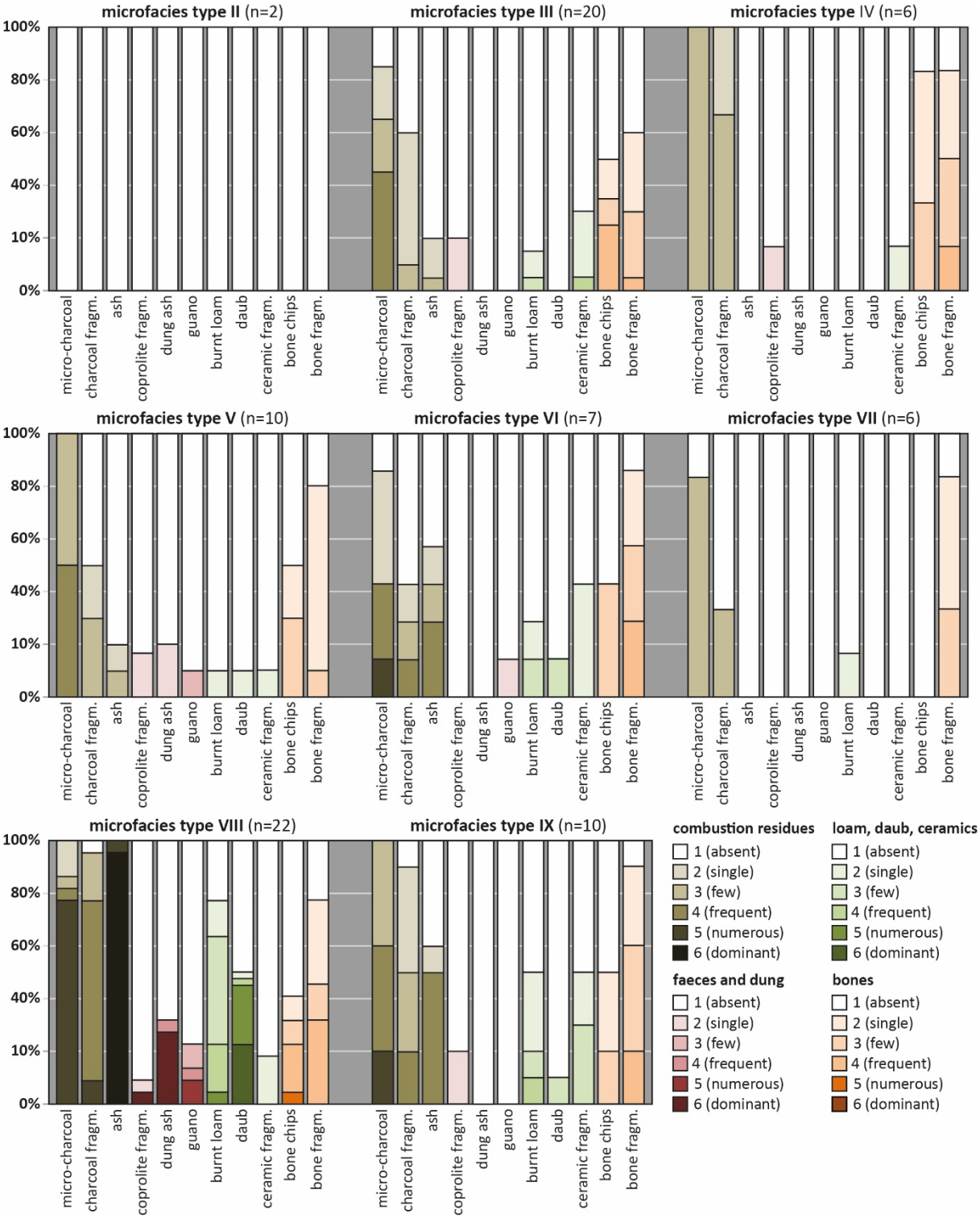


Fig. 11: *Comparison between the microfacies types MFT II–IX sorted by microfacies types given in a semi-quantitative way (absent [0%] – single [<2%] – few [2–10%] – frequent [10–25%] – numerous [25–50%] – dominant [>50%]).*

Resource and waste management

Bone and pottery fragments

The vast majority of finds from Basel-Gasfabrik appeared in pit fillings (MFT IX). However, initial volume calculations show that the density of finds in occupation layers does not differ greatly from the one in pit fillings. The micromorphological analysis has provided similar results: there is close to no difference in quantity between the amount of ceramic and bone fragments found in pit fillings and in surface layers. However, there is a significant difference between finds from pits and finds from other sediments when it comes to their preservation. Histotaphonomic analyses have shown that animal bones from pit fillings (MFT VIII and IX) exhibit far better collagen preservation and less fungal attack than bones found in occupation layers (MFT III and 4) or ditch fillings (MFT VI) (Brönnimann et al., 2018). Thus, for bone fragments different taphonomic biographies can be postulated. Most bones must have been stored somewhere within the settlement for a period of time. These suspected dumps (= primary refuse) within the settlement allowed for the bone and ceramic fragments to be reused as raw material (repurposing and reusing). For example, pottery fragments might be used as a cover or a support when burning new pottery (Steiner, 2008; 2012) while cow mandibles were used as sled runners (Stopp and Kunst, 2005). Waste from these rubbish dumps was also used to fill in pits (MFT IX) and thus was no longer available as raw material (secondary use). The infilled material therefore is secondary refuse, since it has been proven that those pits were not backfilled successively over a long period of time, but quickly (Brönnimann and Rissanen, 2018). Another indication for a temporary storage of waste and thus for a differentiated waste management can be seen in the preservation of animal bones and ceramic fragments (taphonomic processes), which differs greatly between material from archaeological horizons (MFT III, IV and V) and from pit fillings (MFT IX).

Combustion residues

Micro-charcoal was found in all deposits except for MFT I and II. We suggest that the micro-particles were involuntarily spread by humans, animals, wind and rain. The greatest concentration of charcoal fragments (and ash) was found in pits used as roofed constructions in the context of manual craft (secondary use), where they accumulated over time as de-facto refuse. Both charcoal fragments and ash have been well-preserved in such sheltered pits, while it is difficult to detect ash residues in other structures because of bioturbation, percolating water and the fragility of ash particles. Ash remains are also quite frequent in ditches (MFT VI); however, there it was washed in from the surface. It can therefore be assumed that ashes – just like micro-charcoal – were spread by wind and water across the settlement, but have not been preserved in heavily trampled areas (MFT IV). The presence of ash residue in areas which might have been used as gardens (MFT V) could indicate that ash was occasionally used as a fertiliser.

Faeces and dung

Using thin section analysis, it is rarely possible to identify human faeces for certain (Brönnimann et al., 2017b). Micromorphological and paleoparasitological analysis of coprolites that were found in pits and were preserved in their entirety show that the majority of faeces are from carnivores (probably dogs) (Pümpin et al., 2015). No latrine sediments, as they are known from Roman and Medieval contexts (Brombacher et al., 1999; Brönnimann

et al., 2017b), were identified in Basel-Gasfabrik yet. Thus, it remains unclear what happened with human faeces. As the human occupants and their animals lived side by side, faeces often found their way into the soil – probably sometimes as fertiliser. Most sediments contain small bits of coprolite that are too small to be determined to species level (omnivore /carnivore 0.5–2 mm) (figure 11). The parasite infestation of occupants and domestic animals might have been the result of faeces, which were embedded in the soil, being washed into the drinking water (e.g. in wells) polluting it (Pichler et al., 2014).

The dung spherulites in herbivore dung (cows, sheep, goats) make it possible to easily identify this kind of dung (Shahack-Gross, 2011; Brönnimann et al., 2017a; Canti and Brochier, 2017b). MFT V contained few poorly preserved dung remains, while dung ash is one of the components of MFT VIII in pit 302. It is therefore likely that herbivore dung was used as a fertiliser in Basel-Gasfabrik and certain that it was used as a source of fuel. The latter might be due to a lack of firewood within the vicinity of the settlement, since palynological and isotopic results show an open landscape (Guélat and Richard, 2014; Wick, 2015; Knipper et al., 2017). In summary, it can be said that for Iron Age people faeces and dung was a resource and not just waste. However, from a modern perspective, this entailed poor hygiene, which, for example, led to the spread of intestinal parasites.

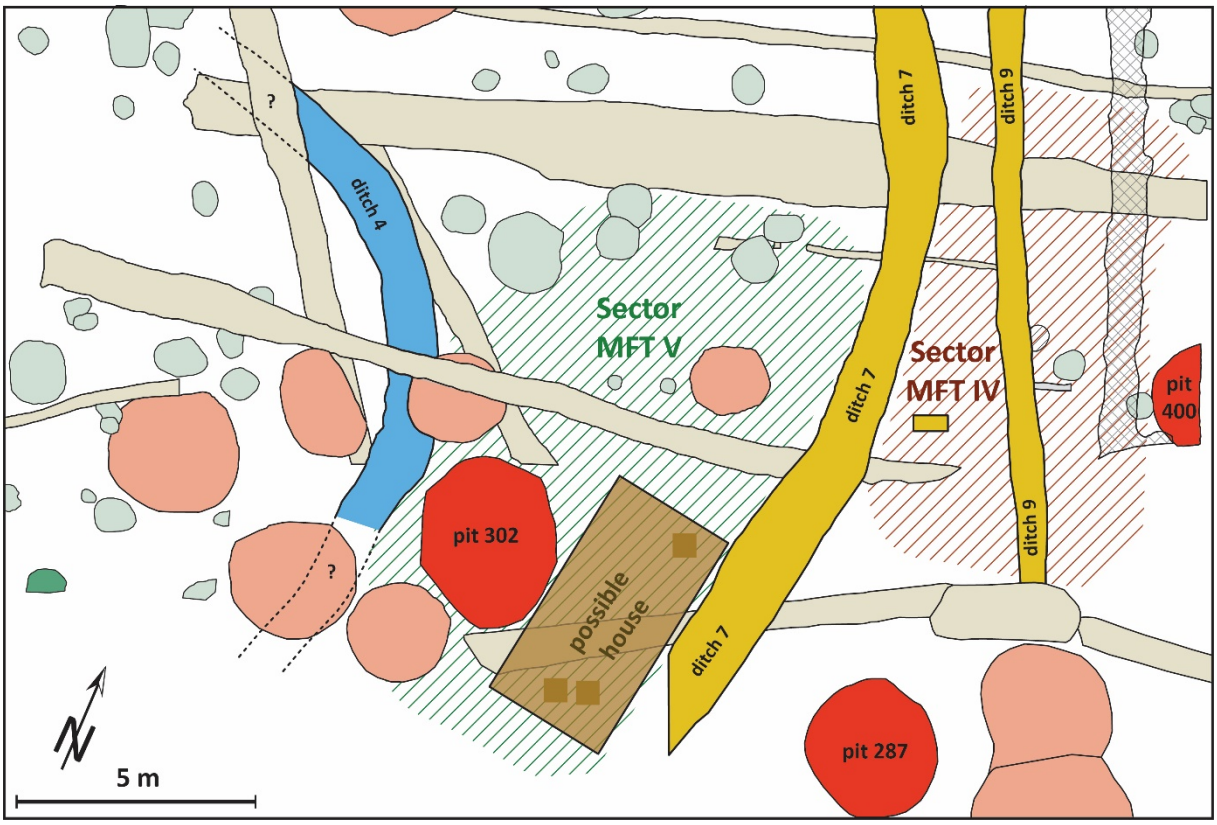


Fig. 12: *Interpretation and contextualisation of the geoarchaeological results: Two different sectors (sector MFT V and MFT IV), separated by ditch 7. One house ground (brown) and a water canal (blue) are postulated.*

Excavation material

Geoarchaeological analyses has shown that the local geological substrates were used in various ways. For example, the calcareous overbank deposit (C horizon) served as daub; the loamy overbank deposit (Bt horizon) was used for making pottery, hearths and ovens (Rentzel, 1998; Steiner, 2008; 2012). The use of Rhine gravel on the other hand has remained unclear. While pebbles were used for levelling the area (MFT X; levelling layer), this is only a fraction of the large amounts of gravel that were excavated when making pits. It is also possible that calcareous sandy gravel was sometimes employed to fix surfaces and used as marl to fertilise the soil.

Contextualisation of the micromorphological results

Our results show that the site was levelled into different "sectors" by truncating the terrain during an early settlement phase (figure 12). Those probable parcels are separated from one another by ditches and show slightly different surface heights. The initial trampling horizon (MFT III), which is directly above this levelled surface, is present in every part of the examined area and might be connected to the preparation of the terrain. The occupation layers are weakly layered (MFT IV) or rather homogenous (MFT V). Mapping these two microfacies types illustrates that the spatial organisation of the site corresponds to the supposed parcelling. While MFT IV is most probably the result of constant accumulation due to domestic and economic activities, MFT V might be connected to intensive garden cultivation. This is the first time that a difference in use can be linked to different areas within Basel-Gasfabrik. This casts an entirely new light on the organisation of settlements of the younger Iron Age. The spatial organisation manifests itself in various features (ditches, difference in use and different levels) and seems to have played a crucial role in the settlement of Basel-Gasfabrik. However, the fact that a cover of gravel and pebble was distributed at a later time (cannot be estimated precisely) over a large area (MFT X) suggests that there was an overarching concept, for this layer makes a clear break with the earlier spatial organisation. Whether this break was followed by a new settlement phase (which is no longer tangible), whether the area was repurposed as an open public space or whether it was then abandoned is unknown.

The geoarchaeological results show that the ditches had several functions. Some were used to organise the settlement spatially. Their filling accumulated steadily and consists of surface material that was washed in. It is likely that those ditches were also used to drain surface water. By contrast, ditch 7 is to be interpreted as a canal. While the running water from the canal was probably not used as the main source of drinking water (there were several wells in the settlement), it might have been of importance for artisan work.

In the settlement pits, no traces of their primary use have been preserved (probably as cellar and storage areas). The finely-layered ash- and charcoal-rich trampled layers in the micromorphologically investigated pits 287, 302 and 400 suggest that those pits were later used as roofed construction in the context of manual craft (secondary use; maybe as part of a workshop). The abundance of glass droplets in pit 400 suggest that the secondary use of this pit was probably in the context of glass craft. Once the pits were no longer used, they were filled in intentionally over a short period of time using charcoal-rich sediments from within the settlement. These fillings are similar to MFT IV, V and VI. At the same time, well-preserved ceramic and animal bone fragments, probably from rubbish dumps inside the settlement, entered the ditch fillings.

Three investigated profiles feature a simple rammed earth floor made of loam, which might have belonged to the same building. On this loam floor, no occupation layer was observed. An explanation for this could be that the floor was covered by some kind of mat, for which, however, no evidence (such as phytolith accumulation) was observed. The lack of defacto refuse also means that no traces of domestic activities can be found in the suspected house.

The geoarchaeological analysis has also shown that the ways in which the occupants of Basel-Gasfabrik used resources and waste were strikingly varied and the use of different materials can be multifaceted. Dumps with animal bones and ceramic fragments were postulated, which probably have served as easily accessible material depots. Thus, the boundary between waste and raw material was fluid and ever-changing. For example, faeces were used in various ways: herbivore dung was used as fuel and possibly as a fertiliser. The latter might also be true for pig manure. It is still unclear how the occupants dealt with human faeces as no latrine sediments were found. The way in which local raw materials such as loam and Rhine gravel was used is also very complex and highly regulated. Loam from calcareous overbank deposits was used as daub; the loamy Bt horizon material for making pottery, ovens and hearths; and large pebbles and gravel for stabilising and covering surfaces.

Conclusions

It is only possible to interpret archaeological artefact assemblages if the formation and transformation processes can be reconstructed. This is especially true for archaeological layers and the (micro-) artefacts embedded in them. Only if layer formation and postsedimentary processes are identified, can we discern cultural practices and patterns of behaviour. Waste and resource management are two of these patterns that influence the formation of the artefact assemblages to a great extent.

Thanks to micromorphological analyses, it was possible to reconstruct natural and anthropogenic layer formation processes and taphonomic alterations in a well-preserved area of the younger La Tène settlement of Basel-Gasfabrik. Several archaeological features like settlement pits, ditches, house floors, occupation layers and trampling horizons were included in this analysis. The definition and mapping of microfacies types turned out to be a useful approach to reconstruct everyday practices and spatial organisation within a settlement. It also helps to reconstruct the use, reuse and disposal of different objects or material groups and offers a first insight into the occupants' waste and resource management.

For a more profound understanding of these processes, a larger database is necessary. The integration of archaeological and zooarchaeological results will allow to retrace the use, reuse, and disposal of different material groups. This will help to sketch behavioural patterns and to delve further into the problems discussed here.

Acknowledgements

The geoarchaeological analyses were funded by Archäologische Bodenforschung Basel-Stadt. The authors would like to thank Johannes Wimmer and Milena Müller-Kissing for their help and support as well as Thomas Beckmann for making the thin sections. We also would like to thank Olivia L. Klee for translating this text into English, the editors and the anonymous reviewers whose comments have greatly improved this manuscript.

Data Availability Statement

The data that support the findings of this study are openly available in "Zenodo" at http://doi.org/10.5281/zenodo.3256487.

References (chapter 3)

Adderley, W.P., Wilson, C.A., Simpson, I.A., Davidson, D.A., 2010. Anthropogenic Features, in: Stoops, G., Marcelino, V., Mees, F. (Eds.), Interpretation of micromorphological features of soils and regoliths. Elsevier, Amsterdam, Oxford, pp. 569–588.

Amoroso, H., Schenk, A., 2018. Quoi de neuf chez les Helvètes d'Avenches? Archäologie Schweiz 41 (1), 16–23.

Banerjea, R.Y., Bell, M., Matthews, W., Brown, A., 2015a. Applications of micromorphology to understanding activity areas and site formation processes in experimental hut floors. Archaeological and Anthropological Sciences 7 (1), 89–112.

Banerjea, R.Y., Fulford, M.G., Bell, M., Clarke, A.S., Matthews, W., 2015b. Using experimental archaeology and micromorphology to reconstruct timber-framed buildings from Roman Silchester: a new approach. Antiquity 89 (347), 1174–1188.

Beck, M.E., Hill, Matthew E. Jr., 2004. Rubbish, relatives, and residence: The family use of middens. Journal of Archaeological Method and Theory 11 (3), 297–333.

Binford, L.R., 1981. Behavioral archaeology and the "Pompeii premise". Journal of Archaeological Research 37 (3), 195–208.

Borderie, Q., Devos, Y., Nicosia, C., Cammas, C., Macphail, R.I., 2014. Dark Earth in the geoarchaeological approach to urban contexts, in: Arnaud-Fassetta, G., Carcaud, N. (Eds.), La géoarchéologie française au XXIè siècle. CNRS Éditions, Paris.

Bresson, L.-M., Valentin, C., 1994. Soil surface crust formation: contribution of micromorphology, in: Soil micromorphology: Studies in management and genesis. Proceedings of the IXth International Working Meeting on Soil Micromorphology, Townsville, Australia, July 1992, Amsterdam, pp. 737–762.

Brestel, T.J., 2015. Becoming visible: The formation of urban boundaries in the oppidum of Manching (Bavaria), in: Dalton, M., Peters, G., Tavares, A. (Eds.), Seen & unseen spaces. Archaeological Review from Cambridge 30.1. ARC, Cambridge, pp. 44–51.

Brombacher, C., Helmig, G., Hüster Plogmann, H., Klee, M., Rentzel, P., Rodel, S., Veszeli, M., 1999. … und was davon übrig bleibt - Untersuchungen an einem mittelalterlichen Latrinenschacht an der Bäumleingasse 14 (1992/20). Jahresbericht der Archäologischen Bodenforschung des Kantons Basel-Stadt 1998, 93–131.

Brönnimann, D., 2019. Geoarchäologische Untersuchungen zum Abfall- und Ressourcen-Management in der jüngerlatènezeitlichen Siedlung Basel-Gasfabrik. Inauguraldissertation zur Erlangung der Würde eines Doktors der Philosophie vorgelegt der Philosophisch-Naturwissenschaftlichen Fakultät der Universität Basel von David Simon Brönnimann aus der Schweiz. Basel.

Brönnimann, D., Rissanen, H., 2018. Vivre et mourir sur le site La Tène de Bâle-Gasfabrik (Suisse): L'étude interdisciplinaire de structures d'habitat choisies et de deux nécropoles donne un aperçu de la société à la fin de l'âge du Fer, in: Interdisciplinarity and new approaches in the research of the Iron Age. International Doctoral Conference 2015. Rencontres doctorales archéologiques de l'Ecole Européenne de Protohistoire de Bibracte, Glux-en Glenne. 28.-30. April 2015. Dissertationes Archaeologicae Brunenses/Pragensesque, Glux-en Glenne, Brno, pp. 87–91.

Brönnimann, D., Ismail-Meyer, K., Rentzel, P., Pümpin, C., Lisá, L., 2017a. Excrements of herbivores, in: Nicosia, C., Stoops, G. (Eds.), Archaeological soil and sediment micromorphology. Wiley Blackwell, Hoboken, pp. 55–65.

Brönnimann, D., Pümpin, C., Ismail-Meyer, K., Rentzel, P., Egüez, N., 2017b. Excrements of omnivores and carnivores, in: Nicosia, C., Stoops, G. (Eds.), Archaeological soil and sediment micromorphology. Wiley Blackwell, Hoboken, pp. 67–81.

Brönnimann, D., Portmann, C., Pichler, S.L., Booth, T.J., Röder, B., Vach, W., Schibler, J., Rentzel, P., 2018. Contextualising the dead – Combining geoarchaeology and osteo-anthropology in a new multi-focus approach in bone histotaphonomy. Journal of Archaeological Science (98), 45–58.

Bullock, P., Fédoroff, N., Jongerius, A., Stoops, G., Tursina, T.V., 1985. Handbook for soil thin section description. Waine Research, Albrighton, 152 pp.

Canti, M.G., Brochier, J.-É., 2017a. Plant ash, in: Nicosia, C., Stoops, G. (Eds.), Archaeological soil and sediment micromorphology. Wiley Blackwell, Hoboken, pp. 147–154.

Canti, M.G., Brochier, J.-É., 2017b. Faecal spherulites, in: Nicosia, C., Stoops, G. (Eds.), Archaeological soil and sediment micromorphology. Wiley Blackwell, Hoboken, pp. 51–54.

Courty, M.-A., 2001. Microfacies analysis assisting archaeological stratigraphy, in: Goldberg, P., Holliday, V.T., Ferring, C.R. (Eds.), Earth sciences and archaeology, New York, pp. 205–239.

Couture, A., Bhiry, N., Woollett, J., 2017. Micromorphological Analyses of Inuit Communal Sod Houses in Northern Labrador, Canada. Geoarchaeology 32 (2), 267–282.

Deák, J., Gebhardt, A., Lewis, H., Usai, M.R., Lee, H., 2017. Soils disturbed by vegetation clearance and tillage, in: Nicosia, C., Stoops, G. (Eds.), Archaeological soil and sediment micromorphology. Wiley Blackwell, Hoboken, pp. 233–264.

Devos, Y., Nicosia, C., Vrydaghs, L., Speleers, L., van der Valk, J., Marinova, E., Claes, B., Albert, R.M., Esteban, I., Ball, T.B., Court-Picon, M., Degraeve, A., 2017. An integrated study of Dark Earth from the alluvial valley of the Senne river (Brussels, Belgium). Quaternary International 460, 175–197.

Friesem, D.E., 2016. Geo-ethnoarchaeology in action. Journal of Archaeological Science 70, 145–157.

Friesem, D.E., Lavi, N., Madella, M., Ajithprasad, P., French, C., 2016. Site formation processes and hunter-gatherers use of space in a tropical environment: A geo-ethnoarchaeological approach from South India. PLoS ONE 11 (10), 1-30.

Gé, T., Courty, M.-A., Matthews, W., Wattez, J., 1993. Sedimentary formation processes of occupation surfaces, in: Gold-

berg, P., Nash, D.T., Petraglia, M.D. (Eds.), Formation processes in archaeological context. Monographs in World Archaeology 17, Madison, Wisconsin, pp. 149–163.

Gebhardt, A., 1995. Soil micromorphology data from traditional and experimental agriculture, in: Archaeological sediments and soils. Analysis, interpretation and management : papers from the Tenth Anniversary Conference of the Association for Environmental Archaeology held at the Institute of Archaeology, UCL, July 1989. Tenth Anniversary Conference of the Association for Environmental Archaeology. Juli 1989. Institute of Archaeology, London, pp. 25–39.

Gebhardt, A., Langohr, R., 1999. Micromorphological study of construction materials and living floors in the Medieval motte of Werken (West Flanders, Belgium). Geoarchaeology: An International Journal 14 (7), 595–620.

Georges-Leroy, M., Heckenbenner, D., Laffite, J.-D., Meyer, N., 2007. Les parcellaires anciens fossilisés dans les forêts lorraines, in: La mémoire des forêts. Actes du colloque « Forêt, archéologie et environnement » 14-16 décembre 2004. Forêt, archéologie et environnement. 14.-16. Dezember 2014, Paris, pp. 121–131.

Gifford-Gonzalez, D., 2014. Constructing community through refuse disposal. Afr Archaeol Rev 31 (2), 339–382.

Giles, M., 2007. Good fences make good neighbours? Exploring the ladder enclosures of Late Iron Age East Yorkshire, in: Haselgrove, C., Moore, T. (Eds.), The Later Iron Age in Britain and beyond. Oxbow Books; David Brown Book Co, Oxford, pp. 235–249.

Goldberg, P., 1980. Micromorphology in Archaeology and Prehistory. Paléorient 6, 159–164.

Goldberg, P., Macphail, R.I., 2006. Practical and theoretical geoarchaeology. Blackwell Publishers, Malden, MA, Oxford, 454 pp.

Guélat, M., Richard, H., 2014. Holocene environmental changes and human impact in the northern Swiss Jura as reflected by data from the Delémont valley. Swiss Journal of Geosciences 107 (1), 1–21.

Hecht, Y., Niederhäuser, A., 2011. Alltagskultur und Totenrituale der Kelten: Ein Siedlungszentrum am Oberrhein um 100 v. Chr. Merian, Basel, 113 pp.

Hollund, H.I., Jans, M.M., Collins, M.J., Kars, H., Joosten, I., Kars, S.M., 2012. What happened here?: Bone histology as a tool in decoding the postmortem histories of archaeological bone from castricum, the Netherlands. International Journal of Osteoarchaeology 22, 537–548.

WRB (Ed.), 2006. World Reference Base for Soil Resources 2006: A Framework for International Classification, Correlation and Communication. World Soil Resources Report 103. Food and agriculture organization of the United Nations, Rom, 145 pp.

Jones, A.M., 2015. Ritual, rubbish or everyday life? Evidence from a Middle Bronze Age settlement in Mid-Cornwall. Archaeological Journal 172 (1), 30–51.

Jud, P., Spichtig, N., 1995. Vorbericht über die Grabungen 1992 in der spätkeltischen Siedlung Basel-Gasfabrik. Jahresbericht der Archäologischen Bodenforschung des Kantons Basel-Stadt 1992, 19–35.

Karkanas, P., Efstratiou, N., 2009. Floor sequences in Neolithic Makri, Greece: Micromorphology reveals cycles of renovation. Antiquity 83 (322), 955–967.

Karkanas, P., Brown, K.S., Fisher, E.C., Jacobs, Z., Marean, C.W., 2015. Interpreting human behaviour from depositional rates and combustion features through the study of sedimentary microfacies at site Pinnacle Point 5-6, South Africa. Journal of Human Evolution 85, 1–21.

Knipper, C., Pichler, S.L., Rissanen, H., Stopp, B., Kühn, M., Spichtig, N., Röder, B., Schibler, J., Lassau, G., Alt, K.W., 2017. What is on the menu in a Celtic town?: Iron Age diet reconstructed at Basel-Gasfabrik, Switzerland. Archaeological and Anthropological Sciences 9, 1307–1326.

Kock, S., Huggenberger, P., Preusser, F., Rentzel, P., Wetzel, A., 2009. Formation and evolution of the Lower Terrace of the Rhine River in the area of Basel. Swiss Journal of Geosciences 102 (2), 307–321.

Lewis, H., 2002. An investigation of ancient cultivation remains at Hengistbury Head Site 6, Christchurch, Dorset. Proceedings of the Prehistoric Society 68, 83–102.

Lewis, H., 2012. Investigating ancient tillage: An experimental and soil micromorphological study. BAR international series 2388. Archaeopress, Oxford.

Lisá, L., Komoróczy, B., Vlach, M., Válek, D., Bajer, A., Kovárník, J., Rajtár, J., Hüssen, C.-M., Šumberová, R., 2015. How were the ditches filled? Sedimentological and micromorphological classification of formation processes within graben-like archaeological objects. Quaternary International 370, 66–76.

Macphail, R.I., 2000. Soils and microstratigraphy: a soil micromorphological and micro-chemical approach, in: Lawson, A.J. (Ed.), Potterne 1982-5. Animal Husbandry in Later Prehistoric Wiltshire. Wessex Archaeology Report 17. Trust for Wessex Archaeology, Salisbury, pp. 47–71.

Macphail, R.I., 2010. Dark earth and insights into changing land use of urban areas, in: Debating urbanism within and beyond the walls A. D. 300-700. Proceedings of a conference held at the University of Leicester, 15th Novemer 2008, Leicester. 15. November 2008, Leicester, pp. 145–165.

Macphail, R.I., Cruise, G.M., Allen, M.J., Linderholm, J., Reynolds, P., 2004. Archaeological soil and pollen analysis of experimental floor deposits; with special reference to Butser Ancient Farm, Hampshire, UK. Journal of Archaeological Science 31, 175–191.

Matthews, R. (Ed.), 2003a. Excavations at Tell Brak, Vol. 4: Exploring an Upper Mesopotamian regional centre, 1994 - 1996. McDonald Institute monographs. British School of Archaeology in Iraq, London, 446 pp.

Matthews, W., 2003b. Microstratigraphic sequences: Indications of uses and concepts of space, in: Matthews, R. (Ed.), Excavations at Tell Brak, Vol. 4. Exploring an Upper Mesopotamian regional centre, 1994 - 1996. McDonald Institute monographs. British School of Archaeology in Iraq, London, pp. 377–388.

Matthews, W., 2012. Household life histories and boundaries: Microstratigraphy and micromorphology of architectural surfaces in building 3 (BACH), in: Tringham, R.E., Stevanović, M. (Eds.), Last house on the hill. BACH area reports from Çatalhöyük, Turkey. Çatalhöyük research project series 11. Cotsen Inst. of Archaeology Press, Los Angeles, California, pp. 205–222.

Matthews, W., French, C., Lawrence, T., Cutler, D., 1996. Multiple surfaces: The Micromorphology, in: Hodder, I. (Ed.), On the surface. Çatalhöyük 1993 - 95. Çatalhöyük Project Volume 1. BIAA Monograph 22. McDonald Inst. for Archaeological Research, Cambridge, pp. 301–342.

Milek, K.B., 2012. Floor formation processes and the interpretation of site activity areas: An ethnoarchaeological study of turf buildings at Thverá, northeast Iceland. Journal of An-

thropological Archaeology 31 (2), 119–137.

Miller, C.E., Conard, N.J., Goldberg, P., Berna, F., 2010. Dumping, sweeping and trampling: Experimental micromorphological analysis of anthropogenically modified combustion features, in: The taphonomy of burned organic residues and combustion features in archaeological contexts. Centre d'Étude Préhistoire, Antiquité, Moyen Âge - UMR 6130. Proceedings of the round table, May 27-29 2008, CEPAM. Round table, May 27-29 2008, CEPAM. 27.-29. Mai 2008, pp. 25–37.

Müller-Scheessel, N., Hofmann, R., Müller, J., Rassmann, K., 2010. Müllmanagement in einem spätneolithischen Tell Zentralbosniens. Tübinger Verein zur Förderung der Ur- und Frühgeschichtlichen Archäologie 11, 67–79.

Passard, F., Urlacher, J.-P., 1997. Besançon, Saint-Jean (Doubs): structures en fosses et puits en contextes laténien et gallo-romain (1er siècle avant J.-C. - 1er siècle après J.-C.). Revue Archéologique de l'Est 48, 167–218.

Passard, F., Urlacher, J.-P., Avanzi, V., 1991. L'horizon laténien du site de Saint-Jean à Besançon, in: Curdy, P., Kaenel, G., Roulière-Lambert, M.-J. (Eds.), Les Celtes dans le Jura. L'âge du Fer dans le massif jurassien (800-15 av. J.-C.). Ausstellungskatalog, Yverdon-les-Bains, pp. 95–97.

Pichler, S.L., Rissanen, H., Spichtig, N., Alt, K.W., Röder, B., Schibler, J., Lassau, G., 2013. Die Regelmäßigkeit des Irregulären: Menschliche Skelettreste vom spätlatènezeitlichen Fundplatz Basel-Gasfabrik, in: ‚Irreguläre' Bestattungen in der Urgeschichte: Norm, Ritual, Strafe …? Akten der Internationalen Tagung in Frankfurt a. M. vom 3. bis 5. Februar 2012, Frankfurt. 3.-5.2.2012. Dr. Rudolf Habelt GmbH, Bonn, pp. 471–484.

Pichler, S.L., Pümpin, C., Brönnimann, D., Rentzel, P., 2014. Life in the proto-urban style: the identification of parasite eggs in micromorphological thin sections from the Basel-Gasfabrik Late Iron Age settlement, Switzerland. Journal of Archaeological Science 43, 55–65.

Pichler, S.L., Rissanen, H., Spichtig, N., 2015. Ein Platz unter den Lebenden, ein Platz unter den Toten – Kinderbestattungen des latènezeitlichen Fundplatzes Basel-Gasfabrik, in: Kory, R.W. (Ed.), Lebenswelten von Kindern und Frauen in der Vormoderne. Archäologische und anthropologische Forschungen in memoriam Brigitte Lohrke. Paläowissenschaftliche Studien 4. curach bhán publications, Berlin, pp. 257–273.

Pichler, S.L., Röder, B., Brönnimann, D., Knipper, C., Kühn, M., Rentzel, P., Rissanen, H., Stopp, B., Vach, W., Warnberg, O., Alt, K.W., Schibler, J., Lassau, G., 2017. The Basel-Gasfabrik research project: Addressing complex topics by an integrative approach, in: Multidisciplinary approach to archaeology: Recent achievements and prospects. Proceedings of the international symposium "Multidisciplinary Approach to Archaeology: Recent achievements and prospects" (June 22-26, 2015, Novosibirsk). Multidisciplinary Approach to Archaeology: Recent achievements and prospects, Novosibirsk. 22.-25. June 2016. IAET SB RAS Publishing, Novosibirsk, pp. 240–247.

Pümpin, C., Pichler, S.L., Maicher, C., Le Bailly, M., 2015. Basel - Gasfabrik: Untersuchung der Koprolithen aus der Grube 283 und der Grube 321: Mikromorphologische und paläoparasitologische Analysen. Universität Basel, Basel.

Rentzel, P., 1994. Geologische Untersuchungen auf dem Gelände der spätlatènezeitlichen Siedlung Basel-Gasfabrik. Eine erste Bilanz, in: Die spätkeltische Zeit am südlichen Oberrhein. Kolloquium Basel, Basel. 17.-18. Oktober 1991. Archäologische Bodenforschung des Kantons Basel-Stadt, Basel, pp. 49–55.

Rentzel, P., 1997. Geologisch-bodenkundliche Untersuchungen an den Niederterrassenfeldern bei Basel unter besonderer Berücksichtigung der spätlatènezeitlichen Fundstelle Basel-Gasfabrik. JbABBS 1994, 31–52.

Rentzel, P., 1998. Ausgewählte Grubenstrukturen aus der spätlatènezeitlichen Fundstelle Basel-Gasfabrik. JbABBS 1995, 35–79.

Rentzel, P., Pümpin, C., Brönnimann, D., 2015. Geoarchäologischer Report: Eine kurze Geschichte des Rheins: Geologische und archäologische Impressionen aus Basel. JbABBS 2014, 108–135.

Rentzel, P., Nicosia, C., Gebhardt, A., Brönnimann, D., Pümpin, C., Ismail-Meyer, K., 2017. Trampling, poaching and the effect of traffic, in: Nicosia, C., Stoops, G. (Eds.), Archaeological soil and sediment micromorphology. Wiley Blackwell, Hoboken, pp. 281–297.

Rodríguez-Morelos, V.H., Soto-Estrada, A., Pérez-Moreno, J., Franco-Ramírez, A., Díaz-Rivera, P., 2014. Arbuscular mycorrhizal fungi associated with the rhizosphere of seedlings and mature trees of Swietenia macrophylla (Magnoliophyta: Meliaceae) in Los Tuxtlas, Veracruz, Mexico. Rev. Chil. de Hist. Nat. 87 (1), 261.

Röpke, A., Dietl, C., 2017. Burnt soils and sediments, in: Nicosia, C., Stoops, G. (Eds.), Archaeological soil and sediment micromorphology. Wiley Blackwell, Hoboken, pp. 173–180.

Roth-Zehner, M., 2005. Sites et structures d'habitat à La Tène finale et au début de l'époque romaine dans la plaine d'Alsace, in: Colloquium Turicense. Siedlungen, Baustrukturen und Funde im 1. Jh. v. Chr. zwischen oberer Donau und mittlerer Rhone (Kolloquium in Zürich, 17./18. Januar 2003). Sites, structures d'habitat et trouvailles du 1er s. av. J.-C. entre le Haut-Danube et la moyenne vallée du Rhône, Zürich. 17.-18. Januar 2003, Lausanne, pp. 209–222.

Sageidet, B.M., 2013. Soil micromorphological evidence from Iron Age land use at Tornby and Mörtlösa in Linköping, Sweden. Quaternary International 315, 116–130.

Schiffer, M.B., 1972. Archaeological context and systemic context. American Antiquity 37 (2), 156–165.

Schiffer, M.B., 1983. Toward the identification of formation processes. American Antiquity 48 (4), 675–706.

Schiffer, M.B., 1987. Formation processes of the archaeological record. University of New Mexico Press, Albuquerque.

Schmidt, D., 2005. Die Lesbarkeit des Abfalls: Zur Entdeckung materieller Unkultur als Objekt archäologischen Wissens, in: Die Dinge als Zeichen. Kulturelles Wissen und materielle Kultur. Internationale Fachtagung an der Johann-Wolfgang-Goethe-Universität Frankfurt am Main 3. - 5. April 2003, Frankfurt. 3.-5. April 2003. Habelt, Bonn, pp. 239–252.

Shahack-Gross, R., 2011. Herbivorous livestock dung: Formation, taphonomy, methods for identification, and archaeological significance. Journal of Archaeological Science 38 (2), 205–218.

Shahack-Gross, R., 2017. Archaeological formation theory and geoarchaeology: State-of-the-art in 2016. Journal of Archaeological Science 79, 36–43.

Shillito, L.-M., 2011. Simultaneous thin section and phytolith observations of finely stratified deposits from Neolithic Çatalhöyük, Turkey: implications for paleoeconomy and Early Holocene paleoenvironment. Journal of Quaternary Science 26 (6), 576–588.

Shillito, L.-M., Matthews, W., 2013. Geoarchaeological Investigations of Midden-Formation Processes in the Early to Late Ceramic Neolithic Levels at Çatalhöyük, Turkey ca . 8550-8370 cal BP. Geoarchaeology 28 (1), 25–49.

Shillito, L.-M., Ryan, P., 2013. Surfaces and streets: phytoliths, micromorphology and changing use of space at Neolithic Çatalhöyük (Turkey). Antiquity 87, 684–700.

Shillito, L.-M., Matthews, W., Almond, M.J., Bull, I.D., 2011. The microstratigraphy of middens: Capturing daily routine in rubbish at Neolithic Çatalhöyük, Turkey. Antiquity 85 (329), 1024–1038.

Steiner, S., 2008. Fundmaterial aus einem Töpferofen: Eine Studie zur Keramikproduktion in der spätlatènezeitlichen Siedlung Basel-Gasfabrik. Unpublizierte Diplomarbeit, Basel.

Steiner, S., 2012. Zur Keramikherstellung in der Spätlatènezeit: Neue Forschungsansätze von Funden aus Basel-Gasfabrik, Schweiz, in: Kern, A., Koch, J.K., Balzer, I., Fries-Knoblach, J., Kowarik, K., Later, C., Ramsl, P.C., Trebsche, P., Wiethold, J. (Eds.), Technologieentwicklung und -transfer in der Hallstatt- und Latènezeit. Beiträge zur internationalen Tagung der AG Eisenzeit und des Naturhistorischen Museums Wien, Prähistorische Abteilung - Hallstatt 2009. Beiträge zur Ur- und Frühgeschichte Mitteleuropas 65. Beier & Beran, Langenweissbach, pp. 145–148.

Stoops, G., 2003. Guidelines for analysis and description of soil and regolith thin sections. Soil Science Society of America, Madison, 184 pp.

Stopp, B., Kunst, G.K., 2005. Sledge runners made of cattle mandibles? – Evidence for jawbone sledges from the Late Iron Age and the Roman Period in Switzerland and Austria, in: Luik, H., Choyke, A.M., Batey, C.E., Lõugas, L. (Eds.), From hooves to horns, from mollusc to mammoth. Manufacture and use of bone artefacts from prehistoric times to the present ; proceedings of the 4th Meeting of the ICAZ Worked Bone Research Group at Tallinn, 26th - 31st of August 2003. Muinasaja teadus 15. Tallinn Book Printers, Tallinn, pp. 187–198.

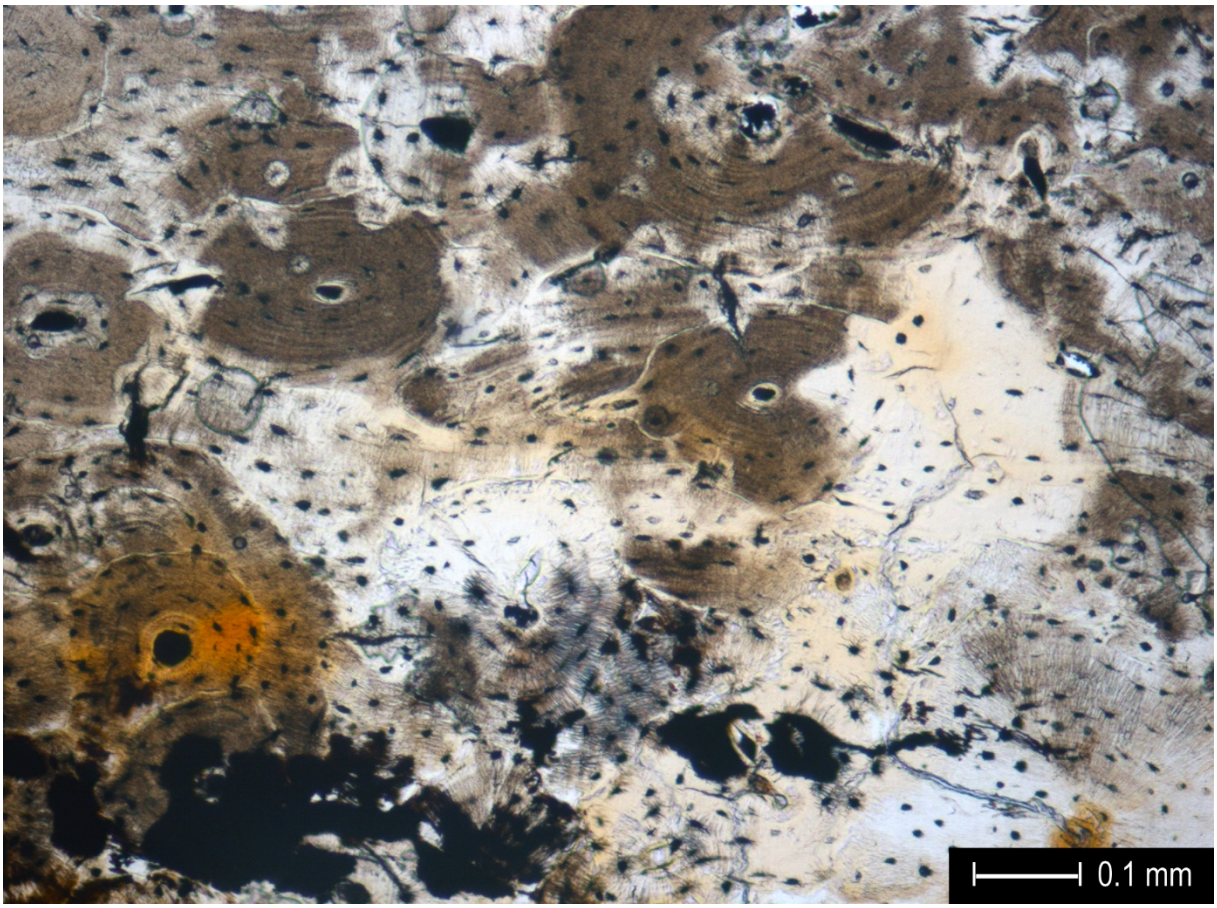
Wendling, H., 2010. Landbesitz und Erbfolge: Ein ethnographisches Modell zur Sozialstruktur und Raumgliederung der mitteleuropäischen Latènezeit, in: Trebsche, P., Müller-Scheessel, N., Reinhold, S. (Eds.), Der gebaute Raum. Bausteine einer Architektursoziologie vormoderner Gesellschaften. Tübinger Archäologische Taschenbücher 7. Waxmann, Münster, New York, München, Berlin, pp. 325–354.

Wick, L., 2015. Das Hinterland von Augusta Raurica: Paläoökologische Untersuchungen zur Vegetation und Landnutzung von der Eisenzeit bis zum Mittelalter. Jahresberichte aus Augst und Kaiseraugst 36, 209–215.

Wolfram, S., 2003. Der Müll, Archäologie und die Steinzeit, in: Fansa, M., Wolfram, S. (Eds.), Müll - Facetten von der Steinzeit bis zum Gelben Sack. Begleitschrift zur Sonderausstellung Müll - Facetten von der Steinzeit bis zum Gelben Sack vom 06. September bis 30. November 2003 in Oldenburg anschließend in Hanau. Schriftenreihe des Landesmuseums für Natur und Mensch Oldenburg 27. von Zabern, Mainz am Rhein, pp. 17–34.

Wouters, B., Devos, Y., Milek, K.B., Vrydaghs, L., Bartholomieux, B., Tys, D., Moolhuizen, C., van Asch, N., 2017. Medieval markets: A soil micromorphological and archaeobotanical study of the urban stratigraphy of Lier (Belgium). Quaternary International 460, 48-64.

[dataset]Brönnimann, D., Röder, B., Spichtig, N., Rissanen, H., Lassau, G., Rentzel, P.; 2019; The Hidden Midden – Geoarchaeological investigation of sedimentation processes, waste disposal practices and resource management at the La Tène settlement of Basel-Gasfabrik (Switzerland) - Dataset; Zenodo; Version 1; http://doi.org/10.5281/zenodo.3256487



Mikroskop-Foto (parallele Polarisatoren) von einem Tierknochen in einem Bodendünnschliff. Mehrere der Osteonen weisen eine deutliche Bioerosion (Wedl Type 2) auf. Ausserdem sind rostbraune und schwarze Eisen-Mangan-Oxidausfällungen zu erkennen.

Kapitel 4

Contextualising the dead – Combining geoarchaeology and osteo-anthropology in a new multi-focus approach in bone histotaphonomy

David Brönnimann, Cordula Portmann, Sandra L. Pichler, Thomas J. Booth, Brigitte Röder, Werner Vach, Jörg Schibler, Philippe Rentzel

Journal of Archaeological Science 98 (2018) 45–58.

DOI: 10.1016/j.jas.2018.08.005

Keywords: histotaphonomy, animal bones, human remains, geoarchaeology, physical anthropology, funerary archaeology, Iron Age, micromorphology

Abstract

Histotaphonomy has become an important area of research in funerary archaeology. It focuses on diagenetic alterations in bone microstructure and the reconstruction of post-mortem processes. Microbial bioerosion is the most common diagenetic change observed in archaeological bone, and its probable causes have been the subject of ongoing discussions.

This paper presents a new integrative approach that combines methods from physical anthropology and geoarchaeology. The aim is to contextualise samples in regard to their sedimentary milieu (sediment type), the sedimentation processes they underwent, and the specific archaeological features they originate from. The analysis is based on 208 human and animal skeletal fragments from the Late La Tène site of Basel-Gasfabrik recovered from various feature types and embedded in different sediments. Both 80 µm and 30 µm thin sections were graded semi-quantitatively on a scale of 0 or 1 to 5 in regard to bacterial attack (BAI), Wedl tunnels (WTI), cyanobacterial attack (CAI), the formation of cracks (CRI), the collagen content (COI), and thermal alterations (HEI).

Our results evinced no correlations between the intensity of bacterial attack and sediment types or sedimentation processes respectively. We therefore deduce that bacterial degradation of bone is mainly caused by endogenous gut bacteria. Wedl tunnels, on the other hand, are chiefly found in bones from exposed surfaces. Bone collagen content, as measured by birefringence, is dependent on a variety of factors, with thermal alteration being among the most important. Unlike the 80 µm sections used in anthropological investigations, the 30 µm thin sections typically utilized in geoarchaeological analyses permitted a reliable distinction of microbial bioerosion types. Our context-oriented

histotaphonomic approach allows detailed conclusions on the causes of microbial bioerosion in bone. Moreover, it provides an important tool for reconstructing the post-mortem biographies of human and animal remains, especially in regard to (multi-stage) mortuary practices and the analysis of sedimentation processes. Thus, this novel approach generates a wealth of information from individual skeletal elements as well as from bone fragments embedded in soil samples.

Introduction

Histotaphonomy is a field of research related to forensics, physical anthropology and palaeoenvironmental investigations, and is concerned with the description, evaluation and interpretation of taphonomic processes in bone on a microstructural level (Bell, 2012a; Jans, 2013, Turner-Walker and Jans, 2008). It provides information on the post-mortem fate of human or animal bodies (death history), on the embedding of bones into the soil, on their sedimentary milieus as well as on post-sedimentary processes. Here, we apply a new approach to assessing the complex interplay of factors affecting the diagenesis of human and animal remains. By combining anthropological and geoarchaeological approaches with histotaphonomy, a variety of questions can be addressed. These include the reconstruction of mortuary practices as well as the identification of animal sacrifices, interpreting (human and animal) depositions, and more generally, the handling of bones as waste, technical raw material, and/or as objects of symbolic value. Thus, histotaphonomy becomes an effective tool not only in funerary archaeology but also for the reconstruction of domestic and/or ritual activities. The Late La Tène site of Basel-Gasfabrik (Switzerland) served as a case study since it has been intensely studied and provides comprehensive (bio-) archaeological, archaeoanthropological and geoarchaeological data.

The development of histotaphonomy

Initial histotaphonomic observations go back to the 19th century, when Carl Wedl described microstructural changes in a human tooth caused by microbial activity (Wedl, 1864). The actualistic experiments of Johannes Weigelt and Ivan Efremov in the first half of the 20th century established the term “taphonomy” in histology (Weigelt, 1927; Efremov, 1940). From the second half of the 20th century onwards, microbial bioerosion in hard tissues was studied systematically (Bell, 2012a). At that time also, Cecil J. Hackett first described three other microbial phenomena in bone in addition to the so-called Wedl tunnels (Hackett, 1981). These microbial bioerosion patterns are collectively called microscopical focal destruction (mfd) and include linear longitudinal, budded, and lamellate mfd (Fig. 1). Robert E. M. Hedges and Andrew R. Millard developed the Oxford Histological Index (OHI), a well-established tool for assessing bone preservation semi-quantitatively (Hedges and Millard, 1995; Millard 2001). In the OHI, bones are graded on a scale of 0 to 5 depending on the percentage of their micro-

structure that is free from microbial bioerosion (Tab. 1).

In archaeology, histotaphonomic research was pursued intensely over the past 20 years. The main focus has been on human remains (Bell and Elkerton, 2008; Booth, 2014; Booth et al., 2015; Booth, 2016; Booth and Madgwick, 2016; Jackes et al., 2001; Hollund et al., 2012; Turner-Walker and Jans, 2008; Turner-Walker and Mays, 2008), while animal bones from archaeological contexts have been analysed only rarely (Huisman et al., 2017; Jans et al., 2004; Jans, 2005; Müller et al., 2011; Nielsen-Marsh et al., 2007). There are, however, a number of studies that have examined microbial bioerosion in modern animal bones (Fernández-Jalvo et al., 2010; Fernández-Jalvo and Andrews, 2016; Kontopoulos et al., 2016; Nicholson, 1996, 1998; Turner-Walker and Peacock, 2008; Turner-Walker, 2012; White and Booth, 2014).

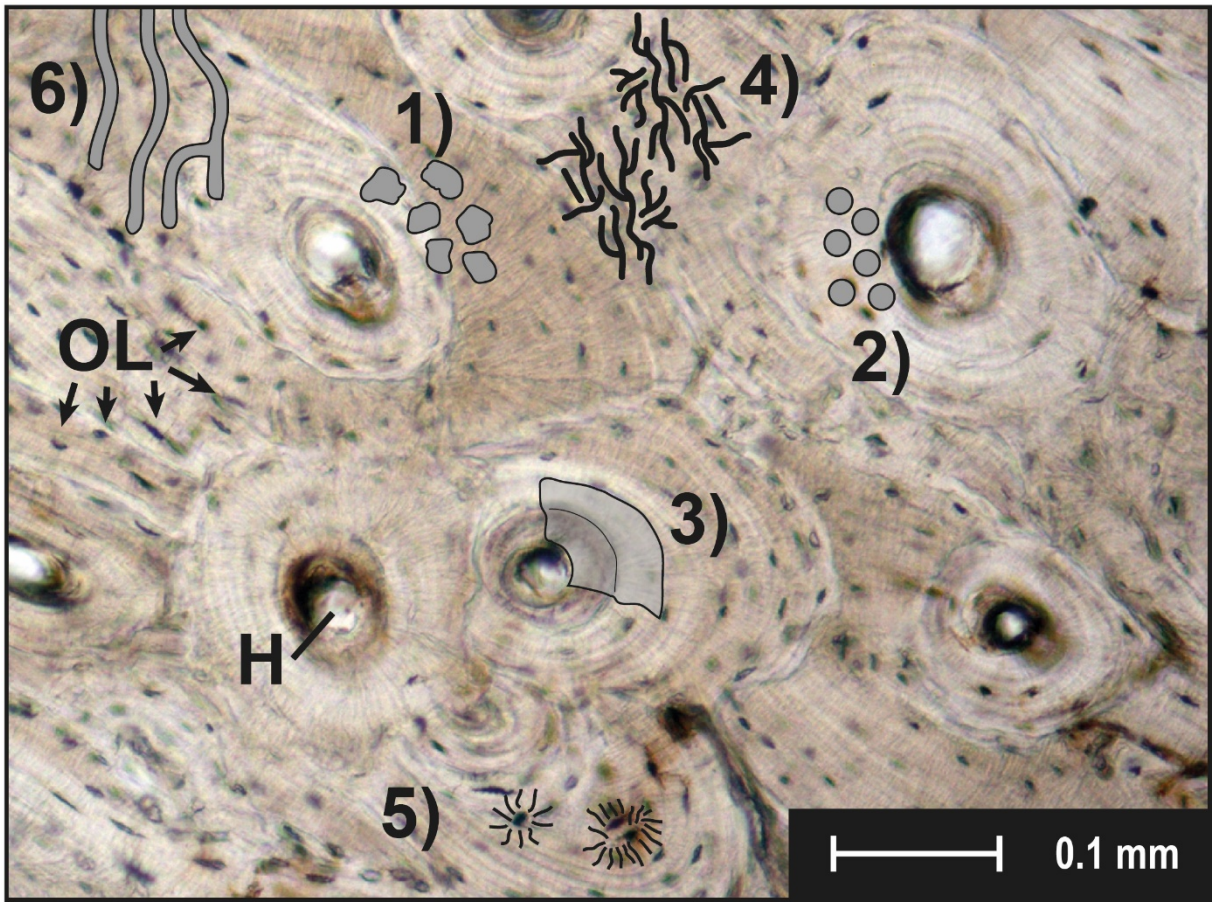


Fig. 1: *Schematic representation of bioerosive features in bone: 1)* budded mfd*; 2)* linear longitudinal mfd*; 3)* lamellate mfd*; 4) Wedl tunnelling; 5) enlarged canaliculi (Wedl type 2); 6) cyanobacteria tunnelling. Note the numerous Haversian canals (H) and osteocyte lacunae (OL).*

Until the 1990s, post-mortem diagenetic alteration of bone – and therefore also microbial bioerosion – was perceived as a postsedimentary process which took place only after skeletonisation. It was thus (implicitly) assumed that microbial degradation could not stem from other factors such as putrefaction during the early phases of decay (Bell, 2012a). The first ones to challenge this assumption were Lynne S. Bell and others (Bell et al., 1996; Child, 1995). Based on SEM observations, Bell concluded that cer-

tain microbial changes in bone occur already during the first few days or weeks after death, induced by endogenous gut bacteria. The idea was taken up and further developed subsequently (Jans et al., 2004; Jans, 2013; Nielsen-Marsh et al., 2007; Trueman and Martill, 2002; White and Booth, 2014). It regards the intensity of bacterial attack as an indicator of the early post-mortem biography of the body, which represents a novel approach to the reconstruction of mortuary practices (Booth et al., 2015; Booth and Madgwick, 2016; Hollund et al., 2012; Jans, 2013). Other authors however suggest that bacterial decomposition is largely due to soil micro-organisms and therefore dependent on exogenous factors (Grine et al., 2015; Kendall et al., 2018; Kontopoulos et al., 2016; Morales et al., 2017; Turner-Walker, 2012).

OHI	intact bone [%]	Description
5	> 95	Very well preserved, virtually indistinguishable from fresh bone
4	> 85	Only minor amounts of destructive foci, otherwise generally well preserved
3	> 67	Clear preservation of some osteocyte lacunae
2	< 33	Clear lamellate structure preserved between destructive foci
1	< 15	Small areas of well-preserved bone, or some lamellar structure preserved by pattern of destructive foci
0	< 5	No original features identifiable, other than Haversian canals

Tab. 1: Oxford Histological Index (OHI) after Hedges and Millard, 1995, table 1.

Histotaphonomy in archaeoanthropology and geoarchaeology

There are some fundamental differences between histological research in physical anthropology and geoarchaeology in regard to topics, methods and the collection of data. Anthropological bone histology focusses on the human individual or on a precise skeletal element, while (archaeological) contexts and specific sediment characteristics are rarely taken into account. Bones are usually histotaphonomically analysed using a polarisation microscope and thin sections (Jans, 2013, Portmann et al., in prep.), by scanning electron microscopy (SEM) (Bell, 2012a, 2012b), or by microtomography (micro-CT), which permits examination of complete bone specimens (Booth et al., 2016). While SEM images offer high resolution even under high magnification, thin sections have the advantage of making changes in colour visible (e.g. due to thermal alteration or staining) and, with the aid of a polarising filter, permitting an assessment of collagen content. Here, skeletal elements and section planes are selected deliberately. Microbial degradation is commonly assessed using either the Oxford Histological Index (OHI) (Hedges & Millard, 1995; Millard 2001) or the General Histological Index (GHI) (Hollund et al., 2012). Both indices rate the degradation in toto without distinguishing between specific kinds of microbial erosion. However, as particular taphonomic indicators like microscopical focal destruction (mfd), cracks, and collagen content can be traced back to different causes, Miranda Jans suggests a more detailed assessment of the different phenomena (Jans, 2013).

Micromorphology, an analytical technique in the frame of geoarchaeological research, examines (archaeological) sediments and features using soil thin sections. In general, bone is not specifically targeted in such analyses; instead, small bone fragments and splinters may be included at random in

such thin sections as components of archaeological layers. Section planes, skeletal elements and species identity of the included bone fragments are unknown and incidental. It is not always possible to distinguish human and animal bone, and anthropological (osteological) data (estimation of age, pathologies) can rarely be gathered. In geoarchaeological thin sections, bone fragments are identified and quantified; however, little attention is usually paid to their preservation, besides the evaluation of thermal alterations (Pérez et al., 2017; Reidsma et al., 2016; Villagran et al., 2017b). The practice of describing histotaphonomical features and microstructural changes in bone in more detail is only a recent development in geoarchaeological studies (Huisman, 2009; Huisman et al., 2017; Ismail-Meyer and Rentzel, 2017; Villagran et al., 2017a), and soil thin sections still represent a largely untapped yet potentially profitable source of taphonomic information.

The aim of our histotaphonomic analysis was to evaluate the various taphonomic phenomena in detail considering the individual data of each bone/fragment and contextualizing these comprehensively with regard to archaeological features and sediment types. In order to do so, geoarchaeological and anthropological methods were combined using an integrative approach. The focal questions were as follows:

1. Which phenomena of microbial bioerosion and other taphonomic characteristics (collagen preservation, crack intensity, thermal alteration) can be observed?
2. Are there any differences in the quality or quantity of these characteristics between
    a. human and animal remains
    b. bone embedded in different sediment types
    c. bones from discrete archaeological features

Materials and methods

The Basel-Gasfabrik La Tène central site

The La Tène central site of Basel-Gasfabrik (Switzerland, chiefly 200/150-80 BC) is situated in today's city of Basel in the north-west of Switzerland (Fig. 2). It includes an unfortified settlement area of ca. 150,000 m2 with hundreds of archaeological structures (pits, ditches, post holes), archaeological layers as well as two cemeteries with about 170 inhumation graves (Hecht and Niederhäuser, 2011). Furthermore, a number of complete human skeletons as well as hundreds of isolated human bones were recovered from various features within the settlement, some of which bear traces of peri- and post-mortem manipulations (Pichler et al., 2013; Pichler et al., 2015; Pichler, in prep.). The human remains are currently interpreted as the relicts of various, in part multi-stage mortuary practices (Harding, 2016; Jud, 2008; Pichler et al., in prep.). In addition to a large number of archaeological finds, there are hundreds of thousands of faunal remains. Pit 321, for example, which was about 3 m wide

and at least 2.7 m deep, yielded the complete skeletons of two young men as well as hundreds of animal bone fragments embedded in the dark, charcoal-rich loam used to fill in the pit. This will be discussed in more detail in ch. 3.4, where pit 321 will serve as a case study.

The investigation of Basel-Gasfabrik has been underway since 1911, with modern methods being used for more than 25 years. Furthermore, the multifarious treatment of the dead in Basel-Gasfabrik has recently been investigated as part of an interdisciplinary research project (Pichler et al., 2017). All human remains from the site were analysed by classical osteological methods (White and Folkens, 2010) while 25 specifically selected human skeletal elements were examined histologically (Portmann, 2015; Portmann and Pichler, in prep.). Moreover, zooarchaeological data of several hundred thousand faunal remains are at hand as well as extensive geoarchaeological information on sediment types and sediment formation processes (Brönnimann and Rissanen, 2017; Brönnimann et al., in prep; Rentzel, 1997, 1998; Rentzel and Narten, 2000, Stopp, 2008, Schaer and Stopp, 2005). This favourable setting makes Basel-Gasfabrik an ideal site for our novel interdisciplinary approach.

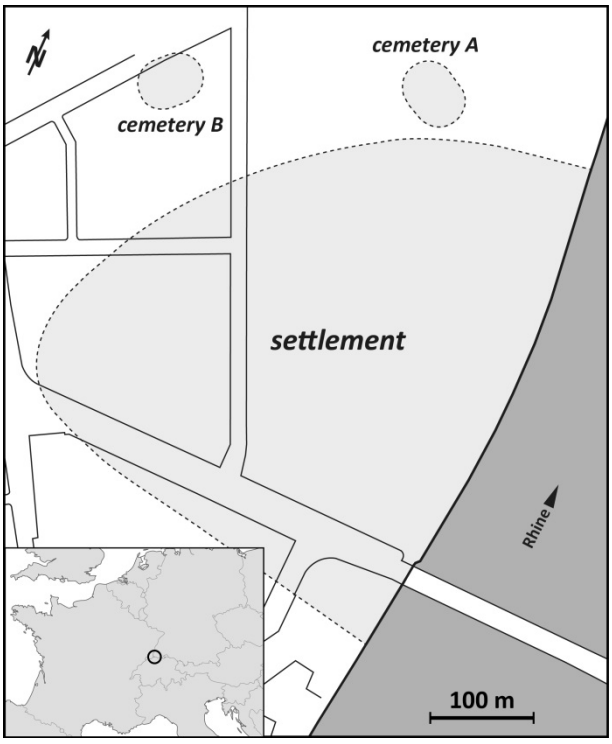


Fig. 2: Location of the Basel-Gasfabrik site in north-western Switzerland (inset). Expansion of the settlement (grey area) and associated cemeteries A and B.

Histological samples

The archaeoanthropological sample consisted of a total of 124 thin sections of 25 human skeletal elements belonging to 20 adult individuals, both male and female (see supplementary information). Amongst them, five complete skeletons (4 burials from the cemeteries and one from a settlement pit) were sampled on both, the right humerus and femur. In addition, 15 isolated bones (5 femora and 10 humeri) from various archaeological features from within the settlement were analysed. Before being sampled they were examined using classical-osteological methods (Pichler in prep.; Portmann and

Pichler, in prep).

For the animal bone sample, 210 soil thin sections from eight excavation campaigns were examined in regard to randomly embedded bone fragments. From a statistical point of view, this corresponds to the principle of simple random sampling. Drawing on the accumulated knowledge of routine geoarchaeological investigations, the use of the thin sections rather than complete bone specimens from zooarchaeological analyses ensured the best possible correlation of samples and sediments. A total of 183 bone fragments were evaluated histotaphonomically and the corresponding sediments were characterised (see supplementary information). The analysed fragments, as far as they were identifiable, all represent animal bones, which is also supported by statistical considerations on the frequency of animal versus human bones at the site (ca. 1'600'000 animal bones versus a few thousand human remains). The soil thin sections were taken from various features including trampled loamy surfaces (36 layers), pits (n = 10), ditches (n = 3), one post hole and two shallow depressions (see supplementary information).

Methods

Human skeletal elements

Rectangular transverse sections of compact bone measuring 10 x 15 mm were taken on humeri and femora at the anterior side of the proximal third of the diaphysis, perpendicular to the longitudinal axis of the bone. Samples were embedded in epoxy resin (Biodur E1/E12, Biodur Products, Heidelberg, D) following the protocol for undecalcified bone (Hagens, 1979; Schultz, 2001; Nicklisch, 2013). The sample blocks were then cut into five consecutive thin sections each using a saw microtome (Leica SP1600); in one case only four cuts were made due to poor preservation. As the human thin sections were originally meant to be used for age estimation and histopathology (Portmann, 2015; Portmann and Pichler, in prep.) a section thickness of 70-80 µm was selected. For the histotaphonomic analysis, we examined all 124 thin sections using transmitted light microscopy with polarizer and a λ/2 wave lambda plate (Schultz, 2001). Since no significant differences between separate thin sections of the same bone were detected, results are reported for individual bones, not for each thin section (see supplementary information).

Animal bones in geoarchaeological samples

Soil samples were taken en bloc from profiles during the course of the excavations. These block samples (usually 20–30 x 10 x 10 cm) were hardened with epoxy resin (Laromin C260, Araldite DY 026 SP, acetone), preserving the texture and microstructure of the original settings, and cut into polished sections using a diamond blade. The covered thin sections of 30 µm thickness were then processed in a specialised laboratory in Braunschweig (Germany). For the analysis, we used an optical microscope

(Leica DM-RXP) with polarisation filter and 16-630x magnification in accordance with the guidelines for the micromorphological examination of archaeological sediments (Stoops, 2003; Goldberg and Macphail, 2006). Sediments were analysed with regard to grain size, texture and content of calcium carbonate.

2.3.4 Statistical analyses

For the statistical analyses we considered the indices defined as variables with an ordinal scale. The Wilcoxon rank sum test was used to compare two groups, the Kruskal-Wallis-test to compare three groups. For both tests an adjustment for ties was used. Associations between two indices were assessed using the Spearman correlation coefficient. All computations were made with Stata 14.2.

2.3.4 Nomenclature and acquisition of data

Histotaphonomic features of human remains and animal bone fragments were characterised based on Hackett's terminology (Hackett, 1981), and on the work of Jans and Bell (Bell, 2012b; Jans, 2013). Budded mfd, linear longitudinal mfd and lamellate mfd were summed up as bacterial attack (Fernández-Jalvo and Andrews 2016; Hackett, 1981; Jans, 2013; Trueman and Martill, 2002). Bacterial attack and Wedl tunnels were each graded on a scale of 0 to 5, similar to the OHI (after Hollund et al., 2012; 5 = perfect preservation; 0 = completely destroyed microstructure; Tab. 1) and labelled as Bacterial-Attack-Index (BAI) and Wedl-Tunnel-Index (WTI) respectively (Tab. 2). The same applies to suspected cyanobacterial attack (Cyanobacterial-Attack-Index = CAI) and the intensity of crack formation (Crack-Index = CRI) (Tab. 2). The former are easily distinguished from mfd features due to their larger diameter and their characteristic shape and appearance within the bone (Fig. 1). Collagen preservation was likewise graded on a scale of 1 to 5 (5 = perfect preservation; 1= completely dissolved), based mainly on the intensity of birefringence when using crossed polarisers during microscopy (collagen index = COI). Although both bioapatite and collagen produce interference colours, experiments on fresh bone show that the occurrence of interference colours and particularly their strength is mostly due to collagen (Karkanas and Goldberg, 2010; Villagran et al., 2017a). Thermal alteration was determined on the basis of bone colour, mineral structure (collagen fibres, formation of crystals after Fernández Castillo et al., 2013a and Fernández Castillo et al., 2013b) and the recognisability of characteristics in the bone microstructure (Heat-Index = HEI) using a modified scale after Squires et al., 2011 (Tab. 3). Intermediate stages were introduced (0.5, 1.5 and 2.5), whereby 0.5 was selected for probable thermal alteration. Colouring can also occur due to iron- or manganese precipitations, which is generally easily distinguished from thermal alteration.

Index	Sign.	Scale	Description
Bacterial-Attack-Index	BAI	0-5	Intensity of bacterial attack (*budded mfd, linear longitudinal mfd, lamellate mfd*), based on the OHI (% of intact bone microstructure)
Wedl-Tunnel-Index	WTI	0-5	Intensity of Wedl tunnels (supposed fungal attack), based on the OHI (% of intact bone microstructure)
Cyanobacterial-Attack-Index	CAI	0-5	Intensity of cyanobacterial attack, based on the OHI (% of intact bone microstructure)
Crack-Index	CRI	0-5	Intensity of crack formation, based on the OHI (% of intact bone microstructure)
Collagen-Index	COI	1-5	Collagen preservation, based on the intensity of birefringence using crossed polarisers
Heat-Index	HEI	0-3 (0.5-steps)	Thermal alteration, based on colour, collagen content, preservation of the microstructure after Squires et al., 2011

Tab. 2: Indices used in our research and their definitions: Bacteria-Attack-Index (BAI), Wedl-Tunnel-Index (WTI), Cyanobacterial-Attack-Index (CAI), Crack-Index (CRI) and Collagen-Index (COI).

HEI	colouring	bone microstructure	mineral structure	description
0	-	no change in microstructure (100% preserved)	collagen fibres well visible	no thermal alteration
0.5	weak, orange-brown	no change in microstructure (100% preserved)	collagen fibres well visible	probable thermal alteration (uncertain)
1	weak, orange-brown	minor changes in microstructure (> 80% preserved)	collagen fibres visible; longitudinal microfractures	weak thermal alteration
1.5	distinct, orange-brown	minor changes in microstructure (> 80% preserved)	collagen fibres still visible; longitudinal microfractures; first formation of crystalline structures	moderate thermal alteration
2	distinct, brown	partly destroyed microstructure (< 50% preserved)	formation of large (cubic) crystalline structures	distinct thermal alteration
2.5	strong, brown-grey	mostly destroyed microstructure (only Haversian canals visible; < 20% preserved)	formation of large (cubic) crystalline structures	strong thermal alteration
3	strong, brown-grey	microstructure destroyed (0% preserved)	the granular structure has completely disappeared	very strong thermal alteration

Tab. 3: Definition of the heat index (HEI), based on the three-stage scale of Squieres et al., 2011, table 2 and after Fernández Castillo et al., 2013a and Fernández Castillo et al., 2013b. This scale was expanded by stages 0.5, 1.5 and 2.5, where stage 0.5 denotes bone with assumed but uncertain thermal alteration.

Results

Methodological results

The analysis of the anthropological and the geoarchaeological samples showed that the assessment of the collagen content (COI) and crack intensity (CAI) are not affected by the thickness of the thin sections. However, there were major differences between the thin sections of 30 µm and 80 µm thickness when it came to the identification of microbial bioerosion. As the 2-10 µm sized microbial structures would overlap several times in the 80 µm anthropological thin sections, differentiation of bioerosive patterns was hampered, especially in poorly preserved bone (Fig. 3). While grading these thin sections according to the OHI was possible, Wedl tunnels and bacterial alteration could not always be distinguished (see supplementary information).

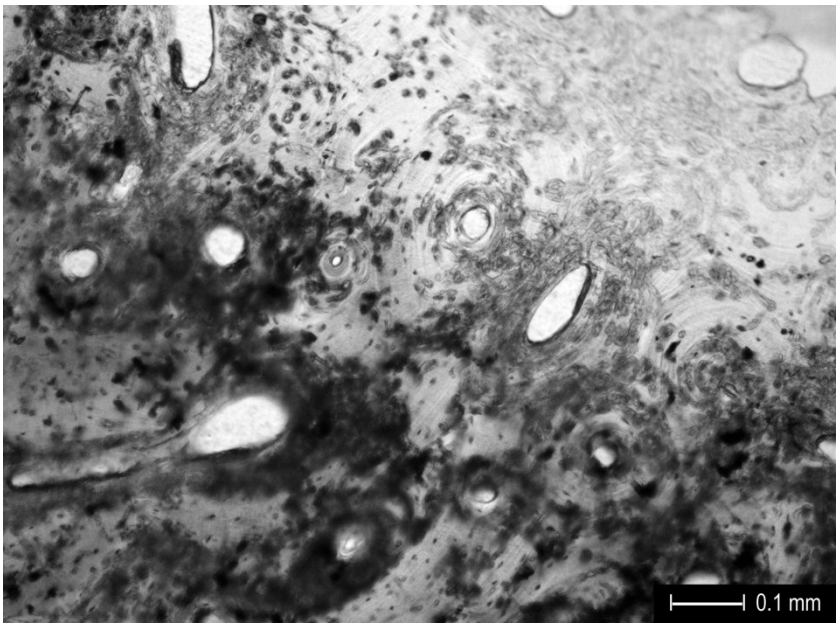


Fig. 3: *Microscope photo of a faulty 80 µm thin section (human bone), which becomes increasingly thin top right. In the thin part linear longitudinal mfd around Haversian canals are recognized without difficulty, while in the thicker part (bottom left) they appear a diffuse and undifferentiated grey mass. Plane polarized light (PPL), 100x magnification.*

Histotaphonomic features

The thinness of the soil thin sections (30 µm) meant that differentiation between Wedl tunnels and bacterial mfd was mostly unproblematic. Our research has shown that budded mfd (Fig. 4A) are frequently grouped around Haversian canals (Fig. 3), while linear-longitudinal mfd tend to run parallel to the bone's lamellar structure (Fig. 4B). Wedl tunnels, on the other hand, occurred independent of bone microstructure and were easily distinguishable from bacterial attack due to their dendritic form and small diameter (Fig. 4C and 4F). Lamellate mfd showed up rarely and were only found in conjunction with other kinds of bacterial degradation (Fig. 4D). Enlarged canaliculi (also called Wedl type 2; Jans, 2008; Trueman and Martill, 2002) were encountered mainly around osteocyte lacunae (Fig. 4E) and especially near Haversian canals (Fig. 4F). These enlarged canaliculi do not look like the phenomenon on modern bones that Yolanda Fernández-Jalvo and co-authors interpreted as being the result of acidic erosion (Fernández-Jalvo et al., 2010; Fernández-Jalvo and Andrews, 2016). Suspected cyanobacterial attack was rarely observed and limited to the outward 1-2 mm bone surfaces (Fig. 4G), which is consistent with previous observations (Bell and Elkerton, 2008; Huisman et al., 2017; Turner-Walker, 2008, 2012; Turner-Walker and Jans, 2008). Iron-manganese precipitations were regularly found on bone surfaces, in Haversian canals, osteocyte lacunae, Wedl tunnels, enlarged canaliculi, and more rarely in cracks (Fig. 4D, E, F and 4H). Wedl tunnels (Fig. 4C and 4F) and all types of microscopical focal destruction (mfd) (Fig. 1) were observed in both human and animal bone fragments (see supplementary information); however, there were some differences in their quality and quantity. 32% of the 208 analysed bone specimens showed signs of bacterial attack; 42% displayed Wedl tunnels (Tab. 4). Comparing their intensity, one finds that bacterial attack caused the extensive or complete destruction of bone microstructure (BAI = 0-2) in 21% of cases, whereas this is considerably lower in Wedl tunnels

(WTI = 0-2; 9%). Only 6% of bones showed suspected cyanobacterial attack (CAI), and in all cases it was not very marked (Tab. 4). Cracks, however, were detected in almost half of the bones (44%), though a marked or severe degradation was rare (CRI = 0-3; 15%).

Collagen content varied considerably (Tab. 4): while 26% of samples exhibited (very) good preservation (COI = 4-5), 33% showed a moderate (COI = 3) and 40% a (very) bad collagen preservation (COI = 1-2). The analysis of thermal alterations (HEI; Tab. 4) showed that about a third of the bones (32%) displayed discernible burn marks (HEI = 1-3); 14% were strongly burnt (HEI = 2-3) and about another third of the bones showed no sign of thermal alteration at all (HEI =0; 35%). However, for 27% of the bones it was not possible to distinguish between burnt and unburnt (HEI = 0.5). All burnt bones (HEI = 1-3) represent probable animal bone fragments, while the human remains showed no conclusive thermal alterations (see supplementary information). A comparison of thermal alterations (HEI) and collagen content (COI) produced a statistically significant correlation (correlation coefficient = -0.42, p = 0.0000) (Tab. 5, Fig. 5). Thus, with increased burning, the collagen content decreases markedly.

	BAI		WTI		CAI		CRI		COI	
index	num.	%	num.	%	num.	%	num.	%	num.	%
5	142	68	107	51	186	89	114	55	16	8
4	11	5	55	26	8	4	61	29	37	18
3	11	5	25	12	4	2	28	13	68	33
2	11	5	10	5	0	0	3	1	51	25
1	10	5	3	1	0	0	0	0	32	15
0	23	11	5	2	0	0	0	0		
indet	*0*	*0*	*3*	*1*	*10*	*5*	*2*	*1*	*4*	*2*

	HEI	
index	num.	%
0	73	35
0.5	57	27
1	25	12
1.5	12	6
2	19	9
2.5	7	3
3	4	2
indet	*11*	*5*

Tab. 4: *Observed histotaphonomic features in animal and human bone (n=208). BAI = Bacterial-Attack-Index; WTI = Wedl-Tunnel-Index; CAI = Cyanobacteria-Attack-Index; CRI = Crack-Index; COI = Collagen-Index; HEI = Heat-Index. Indet = not observable due to severe degradation.*

	Collagen-Content-Index (COI)													
index	HEI 0 (n=73)		HEI 0.5 (n=57)		HEI 1 (n=25)		HEI 1.5 (n=12)		HEI 2 (n=19)		HEI 2.5 (n=7)		HEI 3 (n=4)	
	num.	%	num.	%	num.	%	num.	%	num.	%	num.	%	num.	%
5	13	18	2	4	1	4	0	0	0	0	0	0	0	0
4	22	30	10	18	5	20	0	0	0	0	0	0	0	0
3	16	22	26	46	12	48	2	17	5	26	1	14	1	25
2	14	19	14	25	4	16	9	75	5	26	1	14	0	0
1	7	10	5	9	2	8	1	8	8	42	5	71	3	75
0	0	0	0	0	0	0	0	0	0	0	0	0	0	0
indet	*1*	*1*	*0*	*0*	*1*	*4*	*0*	*0*	*1*	*5*	*0*	*0*	*0*	*0*

Tab. 5: *Comparison of collagen content (COI) in animal bone fragments (n=197) in relation to thermal alteration (HEI). Indet = not observable due to severe degradation.*

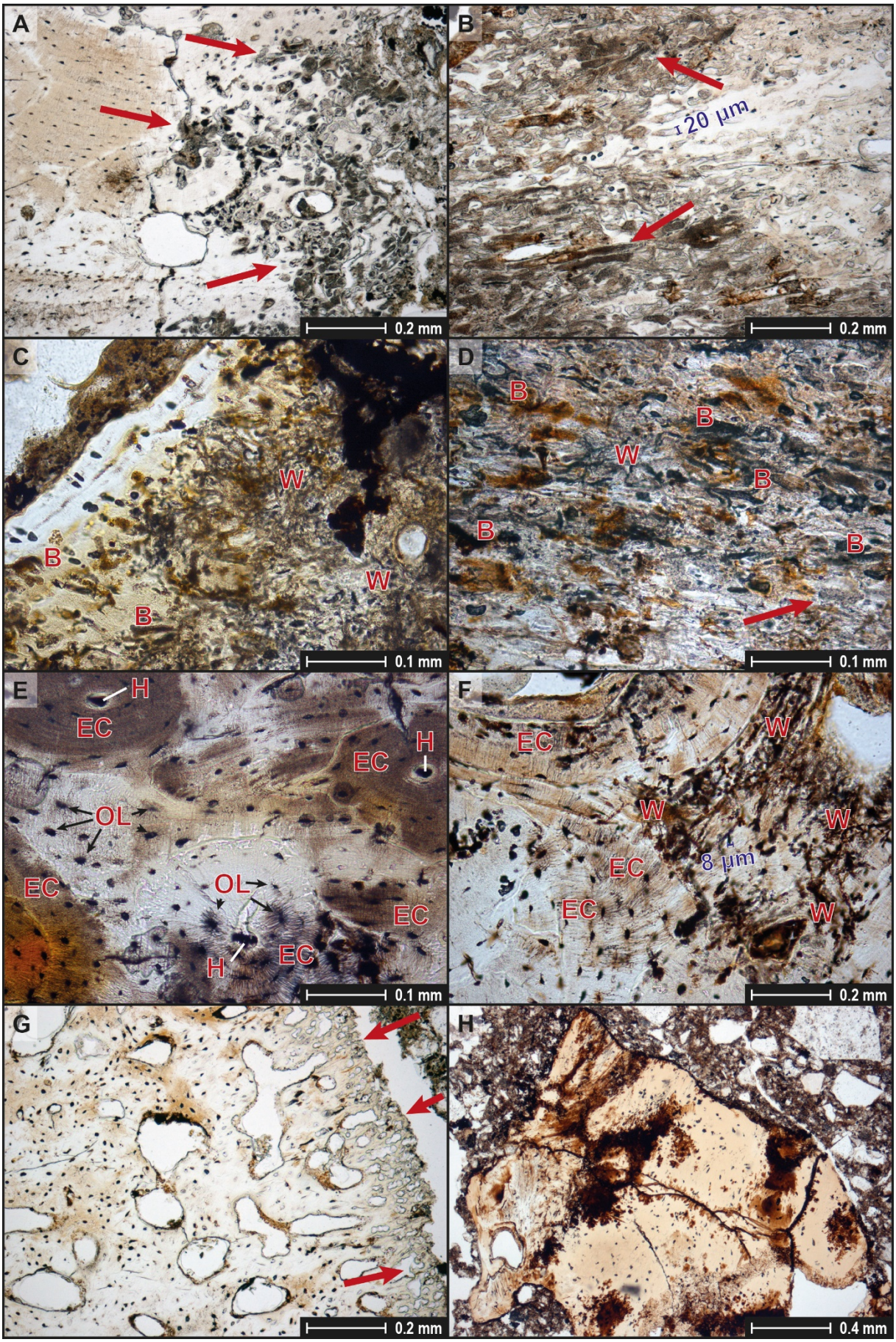

A
0.2 mm
B
20 µm
0.2 mm
C
W
B
W
B
0.1 mm
D
B
B
W
B
B
B
0.1 mm
E
H
EC
EC
H
OL
EC
OL
EC
H
EC
0.1 mm
F
EC
W
W
W
EC
8 µm
EC
W
0.2 mm
G
0.2 mm
H
0.4 mm

Fig. 4: *Histotaphonomic features of bone fragments in 30 µm geoarchaeological thin sections. All images in plane polarized light (PPL) and 100x magnification, unless indicated otherwise.* ***4A)*** *Distinct microbial degradation; arrows indicate budded tunnelling.* ***4B)*** *Intense microbial degradation, mainly linear longitudinal tunnelling (arrows). Blue letters: diameter of the budded tunnels (20 µm).* ***4C)*** *Wedl tunnels, often with reddish-brown iron-manganese-precipitations.* ***4D)*** *Bone extensively degraded by bacterial and fungal attack with suspected Wedl tunnelling (W), budded tunnels (B) and lamellate mfd (arrow); 200x magnification.* ***4E)*** *Strongly pronounced enlarged canaliculi (EC; Wedl type 2) mainly grouped around Haversian canals (H) and appearing to emanate from osteocyte lacunae (OL); 200x magnification.* ***4F)*** *Wedl tunnels (W) filled with reddish-brown iron-manganese precipitations, and enlarged canaliculi (EC; Wedl type 2) emanating from osteocyte lacunae. Blue letters: diameter of Wedl tunnels (8 µm); 200x magnification.* ***4G)*** *Suspected cyanobacterial attack (arrow) on the surface of a bone chip.* ***4H)*** *Distinct reddish-brown precipitations (presumably iron oxide) along tunnels and cracks and on the bone surface; 50x magnification.*

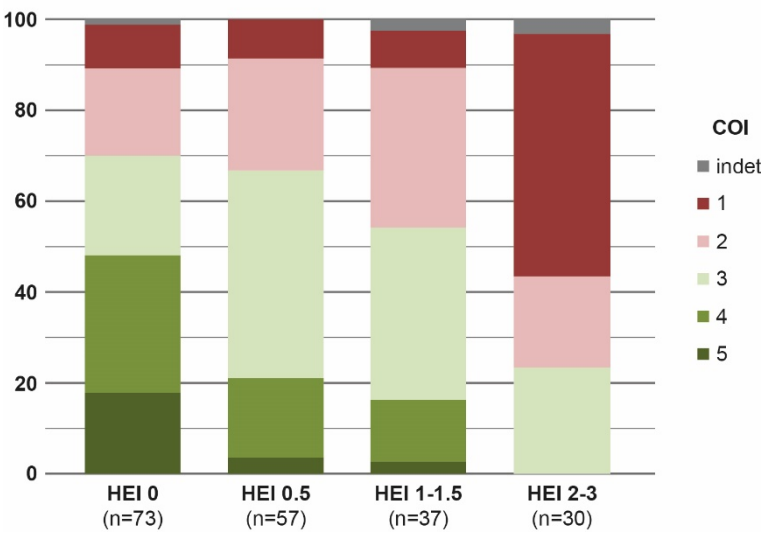


Fig. 5: *Comparison of collagen content (COI) in relation to thermal alteration (HEI); data shown as percentages.*

Histotaphonomic patterns in context

For the contextualisation of the histotaphonomic data, we focused on bacterial attack, Wedl tunnels and on collagen content. Neither the overprint by cracks or cyanobacteria plays a major role in our research questions, which is why the corresponding results are not included here.

Differences between human and animal bones

When comparing the BAI (Bacterial Attack Index) of the 25 human samples and of the 184 animal bone fragments, (Tab. 5; Fig. 6) there are some major differences. While only 23% of the animal bone fragments were affected, the human skeletal elements, with one exception, all exhibit signs of bacterial degradation (96%). The bacterial attack is very pronounced (BAI = 0-2) in most human bones (92%), but not in animal bone fragments (12%). In terms of the WTI (Wedl-Tunnel-Index), the differences are significantly less marked, albeit some of the human bones could not be assessed due to the intensity of the bacterial attack (given as indet). Overall, human skeletal elements were affected by Wedl tunnels somewhat more frequently (56%) than animal bone fragments (46%), though the latter showed severe degradation by Wedl tunnels more often (WTI = 0-2; 9%) than human bones (4%). In

summary, the difference between human and animal remains in the BAI is statistically highly significant (p = 0.0000), whereas no such difference can be seen in the WTI (p = 0.4055). The same can be seen when only the unburnt bones are taken into account (see supplementary information).

	BAI human		BAI animal		WTI human		WTI animal	
index	num.	%	num.	%	num.	%	num.	%
5	1	4	141	77	8	32	99	54
4	0	0	11	6	11	44	44	24
3	1	4	10	6	2	8	23	13
2	1	4	10	6	0	0	10	6
1	2	8	8	4	1	4	2	1
0	20	80	3	2	0	0	5	3
indet	*0*	*0*	*0*	*0*	*3*	*12*	*0*	*0*

Tab. 6: *Comparison of bacterial attack (BAI) and suspected fungal attack (Wedl tunnels = WTI) in human (n=25) and animal bones (n=183). Indet = not observable due to severe degradation.*

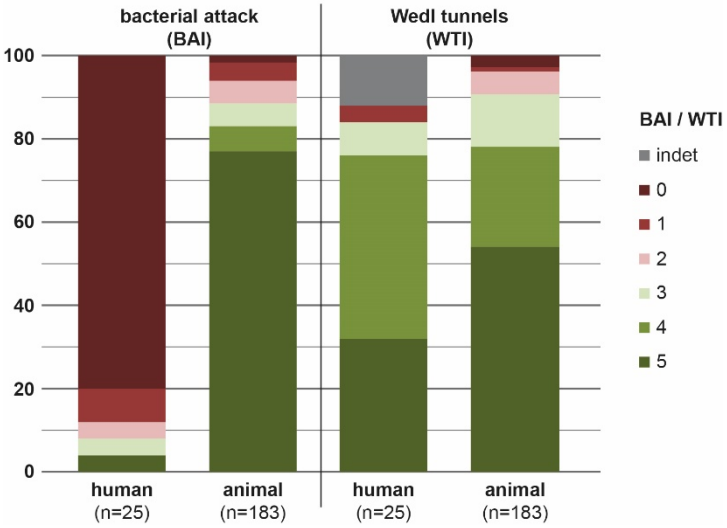


Fig. 6: *Comparison of bacterial attack (BAI) and Wedl tunnels (WTI, suspected fungal attack) in human (n=25) and animal bone (n=183); data shown as percentages.*

Differences between sediment types

As some of the human bones stem from old excavations, we do not have any knowledge about their specific (geo-) archaeological contexts. Hence, only the (animal) bone fragments embedded in the geoarchaeological thin sections were considered for this chapter. For these, three sediment types were distinguished: LB (B horizon loam), LC (C horizon loam) and TSM (topsoil material), all of which differ in regard to their content of calcium carbonate, their pedological characteristics and embedded components (Tab. 7). Three bone fragment samples from archaeological features other than ditches, pits and exposed surfaces were excluded, bringing the sample size to n=180 bone fragments.

The majority of bone fragments (n = 104) were allocated to sediment type TSM, while fewer occurred in LB (n = 60) and LC (n = 16). Those from TSM were somewhat less affected by bacterial attack (84% with a BAI = 5) than the ones from LC (75%) and LB (68%). However, these differences are not statistically significant (p = 0.1201) (Tab. 8; Fig. 7). The same applies to the intensity of the bacterial attack (BAI = 0-2; TSM = 11%, LC = 6%, LB = 13%). There is, however, a significant difference between sediment type TSM and the sediment types LC and LB when considering the overprint by Wedl tunnels (p = 0.0001). Only 33% of bones in TSM show Wedl tunnels, whereas in LB and LC, 68% resp. 56% were

affected (Fig. 7). Again, the same tendencies can be observed if only unburnt bones were considered (see supplementary information).

When assessing the collagen content, only bone fragments without thermal alterations (HEI= 0-0.5; n = 113) were considered, as collagen is destroyed under the effect of heat (Fernández Castillo et al., 2013a; Fernández Castillo et al., 2013b; Reidsma et al., 2016; Villagran et al., 2017a) (see also ch. 4.1.3). Collagen was significantly better preserved in the calcareous sediment types TSM and LC than in sediment type LB (P = 0.0003). This is demonstrated both by the proportion of (very) well-preserved bones (COI = 4-5; TSM = 46%, LC = 43%, LB = 22%) and the percentages of bones with low collagen content (COI = 1-2; TSM = 17%, LC = 29%, LB = 56%) (Fig. 7).

type	description	lime cont.	charcoal	ash	coprolites	Fe/Mn	pH
LB	**Loam B horizon:** Silty-sandy loam, mainly based on B-horizon material	-	+	-	-	++	6.8 - 7.5
LC	**Loam C horizon:** Silty-sandy loam, mainly based on C(v)-horizon material	++	+	-	-	+	7.7 - 8.0
TSM	**Topsoil material:** Silty-sandy, gravelly loam, partly based on topsoil-material and on rhine gravel	++/+++	++/+++	+/+++	++	+++	7.5 - 7.7

Tab. 7: *Summary of the characteristics of micromorphologically analysed sediment types with embedded bone fragments. The various components like e. g. charcoal are listed semiquantitatively: - not present; + isolated; ++ frequent; +++ numerous.*

	BAI						WTI						COI					
	LB		LC		TSM		LB		LC		TSM		LB		LC		TSM	
index	num.	%	num.	%	num.	%	num.	%	num.	%	num.	%	num.	%	num.	%	num.	%
5	41	68	12	75	87	84	19	32	7	44	70	67	0	0	3	21	10	19
4	5	8	3	19	3	3	12	20	4	25	28	27	10	22	3	21	15	28
3	6	10	0	0	3	3	17	28	2	13	4	4	10	22	4	29	19	35
2	5	8	0	0	4	4	7	12	2	13	1	1	17	38	4	29	5	9
1	2	3	1	6	5	5	1	2	1	6	0	0	8	18	0	0	4	7
0	1	2	0	0	2	2	4	7	0	0	1	1						
indet	*0*	*0*	*0*	*0*	*0*	*0*	*0*	*0*	*0*	*0*	*0*	*0*	*0*	*0*	*0*	*0*	*1*	*2*

Tab. 8: *Comparison of bacterial attack (BAI) and suspected fungal attack (Wedl tunnels = WTI) in animal bone fragments (n=180) in relation to sediment type. For collagen content (COI), only unburned bones (n=113) were scored. Indet = not observable due to severe degradation.*

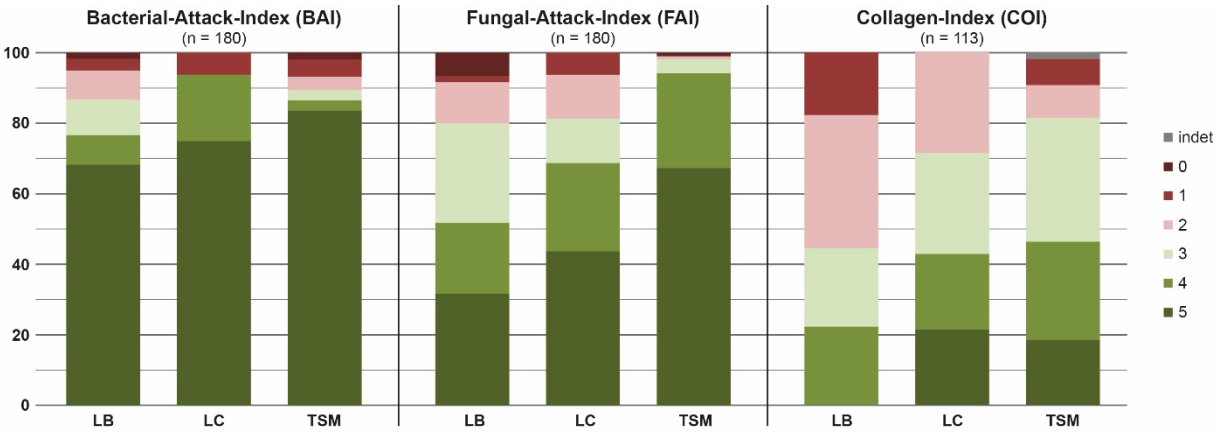


Fig. 7: *Comparison of bacterial attack (BAI), Wedl tunnels (WTI, suspected fungal attack) and collagen content (COI) in relation to sediment type; data shown as percentages.*

Differences between archaeological features

Only the bone fragments from geoarchaeological thin sections were taken into account when evaluating the results in regard to archaeological feature types in order to ensure for the data to be comparable. Here, we distinguished between loamy, possibly trampled surfaces (n = 72), pits (n = 89) and ditches (n = 17). This comparison showed that bone fragments from pits are less frequently affected by bacteria (17%) than those from surfaces (31%). However, the percentage of bone fragments extensively degraded by bacteria (11%, BAI = 0-2) is about the same for both (Tab. 9; Fig. 8). Bone fragments found in ditches exhibit less bacterial attack; however, this may also be due to the small number of samples (n = 17) and the small size of the fragments. Overall, there is no clear correlation between bacterial attack and archaeological feature types (p = 0.0423). The WTI provides a completely different picture (Fig. 8). Only 27% of bone fragments found in pits show Wedl tunnels, whereas the numbers are far higher for fragments from ditches (53%) or surfaces (69%). The same is the case for the intensity: no fragments found in pits show extensive overprint by Wedl tunnels (WTI = 0-2, 0%); while 12% of fragments from ditches and 21% of fragments from surfaces were strongly affected. This trend is confirmed by statistical analyses which show a highly significant correlation between Wedl tunnels (WTI) and archaeological feature types (p = 0.0001).

Again we used only the unburnt bones (HEI= 0-0.5; n = 110) when comparing the collagen content in bone fragments from different features. Our evaluation showed that more than half of the bone fragments from pits (56%) exhibit a high collagen content; only 17% showing a low collagen content (COI = 1-2). By comparison, the ratio for bone fragments found on surfaces (22% high COI; 51% low COI) is roughly the opposite (Fig. 8). This correlation between collagen content and the type of archaeological feature has also been statistically verified and confirmed (p = 0.0001).

	BAI						WTI						COI					
	pits		ditches		surfaces		pits		ditches		surfaces		pits		ditches		surfaces	
index	num.	%	num.	%	num.	%	num.	%	num.	%	num.	%	num.	%	num.	%	num.	%
5	74	83	16	94	50	69	65	73	8	47	22	31	10	24	3	21	0	0
4	2	2	1	6	8	11	22	25	5	29	17	24	13	32	2	13	12	22
3	3	3	0	0	6	8	2	2	2	12	18	25	11	27	7	50	15	27
2	4	4	0	0	3	4	0	0	1	6	9	13	3	7	2	14	21	38
1	4	4	0	0	4	6	0	0	0	0	2	3	4	10	0	0	7	13
0	2	2	0	0	1	1	0	0	1	6	4	6						
indet	*0*	*0*	*0*	*0*	*0*	*0*	*0*	*0*	*0*	*0*	*0*	*0*	*0*	*0*	*0*	*0*	*0*	*0*

Tab. 9: *Comparison of bacterial attack (BAI) and suspected fungal attack (Wedl tunnels = WTI) in animal bone fragments (n=178) in relation to archaeological feature type. For collagen content (COI), only unburned bones (n=110) were scored. Indet = not observable due to severe degradation.*

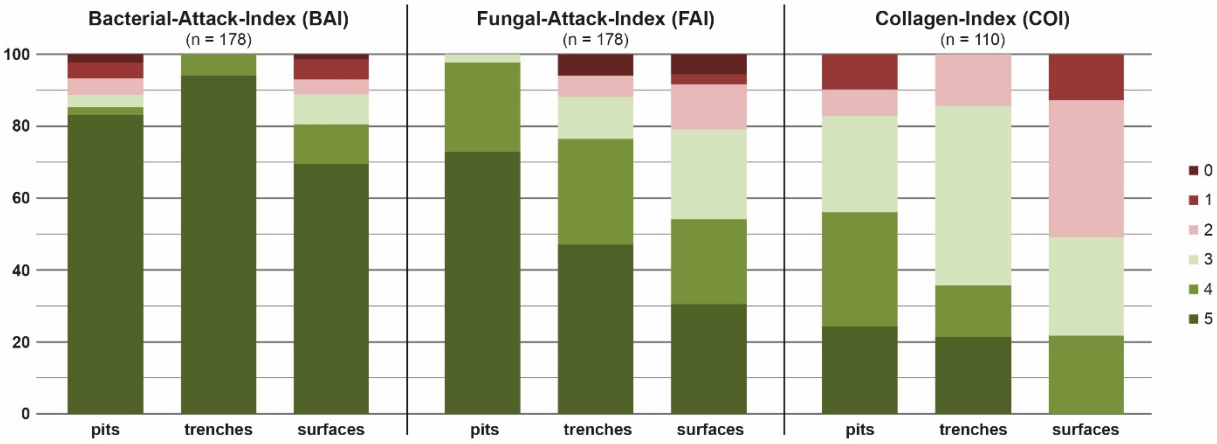


Fig. 8: *Comparison of bacterial attack (BAI), Wedl tunnels (WTI, suspected fungal attack) and collagen content (COI) in relation to archaeological feature type; data shown as percentages.*

Case study – Bone Preservation in pit no. 321

Geoarchaeological data suggested that settlement pit 321 had been infilled intentionally with dark sediments rich in archaeological finds (sediment type TSM) within a short space of time (Brönnimann and Rissanen, 2017; Brönnimann et al., accepted). In addition to more than 13'000 animal bones, which are interpreted as waste on the basis of archaeozoological analyses (Brönnimann and Rissanen, 2017), the pit contained the complete articulated skeletons of two young men (Hüglin and Spichtig, 2010; Pichler et al., 2013). The humerus and femur of one of the two individuals (samples BGS 6-1 and 6-2) as well as 13 probable animal bone fragments from geoarchaeological samples were assessed histotaphonomically (Tab. 10). All of the bone remains were allocated to the midden-like sediment type TSM. Thus, it can be assumed that all samples have been subject to similar ambient conditions. With the exception of one animal bone fragment, the human and animal remains display no or only very few Wedl tunnels (WTI = 4-5). However, in regard to bacterial attack, there are clear differences. The human skeletal remains exhibit severe bacterial degradation (BAI = O) (Figure 9A and 9B), while only two of the 13 animal bone fragments show this to a similar extent (BAI= 0-2) (Figure 9C–9F). In contrast, the majority of animal bone fragments (n = 10) exhibit little or no bacterial attack (BAI = 4-5) (Figure 9C and 9E). Collagen content was identical in both human bones (COI = 3), but differed greatly in the animal bone fragments, ranging from good (COI = 4-5; n = 3) to medium (COI = 3; n = 5) or even poor preservation (COI = 4-5; n = 3).

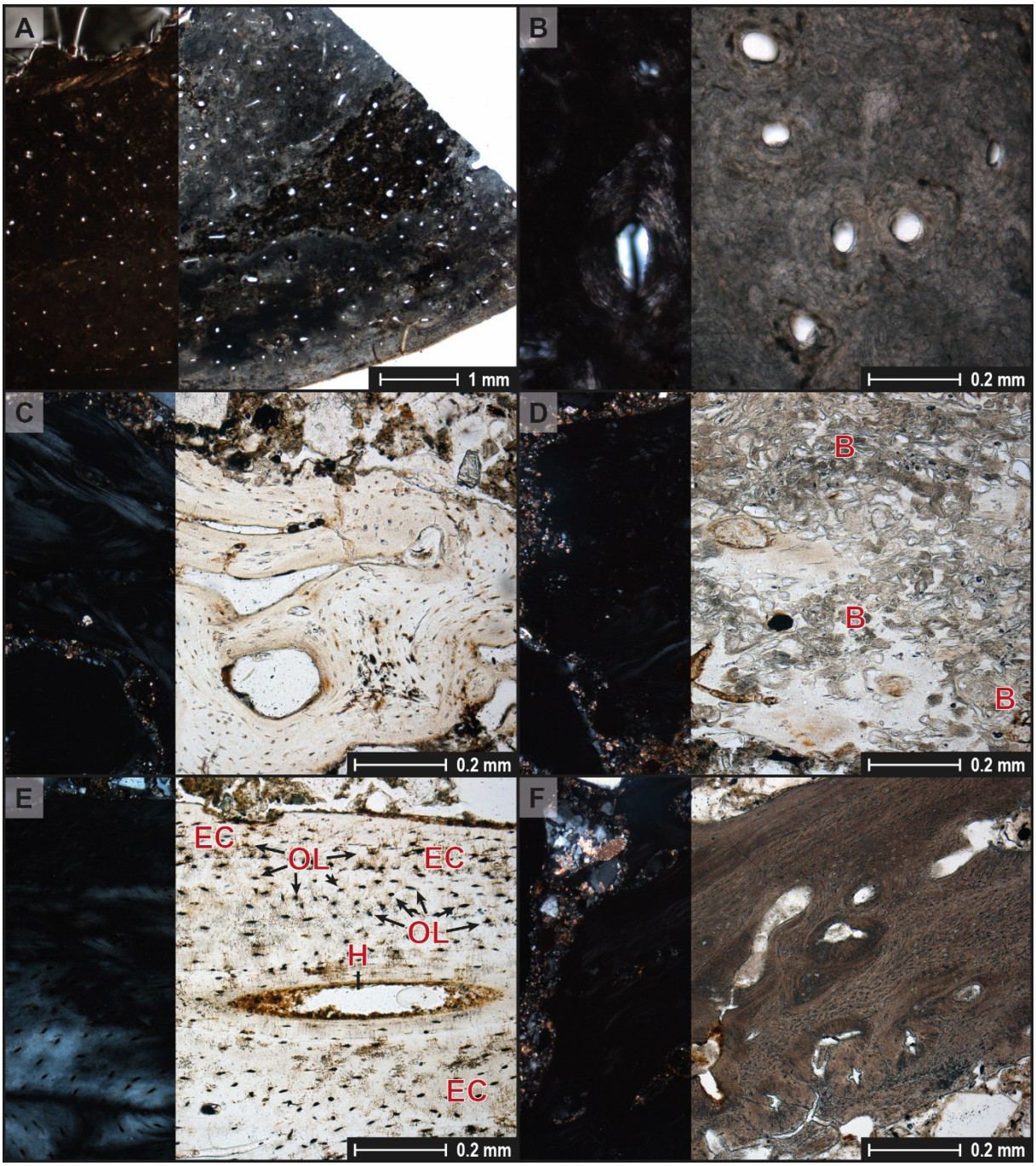


Fig. 9: *Histotaphonomic features of bone fragments of pit 321. All images with 100x magnification and in plane polarized light (PPL) with a left part in crossed polarized light (XPL), unless indicated otherwise.* ***9A)*** *Thin section (80 micrometres) of the humerus of a complete human skeleton. Very intense bacterial attack (BAI = 0) without any bone microstructure preserved; 16x magnification.* ***9B)*** *'Same sample with 100x magnification. Mostly budded tunnels can be detected, which overlap several times, leading to a grey mass.* ***9C)*** *Very well preserved suspected animal bone fragment with no bioerosion (BAI and WTI = 0). The collagen is quite well preserved (COI = 4). A slight brown colouring (HEI = 0.5) is visible, which is probably due to iron oxide precipitations (thin section 1996/01/3.3).* ***9D)*** *Small bone splinter (suspected animal bone fragment) with quite intense bacterial attack (mostly budded tunnels indicated with B; BAI = 2) with some unaffected areas. No collagen preserved (COI = 1) (thin section 1996/01/3.3).* ***9E)*** *Very well preserved suspected animal bone fragment with no bioerosion (BAI and WTI = 0). The collagen is well preserved (COI = 5). Osteocyte lacunae (OL) with some (enlarged) caniculi (EC) and a longitudinally cut Haversian canal (H) are visible (thin section 1996/01/4.1).* ***9F)*** *Heavily burnt bone chip (suspected animal bone fragment) with grey coloration and the formation of cubic crystals (not visible in the picture; HEI = 2.5) (thin section 1996/01/7.2).*

sample	sample size	kind of sample	BAI	WTI	COI	HEI
1996/01/1	small frgm.	prob. animal	0	5	2	0
1996/01/1	small frgm.	prob. animal	3	3	1	0
1996/01/2.0	small frgm.	prob. animal	5	5	4	1
1996/01/2.1	small frgm.	prob. animal	5	4	3	0.5
1996/01/3.1	small frgm.	Tooth	5	5		0.5
1996/01/3.1	small frgm.	prob. animal	4	4	3	0
1996/01/3.2	small frgm.	prob. animal	5	5	1	2
1996/01/3.3	small frgm.	prob. animal	5	5	4	0.5
1996/01/3.3	bone chip	prob. animal	2	5	1	0.5
1996/01/3.3	small frgm.	prob. animal	5	5	4	1
1996/01/3.3	bone chip	prob. animal	5	5		2
1996/01/4.1	big fragm.	prob. animal	5	5	5	0
1996/01/5.1	bone chip	prob. animal	5	4	3	1
1996/01/7.2	bone chip	prob. animal	5	5	2	2.5
BGS 6-1	bone section	human (hum.)	0	5	3	0.5
BGS 6-2	bone section	human (fem.)	0	4	3	0.5

Tab. 10: Histotaphonomic results of human- and animal bone from pit 321. BAI = Bacterial-Attack-Index; suspected fungal attack (WTI); COI = Collagen-Index; HEI = Heat-Index (thermal alteration). Bone chip: < 2mm; small fragment: 2-10 mm; bone section: thin section from complete bone.

Discussion

The 25 human and 183 animal bone samples assessed during our histotaphonomic investigations exhibited the entire range of microscopical focal destruction features (mfd) including Wedl tunnels and enlarged canaliculi (Wedl type 2) (Fig. 1). Wedl tunnels (47% of bones) and bacterial attack (32% of bones) represented the most common phenomena. However, we detected major differences in their frequency and intensity between bones and feature or sediment types. The observed differences, correlations and trends emerge regardless of whether bones are burnt or not (see supplementary information). Thermal alterations therefore appear not to significantly affect the phenomena discussed below.

Bioerosion phenomena and their Interpretation

Bacterial attack

Budded and *linear longitudinal mfd* are generally regarded as bacteria induced degradations in bone microstructure (Bell, 2012a; Jans, 2013; Trueman and Martill, 2002, Turner-Walker and Mays, 2008). Of the 208 analysed bones from Basel-Gasfabrik, 32% exhibited such bacterial bioerosion. However, neither the presence nor the intensity of bacterial attack depend on sediment type (Fig. 7) or the type of archaeological feature (Fig. 8). This corresponds to the observations of Miranda Jans (2005), Christina Nielsen-Marsh et al. (2007), and Tom J. Booth (2016). There were, however, fundamental differences between human and animal bones. The vast majority (96%) of human bones exhibited intense bacterial degradation, but only 23% of the animal bone fragments (Fig. 6). This stark contrast was also noted by Jans (74% bacterial degradation in human vs. 34% in animal bone fragments).

There are differing views as to what causes bacterial degradation in bone. Some postulate that it is mainly induced by endogenous gut bacteria that spread throughout the body shortly after death and play an important role in the process of putrefaction and decay (Bell et al., 1996; Bell, 2012a; Hedges

and Millard, 1995; Huisman, 2009; Jans, 2008, 2013; White and Booth, 2014). Others propose that soil bacteria entering the bones post-skeletonisation are partly or even exclusively responsible for the degradation of the microstructure (Kendall et al., 2018; Kontopoulos et al., 2016; Turner-Walker, 2012; Morales et al., 2017). Soil organisms certainly play a central role in the body's decay (Pokines and Symes, 2013; Lauber et al., 2014; Gutiérrez et al., 2016; Szelecz et al., 2016). However, our data shows that there are no significant differences concerning the quality and quantity of bacterial attack between sediment types TSM, LB and LC (Fig. 7).This result is exhibited most clearly in sediment type TSM. One would assume that it contained the highest amount of soil bacteria due to its midden-like nature and its share of topsoil (Brönnimann and Rissanen, 2017; Brönnimann et al., accepted). Nevertheless, bacterial attack was not increased in the skeletal elements embedded in this sediment type. This was also illustrated by the case study on pit 321. The bones from this pit display considerable variation regarding their BAI (Tab. 10). If the intensity of the bacterial attack was largely dependent on the type of sediment, one would expect bones embedded in sediment type TSM to exhibit extensive bacterial degradation throughout. However, no such uniform pronounced bacterial attack was observed. Furthermore, bacterial bioerosion tends to be absent or low in bones recovered from anoxic or waterlogged contexts (Booth, 2016; Hollund et al., 2012; Turner-Walker and Jans, 2008). However, there was no evidence that the archaeological contexts at Basel-Gasfabrik had been waterlogged. In conclusion, our results support the hypothesis that bacterial degradation of bone is mainly caused by endogenous gut bacteria rather than exogenous soil bacteria.

This is also reflected in the differential preservation of human and animal bones. The animal bones found in Basel-Gasfabrik, as well as in other archaeological contexts, represent slaughter waste (Stopp et al., 1999; Stopp, 2008). Soon after the animals are killed, their entrails are removed and their bodies dismembered. This prevents the endogenous gut bacteria from spreading through the body, which provides a conclusive explanation for the significantly lower intensity of bacterial attack in animal bones. Clearly, some presumably butchered animal bones do exhibit some bacterial bioerosion, although this could be related to the efficiency and timing of butchery: intrinsic bacteria are still occasionally recovered from meat processed in modern slaughterhouses (Chaillou et al., 2015). The consistency in the lack of bacterial attack in the animal bones examined here is remarkable given the likely random and eclectic selection of skeletal elements combined with evidence for intra-skeletal variation in bacterial bioerosion (in human bones at least). However, previous studies have suggested that bioerosion is invariable in long bones or skeletal elements containing high proportions of cortical bone and the results from Basel-Gasfabrik suggest this may also be largely true of faunal skeletal elements recovered as part of butchery waste (Booth et al., 2016; Kontopoulos et al., 2016).

Researchers who favour an exogenous model of bacterial bioerosion have explained previous observa-

tions of discrepancies between human and faunal remains as a result of differences in bone porosity which affect the ease of bacterial penetration. For instance, the bones of juvenile animals which are predominantly slaughtered for meat will have undergone lower levels of age-related remodelling that would have increased bone porosity (Turner-Walker, 2008; 2012). However, the lack of progressive age-related variation in the bacterial bioerosion of human remains runs counter to this theory (Booth, 2016). Bones of large-bodied domesticates are intrinsically less porous than human bones and it could be that bones from these domesticates are more resistant to bacterial invasion. However, it is difficult to reconcile this explanation with the small but considerable proportion of faunal remains from Basel-Gasfabrik and other archaeological/modern sites that have been extensively attacked by bacteria. This is particularly true for the bias towards bones from articulated animal skeletons, the lack of evidence for species-specific variation in bioerosion of faunal remains, as well as the numerous human bones recovered from aerobic burial contexts that show little or no bacterial bioerosion (Booth, 2016; Fernández -Jalvo et al., 2010; Jans et al., 2004; Kontopoulos et al., 2016; Mulville et al., 2012; Nielsen-Marsh et al., 2007; White and Booth, 2014).

In human skeletal remains, it has been suggested that the intensity of bacterial attack can yield information on the mortuary practices the bodies underwent. Acts of slowing down the process of decay or even bringing it to a halt (e.g. different kinds of artificial or natural mummification) as well as cutting off limbs may influence the bacterial degradation of the body (Booth et al., 2015; Booth, 2016; Booth and Madgwick, 2016). These insights make histotaphonomy an interesting tool for reconstructing single or multi-stage burial practices.

Wedl-tunnels

Wedl tunnels were found in 47% of the analysed bones from Basel-Gasfabrik and were the most common taphonomic phenomena (Tab. 4). They are characterised by their dendritic shape (Fig. 4C and 4F) and are associated with fungal attack (Fernández-Jalvo and Andrews 2016; Fernández-Jalvo et al., 2010; Hackett, 1981; Jans, 2013; Trueman and Martill, 2002). Gordon Turner-Walker (2012) has questioned the association of Wedl tunnelling with fungal activity, particularly the study which originally made this association (Marchiafava et al., 1974), but more recent work by other researchers has reasserted this link (Fernández -Jalvo et al., 2010). Our research has shown that this presumed fungal attack is connected to fundamentally different processes than bacterial degradation. Firstly, no clear difference in WTI was detected between human and animal remains (Tab. 6; Fig. 6). Secondly, there are striking contrasts between different types of archaeological features (Fig. 8): only 27% of bone fragments found in pits show Wedl tunnels, whereas 69% of specimens from the surface do. One may assume that differing processes of sedimentation represent decisive factors for this. Geoarchaeological investigations have shown that settlement pits at Basel-Gasfabrik were usually filled in quickly and

intentionally (Brönnimann and Rissanen, 2017; Brönnimann et al., accepted). As a result, bones in these pits were embedded quickly. Exposed surfaces and ditches, however, have far lower rates of sedimentation (Brönnimann et al., accepted.). Based on these observations, we hypothesise that Wedl tunnels go back to fungal attack and thus were mainly found on bone fragments that were once exposed. This corresponds to the observations of Hans Huisman that fungal activity is connected to aerobic conditions (Huisman, 2009; Huisman et al., 2017). Thus, the WTI can be used as an indicator of exposed and defleshed bones and therefore also of exposed surfaces and structures. However, the intensity of fungal attack is also dependent on other factors such as soil humidity, oxygen availability, content of calcium carbonate and pH value. As the pH value is fairly similar in all sediment types in Basel-Gasfabrik (6.8 – 7.7), it probably had no significant influence on fungal attack intensity. Unlike Huisman (Huisman et al., 2017), we also detected fungal attack in calcareous sediments. Thus, at Basel-Gasfabrik fungal attack on bone was mainly dependent on the type of archaeological feature, and by implication on the rate of sedimentation, while the type of substrate was not of great significance. The causes why canaliculi (Wedl type 2) are formed remain unclear. Further investigations will be needed in order to determine whether they really are the result of acids entering the bone (Trueman and Martill, 2002; Jans, 2008).

Collagen content

Contextualising our data has shown that collagen preservation is linked to the type of both sediment and archaeological feature (Tab. 8 and 9). The poorest collagen preservation is found in bones embedded in the decalcified sediment type LB and in bones from exposed surfaces. This reflects the observation of other authors that collagen content is dependent on a whole series of factors, such as pH value, varying soil humidity, exposition of bones etc. (Fernández-Jalvo et al., 2010; Hollund et al., 2012; Huisman, 2009; Huisman et al., 2017; Nicholson, 1996, 1998; Trueman and Martill, 2002; Turner-Walker, 2008; Villagran et al., 2017a). One of the most important factors, however, appears to be the impact of thermal alteration. Our results show that there is a highly significant correlation between burning and collagen content, whereby high temperature burning (HEI = 1-2) leads to a massive loss of collagen (Tab. 5, Fig. 5).

Cyanobacteria

6% of the animal bone fragments showed signs of suspected cyanobacterial attack, which represents quite a low value compared to fungal and bacterial attack. This result is not very surprising given the terrestrial condition of the site, since cyanobacterial attack only occurs in connection with water (Bell and Elkerton, 2008; Huisman et al., 2017; Jans, 2008; Turner-Walker, 2012; Villagran et al. 2017a). It can be therefore assumed that there was occasionally stagnant water in pits or ditches as well as on surfaces (puddles, etc.) within the settlement due to the partly clayey and impermeable subsoil.

Methodological considerations

Our histotaphonomic analyses have shown that not only bacterial (budded, linear-longitudinal and lamellate mfd) but also fungal attack (Wedl tunnels) can lead to severe degradation of bone microstructure. However, the causes of these two types of degradation are vastly different. It is therefore essential to differentiate between bacterial attack and Wedl tunnels with regard to specific research issues, for example when reconstructing mortuary practises. We therefore propose the use of different indices for bacterial attack (BAI) and fungal attack (WTI), and – where called for with regard to specific research questions - also for cyanobacterial attack (CAI) and cracking (CRI) using scales from 0 to 5 (based on the OHI) for each. Furthermore, collagen preservation (COI) and thermal alteration (HEI) (Tab. 2) can provide additional insights. Using thin sections of both 80 µm (anthropology) and 30 µm (geoarchaeology) thickness, it has become very clear that the various kinds of microbial bioerosion were more easily distinguished in preparations of 30 µm thinness. In thin sections, microbial structures as small as 2-10 µm can overlap several times, rendering differentiation impossible, especially in much degraded specimens. We therefore recommend using thin sections of 30 µm thickness when analysing microbial bioerosion types in detail. In order to produce such thin sections from archaeological, potentially fragile skeletal material, it is essential to embed the bones in epoxy resin. We have found it useful to follow a protocol that includes prior saturation of samples in an intermedium. Depending on the fragility of the bone, grinding rather than cutting the samples to the required thickness is advisable.

As the example of the Basel-Gasfabrik site clearly showed, combining anthropological and geoarchaeological perspectives is an advantageous new approach in histotaphonomy. It enables a detailed assessment of the sediments surrounding each sample and thus the in-depth contextualisation of the bones. One disadvantage of investigating bone fragments from geoarchaeological thin sections is that, due to the small size of the fragments, it is not always possible to distinguish human from animal bones or to include more specific information on the individual specimen (species, age, pathologies, as well as the section plane). Additionally, there is evidence that bioerosion phenomena may vary even within individual bones (e.g. Kontopoulos et al., 2016). This phenomenon cannot always be taken into account sufficiently when dealing with randomly cut bone fragments. Nevertheless, it has become obvious that analysing bone fragments in geoarchaeological thin sections in regard to histotaphonomy and relating these results to observations from histological analyses on human remains enables a gain in knowledge both in regards to methodology and the individual object under observation. It is only through this interdisciplinary approach that correlations between histotaphonomic phenomena, sediment characteristics and sedimentation processes can be identified and made useful for further interpretation.

For future research, a database of (soil) thin sections and corresponding data on archaeological contexts, sediment characteristics, individual data of bone specimens contained therein, etc. would constitute a useful basis for a better understanding of taphonomic processes in bone. Such a database is currently under construction in our working group and establishment of such an open access database with a wide range of contributors will represent a valuable asset for researchers from various fields.

Conclusions

For a working protocol in histotaphonomic analysis, we recommend embedding bone samples in epoxy resin and using thin sections of 30 µm thickness regardless of the specific topics under investigation. Moreover, grading the different bioerosional phenomena from 0 to 5 in a semi-quantitative fashion in accordance with the OHI has proved positive. We recommend separate scoring of microscopical focal destruction (mfd) (=bacterial attack index BAI) and Wedl tunnels (=Wedl-Tunnel-Index WTI) (Tab. 2). Furthermore, evaluating collagen content and thermal alterations generated valuable additional information.

The histotaphonomic analysis of 208 human and animal bone specimens from the La Tène settlement of Basel-Gasfabrik to our knowledge represents the largest data set for one single site so far. Thus, it forms an ideal basis for the research on microbial bioerosive processes. For our investigation, we applied a combination of anthropological and geoarchaeological methods. This novel approach included the detailed analysis of the different bioerosive patterns and contextualising the bones in regard to their archaeological feature, the sediment type they were embedded in and the sedimentation process they underwent.

Our results show that Wedl tunnels are most likely caused by fungal attack and that this kind of bioerosion is relatively common in both human and animal bones. While no significant connection between sediment type and fungal attack was detected, there emerged a clear correlation between fungal attack, the type of archaeological feature and the associated sedimentation processes affecting the specific samples. Fungal attack tends to primarily involve bone from exposed surfaces or structures, while few such signatures were found in specimens from quickly filled pits. Thus, (severe) fungal degradation can be considered a strong indicator that bones lay exposed. By contrast, bacterial attack is far more frequent and intense in human skeletal remains than in animal bone fragments. There were no indications for a connection between bacterial attack and sediment type or sedimentation processes. It follows that the bacterial degradation observed in bones from Basel-Gasfabrik does not derive from exogenous soil bacteria but mainly from endogenous putrefactive gut bacteria. Thus, bone degradation caused by bacteria greatly results from the putrefaction of the body and its post mortem fate. An assessment of the intensity of bacterial attack in human skeletal remains can therefore make

an essential contribution to the reconstruction of the handling of the dead and single or multi stage mortuary practices.

The combination of anthropological and geoarchaeological methods proved to be a promising approach in histotaphonomy. It generates a wealth of valuable information even from tiny bone fragments while putting each specimen or individual into a clearly defined context. Our integrative approach provides a novel tool for the analysis of complex processes in the handling of the dead in former communities. Moreover, it can aid in developing new perspectives, e.g. on sedimentation processes, the identification of animal or human sacrifices, ancient feasting and disposal practices in general.

Acknowledgements

The histotaphonomic and geoarchaeological investigations at Basel-Gasfabrik were funded by the Archäologische Bodenforschung Basel-Stadt and the Swiss National Research Foundation. The Institute of Anatomy, University of Basel enabled production of the anthropological thin sections. The authors would like to thank Guido Lassau, Hannele Rissanen, Norbert Spichtig, Richard Madgwick, Kristin Ismail-Meyer, Christine Pümpin and Nicole Nicklisch for their advice and support. Furthermore, we owe thanks to Thomas Beckmann for preparation of the soil thin sections. We also thank Olivia Klee for translating the text into English.

References (chapter 4)

Bell, L.S., 2012a. Histotaphonomy, in: Crowder, C., Stout, S. (Eds.), Bone histology. An anthropological perspective. CRC Press, Boca Raton, pp. 241–251.

Bell, L.S., 2012b. Identifying postmortem microstructural change to skeletal and dental tissues using backscattered electron imaging, in: Bell, L.S. (Ed.), Forensic microscopy for skeletal tissues. Methods and protocols. Methods in Molecular Biology 915. Humana Press, Totowa, NJ, pp. 173–190.

Bell, L.S., Elkerton, A., 2008. Unique marine taphonomy in human skeletal material recovered from the medieval warship Mary Rose. International Journal of Osteoarchaeology 18 (5), 523–535.

Bell, L.S., Skinner, M.F., Jones, S.J., 1996. The speed of post mortem change to the human skeleton and its taphonomic significance. Forensic Science International 82 (2), 129–140.

Booth, T.J., 2014. An investigation into the relationship between bone diagenesis and funerary treatment. PhD Thesis, Sheffield.

Booth, T.J., 2016. An investigation into the relationship between funerary treatment and bacterial bioerosion in european archaeological human bone. Archaeometry 58 (3), 484–499.

Booth, T.J., Chamberlain, A.T., Parker Pearson, M., 2015. Mummification in Bronze Age Britain. Antiquity 89 (347), 1155–1173.

Booth, T.J., Madgwick, R., 2016. New evidence for diverse secondary burial practices in Iron Age Britain: A histological case study. Journal of Archaeological Science 67, 14–24.

Booth, T.J., Redfern, R.C., Gowland, R.L., 2016. Immaculate Conceptions: Micro-CT analysis of diagenesis in Romano-British infant skeletons. Journal of Archaeological Science 74, 124–134.

Brönnimann, D., Rentzel, P., Röder, B., Spichtig, N., Rissanen, H., Lassau, G., accepted. The hidden midden – Geoarchaeological investigation of sedimentation processes, waste disposal practices and resource management at the Latène settlement Basel-Gasfabrik (Switzerland). Geoarchaeology: An International Journal.

Brönnimann, D., Rentzel, P., in prep. Geoarchäologische Untersuchungen an zwei Siedlungsgruben sowie an Grabgruben und Gräben innerhalb der beiden Gräberfeldern der spätlatènezeitlichen Siedlung Basel-Gasfabrik, in: Pichler, S.L., Alt, K.W., Lassau, G., Röder, B., Schibler, J. (Eds.), Über die Toten zu den Lebenden. Interdisziplinäre Synthese. Materialhefte der Archäologischen Bodenforschung Basel-Stadt. Archäologische Bodenforschung Basel-Stadt, Basel.

Brönnimann, D., Rissanen, H., 2017. Vivre et mourir sur le site La

Tène de Bâle-Gasfabrik (Suisse) – l'étude interdisciplinaire de structures d'habitat choisies et de deux nécropoles donne un aperçu de la société à la fin de l'âge du Fer, in: Interdisciplinarité et nouvelles approches dans les recherches sur l'âge du Fer. Interdisciplinarity and New Approaches in the Research of the Iron Age. International Doctoral Conference 2015. Bibracte (France), 2015. Interdisciplinarity and New Approaches in the Research of the Iron Age, Bibracte. 28.-30. April 2015. Masarykova univerzita, Brno, pp. 93–97.

Chaillou, S., Chaulot-Talmon, A., Caekebeke, H., Cardinal, M., Christieans, S., Denis, C., Desmonts, M.H., Dousset, X., Feurer, C., Hamon, E., Joffraud, J.-J., La Carbona, S., Leroi, F., Leroy, S., Lorre, S., Macé, S., Pilet, M.-F., Prévost, H., Rivollier, M., Roux, D., Talon, R., Zagorec, M., Champomier-Vergès, M.-C., 2015. Origin and ecological selection of core and food-specific bacterial communities associated with meat and seafood spoilage. The ISME Journal 9 (5), 1105–1118.

Child, A.M., 1995. Microbial taphonomy or archaeological bone. Studies in Conservation 40, 19–30.

Efremov, I.A., 1940. Taphonomy: a new branch of paleontology. Pan-American Geologist 74 (2), 81–93.

Fernández Castillo, R., Ubelaker, D.H., Acosta, J.A.L., La Fuente, G.A.C. de, 2013a. Effects of temperature on bone tissue. Histological study of the changes in the bone matrix. Forensic Science International 226 (1-3), 33–37.

Fernández Castillo, R., Ubelaker, D.H., Acosta, J.A.L., La Rosa, R.J.E. de, Garcia, I.G., 2013b. Effect of Temperature on Bone Tissue: Histological Changes. J Forensic Sci 58 (3), 578–582.

Fernández-Jalvo, Y., Andrews, P., 2016. Atlas of taphonomic identifications: 1001 + images of fossil and recent mammal bone modification. Vertebrate Paleobiology and Paleoanthropology Series. Springer, Dordrecht, Heidelberg, New York, London.

Fernández-Jalvo, Y., Andrews, P., Pesquero, D., Smith, C., Marín-Monfort, D., Sánchez, B., Geigl, E.-M., Alonso, A., 2010. Early bone diagenesis in temperate environments. Palaeogeography, Palaeoclimatology, Palaeoecology 288 (1-4), 62–81.

Goldberg, P., Macphail, R.I., 2006. Practical and theoretical geoarchaeology. Blackwell Publishers, Malden, MA, Oxford, p. 454.

Grine, F.E., Bromage, T.G., Daegling, D.J., Burr, D.B., Brain, C.K., 2015. Microbial osteolysis in an Early Pleistocene hominin (Paranthropus robustus) from Swartkrans, South Africa. Journal of Human Evolution 85, 126–135.

Gutiérrez, A., Nociarová, D., Malgosa, A., Armentano, N., 2016. The taphonomic effects comparison in two empty space burial structures. Spanish Journal of Legal Medicine 42 (3), 98–104.

Hackett, C.J., 1981. Microscopical focal destruction (tunnels) in exhumed human bones. Medicine, science, and the law 21 (4), 243–265.

Hagens, G. von, 1979. Impregnation of soft biological specimens with thermosetting resins and elastomers. The Anatomical Report 194, 247–256.

Harding, D.W., 2016. Death and burial in Iron Age Britain. Oxford University Press, Oxford.

Hecht, Y., Niederhäuser, A., 2011. Alltagskultur und Totenrituale der Kelten: Ein Siedlungszentrum am Oberrhein um 100 v. Chr. Merian, Basel.

Hedges, R.E.M., Millard, A.R., 1995. Measurements and relationships of diagenetic alteration of bone from three archaeological sites. Journal of Archaeological Science 22, 201–209.

Hollund, H.I., Jans, M.M., Collins, M.J., Kars, H., Joosten, I., Kars, S.M., 2012. What happened here?: Bone histology as a tool in decoding the postmortem histories of archaeological bone from castricum, the Netherlands. International Journal of Osteoarchaeology 22, 537–548.

Hüglin, S., Spichtig, N., 2010. War crime or élite burial: Interpretations of human skeletons within the Late La Tène settlement Basel-Gasfabrik, Basel, Switzerland. European Journal of Archaeology 13 (3), 313–335.

Huisman, D.J. (Ed.), 2009. Degradation of archaeological remains. Sdu Uitgevers, Den Haag.

Huisman, H., Ismail-Meyer, K., Sageidet, B.M., Joosten, I., 2017. Micromorphological indicators for degradation processes in archaeological bone from temperate European wetland sites. Journal of Archaeological Science 85, 13–29.

Ismail-Meyer, K., Rentzel, P., 2017. Paludal settings (wetland archaeology), in: Gilbert, A.S., Goldberg, P., Holliday, V.T., Mandel, R.D., Sternberg, R.S. (Eds.), Encyclopedia of geoarchaeology. Encyclopedia of Earth Sciences Series. Springer Reference, Dordrecht, Heidelberg, New York, London, Dordrecht, Heidelberg, New York, London, pp. 628–644.

Jackes, M., Sherburne, R., Lubell, D., Barker, C., Wayman, M., 2001. Destruction of microstructure in archaeological bone: A case study from Portugal. International Journal of Osteoarchaeology 11 (6), 415–432.

Jans, M.M., 2005. Histological characterisation of diagenetic alteration of archaeological bone. Geoarchaeological and Bioarchaeological Studies 4, Amsterdam.

Jans, M.M., 2008. Microbial bioerosion of bone – a review, in: Wisshak, M., Tapanila, L. (Eds.), Current developments in bioerosion, 1. Aufl. ed. Erlangen Earth Conference Series. Springer, Berlin, Heidelberg, pp. 397–413.

Jans, M.M., 2013. Microscopic destruction of bone, in: Pokines, J.T., Symes, S.A. (Eds.), Manual of forensic taphonomy. CRC Press, Taylor & Francis Group, Boca Raton, pp. 19–35.

Jans, M.M., Nielsen-Marsh, C., Smith, C.I., Collins, M.J., Kars, H., 2004. Characterisation of microbial attack on archaeological bone. Journal of Archaeological Science 31 (1), 87–95.

Jud, P. (Ed.), 2008. Die Töpferin und der Schmied: Basel-Gasfabrik, Grabung 1989/5. Dissertation 2004, Teil I: Text. Materialhefte zur Archäologie in Basel 20:1. Archäologische Bodenforschung des Kantons Basel-Stadt, Basel.

Karkanas, P., Goldberg, P., 2010. Phosphatic features, in: Stoops, G., Marcelino, V., Mees, F. (Eds.), Interpretation of micromorphological features of soils and regoliths. Elsevier, Amsterdam, Oxford, pp. 521–541.

Kendall, C., Eriksen, A.M.H., Kontopoulos, I., Collins, M.J., Turner-Walker, G., 2018. Diagenesis of archaeological bone and

tooth. Palaeogeography, Palaeoclimatology, Palaeoecology 491, 21–37.

Kontopoulos, I., Nystrom, P., White, L., 2016. Experimental taphonomy: Post-mortem microstructural modifications in Sus scrofa domesticus bone. Forensic Science International 266, 320–328.

Lauber, C.L., Metcalf, J.L., Keepers, K., Ackermann, G., Carter, D.O., Knight, R., 2014. Vertebrate decomposition is accelerated by soil microbes. Applied and environmental microbiology 80 (16), 4920–4929.

Marchiafava, V., Bonucci, E., Ascenzi, A., 1974. Fungal osteoclasia: a model of dead bone resorption. Calcified Tissue International 14, 195–210.

Millard, A.R., 2001. The deterioration of bone, in: Brothwell, D.R., Pollard, A.M. (Eds.), Handbook of archaeological sciences. John Wiley & Sons, Chichester, New York, pp. 636–647.

Morales, N.S., Catella, L., Oliva, F., Sarmiento, P.L., Barrientos, G., 2017. A SEM-based assessment of bioerosion in Late Holocene faunal bone assemblages from the southern Pampas of Argentina. Journal of Archaeological Science: ReportsReports (2017), http://dx.doi.org/10.1016/j.jasrep.2017.07.012.

Müller, K., Chadefaux, C., Thomas, N., Reiche, I., 2011. Microbial attack of archaeological bones versus high concentrations of heavy metals in the burial environment. A case study of animal bones from a mediaeval copper workshop in Paris. Palaeogeography, Palaeoclimatology, Palaeoecology 310 (1-2), 39–51.

Mulville, J., Madgwick, R., Powell, A., Parker Pearson, M., 2012. Flesh on the bones: animal bodies in Atlantic roundhouses, in: Pluskowski, A. (Ed.), The ritual killing and burial of animals. European perspectives. Oxbow Books, Oxford, pp. 205–219.

Nicholson, R.A., 1996. Bone degradation, burial medium and species representation: Debunking the myths, an experiment-based approach. Journal of Archaeological Science 23, 513–553.

Nicholson, R.A., 1998. Bone degradation in a compost heap. Journal of Archaeological Science 25 (5), 393–403.

Nicklisch, N., 2013. Einbettung mit Biodur-Harz: Labor-Protokoll, Mainz.

Nielsen-Marsh, C.M., Smith, C.I., Jans, M.M., Nord, A., Kars, H., Collins, M.J., 2007. Bone diagenesis in the European Holocene II: Taphonomic and environmental considerations. Journal of Archaeological Science 34 (9), 1523–1531.

Pérez, L., Sanchis, A., Hernández, C.M., Galván, B., Sala, R., Mallol, C., 2017. Hearths and bones: An experimental study to explore temporality in archaeological contexts based on taphonomical changes in burnt bones. Journal of Archaeological Science: Reports 11, 287–309.

Pichler, S.L., in prep. Die menschlichen Skelettreste vom Fundplatz Basel-Gasfabrik. In: Pichler, S.L., Alt, K.W., Lassau, G., Röder, B., Schibler, J. (Eds.), Über die Toten zu den Lebenden. Interdisziplinäre Synthese. Materialhefte der Archäologischen Bodenforschung Basel-Stadt. Archäologische Bodenforschung Basel-Stadt, Basel.

Pichler, S.L., Alt, K.W., Lassau, G., Röder, B., Schibler, J. (Eds.), in prep. Über die Toten zu den Lebenden: Interdisziplinäre Synthese. Materialhefte der Archäologischen Bodenforschung Basel-Stadt. Archäologische Bodenforschung Basel-Stadt, Basel.

Pichler, S.L., Rissanen, H., Spichtig, N., 2015. Ein Platz unter den Lebenden, ein Platz unter den Toten – Kinderbestattungen des latènezeitlichen Fundplatzes Basel-Gasfabrik, in: Kory, R.W. (Ed.), Lebenswelten von Kindern und Frauen in der Vormoderne. Archäologische und anthropologische Forschungen in memoriam Brigitte Lohrke. Paläowissenschaftliche Studien 4. curach bhán publications, Berlin, pp. 257–273.

Pichler, S.L., Rissanen, H., Spichtig, N., Alt, K.W., Röder, B., Schibler, J., Lassau, G., 2013. Die Regelmäßigkeit des Irregulären: Menschliche Skelettreste vom spätlatènezeitlichen Fundplatz Basel-Gasfabrik, in: ‚Irreguläre' Bestattungen in der Urgeschichte: Norm, Ritual, Strafe …? Akten der Internationalen Tagung in Frankfurt a. M. vom 3. bis 5. Februar 2012, Frankfurt. 3.-5.2.2012. Dr. Rudolf Habelt GmbH, Bonn, pp. 471–484.

Pichler, S.L., Röder, B., Brönnimann, D., Knipper, C., Kühn, M., Rentzel, P., Rissanen, H., Stopp, B., Vach, W., Warnberg, O., Alt, K.W., Schibler, J., Lassau, G., 2017. The Basel-Gasfabrik research project: Addressing complex topics by an integrative approach, in: Multidisciplinary approach to archaeology: Recent achievements and prospects. Proceedings of the international symposium "Multidisciplinary Approach to Archaeology: Recent achievements and prospects" (June 22-26, 2015, Novosibirsk). Multidisciplinary Approach to Archaeology: Recent achievements and prospects, Novosibirsk. 22.-25. June 2016. IAET SB RAS Publishing, Novosibirsk, pp. 240–247.

Pokines, J.T., Symes, S.A. (Eds.), 2013. Manual of forensic taphonomy. CRC Press, Taylor & Francis Group, Boca Raton.

Portmann, C., 2015. Histologische Sterbealterbestimmung an menschlichen Langknochen aus der latènezeitlichen Siedlung Basel-Gasfabrik (BS) und Überlegungen zur Befundentstehung anhand archäologischer und ethnologischer Vergleiche. Unpublizierte Masterarbeit, Basel.

Portmann, C., Pichler, S.L., in prep. Histologische Untersuchungen an menschlichen Langknochen aus dem Siedlungskontext und den Gräberfeldern, in: Pichler, S.L., Alt, K.W., Lassau, G., Röder, B., Schibler, J. (Eds.), Über die Toten zu den Lebenden. Interdisziplinäre Synthese. Materialhefte der Archäologischen Bodenforschung Basel-Stadt. Archäologische Bodenforschung Basel-Stadt, Basel.

Portmann, C., Brönnimann, D., Pichler, S.L., Rentzel, P., Schibler, J., Röder, B., Rissanen, H., Lassau, G., in prep. Retracing late Iron Age multi-stage burial processes by a combined interdisciplinary histotaphonomical approach.

Reidsma, F.H., van Hoesel, A., van Os, B.J.H., Megens, L., Braadbaart, F., 2016. Charred bone: Physical and chemical changes during laboratory simulated heating under reducing conditions and its relevance for the study of fire use in archaeology. Journal of Archaeological Science: Reports 10, 282–292.

Rentzel, P., 1997. Geologisch-bodenkundliche Untersuchungen an den Niederterrassenfeldern bei Basel unter besonderer Berücksichtigung der spätlatènezeitlichen Fundstelle Basel-Gasfabrik. Jahresbericht der Archäologischen Bodenforschung des Kantons Basel-Stadt 1994, 31–52.

Rentzel, P., 1998. Ausgewählte Grubenstrukturen aus der spätlatènezeitlichen Fundstelle Basel-Gasfabrik. Jahresbericht der Archäologischen Bodenforschung des Kantons Basel-Stadt 1995, 35–79.

Rentzel, P., Narten, G.-B., 2000. Zur Entstehung von Gehniveaus in sandig-lehmigen Ablagerungen - Experimente und archäologische Befunde. Jahresbericht der Archäologischen Bodenforschung des Kantons Basel-Stadt 1999, 107–127.

Schultz, M., 2001. Paleohistopathology of bone: A new approach to the study of ancient diseases. Yearbook of Physical Anthropology 44, 106–147.

Squires, K.E., Thompson, T.J.U., Islam, M., Chamberlain, A., 2011. The application of histomorphometry and Fourier Transform Infrared Spectroscopy to the analysis of early Anglo-Saxon burned bone. Journal of Archaeological Science 38 (9), 2399–2409.

Stoops, G., 2003. Guidelines for analysis and description of soil and regolith thin sections. Soil Science Society of America, Madison.

Stopp, B., 2008. Archäozoologische Untersuchung der Tierknochen aus Gruben der spätlatènezeitlichen Siedlung Basel-Gasfabrik, Grabung 1989/5, in: Jud, P. (Ed.), Die Töpferin und der Schmied. Basel-Gasfabrik, Grabung 1989/5. Dissertation 2004, Teil I: Text. Materialhefte zur Archäologie in Basel 20:1. Archäologische Bodenforschung des Kantons Basel-Stadt, Basel, pp. 249–292.

Schaer, N., Stopp, B., 2005. Bestattet oder entsorgt? Das menschliche Skelett aus der Grube 145/230 von Basel-Gasfabrik. Materialhefte zur Archäologie in Basel 19. Archäologische Bodenforschung des Kantons Basel-Stadt, Basel.

Stopp, B., Iseli, M., Jacomet, S., 1999. Die Landwirtschaft der späten Eisenzeit. Archäologie Schweiz 22 (1), 27–30.

Szelecz, I., Sorge, F., Seppey, C.V.W., Mulot, M., Steel, H., Neilson, R., Griffiths, B.S., Amendt, J., Mitchell, E.A.D., 2016. Effects of decomposing cadavers on soil nematode communities over a one-year period. Soil Biology and Biochemistry 103, 405–416.

Trueman, C.N., Martill, D.M., 2002. The long-term survival of bone: The role of bioerosion. Archaeometry 44 (3), 371–382.

Turner-Walker, G., 2008. The chemical and microbial degradation of bones and teeth, in: Pinhasi, R., Mays, S. (Eds.), Advances in human palaeopathology. John Wiley & Sons, Hoboken, pp. 3–29.

Turner-Walker, G., 2012. Early bioerosion in skeletal tissues: persistence through deep time. Neues Jahrbuch für Geologie und Paläontologie - Abhandlungen 265 (2), 165–183.

Turner-Walker, G., Jans, M.M., 2008. Reconstructing taphonomic histories using histological analysis. Palaeogeography, Palaeoclimatology, Palaeoecology 266, 227–235.

Turner-Walker, G., Mays, S., 2008. Histological studies on ancient bone, in: Pinhasi, R., Mays, S. (Eds.), Advances in human palaeopathology. John Wiley & Sons, Hoboken, pp. 121–146.

Turner-Walker, G., Peacock, E.E., 2008. Preliminary results of bone diagenesis in Scandinavian bogs. Palaeogeography, Palaeoclimatology, Palaeoecology 266 (3-4), 151–159.

Villagran, X.S., Huisman, D.J., Mentzer, S.M., Miller, C.E., Jans, M.M., 2017a. Bone and other skeletal tissues, in: Nicosia, C., Stoops, G. (Eds.), Archaeological soil and sediment micromorphology. Wiley Blackwell, Hoboken, pp. 11–38.

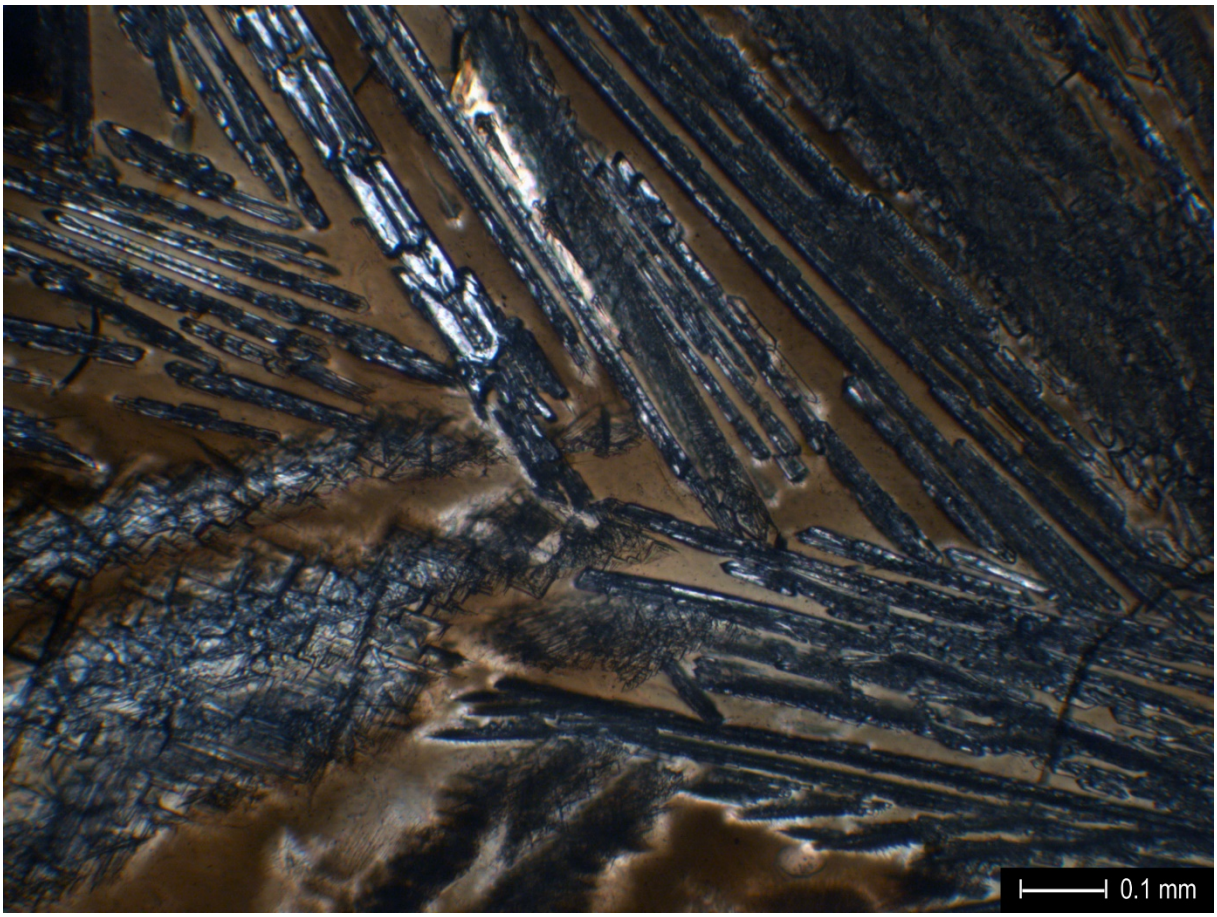
Villagran, X.S., Strauss, A., Miller, C.E., Ligouis, B., Oliveira, R., 2017b. Buried in ashes: Site formation processes at Lapa do Santo rockshelter, east-central Brazil. Journal of Archaeological Science 77, 10–34.

Wedl, C., 1864. Über einen im Zahnbein und Knochen keimenden Pilz. Sitzungsberichte der kaiserlichen Akademie der Wissenschaften 50, 171–193.

Weigelt, J., 1927. Rezente Wirbeltierleichen und ihre paläobiologische Bedeutung. Palaeontologische Zeitschrift 9 (1-3), 327–328.

White, L., Booth, T.J., 2014. The origin of bacteria responsible for bioerosion to the internal bone microstructure: Results from experimentally-deposited pig carcasses. Forensic Science International 239, 92–102.

White, T., Folkens, P.A., 2005. The human bone manual. Academic Press, Burlington MA.



Mikroskop-Foto (parallele Polarisatoren) einer Eisenschlacke innerhalb einer rasch verfüllten Grube.

Kapitel 5

Zusammenfassung und Synthese

In den nahezu 10 Jahren, während denen ich mich mit der Mikromorphologie befasst habe, durfte ich einige Grundsätze kennenlernen, die wohl nicht nur für dieses eine spezifische Fachgebiet gelten, sondern allgemeingültigen Charakter haben. Besonders beeindruckt hat mich die Erkenntnis, dass man stets nur das finden kann, was einem selber bereits bekannt ist. Zweitens habe ich während den unzähligen Stunden am Mikroskop gelernt, dass eine einzelne Betrachtungsebene alleine niemals ausreicht. Eine stärkere Vergrösserung – der Blick ins Detail also – führt nicht zwangsläufig zu einer tiefergehenden Erkenntnis, sondern erlaubt lediglich die Untersuchung derjenigen Aspekte, die mit geringerer Vergrösserung nicht zu erkennen sind. Gleichzeitig aber geht der Blick fürs Gesamte (für das Gefüge oder die Porosität zum Beispiel) häufig verloren. Für eine möglichst umfassende Analyse brauchen wir also unterschiedliche Vergrösserungen – oder etwas allgemeiner ausgedrückt: Verschiedene Betrachtungsebenen und Blickwinkel. Drittens wird in der Mikromorphologie mit verschiedenen Filtern und Lichtquellen gearbeitet, die die gleichen Objekte verschiedenartig erscheinen lassen und zum Beispiel eine Mineralbestimmung ermöglichen. Die verschiedenen Filter eröffnen uns weitere Betrachtungsweisen und Möglichkeiten, was sich für die Archäologie vielleicht mit der interdisziplinären Arbeitsweise übersetzen lässt.

Deshalb möchte ich das vorliegende Kapitel wie eine mikromorphologische Analyse angehen: Unter Verwendung verschiedener Filter und Vergrösserungen. Jedes der drei Papers ermöglicht eine andere Sicht auf die Siedlung Basel-Gasfabrik, der sich durch die unterschiedlichen Methoden (Filter) und die verschiedenen Blickwinkel und Vergrösserungen ergibt. Das erste Paper befasst sich mit dem Erstellen einer Strontium-Isotopen-Karte vom Umland von Basel-Gasfabrik (Brönnimann et al., 2018a; Kap. 2). Wir betrachten die Siedlung aus der Ferne und betten sie in die umliegende Landschaft ein. Das zweite Paper (Brönnimann et al., accepted; Kap. 3) setzt den Fokus auf Sedimentationsprozesse, Aktivitäten und den Umgang mit verschiedenen Ressourcen innerhalb einer ausgewählten Siedungszone. Das ausgewählte «Okular» weist eine deutlich stärkere Vergrösserung auf und erlaubt detaillierte Einblicke mitten in die Siedlung. Eine noch stärkere Vergrösserung wird für das dritte Paper benötigt (Brönnimann et al., 2018b; Kap. 4), das sich mit bioerosiven Prozessen in Knochen beschäftigt. Die Wahl von Knochen als Untersuchungsobjekt ist nicht zufällig, zumal der relativ weiche und formbare Knochen besonders sensibel auf taphonomische Prozesse reagiert.

5.1 The Lay of Land

Ziele und Probenmaterial

Das Ziel dieser Forschung war die Rekonstruktion des biologisch verfügbaren Strontiums für die EinwohnerInnen der Siedlung Basel-Gasfabrik sowie das Erstellen einer Strontium-Isotopen-Karte für die Region Basel. Hierfür wurden an 51 Standorten moderne Proben von jeweils einer bodennahen Pflanze (wenig tief wurzelnd) und von Baumlaub (tiefwurzelnd) gesammelt, wobei jedes geologische Substrat mit mindestens zwei Standorten vertreten war. Jeder Probenstandort wurde bezüglich geologisch-bodenkundlicher und hydrologischer Aspekte im Feld evaluiert, zumal die geologischen Karten lokale Besonderheiten nicht immer abbilden. Die meisten Proben sind nicht weiter als 20 km von Basel-Gasfabrik entfernt und decken den geografischen Raum ab, für den anhand der archäologischen und archäozoologischen Resultate von einem regen Austausch ausgegangen werden kann. Ausserdem wurden neun Wasserproben aus den acht wichtigsten Fliessgewässern entnommen. Aus der Siedlung Basel-Gasfabrik wurden 28 Milchzähne von 18 Kindern, sechs Zähne von Hausschweinen und fünf Zähne von Hunden ausgewählt (archäologische Proben).

Zusammenfassung der Resultate der $^{87}Sr/^{86}Sr$-Kartierung

Die hohe Variabilität der $^{87}Sr/^{86}Sr$-Werte innerhalb einzelner geologischer Einheiten ist vor allem mit lokalen Gegebenheiten zu begründen. So zeigen die $^{87}Sr/^{86}Sr$-Resultate der Pflanzenproben, dass die Unterschiede zwischen bodennaher und bodenferner Vegetation häufig auf eine Sedimentüberdeckung (z. B. geringmächtige Lössüberdeckung auf Schottern, Verwitterungslehmpaket auf Kalkfelsen etc.) zurückgehen. Ausserdem spielt das Bodenprofil eine wichtige Rolle, da ein entkalkter Bt-Horizont andere $^{87}Sr/^{86}Sr$-Werte aufweist als ein kalkhaltiger C-Horizont (Bullen und Bailey, 2005; Drouet et al., 2007), weshalb Unterschiede zwischen gekappten Bodenprofilen und ungestörten Waldstandorten zu erwarten sind.

Die $^{87}Sr/^{86}Sr$-Resultate der modernen Pflanzenproben haben gezeigt, dass die $^{87}Sr/^{86}Sr$-Werte innerhalb einer geologischen Einheit stark variieren können. Dies gilt insbesondere für die Niederterrassenschotter (0.70830–0.71002) und die Lössablagerungen (0.70842–0.70985). Insgesamt entsprechen die Resultate aber den Erwartungen. So zeigen sich für die Jurakalke (0.70776–0.70864) und für die mit Löss überdeckten vulkanischen Ablagerungen (0.70782–0.70864) die tiefsten Werte und für die triassischen Buntsandsteinablagerungen als auch für das Grundgebirge hohe Werte von > 0.7110. Für die Niederterrasse des Rheins (0.70830–0.71002) sowie für Lössablagerungen (0.70842–0.70985) hingegen ist eine beachtliche Spannbreite zu beobachten. Letzteres kann auf verschiedene Gründe wie (Kalk-) Düngung, gekappte Bodenprofile oder aber kleinräumige geomorphologische und geologische Unterschiede zurückgehen. Die geologische Vielfalt spiegelt sich demnach nur bedingt wider, zumal $^{87}Sr/^{86}Sr$-Werte zwischen 0.70850 und 0.7100 mehrere geologische Einheiten umfassen und unspezifisch sind.

Ein neuer Ansatz in der Strontium-Isotopie: Evaluation der Nutzbarkeit verschiedener Landschaftsformen

Um die Aussagekraft der modernen Pflanzenproben zu erhöhen, wurde für jeden Probenstandort anhand der geologisch-bodenkundliche Beurteilung im Feld sowie auf Basis topografischer und bodenkundlicher Karten (Tiefgründigkeit, Nährstoff- und Wasserspeicherkapazität, Skelettgehalt) das Potential für Ackerbau und Viehwirtschaft (Wald- oder Wiesenweidewirtschaft) evaluiert. Auf diese Weise wurde beurteilt, welche $^{87}Sr/^{86}Sr$-

Werte in die menschliche Nahrungskette integriert worden sein könnten. Dadurch konnten für jeden Landschaftsraum diejenigen Probenstandorte ausgewählt werden, die als landwirtschaftlich geeignet eingestuft wurden (Abb. 4). Für Ackerbau geeignete Böden im näheren Umkreis von Basel (= 7 km Radius) umfassen das lössbedeckte Sundgauer Hügelland, die Niederterrassen des Rheins und die Plateaus des Tafeljuras. Die $^{87}Sr/^{86}Sr$-Werte dieser Pflanzenproben liegen zwischen 0.70830 und 0.71000.

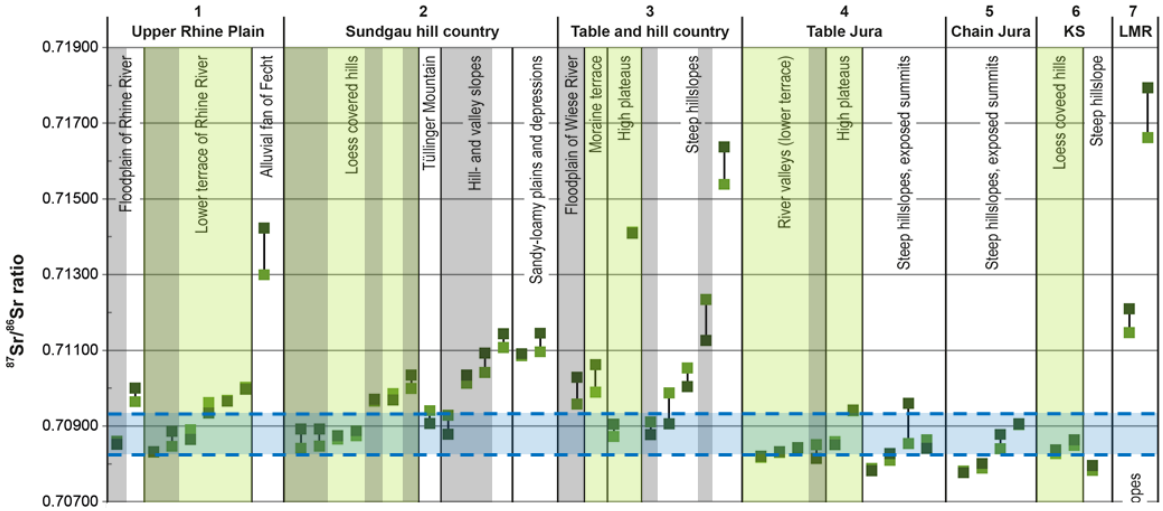


Abb. 4: *$^{87}Sr/^{86}Sr$-Werte der modernen Pflanzenproben (Y-Achse) innerhalb verschiedener Landschaftsformen (KS = Kaiserstuhl; LMR = low mountain range; Grundgebirge). Hellgrüne Werte = Bodenvegetation; dunkelgrüne Werte = Baumlaub. Grün markiert sind die für Ackerbau als geeignet eingestuften Probenstandorte, die grauen Balken zeigen Proben, die maximal 7 km von Basel-Gasfabrik entfernt liegen. Blau eingezeichnet ist der local range I (s. unten).*

Bestimmung des biologisch verfügbaren Strontiums (local range I und II)

Für die Bestimmung des biologisch verfügbaren Strontiums von Basel-Gasfabrik wurden zwei *local ranges* definiert, die auf unterschiedlichen Daten beruhen. *Local range I* basiert auf den $^{87}Sr/^{86}Sr$-Werten der menschlichen Milchzähne. Deren Spannbreite ist mit 0.70832–0.70928 auffallend eng und widerspiegelt kurz zusammengefasst vor allem den pflanzlichen Bestandteil der Ernährung der Mütter. *Local range I* umfasst aber nicht die gesamte $^{87}Sr/^{86}Sr$-Spannbreite, die anhand der Pflanzenproben als mögliches Ackerland definiert wurde (0.70830–0.71000). Daraus folgern wir, dass nicht alle potentiellen Anbauflächen im näheren Umfeld von Basel-Gasfabrik zur Ernährung der Mütter beigetragen haben. Dies deutet auf klar definierte Anbaugebiete hin, wobei die Auswahl der Anbauflächen nicht nur auf utilitaristischen, sondern auch auf kulturellen Aspekten wie zum Beispiel Landnutzungsrechte, Handelsmuster, Verwandtschaft oder Tabus etc. basieren.

Local range II umfasst die $^{87}Sr/^{86}Sr$-Werte der sechs Schweine- und fünf Hundezähnen und ist mit einer Spannbreite von 0.70863–0.71058 deutlich breiter und heterogener als *local range I*. Aus der Archäozoologie wissen wir, dass in der Latènezeit Schweine mit grosser Wahrscheinlichkeit verhandelt wurden (Kühn und Iseli, 2008; Stopp, 2008). Die deutliche Streuung der Schweine-$^{87}Sr/^{86}Sr$-Werte bestätigt diese Hypothese und zeigt, dass die Viehwirtschaft im Gegensatz zum Ackerbau ein deutlich grösseres Einzugsgebiet aufweist.

Fazit zur $^{87}Sr/^{86}Sr$-Kartierung

Insgesamt hat sich gezeigt, dass der kombinierte Ansatz von archäologischem Material (Menschen- und Tierzähne) und von modernen Vegetations- und Wasserproben eine gute Datenbasis für die Rekonstruktion des

lokal biologisch verfügbaren Strontiums darstellt. Allerdings gilt zu beachten, dass eine $^{87}Sr/^{86}Sr$-Kartierung mit modernen Vegetationsproben nur dann zuverlässige Resultate liefert, wenn die wichtigsten geologischen Substrate an mehreren Standorten beprobt und diese bezüglich der geologisch-bodenkundlichen Eigenschaften evaluiert werden. Für die Interpretation von Tierzahnproben ist ausserdem eine enge Zusammenarbeit mit der Archäozoologie notwendig. Der neue Ansatz zur Evaluation der Landschaftsformen zur Eignung als landwirtschaftliche Nutzfläche wurde erfolgreich getestet und erlaubt neuartige Interpretationsmöglichkeiten vor allem im Bereich der Subsistenzwirtschaft. So kann für Basel-Gasfabrik eine differenzierte Nutzung der Landschaft nachgezeichnet werden. Der Anbau und/oder Bezug von pflanzlichen Lebensmitteln ist anders organisiert und verortet als die Viehwirtschaft und scheint strengen Regeln unterworfen zu sein, was zu einem auffallend homogenen Wertespektrum der menschlichen Milchzähne führt. Die Evaluation der Bodenfruchtbarkeit rund um Basel-Gasfabrik legt nahe, dass die Auswahl der Anbaugebiete nicht nur auf utilitaristische Aspekte zurückgeht. Die $^{87}Sr/^{86}Sr$-Werte der Tierzähne hingegen zeigt ein heterogeneres Bild und lässt rege Kontakte mit dem Umland vermuten. Gleiches gilt auch für die erwachsenen Menschen, wie die $^{87}Sr/^{86}Sr$-Werte von Molaren zeigen (Knipper et al., 2018).

Die Ergebnisse zeigen aber auch, dass eine (prähistorische) Siedlung nicht als abgeschlossenes Gebilde, sondern als Bestandteil einer Landschaft betrachtet werden muss. Eine Landschaft, in der sich die Menschen nach ihren eigenen Vorstellungen und kulturellen Prägungen bewegen. Diese Handlungen – zu denen auch die Subsistenzwirtschaft gehört – müssen nicht immer nach für uns „logisch“ erscheinenden Mustern abgelaufen sein. So darf die Landschaft nicht als physische Hülle betrachtet werden, die dem damaligen Menschen bloss als Ressourcen-Quelle diente und mit grösstmöglicher Effizienz ausgebeutet wurde. Diese Vorstellung entspricht vielleicht unserem heutigen kapitalistisch geprägten Denken, muss aber nicht der damaligen Wahrheit gleichkommen. Die Handlungsmuster werden stets vom gesellschaftlichen Umfeld, dem kulturellen Hintergrund, von Tabus und von Idealvorstellungen etc. geprägt, die wir als Aussenstehende oft nicht nachvollziehen können.

5.2 The Hidden Midden

Die Zusammenfassung des zweiten Papers (Kap. 5.2.1) wird mit Ausführungen zum Umgang mit verschiedenen Ressourcen (Kap. 5.2.2) ergänzt, da diese Thematik im Paper aufgrund des beschränkten Platzes nur kurz angesprochen werden konnte. Den nachfolgenden Ausführungen liegen die theoretischen Konzepte und Begriffsdefinitionen zu Grunde, wie sie in Kap. 1.4 erläutert wurden (Abb. 2).

5.2.1 Zusammenfassung des Papers

Ziele und Probenmaterial

Eine der wichtigsten Aufgaben der Geoarchäologie und der Mikromorphologie im Speziellen ist die Rekonstruktion von Schichtbildungsprozessen, was für das Verständnis der *site formation processes* essentiell ist. Innerhalb einer Siedlung sind verschiedene Schichtbildungsprozesse wie z. B. die Nutzung von offenen und überdachten Arealen, Aufschüttungen, Einspülen in Senken, Verfüllungen etc. zu erwarten, die fast ausschliesslich von menschlichen Aktivitäten beeinflusst sind (*c-transforms*). Allerdings lassen sich auch postsedimentäre Prozesse wie Eisen- und Phosphatausfällungen, Verwitterungs- oder Zersetzungsprozesse etc. nachvollziehen (*n-transforms*). Und schliesslich können im Dünnschliff verschiedene Mikroartefakte identifiziert werden, die makroskopisch nicht zu erkennen sind (Glassplitter, Fäkalien- oder Dungreste, Aschen etc.).

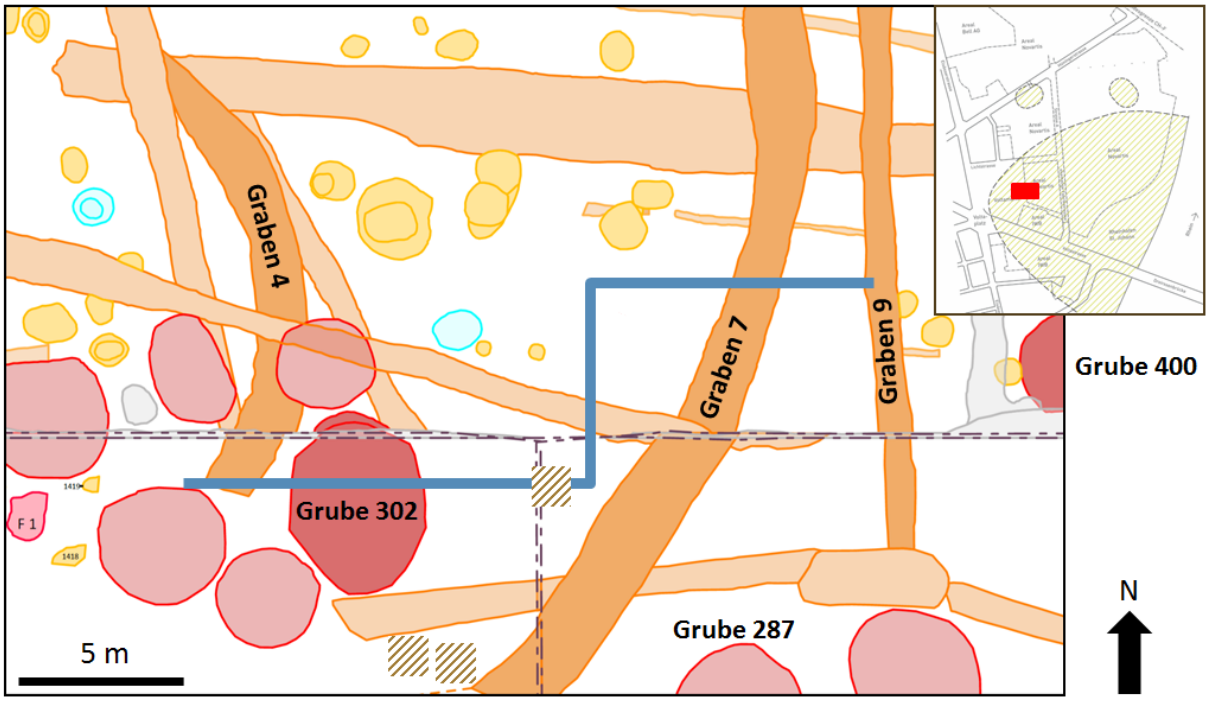


Abb. 5: *Der untersuchte Siedlungsbereich liegt im Westen der Siedlung (kleine Karte oben rechts). Der dargestellte Siedlungsausschnitt zeigt eine Vielzahl von Gruben (rot), Gräben (orange) und Pfostengruben (gelb) (hellblau = neuzeitliche Befunde; grau = Störungen). Die mikromorphologisch untersuchten Strukturen sind mit Nummern beschriftet. Braune Quadrate: Stampflehmboden. Blaue Linie: Lage des schematischen West-Ost-Profils in Abb. 6.*

Bei den vorliegenden Untersuchungen wurde der Fokus nicht primär auf Siedlungsgruben, sondern auf Gräben und Flächen („Kulturschichten") gelegt. Hierfür wurde ein sehr gut erhaltener Siedlungsbereich in einer mit Hochflutsand verfüllten Senke im Westen der Fundstelle ausgewählt (Grabungen 1990/42, 1992/34, 1994/01 und 2002/13) (Abb. 5). Dabei wurden mit 89 Dünnschliffen aus 25 Profilen 124 Schichten aus drei Gruben (Grube

287, 302 und 400), vier Gräben (Graben 4, 7, 9 und ein weiterer Graben ausserhalb des Siedlungsbereichs), drei Hausböden, eine Pfostengrube sowie 16 Profile mit archäologischen Schichten analysiert.

Zusammenfassung der Resultate zu den Schichtbildungsprozessen

Auf Basis der geoarchäologischen Resultate (Sedimenteigenschaften, Mikrokomponenten, Schichtbildungsprozesse) wurden elf Mikrofazies-Typen definiert (MFT I–XI; Tab. 2). Die rekonstruierten Sedimentationsprozesse wurden fast ausschliesslich durch menschliche Aktivitäten innerhalb der Siedlung initiiert (*c-transforms*) und unterscheiden sich zwischen den verschiedenen Befundtypen stark (Tab. 2).

Anhand bodenkundlicher Überlegungen zeigt sich, dass das Gelände einst eine Mikro-Topografie mit Senken und (Kies-) Hochrücken aufwies. Spätestens mit der geoarchäologisch untersuchten Siedlungsphase wurde das Gelände allerdings ausnivelliert, wobei innerhalb eines Areals („Parzelle“) jeweils ein einheitliches Level geschaffen wurde (± 2 cm). Auf dieser gekappten Lehmoberfläche hat sich ein 2-5 cm mächtiger, initialer Tramplinghorizont ausgebildet (MFT 3), der sich als diffuse Kiesschicht manifestiert. Bei längerer Nutzung und Begehung erfolgte eine Sedimentakkumulation mit schwacher Feinschichtung (MFT 4). Andernorts zeigt sich ein durchwegs homogenes Schichtpaket (MFT 5), das kleine Fäkalienstückchen und Asche enthält und möglicherweise von einer Bodenbearbeitung (und Düngung) überprägt ist. Mit MFT 2 wurde verschiedentlich ein Stampflehmboden gefasst, der sich in einem überdachten Bereich direkt auf dem gekappten Lehm ausgebildet hat. Das Fehlen von Mikroartefakten oder einer Nutzungsschicht legt den Schluss nahe, dass der Boden von einer mutmasslichen Matte oder ähnlichem überdeckt wurde.

In drei der vier untersuchten Gräben wurde eine Akkumulation von eingespültem Oberflächenmaterial festgestellt, was zu einer allmählichen Verfüllung der Gräben mit mikroholzkohlehaltigem Feinsediment führte (MFT 6). Eine Ausnahme bildet Graben 4, dessen gut sortierte Sandschichten (MFT 7) auf fliessendes Wasser hindeuten. Es bleibt unklar, ob es sich hierbei um einen kanalisierten Bach oder um sporadisch fliessendes Wasser handelte.

In den Gruben schliesslich konnten feingeschichtete, kompaktierte Asche- und Holzkohleschichten identifiziert werden (MFT 8). Dabei dürfte es sich um eine Akkumulation von Ofenausraum handeln (Defacto-Abfall), wobei die Feinschichtung und Kompaktion auf eine Begehung in einem überdachten Bereich schliessen lassen. Entsprechend wird eine Sekundärnutzung der Gruben als überdachter Werkplatz postuliert. Allen Gruben gemein ist eine nachfolgende rasche Verfüllung mit holzkohlehaltigen Sedimenten (MFT 9) und zahlreichen Keramik- und Tierknochenfragmenten (Sekundär-Abfall). Das eingefüllte Sediment ähnelt den MFT 4, 5 und 6.

MFT	Befunde	(Sedimentations-) Prozesse	Menschliche Aktivitäten	Interpretation
I	Anstehende Sedimente			Natürlich anstehender Lehm
II	Hausboden	Kompaktion	Begehung innerhalb eines überdachten Bereichs	Stampflehmboden
III	Offene Areale; Nutzungsschicht	Kontinuierliche Akkumulation; Exponierung	Begehung einer lehmigen Oberfläche; ungeschützter Bereich	Initialer Trampling-horizont
IV	Offene Areale; Nutzungsschicht	Kontinuierliche Akkumulation; Einarbeitung von Holzkohlen und Mikroartefakten	Begehung Aussenbereich; häusliche und handwerkliche Aktivitäten	Feingeschichtete Nutzungsschicht
V	Offene Areale; Nutzungsschicht	Homogenisierung; Einarbeitung von Aschen, Mikroholzkohlen, wenig Dung und Koprolith-Stückchen	Mutmassliche Bodenbearbeitung und Düngung	Mutm. Gartenwirtschaft
VI	Gräben	Kontinuierliche Akkumulation von eingespültem Material		Natürliche Grabenverfüllung
VII	Gräben	Durch fliessendes Wasser abgelagerter Sand		Wasserkanal
VIII	Gruben	Kontinuierliche Akkumulation und Kompaktion von Aschen, Holzkohlen und verziegeltem Lehm	Begehung innerhalb einer vor Witterung geschützten Grube; handwerkliche Aktivitäten (Glas-, Metallhandwerk)	Überdachte Werkgrube
IX	Gruben	Verfüllung	Rasche, intentionelle Verfüllung mit Sediment und "Abfall" (Keramik, Knochen)	Grubenverfüllung
X	Offene Areale	Planie	Flächiges Ausplanieren von grössenselektierten Kieseln und Geröllen	Intentionelle Geröll-Auflage
XI	Überall	Verwitterung durch langanhaltende Exposition und Bioturbation	Moderne Bodenbearbeitung	Stark verwittertes, *dark earth*-ähnliches oberstes Schichtpaket

Tab. 2: *Überblickstabelle zu den verschiedenen Mikrofazies-Typen (MFT I-XI) und den dazugehörigen Befunden, den (Sedimentations-) Prozessen, den damit assoziierten Aktivitäten und der dazugehörigen Interpretationen.*

Räumliche Gliederung und Ereignisabfolge

Anhand des in drei Profilen festgestellten Stampflehmbodens ist im südlichen Bereich des Untersuchungsgebietes ein Haus zu postulieren (Abb. 5). Dieses dürfte aufgrund stratigrafischer Überlegungen einer vorangehenden Siedlungsphase angehören. Von dieser älteren Phase ist – abgesehen von diesem Boden – offenbar nichts mehr vorhanden, was mit der Ausnivellierung des Geländes zusammenhängen dürfte.

Die Kartierung der Mikrofazies-Typen hat gezeigt, dass gewisse räumliche Unterschiede zu erkennen sind. So findet sich MFT 4 ausschliesslich östlich von Graben 7, während MFT 5 nur westlich davon auftritt (Abb. 5). Ausserdem besteht zwischen dem westlichen und östlichen Bereich bei der Oberkante des anstehenden Lehmes ein Höhenunterschied von etwa 10 cm. Es liegt deshalb der Schluss nahe, dass Graben 7 eine Parzellengrenze darstellt, wobei Unterschiede in der jeweiligen Nutzung der beiden Parzellen festzustellen sind. So wird für den westlichen Bereich eine Gartenwirtschaft und im östlichen Bereich eine offenliegende, über längere Zeit begangene Oberfläche postuliert. Mehrere in Grube 400 identifizierte Glastropfen- und Splitter lassen für diesen Bereich handwerkliche Aktivitäten (Glashandwerk) vermuten.

Die stratigrafische Einordnung der Mikrofazies-Typen ergibt ausserdem eine relative Abfolge der rekonstruierten Aktivitäten. Die daraus resultierende Ereignisabfolge wird in Abb. 6 schematisch dargestellt. Der Einfachheit wegen ist die festgestellte ältere Siedlungsphase nicht aufgeführt. Beim dargestellten Haus handelt sich um einen Analogie-Schluss zum stratigrafisch älteren Hausboden MFT 2.

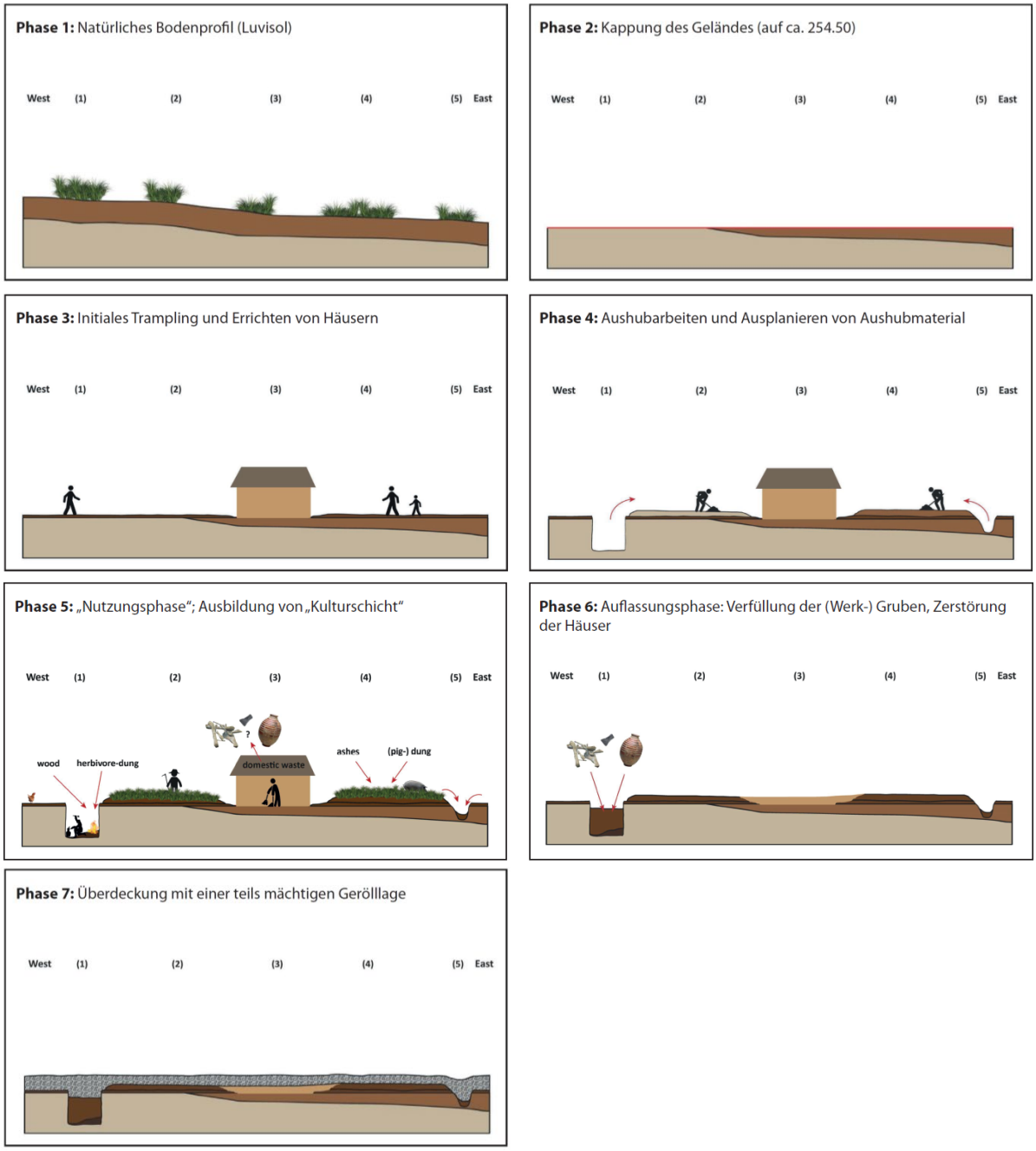


Abb. 6: *Schematisches West-Ost-Profil (zur Position des schematischen Profils siehe Abb. 5). Rekonstruktion der Ereignisabfolge anhand der mikromorphologischen Resultate:* ***Phase 1)*** *Ursprüngliche Mikrotopografie und holozänes Bodenprofil eines Luvisols (dunkelbraun) vor der Besiedlung;* ***Phase 2)*** *Das Gelände wird ausnivelliert (ältere Siedlungsspuren werden zerstört). Areale weisen verschiedene Höhen-Niveaus auf;* ***Phase 3)*** *Initiale Begehung (MFT 3), möglicherweise im Zusammenhang mit den Nivellierungsarbeiten und/oder dem Ausheben von Gräben und Gruben;* ***Phase 4)*** *Akkumulation infolge alltäglicher (Siedlungs-) Aktivitäten (MFT 4) und Ausplanieren von Aushubmaterial (MFT 5);* ***Phase 5)*** *Im Zuge der Siedlungsaktivitäten fallen grosse Mengen an Keramikscherben, Tierknochenfragmenten, Holzkohlen, Aschen, Fäkalien etc. an. Es wird ein differenzierter Umgang mit den verschiedenen Materialien sowie (verschiedene) Abfallhaufen vermutet (Primär-Abfall). In situ liegende Nutzungsschichten innerhalb von Häusern (Defacto-Abfall) sind keine bekannt. Es wird eine Sekundärnutzung von Gruben zu handwerklichen Zwecken vermutet (MFT 8);* ***Phase 6)*** *Gruben werden mit (gelagertem) Abfall (Sekundär-Abfall) und mit unterschiedlichen Sedimenten verfüllt (MFT 9). Dabei handelt es sich evtl. um in Gräben akkumulierte Ablagerungen, das beim Erneuern von Gräben als Aushubmaterial anfällt;* ***Phase 7)*** *Die Siedlungsphase wird von einem mächtigen, jüngerlatènezeitlichen Geröllpaket abgeschlossen (MFT 10).*

5.2.2 Der Umgang mit verschiedenen Materialien

Auf Basis der geoarchäologischen Untersuchungen ist es möglich, die Nutzung und Entsorgung einzelner Materialien teilweise nachzuvollziehen. Dies kann als ein erster Schritt zur Rekonstruktion des Abfallverhaltens einer (prähistorischen) Gesellschaft betrachtet werden.

Aushubmaterial als natürliche Ressourcen

Beim Ausheben einer Grube variiert die dabei anfallende Menge der anstehenden Sedimente stark. Dieser Umstand soll mit einem Gedankenexperiment nachvollzogen werden. Anhand der 2.7 m tief erhaltenen Grube 321 wurde ausgerechnet, wie viel Material von den einzelnen anstehenden Sedimenten relativ zueinander anfällt (Tab. 3). Dabei werden sowohl die obersten latènezeitlichen Schicht (Kulturschicht) als auch der Bt-, Cv- und C-Horizont des Hochflutsandes komplett durchschlagen. Die untersten 1.8 m der Grube sind im kalkhaltigen Rheinschotter (IIC) eingetieft. Somit fällt beim Ausheben der Grube mit 66% (Volumen) vor allem Material des sandig-kiesigen Rheinschotters an. 16% sind dem kalkhaltigen C- und Cv-Horizont und 7% dem Bt-Horizont zuzurechnen, während nur 11% anthropogen überprägte Sedimente (Kulturschicht) ausmachen (Tab. 3).

Horizont	Mächtigkeit [cm]	Aushub [%]	Verfüllung [%]
Kulturschicht	30	**11**	**70**
Bt	18	**7**	**5**
Cv	22	**8**	**15**
C	22	**8**	**0**
IIC	178	**66**	**10**

Tab. 3: Anstehende Substrate und ihre Mächtigkeit bei Grube 321 sowie deren prozentualen Volumen-Anteile im Aushub und Verfüllung (Gedankenexperiment).

Der Vergleich der Zusammensetzung des Aushubs und der Grubenverfüllung (Tab. 3) zeigt, dass letztere nicht aus frischem Aushubmaterial (zum Beispiel von einer benachbarten Grube) besteht. Insbesondere der kalkhaltige Rheinschotter, aber auch der Hochflutsand ist (deutlich) unterrepräsentiert, während bei der Verfüllung das Kulturschichtmaterial mit 70% stark überrepräsentiert ist. Die Untervertretung von Hochflutsandlehm ist keine Überraschung, zumal der kalkhaltige Hochflutsandlehm als Hüttenlehm und der kalkfreie, tonige zum Töpfern (Steiner, 2008) sowie für Ofenkonstruktionen und Herdplatten verwendet wurde. Der Verbleib des Rheinschotters hingegen bleibt unklar. Der unterschiedliche Sand- und Kiesgehalt in den verschiedenen Mikrofazies-Typen deutet allerdings auf eine differenzierte Verwendung und Aufbereitung des Rheinschotters hin: Kalkhaltiger Sand und Feinkies gelangte vor allem in die „Kulturschichten" MFT 4 und 5 und in die Gräben (MFT 6), während sich die Grobkies- und Geröllfraktion vorwiegend auf die Geröllschicht MFT 10 beschränkt.

Zusammenfassend zeigt sich eine regelhafte und differenzierte Nutzung der natürlich anstehenden Ressourcen. Die Eigenschaften der einzelnen Substrate wurden dabei optimal genutzt, was zu einem unterschiedlichen Umgang der Subtraten führte. So findet der Hochflutsandlehm vor allem in Form von verwittertem Wand- und Ofenlehm- sowie von Keramikfragmenten den Weg zurück in die Gruben, während ein Teil des Rheinschotters zur Bildung der Kulturschichten beiträgt. Die differenzierte Nutzung von Lehm während der Latènezeit wurde auch anderweitig – so zum Beispiel auf dem Basler Münsterhügel – festgestellt (Hagendorn et al., 2017).

Zum Umgang mit Fäkalien

Der Umgang mit Fäkalien ist in unserer heutigen Gesellschaft weitestgehend tabuisiert und dank der unter die

Oberfläche verbannten Kanalisation, den farbigen Robidog-Säckchen und der Trennung von Landwirtschaft (Viehzucht) und Wohngebieten kaum mehr im Alltag sicht- und riechbar. Dies hat sich auf die hygienischen und gesundheitlichen Zustände zweifelslos sehr positiv ausgewirkt, führt aber zu einem gesellschaftlich sehr stark geprägten Bild davon, was „sauber" und was „dreckig" ist. In prähistorischen Gesellschaften herrschten ganz andere Realitäten, wie die zahlreichen Fäkalienstückchen in vielen der untersuchten Proben, aber auch der starke Parasitenbefall von Mensch und Tier in Basel-Gasfabrik (Pichler et al., 2014) beweisen. Dass es sich hierbei nicht einfach um Nachlässigkeit, sondern um einen differenzierten Umgang mit Fäkalien handelt, zeigen die bisherigen Resultate für Basel-Gasfabrik, die auf einer ganzen Reihe aufwändiger (und zum Teil noch laufender) Untersuchungen basieren. Grundlage hierfür ist das Erkennen von Fäkalien in bodenkundlichen Dünnschliffen sowie die Identifizierung der jeweiligen Produzenten. Dank einer der europaweit grössten Referenzsammlungen kann die geoarchäologische Forschungsgruppe der IPNA auf einen grossen Erfahrungsschatz bei der Identifikation von Koprolithen zurückgreifen (Brönnimann et al., 2017a; Brönnimann et al., 2017b). Die optischen Untersuchungen von Fäkalien aus Basel-Gasfabrik wurden ausserdem durch paläoparasitologische Analysen (Pümpin et al., 2015) sowie durch neuartige Sterol-Untersuchungen unterstützt. Letztere sind in Form einer Forschungskooperation mit der Universität Mainz momentan am Laufen und erlauben eine Differenzierung von Koprolithen vom Mensch und Schwein. Nachfolgende Erläuterungen umreissen den aktuellen Forschungsstand zu Basel-Gasfabrik.

Kleine **Fäkalienstückchen** (0.5–2 mm) finden sich in den Mikrofazies-Typen 5 und 6 regelmässig. In einigen Gruben konnten ausserdem ganz erhaltene Koprolithe geborgen werden, die – so der heutige Forschungsstand – vor allem Hunden und Schweinen zuzuordnen sind. Gleiches gilt, sofern zu beurteilen, für die obengenannten Fäkalienstückchen. Es ist folglich von einem engen Zusammenleben von Mensch, Schwein und Hund innerhalb der Siedlung auszugehen, was sich auch anhand des paläoparasitologischen Befundes zeigt (Pichler et al., 2014). Eindeutige Latrinensedimente, wie sie aus römerzeitlichen oder mittelalterlichen Latrinen bekannt sind (Brombacher et al., 1999; Brönnimann et al., 2017b; Pümpin, 2013), fehlen bisher weitestgehend.

Herbivoren-Dung findet sich selten in geringer Menge in MFT 5 und deutlich häufiger in mehreren Gruben in Form von Dungasche (MFT 8). Die Nutzung von Herbivoren-Dung als Brennstoff erstaunt nicht, da palynologische Untersuchungen für die späte Eisenzeit eine sehr offene Landschaft postulieren (Guélat und Richard, 2014; Wick, 2015), in der Brennholz wohl knapp war. Ob der seltene Nachweis von Herbivoren-Dung in archäologischen Schichten ein Hinweis auf Viehhaltung innerhalb der Siedlung und/oder für Düngung ist, bleibt unklar.

Eine spezielle Rolle nimmt **Vogel-Guano** ein. So wurde in Grube 400 eine feingeschichtete Abfolge von pflanzlicher Asche und mehreren Guano-Lagen identifiziert. Der wiederholte Eintrag von Guano ist wohl kein zufälliges Ereignis. Die in der Asche eingebetteten Glastropfen- und Splitter lassen im Gegenteil vermuten, dass Guano bei der Glasbearbeitung gezielt verwendet wurde. Dies bestätigte Willem B. Stern, der Guano als stark nitrathaltiges Material bei seinen Experimenten zur Reduzierung der Bläschenbildung verwendet hat (freundliche Mitteilung W. B. Stern). Ein sehr ähnlicher Befund mit feingeschichteten, pflanzlichen Aschen und mehrfachem Eintrag von Vogel-Guano ist des Weiteren aus einer mittelalterlichen Glaswerkstatt in Zürich bekannt (Brönnimann, 2015; Rentzel et al., 2017).

Aufgrund der bisherigen interdisziplinären Resultate zu den Koprolithen aus Basel-Gasfabrik lässt sich zusammenfassen, dass der Umgang mit den menschlichen Ausscheidungen in Basel-Gasfabrik bislang kaum bekannt ist. Dafür zeigt sich, dass gewisse Fäkalien wie Herbivoren-Dung oder Vogel-Guano eine differenzierte Nutzung erfuhren. Fäkalien wurden demnach nicht, wie in der heutigen Gesellschaft, als möglichst rasch zu entsorgendes Übel, sondern als Werkstoff und Rohmaterial betrachtet.

Fazit zu Objektbiografien, Abfallverhalten und Ressourcen-Management

Mit Hilfe geoarchäologischer Methoden lassen sich keine lückenlosen Geschichten einzelner Objektgruppen oder Materialgattungen nacherzählen. Allerdings können auf verschiedenen Stufen Informationen zusammengetragen werden, die in ihrer Summe einen Beitrag zur Rekonstruktion gesellschaftlicher Handlungsmuster liefern können. Die meisten Informationen entnehmen wir den verschiedenen Abfall-Ablagerungen. Dabei handelt es sich meist um Sekundärabfall (MFT 9), seltener auch um Defacto-Abfall (MFT 8) (Abb. 2). Allerdings ist eine Differenzierung von Primär- und Sekundärabfall (und konsequenterweise auch von Tertiärabfall) nur selten möglich.

Die Geoarchäologie leistet insofern einen grossen Beitrag zur Rekonstruktion von Objekt- und Materialbiografien und somit zur Evaluierung vom Abfallverhalten und Ressourcen-Management bei, als dass verschiedene Mikroartefakte und Materialien (wie z. B. Dung) identifiziert und quantifiziert sowie deren Erhaltung evaluiert werden kann. Dabei lassen sich Verwitterungsspuren, Brandüberprägungen, mechanische Einwirkungen etc. beurteilen. Anhand dieser Merkmale lässt sich abschätzen, wie intensiv oder lang der Weg einer Objektgruppe oder einer Materialgattung war – ob die Objektbiografie also viele oder nur wenige Stufen umfasst – und ob die festgestellte Überprägung regelhaft oder nur ausnahmsweise auftritt. Ausserdem ist zur Identifikation von Defacto-Abfall die Mikromorphologie besonders gut geeignet. Beispiele hierfür sind zum Beispiel die *in situ* befindlichen, feingeschichteten Asche- und Holzkohleschichten oder die dem Glashandwerk zugewiesenen Glastropfen und Guano-Stückchen. Aber auch das Fehlen von Defacto-Abfall ist als wichtige Information zu werten – so zum Beispiel im Falle der auffallend reinen Stampflehmboden, was eine Bedeckung des Bodens oder aber ein regelmässiger Unterhalt und Reinigung vermuten lässt. Die geoarchäologischen Analysen können zwar nur einzelne Stufen und Phasen einer Objektbiografie sichtbar machen. Dabei werden aber wertvolle Puzzle-Teile geschaffen, die in Kombination mit anderen Disziplinen helfen, das grosse Ganze besser zu verstehen.

5.3. Contextualising the Dead

Ein differenzierter Umgang fand nicht nur mit Objekt- und Materialgruppen, sondern auch mit Lebenden und Toten statt. Mensch und Tier sind im archäologischen Befund aber meist nur noch durch Knochen(-fragmente) repräsentiert. Glücklicherweise erweist sich genau dieses Material als idealer Informationsträger. Das dritte und letzte Paper befasst sich deshalb genau mit dieser Objektgruppe. Knochen sind gegenüber mechanischer Beanspruchung zwar recht resistent, dank ihres biogenen Ursprungs und ihrer differenzierten Mikrostruktur aber hinsichtlich geochemischer Prozesse (Kollagengehalt), Hitzeeinwirkung (Mikrostruktur, Kollagengehalt, Färbung) und Bioerosion ein ausserordentlich vielseitiger Informationsträger. Aus diesem Grund wurde dem Knochen im Rahmen der vorliegenden Dissertation durch neuartige histotaphonomische Untersuchungen besondere Aufmerksamkeit geschenkt. Dabei wird eine besonders starke Vergrösserung benötigt, zumal die bioerosiven Phänomene auf der Ebene von wenigen Mikrometern stattfinden.

Zusammenfassung der Forschungsgeschichte zur Histotaphonomie

Die Histotaphonomie hat ihre Ursprünge – wie die Taphonomie ebenfalls (Kap. 1.4) – in der Paläontologie. So beobachtete Albert Kölliker bereits Mitte des 19. Jh. „Parasiten in den Hartgebilden von Tieren" (Kölliker, 1860), wobei einige dieser in Dünnschliffen von fossilen Spongien und Muschelschalen festgestellten Phänomene tatsächlich Ähnlichkeiten mit Wedl-Tunnels, aber auch mit Cyanobakterien aufweisen. Nur wenig später fand Köllikers damaliger Assistent Karl Joseph Eberth in Menschenzähnen Spuren von Pilzen, die Kölliker auch in Zähnen von fossilen „niederen Tieren" beobachtet haben will (Müller et al., 1863). Die erste publizierte histotaphonomische Arbeit stammt allerdings von Carl Wedl – einem Wiener Pathologen, der – ebenfalls in einem Präparat eines Menschenzahns – Fäden entdeckte, die er als Pilze ansprach (Wedl, 1865). Dieser Aufsatz gilt in der Histotaphonomie gemeinhin als erste Beobachtung bioerosiver Prozesse im Hartgewebe von Menschen[2]. Trotz den Arbeiten von Kölliker, Eberth und Wedl fristete die Histotaphonomie während über 100 Jahren ein eher bescheidenes Dasein, bis die mikroskopische Untersuchung von Menschenknochen- und Zähnen in den 1980er und 1990er Jahren in der physischen Anthropologie und der Forensik wieder aufgegriffen wurde. Es ist Cecil John Hackett, der mit seinem Aufsatz von 1981 die heute gebräuchliche Nomenklatur einführte (Hackett, 1981). Robert Hedges und Andrew Miller schliesslich definierten den *Oxford Histological Index* – eine 6-stufige Skala (0-5), die die Intensität der Bioerosion von 5 (Mikrostruktur komplett erhalten) bis 0 (Mikrostruktur vollständig zerstört) angibt (Hedges und Millard, 1995). Die ersten archäologisch gut verankerten histotaphonomischen Studien stammen von Lynne Bell, die mit einem forensischen Ansatz die Zersetzung von Knochen aufgrund bioerosiver Prozesse studierte (Bell, 1995; Bell et al., 1996). Definitiv aus dem Dornröschenschlaf erwacht ist die Methode vor rund 10 Jahren mit den Forschungsarbeiten von Gordon Turner-Walker und Tom Booth. Es ist dies auch die Geburtsstunde zweier verschiedener Interpretationsansätze zur Ursache der bioerosiven Prozesse: Während Turner-Walker davon ausgeht, dass exogene Bodenbakterien für die im Dünnschliff erkennbare Zerstörung der

[2] Eine eingehende Betrachtung der von Wedl publizierten Zeichnungen lässt allerdings Zweifel aufkommen, ob es sich dabei tatsächlich um das handelt, was Hackett (1981) zu Ehren von Carl Wedl als „Wedl-Tunnel" betitelte. Form und Ausprägung der von Wedl gezeichneten Tunnels erinnern stark an Cyanobakterien. Ausserdem schreibt Wedl, dass er den Zahn einer Leiche zuvor 10-12 Tage in einem Glas mit Wasser zur Reinigung eingelegt habe. Es ist deshalb m. E. möglich, dass es sich bei Wedls Beobachtungen nicht um die von Hackett definierten Wedl-Tunnels, sondern um Cyanobakterien handelt.

Mikrostruktur verantwortlich sind (Turner-Walker, 2008; Turner-Walker und Peacock, 2008; Turner-Walker, 2012), vermutet Booth die körpereigenen Darmbakterien als Hauptverursacher (White und Booth, 2014; Booth et al., 2015; Booth, 2016). Diese beiden Hypothesen stehen sich bis heute gegenüber. Ziel der histotaphonomischen Untersuchungen an Mensch- und Tierknochen von Basel-Gasfabrik war deshalb unter anderem, dieser Grundsatzfrage nachzugehen.

Ein neuer Ansatz in der Histotaphonomie

Um dieser komplexen Fragestellung auf den Grund zu gehen, wurde in Zusammenarbeit mit Cordula Portmann ein neuartiger Ansatz ausgearbeitet, der die methodischen und inhaltlichen Perspektiven zweier Disziplinen – der Anthropologie und der Geoarchäologie – kombiniert. Bisher lag der Fokus bei der Histotaphonomie fast ausschliesslich auf der physischen Anthropologie oder der Archäozoologie (zum Beispiel Jans, 2005). Der (geo-) archäologische Kontext wurde meist nur am Rande miteinbezogen, obschon man sich in der Forschung darüber einig ist, dass die Erhaltung von Knochen auf unterschiedliche Faktoren zurückgeht. Für die histotaphonomischen Untersuchungen von Basel-Gasfabrik wurde das riesige Potential von 210 geoarchäologischen Bodendünnschliffen ausgeschöpft: Die zufällig in den Bodenproben enthaltenen (Tier-) Knochenfragmente wurden nicht nur bezüglich der verschiedenen taphonomischen Phänomene, sondern auch hinsichtlich des umgebenden Sedimentes sowie der Sedimentationsprozesse evaluiert. Die halbquantitativen Daten wurden in einer eigens dafür erstellten Datenbank aufgenommen. Für diesen neuartigen, interdisziplinären Ansatz in der Histotaphonomie schlagen wir deshalb folgendes Protokoll vor:

1. Verwendung von **30 µm dicken Dünnschliffen** (eine Differenzierung der bioerosiven Phänomene ist mit dickeren Präparaten nur beschränkt möglich)
2. **Kontextualisierung** von jeder untersuchten Knochenprobe bezüglich des Befundtyps, des Sedimenttyps und der Sedimentationsprozesse
3. **Differenzierte, halbquantitative Aufnahme der verschiedenen taphonomischen Merkmale** mit unterschiedlichen Indizes (Tab. 4). Dabei wird die 6-stufige Skala des OHI als Vorlage verwendet.

Abk.	Index	Skala	Beschreibung
BAI	*Bacterial Attack Index*	0–5	Gesamtheit der *budded, linear-longitudinal* und der *lamellate mfd*
WTI	*Wedl-Tunnel-Index*	0–5	Gesamtheit der Wedl-Tunnels (ohne *Wedl-Type 2*)
CAI	*Cyanobacterial-Attack-Index*	0–5	Gesamtheit des Cyanobakterienbefalls
CRI	*Crack-Index* (CRI)	0–5	Gesamtheit der Risse
COI	*Collagen-Index*	1–5	Erhaltung des Kollagengehaltes anhand der Intensität der Doppelbrechung des Knochens bei gekreuzten Polarisatoren
HEI	*Heat-Index*	0–3	Einschätzung der Brandüberprägung auf Basis von (Squires et al., 2011) (mit 0.5 = unsichere Brandüberprägung)

Tab. 4: *Zusammenfassung der sechs neu definierten Indizes zur Beurteilung der taphonomischen Phänomene an Knochen.*

Probenmaterial

Für die histotaphonomischen Untersuchungen wurden 25 Knochen von 20 menschlichen Individuen analysiert, wobei für (fast) jeden untersuchten Knochen 5 Dünnschnitte (80 Mikrometer) zur Verfügung standen. Die Untersuchung der Tierknochen erfolgte anhand zufällig in den geoarchäologischen Proben eingebetteten Kno-

chenfragmenten- und Splittern. Dabei standen 210 Dünnschliffe zur Verfügung, innerhalb derer 183 Tierknochenfragmente aus 8 Grabungen[3] histotaphonomisch aufgenommen wurden.

Zusammenfassung der Resultate

Die Kontextualisierung und die differenzierte Aufnahme der verschiedenen histotaphonomischen Phänomene von 208 Knochen(-fragmenten) erlaubte eine fundierte Interpretation der jeweiligen taphonomischen Merkmale. So zeigen die Resultate sehr deutlich, dass die **Wedl-Tunnels (WTI)** eine signifikante Korrelation mit dem Befundtyp, jedoch nicht mit dem Sedimenttyp aufweisen. Aus Gruben stammende Knochen weisen nur selten Wedl-Tunnels auf, während bei Knochen aus Tramplinghorizonten das Gegenteil der Fall ist. Dieser klare Zusammenhang von offenliegenden Oberflächen und rasch verfüllten Gruben lässt darauf schliessen, dass die Wedl-Tunnels tatsächlich auf Pilzbefall zurückgehen und somit einen Indikator zur Rekonstruktion von Sedimentationsprozessen darstellen.

Ganz anders sehen die Resultate zum **Bakterienbefall (BAI)** aus. Weder für den Sediment- noch für den Befundtyp ist eine signifikante Korrelation festzustellen. Umso deutlicher aber sind die Unterschiede zwischen Mensch- und Tierknochen: Weisen bei den Tierknochen nur 23% Bakterienbefall auf, so sind es bei den Menschenknochen mit 96% die grosse Mehrheit. Somit liegt der Schluss nahe, dass der in Knochen festgestellte Bakterienbefall nicht auf exogene Bodenbakterien, sondern primär auf endogene Darmbakterien zurückgeht. Dadurch kann die Überprägung eines Knochens durch Bakterienbefall in einen Zusammenhang mit den Todesumständen eines Individuums gestellt werden. Der geringe Bakterienbefall von Tierknochen erklärt sich dadurch, dass es sich bei den Tierknochen vorwiegend um Schlachtabfälle handelt. Beim Schlachten werden die verschiedenen Körperteilte meist kurz nach dem Tod des Tieres vom Körper abgetrennt, sodass das Ausbreiten körpereigener Darmbakterien im Körper weitestgehend verhindert wird. Bei der Verwesung von ganzen Körpern wie zum Beispiel bei Bestattungen allerdings können sich die endogenen Darmbakterien ungehindert über die Blutbahnen im Körper ausbreiten, was sich in der kompletten Zerstörung der Knochen-Mikrostruktur durch Bakterienbefall manifestiert.

Nur wenige Knochen (7%) weisen einen mutmasslichen Befall von **Cyanobakterien (CAI)** auf. Dieser erinnert in seiner Ausprägung stark an Tierknochen aus einer bronzezeitlichen Gruft in Qatna (Brönnimann, 2017) und zeigt ein etwas anderes Erscheinungsbild als Knochen aus Seeufersiedlungen (Huisman et al., 2017). Trotzdem dürfte es sich mit einiger Wahrscheinlichkeit um Cyanobakterien handeln, zumal sehr ähnliche Phänomene auch von Turner-Walker und Miranda Jans beobachtet wurden (Turner-Walker und Jans, 2008) und es eine Vielzahl verschiedener Cyanobakterien mit unterschiedlichen Ansprüchen gibt. Denkbar ist zum Beispiel, dass es sich um Arten handelt, die keine komplette Wasserüberdeckung, sondern ein feuchtes Milieu bevorzugen.

Die Beurteilung von **Rissen (CRI)** an Knochen zeigt, dass fast die Hälfte (44%) eine Rissbildung aufweisen. Eine Korrelation mit dem Sediment- oder Befundtyp konnte nicht festgestellt werden, allerdings zeigt sich ein signifikanter Zusammenhang mit der Hitzeweinwirkung und dem Kollagengehalt. Es wird deshalb die Hypothese aufgestellt, dass ein reduzierter Kollagengehalt eine erhöhte Rissbildung zur Folge haben kann. Dies ist wenig

[3] Grabungen 1990/32, 1990/42, 1992/34, 1993/13, 1996/01, 2001/25, 2002/13 und 2003/08.

erstaunlich, zumal das Kollagen („Knochenleim“) dem Knochen seine Elastizität verleiht.

Deutlich komplexer gestaltet sich die Beurteilung des **Kollagengehaltes (COI)**. Die Resultate lassen vermuten, dass mehrere Faktoren (pH-Wert, Exponierung, hydrologische Verhältnisse, Brandüberprägung etc.) den Kollagengehalt beeinflussen. So zeigen Knochen aus kalkhaltigen Sedimenten eine etwas bessere Erhaltung. Gleichzeitig ist ein signifikanter Zusammenhang zum Befundtyp und zur Brandüberprägung zu fassen. So zeigen Knochen aus Oberflächen ebenso einen geringen Kollagengehalt auf, wie dies (stark) verbrannte Knochen tun. Die Untersuchung des Kollagengehaltes ist vor allem für die Isotopie und aDNA von Wichtigkeit, da beide Methoden auf eine gute Kollagenerhaltung angewiesen sind (Booth et al., 2016).

Die Untersuchung der **Hitzeüberprägung (HEI)** schliesslich zeigt, dass rund ein Drittel (37%) der Knochen eine eindeutige Brandüberprägung aufweist, wobei der Anteil stark verbrannter Knochen (HEI = 2-3) mit 17% relativ gering ist. Dank statistischer Analysen durch Werner Vach wird klar, dass zwischen der Brandüberprägung und dem Bakterienbefall ein signifikanter Zusammenhang besteht, während dies für den Pilzbefall nicht zutrifft. Da verbrannte Knochen in allen Sediment- und Befundtypen gleichermassen auftreten, spielen etwelche Abhängigkeiten von Hitzeeinwirkung und Bioerosion bei der Interpretation der Daten aber keine Rolle. Eine weitere signifikante Korrelation besteht, wie oben bereits erwähnt, zum Kollagengehalt, der mit zunehmender Hitzeüberprägung abnimmt (Abb. 7).

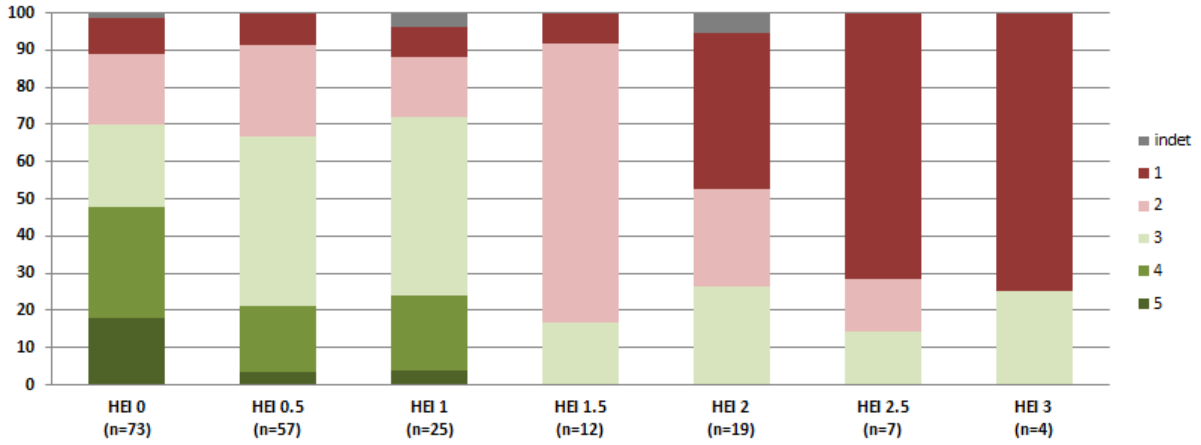


Abb. 7: *Der Kollagengehalt (COI; Säulendiagramme) in Abhängigkeit zur Intensität der Hitzeüberprägung (HEI, X-Achse). HEI 0 = keine Hitzeüberprägung; HEI 0.5 = unsichere Hitzeüberprägung; HEI 1–3 = deutliche bis sehr starke Hitzeüberprägung. COI 1 = keine Kollagenerhaltung; COI 5 = sehr gute Kollagenerhaltung.*

Rekonstruktion der Totenbehandlung – ein Fallbeispiel

Anhand der histotaphonomischen Resultate zu Tier- und Menschenknochen aus Basel-Gasfabrik zeigt sich, dass die Intensität des Bakterienbefalls an Knochen mit der Totenbehandlung des jeweiligen Individuums zusammenhängt. Die Knochen aus den beiden Gräberfeldern von Basel-Gasfabrik sowie das in Grube 321 bestatte männliche Individuum zeigen ein typisches „Körperbestattungs-Signal“ – nämlich die komplette Zerstörung der Mikrostruktur durch Bakterienbefall (Abb. 8.1). Gleiches gilt für die in der Siedlung geborgenen menschlichen Einzelknochen – allerdings stechen hier zwei Ausnahmen ins Auge: Die Knochen BGS 21 und BGS 53 zeigen keinen (BGS 21; Abb. 8.2) respektive einen nur sehr schwachen Bakterienbefall (BGS 53), zusätzlich aber einen schwachen Pilzbefall. Beide Knochen stammen aus ein und derselben Struktur, aus einem als „grosse Mulde“

bezeichneten Befund der Grabung 2003/08 (die nur wenige Dutzend Meter westlich der Grabung 2002/13 liegt). Neueste mikromorphologische Untersuchungen zeigen, dass diese „grosse Mulde“ möglicherweise ein ungewöhnlich grosses (Gruben-) Haus mit Stampflehmboden darstellt. Zwar steht eine Befundauswertung noch aus, die Interpretation der im Feld als Phosphatkruste angesprochenen Schicht als Stampflehmboden ist aber unbestritten. Unabhängig davon, ob es sich bei diesem ausserordentlichen Befund um eine Art Gemeinschaftsgebäude handeln könnte, ist die Tatsache, dass die beiden einzigen Einzelknochen mit abweichender taphonomischer Überprägung aus genau diesem speziellen Befund stammen, wohl nicht bloss Zufall. Für die beiden Einzelknochen (zweier unterschiedlicher Individuen) lässt sich anhand der Histotaphonomie folgende Ereignisabfolge rekonstruieren:

- Das (fast vollständige) Fehlen von Bakterienbefall spricht dafür, dass die beiden Individuen direkt nach ihrem Tod mumifiziert oder aber ihre Gliedmassen abgetrennt wurden.
- Die entfleischten Knochen lagen zu einem späteren Zeitpunkt kurzzeitig an der Oberfläche, was sich am schwachen Pilzbefall nachvollziehen lässt.
- Nach dieser kurzzeitigen Exponierung wurden die Knochen rasch mit Sediment überdeckt, was zum Stopp des Pilzbefalls führte.
- Durch die Lagerung im Sediment haben sich schwache Eisenoxid-Ausfällungen gebildet.

Diese rekonstruierte Totenbehandlung unterscheidet sich wesentlich von derjenigen der anderen histotaphonomisch untersuchten menschlichen Einzelknochen, was anhand klassischer archäoanthropologischen Untersuchungen nicht festgestellt werden könnte. Die Histotaphonomie stellt deshalb eine vielversprechende Methode bei der Untersuchung sterblicher Überreste dar.

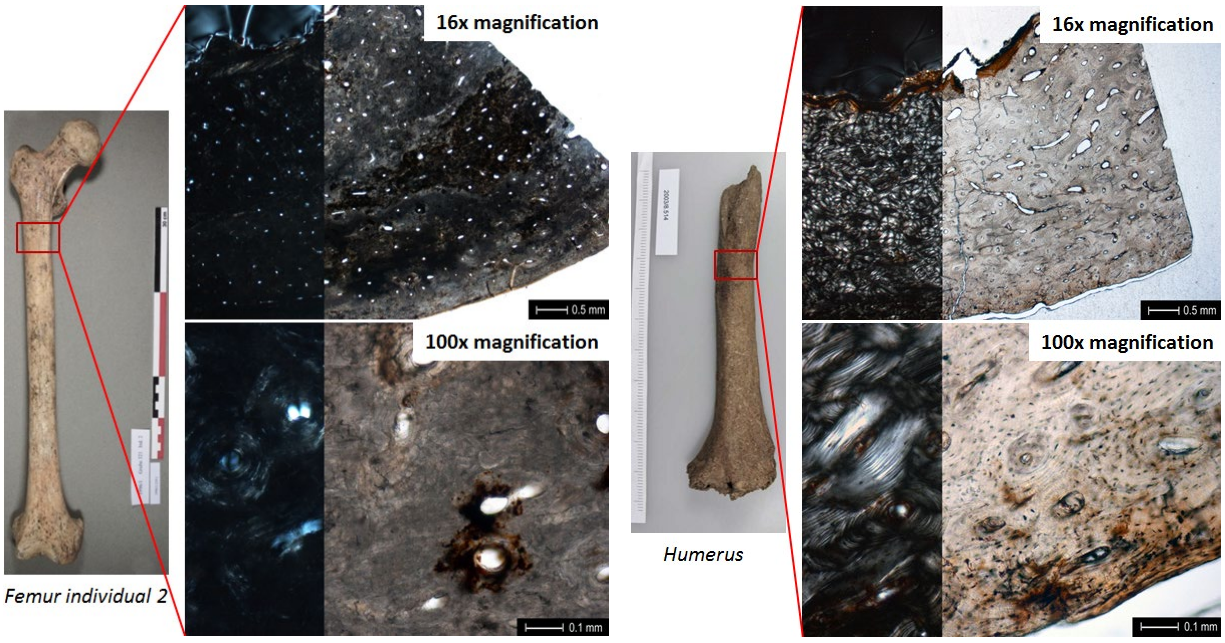


Abb. 8.1(links): *Individuum BGS 6 (Grube 321), Femur und Mikroskop-Fotos mit 16- und 100facher Vergrösserung bei gekreuzten (XPL, links) und parallelen Polarisatoren (PPL, rechts). Die Knochenmikrostruktur ist durch intensiven Bakterienbefall komplett zerstört.* ***Abb. 8.2 (rechts):*** *Individuum BGS 21 (mutm. Grubenhaus), Humerus und Mikroskop-Fotos mit 16- und 100facher Vergrösserung (XPL und PPL). Es zeigt sich kein Bakterienbefall und eine sehr gute Kollagenerhaltung. An der Knochenoberfläche sind schwache Pilzspuren und rostbraune Eisenoxid-Ausfällungen zu erkennen.*

Fazit zu den histotaphonomischen Untersuchungen

Aus methodischer Sicht zeigt sich einmal mehr, dass die Zusammenarbeit verschiedener Disziplinen – die Betrachtung mit verschiedenen Filtern und aus unterschiedlichen Perspektiven – einen substantiellen Mehrwert generiert und eine vielseitige Herangehensweise ermöglicht. Die Verwendung von hochwertigen, 30 µm dünnen Präparaten, die Kontextualisierung der Proben bezüglich des Sediment- und Befundtyps und der Sedimentationsprozesse sowie die differenzierte Aufnahme der verschiedenen taphonomischen Phänomene lieferte eine Datengrundlage, die es erstmals ermöglichte, die Ursache der verschiedenen bioerosiven Prozesse zu beurteilen. Dabei zeigt sich, dass es grosse Unterschiede gibt und teilweise mehrere Faktoren für die taphonomischen Prozesse verantwortlich sind. Anhand unserer Resultate wird klar, dass die Histotaphonomie innerhalb verschiedener Forschungsfelder wertvolle Informationen liefern kann: Bei der Rekonstruktion der Totenbehandlung, bei der Evaluation von Sedimentationsprozessen, aber auch bei der Beurteilung vom Umgang mit Knochen.

Kapitel 6

Ausblick

Im Bereich der Isotopie besteht vor allem bei Tier- und Pflanzenresten aus Basel-Gasfabrik, aber auch aus anderen latènezeitlichen Siedlungen im Umland sehr grosses Potential für weitere Forschungen. Informationen zum Ackerbau sowie zur Viehhaltung und Handel könnten dadurch gewonnen werden. Allerdings sind hierfür in absehbarere Zeit keine Forschungen geplant.

Im Rahmen der bisherigen geoarchäologischen Untersuchungen wurden verschiedene Hypothesen zu Schichtbildungsprozessen, zur Gliederung des Raumes und zu Aktivitätszonen aufgestellt und die Frage nach der Nutzung und dem Umgang unterschiedlicher Ressourcen (Knochen, Keramik, Fäkalien, Rohmaterialien etc.) aufgeworfen. Insbesondere das Forschungsfeld zu taphonomischen Prozessen soll unter Einbezug weiterer Disziplinen intensiv bearbeitet werden. Hierfür werden verschiedene Merkmale wie die Kantenverrundung und Fragmentierung von Keramik- und Knochenfragmenten evaluiert und miteinander verglichen werden. Dies geschieht im Rahmen eines aktuellen interdisziplinären Forschungsprojektes und der engen Zusammenarbeit mit Barbara Stopp (Archäozoologie), Johannes Wimmer (keramisches Fundmaterial und Metallobjekte) und mit Milena Müller-Kissing (Befundauswertung). Dabei wird versucht, verschiedene taphonomische Merkmale unterschiedlicher Disziplinen bezüglich der damit assoziierten Prozesse zu evaluieren und miteinander zu kombinieren. Dadurch soll das Aussagepotential der taphonomischen Phänomene beurteilt und die Hypothesen überprüft werden. Die Resultate werden in einem Paper publiziert, das vom Schreibenden koordiniert wird.

Bei der histotaphonomischen Untersuchung lag der Fokus mit Basel-Gasfabrik auf einer einzelnen Fundstelle. Langfristiges Ziel ist es, den neu ausgearbeiteten Ansatz in zukünftigen Auswertungsprojekten routinemässig anzuwenden und die Daten in einer fundstellenübergreifenden Datenbank zu sammeln. Dadurch soll eine Datenbank wachsen, in der unterschiedlichste Sediment-, Befund- und Siedlungstypen vertreten sind. Diese Datenbasis soll helfen, die verschiedenen taphonomischen Phänomene besser zu verstehen. Daneben sind weitere Papers zur Histotaphonomie in Arbeit. Unter der Federführung von Cordula Portmann entsteht ein Aufsatz, der auf den Fokus auf die Rekonstruktion der Totenbehandlung legt. Unter der Zusammenarbeit mit Tom Booth ist ein Kapitel im *The Routledge Handbook of Archaeothanatology* (Hrsg. Christopher J. Knüsel, Eline M. M. Schotsmans, Dominique Castex) in Arbeit (Booth et al., in Vorb.).

Eine weitere Forschungskooperation besteht mit der Universität Mainz (Geographisches Institut), wo im Rahmen einer Masterarbeit unter der Leitung von Sabine Fiedler Sterol-Analysen an ausgewählten Koprolithen aus Basel-Gasfabrik unternommen werden. Dabei steht die Identifizierung der Produzenten im Vordergrund.

Kapitel 7

(Persönliches) Fazit

Der mit starker Vergrösserung und mehreren Filtern geschärfte, tiefe Blick in die Knochen hat nicht nur eine Vielfalt an taphonomischen Prozessen auf mikroskopischer Ebene (Bakterien- und Pilzbefall etc.) ermöglicht, sondern ist auch für Überlegungen weit darüber hinaus von grosser Wichtigkeit. Anhand der histotaphonomischen Resultate hat sich bestätigt, dass Knochen aufgrund ihrer Mikrostruktur und biogenen Herkunft äusserst sensibel auf eine Vielzahl taphonomischer Prozesse reagieren, wobei diese Prozesse ganz unterschiedliche Ursachen haben. Knochen beinhalten deshalb zahlreiche Informationen zu ihrer Biografie, wie dies kaum eine andere Objekt- oder Materialgattung tut. So konnten beim Fallbeispiel zweier ausserordentlich gut erhaltener Einzelknochen (Kap. 5.3) mehrere Ereignisse in der Biografie der beiden Knochen nachvollzogen werden – darunter auch das, was in Abb. 2 als „Pause“ vermerkt ist (geringer Pilzbefall als Indiz einer kurzfristigen Exponierung). Trotzdem kann – um nochmals auf Abb. 2 zurückzukommen – nur ein Bruchteil dessen rekonstruiert werden, was in der schematischen Darstellung einer Objektbiografie visualisiert ist. Dies gilt auch für die meisten anderen Material- oder Objektgattungen, allerdings in weit dramatischerem Ausmass, zumal nur wenige Materialien derart empfindlich auf Veränderungen reagieren (man denke zum Beispiel an ein Steinartefakt). Die rekonstruierten Objektbiografien bleiben deshalb bestenfalls lückenhaft, meist jedoch fast ganz im Dunkeln. Ganz zu schweigen davon, dass uns kognitive Wahrnehmungen, die Bedeutung von Dingen zum Beispiel, gänzlich verborgen bleiben.

Dies soll aber keinesfalls ein Aufruf zur archäologischen Total-Kapitulation sein, sondern eine Aufforderung, das zur Verfügung stehende Potential auszuschöpfen. Dazu gehört vor allem eine breite Palette an Blickwinkeln (Methoden) und Ebenen (Vergrösserungen). Ein Beispiel dafür ist hoffentlich mit dem Paper „The Hidden Midden“ gelungen (Kap. 5.2): Verschiedene Objekt- und Materialgruppen wie Fäkalien, Aschen oder anstehende Sedimente wurden bis ins Detail untersucht und gleichzeitig durch die Kartierung von Mikrofazies-Typen kontextualisiert. Auf diese Weise können zwar keine Objektbiografien bis ins Detail nachvollzogen, dafür aber eine Vorstellung davon gewonnen werden, wie die EinwohnerInnen von Basel-Gasfabrik mit unterschiedlichsten Ressourcen umgegangen sind. Diese bisher nur auf die Geoarchäologie beschränkte Sichtweise wird durch eine laufende interdisziplinäre Auswertung zu taphonomischen Prozessen an unterschiedlichen Objekt- und Materialgruppen ausgeweitet. Schon jetzt zeigt sich, dass sich durch den Einbezug verschiedener Blickwinkel ein sehr viel differenzierteres Bild ergibt. Die gewonnenen Informationen zum Umgang mit Objekt- und Materialgruppen werden Wesentliches zur Interpretation archäologischer Befunde beitragen. Es ist das Ausarbeiten von Gemeinsamkeiten, von Mustern und Spezialfällen, was mithilft, die damalige Gesellschaft und deren Handlungsmuster Schritt für Schritt sichtbar zu machen.

Schraubt man die Vergrösserung noch etwas zurück, so werden verschiedene Areale innerhalb der Siedlung sichtbar. Areale, die sich durch 10 Zentimeter Niveauunterschied und einen Graben voneinander abgrenzen – eine Hypothese, die durch künftige Untersuchungen aber erst noch bestätigt werden muss. Unterschiede also,

und gleichzeitig auch Gemeinsamkeiten. Dreht man weiter am Rädchen, so erscheint die ganze Siedlung im Blickfeld, die Umgebung schliesslich. Die schematische Darstellung der Objektbiografie weicht einer Karte mit Flüssen und Gebirgszügen, in die mit Pfeilen Beziehungen eingetragen werden können. Beziehungen zum nahen Umfeld zum Beispiel, zum heutigen Allschwil oder Sierentz, wo wir fruchtbare (Schwemm-) Lössböden finden, oder nach Pratteln und Muttenz, wo die Niederterrasse des Rheins oder die mit Lehm bedeckten Plateaus des Tafeljuras mögliche Anbaugebiete für Getreide sind. Etwas weiter und in verschiedene Richtungen weisen die Handelsbeziehungen der Haustiere. Dadurch bettet sich die Zentralsiedlung Basel-Gasfabrik mit jeder neu gewonnen Information besser in die umgebende Landschaft ein, mit einem immer dichter werdenden Netz aus Beziehungen und Zusammenhängen. Zusammenhänge, die sich manchmal nur auf den zweiten Blick, mit verschiedenen vorgehaltenen Filtern und aus unterschiedlichen Perspektiven erkennen lassen.

Meine Dissertation möchte ich so beenden, wie ich sie begonnen habe – mit der Mikroskopie als Metapher. Diese möchte ich zum Schluss dafür verwenden, einige persönliche Gedanken niederzuschreiben, auch wenn dies in wissenschaftlichen Texten nicht üblich ist[4]. Denn anhand der Mikroskopie lassen sich drei wichtige Punkte benennen, die ich mir für die weitere Forschung, aber auch für mich selber so oft wie möglich ans Herzen legen möchte:

1) **Wer sucht, der findet.** Aber nur das, was man kennt. Ungebrochene Neugier, die Freude am Entdecken und am Unbekannten ist ein unabdingbarer Motor. Für die Wissenschaft, und ganz besonders für unsere Gesellschaft. Unwissen schafft Ängste. Die Neugier und Offenheit hilft uns, andere(s) zu verstehen und Vorurteile (Prämissen) zu hinterfragen.
2) **Vor lauter Bäumen den Wald nicht sehen –** für die Mikroskopie vielleicht mit „vor lauter Quarz den Sand nicht sehen“ zu adaptieren. Die Aussage bleibt die gleiche: Probleme und Unstimmigkeiten lassen sich oft nur dann lösen, wenn man es von verschiedenen Seiten, von nah und fern, betrachtet.
3) **Panorama statt Tunnelblick:** Man mag in seinem Fachgebiet noch so gut und von seiner Meinung felsenfest überzeugt sein. Der Einbezug anderer Ansichten und Perspektiven führt immer zu einer Horizonterweiterung. Der Einbezug fremder Ansichten ist keine Schwäche, sondern im Gegenteil eine grosse Stärke.

[4] Was ich persönlich schade finde. Wie oft wird „den Akademikern“ vorgeworfen, keinen Nutzen für die Gesellschaft zu generieren – zum Beispiel der Archäologie. Dabei liegt der Nutzen nicht nur in konkreten Resultaten, in Zahlen und Tabellen, sondern auch in übergeordneten Erkenntnissen, die sich nicht nur in der Wissenschaft, sondern überall anwenden lassen.

Literaturverzeichnis (Kapitel 1 und Kapitel 5–7)

Bell, L.S., 1995. Post mortem microstructural change to the skeleton. A thesis submitted for the degree of Doctor of Philosophy, London.

Bell, L.S., Skinner, M.F., Jones, S.J., 1996. The speed of post mortem change to the human skeleton and its taphonomic significance. Forensic Science International 82 (2), 129–140.

Binford, L.R., 1981. Behavioral archaeology and the „Pompeii premise". Journal of Archaeological Research 37 (3), 195–208.

Bitterli-Brunner, P., 1987. Geologischer Führer der Region Basel. Mit 24 Exkursionen. Veröffentlichungen aus dem Naturhistorischen Museum Basel 19. Birkhäuser, Basel, Boston, 232 pp.

Bitterli-Brunner, P., Fischer, H., Herzog, P., 1984. Geologischer Atlas der Schweiz 1:25'000. Atlasblatt 80 Arlesheim. Bundesamt für Landestopografie swisstopo, Bern.

Blöck, L., Bräuning, A., Deschler-Erb, E., Fischer, A., Hecht, Y., Marti, R., Nick, M., Rissanen, H., Spichtig, N., Roth-Zehner, M., 2012. Die Spätlatènezeitliche Siedlungslandschaft am südlichen Oberrhein, in: Die Eisenzeit zwischen Champagne und Rheintal. 34. Internationales Kolloquium der Association Français pour l'Etude de l'âge du Fer vom 13. bis zum 16. Mai 2010 in Aschaffenburg. 34. Internationales Kolloquium der Association Français pour l'Etude de l'âge du Fer, Aschaffenburg. 13.-15. Mai 2010. Verlag des Römisch-Germanischen Zentralmuseums, Mainz, pp. 381–417.

Booth, T.J., Chamberlain, A.T., Parker Pearson, M., 2015. Mummification in Bronze Age Britain. Antiquity 89 (347), 1155–1173.

Booth, T.J., 2016. An investigation into the relationship between funerary treatment and bacterial bioerosion in European archaeological human bone. Archaeometry 58 (3), 484–499.

Booth, T.J., Redfern, R.C., Gowland, R.L., 2016. Immaculate Conceptions: Micro-CT analysis of diagenesis in Romano-British infant skeletons. Journal of Archaeological Science 74, 124–134.

Booth, T.J., Madgwick, R., Brönnimann, D., Portmann, C., in Vorb. The taphonomic potential of diagenetic alterations to archaeological bones, in: Knüsel, C.J., Schotsmans, E.M.J., Castex, D. (Eds.), The Routledge handbook of Archaeothanatology.

Brombacher, C., Helmig, G., Hüster Plogmann, H., Klee, M., Rentzel, P., Rodel, S., Veszeli, M., 1999. … und was davon übrig bleibt - Untersuchungen an einem mittelalterlichen Latrinenschacht an der Bäumleingasse 14 (1992/20). JbABBS 1998, 93–131.

Brönnimann, D., 2015. Zürich, Münsterhof 10 (Objekt-Nr. 1021): Bericht zu den geoarchäologischen Untersuchungen. IPNA - Universität Basel, Basel.

Brönnimann, D., 2017. Bone taphonomy Qatna 07. IPNA - Universität Basel, Basel.

Brönnimann, D., Rentzel, P., 2014. Naturraum und Geologie, in: Oppler, D. (Ed.), Ausflug in die Vergangenheit. Archäologische Streifzüge durchs Baselbiet. Librum Publisher, Hochwald, pp. 17–24.

Brönnimann, D., Rissanen, H., 2017. Vivre et mourir sur le site La Tène de Bâle-Gasfabrik (Suisse) – l'étude interdisciplinaire de structures d'habitat choisies et de deux nécropoles donne un aperçu de la société à la fin de l'âge du Fer, in: Interdisciplinarité et nouvelles approches dans les recherches sur l'âge du Fer. Interdisciplinarity and New Approaches in the Research of the Iron Age. International Doctoral Conference 2015. Bibracte (France), 2015. Interdisciplinarity and New Approaches in the Research of the Iron Age, Bibracte. 28.-30. April 2015. Masarykova univerzita, Brno, pp. 93–97.

Brönnimann, D., Ismail-Meyer, K., Rentzel, P., Pümpin, C., Lisá, L., 2017a. Excrements of herbivores, in: Nicosia, C., Stoops, G. (Eds.), Archaeological soil and sediment micromorphology. Wiley Blackwell, Hoboken, pp. 55–65.

Brönnimann, D., Pümpin, C., Ismail-Meyer, K., Rentzel, P., Egüez, N., 2017b. Excrements of omnivores and carnivores, in: Nicosia, C., Stoops, G. (Eds.), Archaeological soil and sediment micromorphology. Wiley Blackwell, Hoboken, pp. 67–81.

Brönnimann, D., Knipper, C., Pichler, S.L., Röder, B., Rissanen, H., Stopp, B., Rosner, M., Blank, M., Warnberg, O., Alt, K.W., Lassau, G., Rentzel, P., 2018a. The lay of land: Strontium isotope variability in the dietary catchment of the Late Iron Age proto-urban settlement of Basel-Gasfabrik, Switzerland. Journal of Archaeological Science: Reports 17, 279–292.

Brönnimann, D., Portmann, C., Pichler, S.L., Booth, T.J., Röder, B., Vach, W., Schibler, J., Rentzel, P., 2018b. Contextualising the dead – Combining geoarchaeology and osteoanthropology in a new multi-focus approach in bone histotaphonomy. Journal of Archaeological Science (98), 45–58.

Brönnimann, D., Rentzel, P., Röder, B., Spichtig, N., Rissanen, H., Lassau, G., accepted. The hidden midden – Geoarchaeological investigation of sedimentation processes, waste disposal practices and resource management at the Latène settlement Basel-Gasfabrik (Switzerland). Geoarchaeology: An International Journal.

Brönnimann, D., Rentzel, P., in Vorb. Geoarchäologische Untersuchungen an zwei Siedlungsgruben sowie an Grabgruben und Gräben innerhalb der beiden Gräberfeldern der spätlatènezeitlichen Siedlung Basel-Gasfabrik, in: Pichler, S.L., Alt, K.W., Lassau, G., Röder, B., Schibler, J. (Eds.), Über die Toten zu den Lebenden. Interdisziplinäre Synthese. Materialhefte der Archäologischen Bodenforschung Basel-Stadt. Beiträge zu Basel-Gasfabrik 1. Materialhefte der Archäologischen Bodenforschung Basel-Stadt 24. Archäologische Bodenforschung Basel-Stadt, Basel.

Bullen, T.D., Bailey, S.W., 2005. Identifying calcium sources at an acid deposition-impacted spruce forest: A strontium isotope, alkaline earth element multi-tracer approach. Biogeochemistry 74 (1), 63–99.

Courty, M.-A., Goldberg, P., Macphail, R.I., 1989. Soils and micromorphology in archaeology. Cambridge manuals in archaeology. Cambridge University Press, Cambridge, New York, xx, 344.

Doswald, C., 2004. Historische Verkehrswege im Kanton Basel-Stadt: Eine Publikation zum Inventar historischer Verkehrswege der Schweiz IVS, herausgegeben vom Bundesamt für Strassen (ASTRA). Bundesamt für Strassen (ASTRA). www.ivs.admin.ch.

Drouet, T., Herbauts, J., Gruber, W., Demaiffe, D., 2007. Natural strontium isotope composition as a tracer of weathering patterns and of exchangeable calcium sources in acid leached soils developed on loess of central Belgium. Eur J Soil Science 58 (1), 302–319.

Fischer, A., 2012. Dittingen: ein Mühlstein aus permischer Brekzie. Archäologie Baselland. Jahresbericht. Dokumentation und Funde 2011, 110–115.

Goldberg, P., Aldeias, V., 2016. Why does (archaeological) micromorphology have such little traction in (geo)archaeology? Archaeological and Anthropological Sciences In Press.

Goldberg, P., Macphail, R.I., 2006. Practical and theoretical geoarchaeology. Blackwell Publishers, Malden, MA, Oxford, 454 pp.

Guélat, M., Richard, H., 2014. Holocene environmental changes and human impact in the northern Swiss Jura as reflected by data from the Delémont valley. Swiss Journal of Geosciences 107 (1), 1–21.

Hackett, C.J., 1981. Microscopical focal destruction (tunnels) in exhumed human bones. Medicine, science, and the law 21 (4), 243–265.

Hagendorn, A., Rentzel, P., Pümpin, C., Lanzicher, A.F., 2017. Neue Erkenntnisse zur spätlatène- und frühkaiserzeitlichen Strasse auf dem Basler Münsterhügel. JbABBS 2016, 102–127.

Hahn, H.P., 2015. Dinge sind Fragmente und Assemblagen: Kritische Anmerkungen zur Metapher der "Objektbiografie", in: Boschung, D., Kreuz, P.-A., Kienlin, T.L. (Eds.), Biography of objects. Aspekte eines kulturhistorischen Konzepts. Morphomata 31. Wilhelm Fink, Paderborn, pp. 11–33.

Hecht, Y., Niederhäuser, A., 2011. Alltagskultur und Totenrituale der Kelten: Ein Siedlungszentrum am Oberrhein um 100 v. Chr. Merian, Basel, 113 pp.

Hecht, Y., Rissanen, H., Spichtig, N., Stelzle-Hüglin, S., 2007. Die Suche nach den Namenlosen: Die breite Bevölkerung der spätlatènezeitlichen Siedlung Basel-Gasfabrik, in: Die unteren Zehntausend, auf der Suche nach den Unterschichten der Eisenzeit. Beiträge zur Sitzung der AG Eisenzeit während der Jahrestagung des West- und Süddeutschen Verbandes für Altertumsforschung e.V. in Xanten 2006. Jahrestagung des West- und Süddeutschen Verbandes für Altertumsforschung, Xanten. 2006. Beier & Beran, Langenweissbach, pp. 71–83.

Hedges, R.E.M., Millard, A.R., 1995. Measurements and relationships of diagenetic alteration of bone from three archaeological sites. Journal of Archaeological Science 22, 201–209.

Huisman, H., Ismail-Meyer, K., Sageidet, B.M., Joosten, I., 2017. Micromorphological indicators for degradation processes in archaeological bone from temperate European wetland sites. Journal of Archaeological Science 85, 13–29.

Imhof, B., Jacomet, S., Joos, M., Kissling, H.-R., Ritter, B., Schibler, J., 1977. Naturwissenschaftliche Untersuchungen zur Spätlatène-Siedlung Basel-Gasfabrik, in: Berger, L., Bienz, G., Ewald, J., Joos, M. (Eds.), Festschrift Elisabeth Schmid zu ihrem 65. Geburtstag. Bopp und Schwabe AG, Basel, pp. 91–134.

Jans, M.M., 2005. Histological characterisation of diagenetic alteration of archaeological bone. Geoarchaeological and Bioarchaeological Studies 4, Amsterdam, 163 pp.

Joos, M., 1975. Eine permische Brekzie aus dem Südschwarzwald und ihre Verbreitung als Mühlstein im Spätlatène und in frührömischer Zeit. Archäologisches Korrespondenzblatt 5 (197-199).

Jud, P. (Ed.), 2008. Die Töpferin und der Schmied: Basel-Gasfabrik, Grabung 1989/5. Dissertation 2004, Teil I: Text. Materialhefte zur Archäologie in Basel 20:1. Archäologische Bodenforschung des Kantons Basel-Stadt, Basel, 334 pp.

Knipper, C., Pichler, S.L., Brönnimann, D., Rissanen, H., Rosner, M., Spichtig, N., Stopp, B., Rentzel, P., Röder, B., Schibler, J., Lassau, G., Alt, K.W., 2018. A knot in a network: Residential mobility at the Late Iron Age proto-urban centre of Basel-Gasfabrik (Switzerland) revealed by isotope analyses. Journal of Archaeological Science: Reports 17, 735–753.

Kock, S., Huggenberger, P., Preusser, F., Rentzel, P., Wetzel, A., 2009. Formation and evolution of the Lower Terrace of the Rhine River in the area of Basel. Swiss Journal of Geosciences 102 (2), 307–321.

Kölliker, A., 1854. Mikroskopische Anatomie, oder Gewebelehre des Menschen: Zweiter Band: Specielle Gewebelehre. Verlag von Wilhelm Engelmann, Leipzig.

Kölliker, A., 1860. Ueber das ausgebreitete Vorkommen von pflanzlichen Parasiten in den Hartgebilden niederer Thiere. Zeitschrift für Wissenschaftliche Zoologie 10, 215–232.

Kopytoff, I., 1986. The cultural biography of things: commoditization as process, in: Appadurai, A. (Ed.), The social life of things. Commodities in cultural perspective. Cambridge University Press, Cambridge, pp. 64–91.

Kühn, M., Iseli, M., 2008. Botanische Makroreste aus der spätlatènezeitlichen Siedlung Basel-Gasfasbrik, Grabung 1989/5, in: Jud, P. (Ed.), Die Töpferin und der Schmied. Basel-Gasfabrik, Grabung 1989/5. Dissertation 2004, Teil I: Text. Materialhefte zur Archäologie in Basel 20:1. Archäologische Bodenforschung des Kantons Basel-Stadt, Basel, pp. 293–324.

Leser, H., 1982. Die Landschaft der Basler Region und ihre naturräumliche Gliederungsprobleme. Regio Basiliensis 23 (1-2), 2–23.

Müller, H., Sandberger, F., Schenk, A., 1863. Sitzungsberichte der physikalisch-medicinischen Gesellschaft für das Jahr 1863: III. Sitzung am 10. Januar 1863. Würzburger Naturwissenschaftliche Zeitschrift Vierter Band, II.

Pichler, S.L., Pümpin, C., Brönnimann, D., Rentzel, P., 2014. Life in the proto-urban style: the identification of parasite eggs in micromorphological thin sections from the Basel-Gasfabrik Late Iron Age settlement, Switzerland. Journal of Archaeological Science 43, 55–65.

Pichler, S.L., Röder, B., Brönnimann, D., Knipper, C., Kühn, M., Rentzel, P., Rissanen, H., Stopp, B., Vach, W., Warnberg, O., Alt, K.W., Schibler, J., Lassau, G., 2017. The Basel-Gasfabrik research project: Addressing complex topics by an integrative approach, in: Multidisciplinary approach to archaeology: Recent achievements and prospects. Proceedings of the international symposium "Multidisciplinary Approach to Archaeology: Recent achievements and prospects" (June 22-26, 2015, Novosibirsk). Multidisciplinary Approach to Archaeology: Recent achievements and prospects, Novosibirsk. 22.-25. June 2016. IAET SB RAS Publishing, Novosibirsk, pp. 240–247.

Portmann, C., 2015. Histologische Sterbealterbestimmung an menschlichen Langknochen aus der latènezeitlichen Siedlung Basel-Gasfabrik (BS) und Überlegungen zur Befundentstehung anhand archäologischer und ethnologischer Vergleiche. Unpublizierte Masterarbeit, Basel.

Pümpin, C., 2013. Geoarchäologische Auswertung ausgewählter

Befunde, in: Ackermann, R. (Ed.), Der römische Vicus von Kempraten, Rapperswil-Jona. Neubetrachtung anhand der Ausgrabungen Fluhstrasse 6 -10 (2005 - 2006). Archäologie im Kanton St. Gallen 1. Amt für Kultur des Kantons St. Gallen, St. Gallen, pp. 171–181.

Pümpin, C., Pichler, S.L., Maicher, C., Le Bailly, M., 2015. Basel - Gasfabrik: Untersuchung der Koprolithen aus der Grube 283 und der Grube 321: Mikromorphologische und paläoparasitologische Analysen. Universität Basel, Basel.

Rentzel, P., 1994. Geologische Untersuchungen auf dem Gelände der spätlatènezeitlichen Siedlung Basel-Gasfabrik. Eine erste Bilanz, in: Die spätkeltische Zeit am südlichen Oberrhein. Kolloquium Basel, Basel. 17.-18. Oktober 1991. Archäologische Bodenforschung des Kantons Basel-Stadt, Basel, pp. 49–55.

Rentzel, P., 1997. Geologisch-bodenkundliche Untersuchungen an den Niederterrassenfeldern bei Basel unter besonderer Berücksichtigung der spätlatènezeitlichen Fundstelle Basel-Gasfabrik. JbABBS 1994, 31–52.

Rentzel, P., 1998. Ausgewählte Grubenstrukturen aus der spätlatènezeitlichen Fundstelle Basel-Gasfabrik. JbABBS 1995, 35–79.

Rentzel, P., Nicosia, C., Gebhardt, A., Brönnimann, D., Pümpin, C., Ismail-Meyer, K., 2017. Trampling, poaching and the effect of traffic, in: Nicosia, C., Stoops, G. (Eds.), Archaeological soil and sediment micromorphology. Wiley Blackwell, Hoboken, pp. 281–297.

Rentzel, P., Pümpin, C., Brönnimann, D., 2015. Geoarchäologischer Report: Eine kurze Geschichte des Rheins: Geologische und archäologische Impressionen aus Basel. JbABBS 2014, 108–135.

Schiffer, M.B., 1972. Archaeological context and systemic context. American Antiquity 37 (2), 156–165.

Schiffer, M.B., 1975. Archaeology as behavioral science. American Anthropologist 77 (4), 836–848.

Schiffer, M.B., 1983. Toward the identification of formation processes. American Antiquity 48 (4), 675–706.

Schiffer, M.B., 1987. Formation processes of the archaeological record. University of New Mexico Press, Albuquerque.

Shahack-Gross, R., 2017. Archaeological formation theory and geoarchaeology: State-of-the-art in 2016. Journal of Archaeological Science 79, 36–43.

Sommer, U., 1991. Zur Entstehung archäologischer Fundvergesellschaftungen: Versuch einer archäologischen Taphonomie, in: Mattheußer, E., Sommer, U. (Eds.), Studien zur Siedlungsarchäologie I. Universitätsforschungen zur prähistorischen Archäologie 6. Habelt, Bonn, pp. 51–174.

Sommer, U., 2012. Wer hat Dornröschen aufgeweckt?: Taphonomie und Mainstream-Archäologie, in: Taphonomische Forschungen (nicht nur) zum Neolithikum. Welt und Erde, Kerpen-Loogh, pp. 15–34.

Steiner, S., 2008. Fundmaterial aus einem Töpferofen: Eine Studie zur Keramikproduktion in der spätlatènezeitlichen Siedlung Basel-Gasfabrik. Unpublizierte Diplomarbeit, Basel.

Stoops, G., 2003. Guidelines for analysis and description of soil and regolith thin sections. Soil Science Society of America, Madison, 184 pp.

Stopp, B., 2008. Archäozoologische Untersuchung der Tierknochen aus Gruben der spätlatènezeitlichen Siedlung Basel-Gasfabrik, Grabung 1989/5, in: Jud, P. (Ed.), Die Töpferin und der Schmied. Basel-Gasfabrik, Grabung 1989/5. Dissertation 2004, Teil I: Text. Materialhefte zur Archäologie in Basel 20:1. Archäologische Bodenforschung des Kantons Basel-Stadt, Basel, pp. 249–292.

Stopp, B., Iseli, M., Jacomet, S., 1999. Die Landwirtschaft der späten Eisenzeit. Archäologie Schweiz 22 (1), 27–30.

Turner, S., Shillito, L.-M., Carrer, F., 2018. Landscape archaeology, in: Howard, P., Thompson, I.H., Waterton, E. (Eds.), The Routledge companion to landscape studies, 2nd edition ed. Routledge, Oxford.

Turner-Walker, G., 2008. The chemical and microbial degradation of bones and teeth, in: Pinhasi, R., Mays, S. (Eds.), Advances in human palaeopathology. John Wiley & Sons, Hoboken, pp. 3–29.

Turner-Walker, G., 2012. Early bioerosion in skeletal tissues: persistence through deep time. Neues Jahrbuch für Geologie und Paläontologie - Abhandlungen 265 (2), 165–183.

Turner-Walker, G., Jans, M.M., 2008. Reconstructing taphonomic histories using histological analysis. Palaeogeography, Palaeoclimatology, Palaeoecology 266, 227–235.

Turner-Walker, G., Peacock, E.E., 2008. Preliminary results of bone diagenesis in Scandinavian bogs. Palaeogeography, Palaeoclimatology, Palaeoecology 266 (3-4), 151–159.

Wedl, C., 1865. Über einen im Zahnbein und Knochen keimenden Pilz. Sitzungsberichte der Mathematisch-Naturwissenschaftlichen Classe der Kaiserlichen Akademie der Wissenschaften 50. Band 1. Abteilung. Jahrgang 1864, 171–193.

White, L., Booth, T.J., 2014. The origin of bacteria responsible for bioerosion to the internal bone microstructure: Results from experimentally-deposited pig carcasses. Forensic Science International 239, 92–102.

Wick, L., 2015. Das Hinterland von Augusta Raurica: Paläoökologische Untersuchungen zur Vegetation und Landnutzung von der Eisenzeit bis zum Mittelalter. Jahresberichte aus Augst und Kaiseraugst 36, 209–215.

Wolfram, S., 2003. Der Müll, Archäologie und die Steinzeit, in: Fansa, M., Wolfram, S. (Eds.), Müll - Facetten von der Steinzeit bis zum Gelben Sack. Begleitschrift zur Sonderausstellung Müll - Facetten von der Steinzeit bis zum Gelben Sack vom 06. September bis 30. November 2003 in Oldenburg anschließend in Hanau. Schriftenreihe des Landesmuseums für Natur und Mensch Oldenburg 27. von Zabern, Mainz am Rhein, pp. 17–34.

Supplements

The Lay of Land – Supplement 1	Vegetation samples
The Lay of Land – Supplement 2	Water data literature
The Hidden Midden – Supplement 1	Profiles, polished sections and thin sections
The Hidden Midden – Supplement 2	Micromorphological results
Contextualising the Dead – Supplement 1	Histotaphonomic data
Contextualising the Dead – Supplement 2	Archaeoanthropological data
Contextualising the Dead – Supplement 3	Burnt and unburnt bone samples

The Lay of Land - Supplement 1: Vegetation samples

Locality		GPS coordinates & altitude			Geology and sediment cover			Ground vegetation			Tree leaves			Suitability		
No.	Site	Lat.	Long.	Alt.	System	Serie	Bedrock and sediment cover	Species	$^{87}Sr/^{86}Sr$	± 2 SD	Species	$^{87}Sr/^{86}Sr$	± 2 SD	AC	PA	WP
BG 0	Rosenau	47.61417	7.53743	245	Quarternary	Holocene	Fine grained floodplain sediment of river Rhine	Fern	0.70859	0.00001	Hazel	0.70852	0.00001	--	--	++
BG 1	Bartenheim	47.63760	7.50362	260	Quarternary	Late Pleistocene	(Calcareous) fluvial gravel	Young maple	0.70830	0.00001	Small-leaved linden	0.70831	0.00001	+	++	+
BG 2	Habsheim	47.71325	7.45118	245	Quarternary	Late Pleistocene	Lower terrace deposits (Rhine gravel)	Grasss	0.70967	0.00001	European hornbeam	0.70965	0.00001	--	--	++
BG 3	Munchhouse	47.84613	7.44747	230	Quarternary	Late Pleistocene	Lower terrace deposits (Rhine gravel) with alluvial loam cover	Grass	0.70962	0.00001	Oak	0.70935	0.00001	++	++	+
BG 4	Maugenhard	47.68113	7.62100	310	Paleogene	Oligocene	Sandy-loamy deposits with humus cover	Fern	0.71096	0.00001	European beech	0.71145	0.00001	++	++	+
BG 5	Hügelheim	47.82957	7.63402	275	Quarternary	Late Pleistocene	Loess loam, probably eroded (Ap-C profile)	Ivy	0.70865	0.00001	Elder	0.70874	0.00001	-	o	+
BG 6	Tüllingen	47.60473	7.64037	450	Paleogene	Oligocene	Freshwater limestone (Tüllinger Süsswasserkalk) with humus cover	Young maple	0.70941	0.00001	European beech	0.70907	0.00001	+	++	+
BG 7	Bettingen	47.57458	7.68200	520	Triassic	Keuper (Middle Triassic)	Probably gypsum with humus cover	*Impatiens parviflora*	0.70872	0.00001	European beech	0.70905	0.00001	--	--	+
BG 8	Inzlingen	47.58262	7.68433	420	Triassic	Muschelkalk (Upper Triassic)	Limestone with thin loam cover	Young beech	0.71053	0.00001	European beech	0.71004	0.00001	++	++	+
BG 9	Riehen	47.58842	7.67032	380	Triassic	Upper Buntsandstein (Early Triassic)	Quartz rich sandstone	*Circaea lutetiana*	0.71234	0.00001	Maple	0.71126	0.00001	+	++	+
BG 10	Basel	47.57610	7.62362	265	Quarternary	Holocene	Fluvial gravel (Wiese gravel) with floodplain sediment cover	Young Maple	0.70958	0.00001	European hornbeam	0.71029	0.00001	--	--	+
BG 11	Bickensohl	48.07468	7.64455	315	Neogene	Miocene	Volcanic rock with thick loess loam cover	Ivy	0.70827	0.00001	Largeleaf linden	0.70837	0.00001	++	++	+
BG 12	Bötzingen	48.08433	7.68880	375	Neogene	Miocene	Volcanic rock with thick loess loam cover	*Aegopodium podagraria*	0.70848	0.00001	Hazel	0.70864	0.00001	+	++	+
BG 13	Amoltern	48.12780	7.68242	295	Neogene	Miocene	Tephra (volcanic rock) with thin humus cover	Ivy	0.70782	0.00001	Hazel	0.70795	0.00001	--	--	+
BG 14	Pratteln	47.52660	7.67928	295	Quarternary	Late Pleistocene	Lower terrace deposits (Rhine gravel), probably interlocked with calcareous Ergolz gravel	Young Maple	0.70847	0.00001	European beech	0.70886	0.00002	++	++	+
BG 15	Basel	47.53000	7.59677	355	Quarternary	Early Pleistocene	Early Pleistocene terrace deposits (Rhine gravel) with thin loam cover	*Geum urbanum*	0.71012	0.00001	European beech	0.71035	0.00001	o	+	+
BG 16	Basel	47.52675	7.58095	350	Quarternary	Late Pleistocene	Loess loam, probably erodet (Ap-C profile)	Young ash	0.70847	0.00001	European beech	0.70892	0.00001	o	+	+
BG 17	Reinach	47.51063	7.60722	305	Quarternary	Late Pleistocene	Lower terrace deposits (calcareous Birs gravel) with humus cover	*Geum urbanum*	0.70851	0.00001	European hornbeam	0.70814	0.00001	++	++	+

The Lay of Land - Supplement 1: Vegetation samples

Locality		GPS coordinates & altitude			Geology and sediment cover			Ground vegetation			Tree leaves			Suitability		
No.	Site	Lat.	Long.	Alt.	System	Serie	Bedrock and sediment cover	Species	$^{87}Sr/^{86}Sr$	± 2 SD	Species	$^{87}Sr/^{86}Sr$	± 2 SD	AC	PA	WP
BG 18	Reinach	47.51267	7.59498	355	Quarternary	Middle Pleistocene	High terrace deposits (calcareous Birs gravel) with thin loam cover	Fern	0.70928	0.00001	Robinia	0.70878	0.00001	--	--	+
BG 19	Allschwil	47.53433	7.54577	365	Quarternary	Late Pleistocene	Loess loam, probably heavily weathered (pedogenesis)	Young Maple	0.70966	0.00001	European hornbeam	0.70970	0.00001	--	--	+
BG 20	Oltingue	47.47953	7.40865	435	Paleogene	Oligocene	Sandy-loamy deposit with humus cover	Fern	0.71085	0.00001	European beech	0.71091	0.00001	++	++	+
BG 21	Hagenthal-le-Bas	47.51758	7.48993	430	Quarternary	Late Pleistocene	Loess loam, probably heavily weathered (pedogenesis); probably with underlying gravel	Young ash	0.70999	0.00001	European beech	0.71035	0.00001	--	--	++
BG 22	Schönenbuch	47.53445	7.51773	385	Quarternary	Early Pleistocene	Early Pleistocene terrace deposits (Rhine gravel) with thin loess loam cover	*Impatiens parviflora*	0.71041	0.00001	European hornbeam	0.71093	0.00001	++	++	+
BG 23	Knoeringue	47.55897	7.42178	450	Neogene	Pliocene	Pliocene gravel deposit with thin loess loam cover	Ivy	0.71107	0.00001	European hornbeam	0.71144	0.00001	+	++	+
BG 24	Ranspach-le-Haut	47.57770	7.41062	430	Quarternary	Late Pleistocene	Loess loam, probably heavily weathered (pedogenesis)	Fern	0.70985	0.00001	European beech	0.70969	0.00001	+	++	+
BG 25	Oltingue	47.49332	7.38645	420	Paleogene	Oligocene	Freshwater limestone with humus cover	Ivy	0.70903	0.00001	European beech	0.70906	0.00001	+	++	+
BG 26	Ferrette	47.49668	7.30448	535	Jurassic	Dogger (Middle Jurassic)	Limestone with thin loam cover	Ivy	0.70839	0.00001	European beech	0.70878	0.00001	-	-	++
BG 27	Hésingue	47.57767	7.47647	335	Quarternary	Late Pleistocene	Loess loam, probably erodet (Ap-C profile)	Ivy	0.70842	0.00001	European beech	0.70892	0.00001	+	++	+
BG 28	Hochstetten	48.00318	7.61855	195	Quarternary	Holocene	Gravelly-loamy floodplain sediment of river Rhine	Grass	0.70964	0.00001	Maple	0.71000	0.00001	--	--	o
BG 29	Ostheim	48.16020	7.38060	185	Quarternary	Late Pleistocene	Lower terrace deposits (granitic Fecht gravel) with thin (loess) loam cover	*Geum urbanum*	0.71300	0.00001	European hornbeam	0.71423	0.00001	--	--	o
BG 30	Sierentz	47.64920	7.47233	255	Quarternary	Late Pleistocene	Lower terrace deposits (Rhine gravel) with humus cover	Fern	0.71002	0.00001	Maple	0.70997	0.00001	--	--	o
BG 31	Augst	47.52893	7.72087	295	Quarternary	Late Pleistocene	Lower terrace deposits (calcareous Ergolz gravel)	Ivy	0.70817	0.00001	European hornbeam	0.70820	0.00001	+	++	+
BG 32	Kaiseraugst	47.53783	7.71498	270	Quarternary	Late Pleistocene	Lower terrace deposits (calcareous Ergolz gravel) with humus cover	Ivy	0.70842	0.00001	Hazel	0.70843	0.00001	-	-	++
BG 33	Rheinfelden	47.54428	7.76255	295	Quarternary	Late Pleistocene	Lower terrace deposits (Rhine gravel), probably mixed with calcareous gravel	Fern	0.70890	0.00001	European hornbeam	0.70865	0.00001	--	--	o
BG 34	Pratteln	47.51118	7.70077	430	Jurassic	Dogger (Middle Jurassic)	Limestone debris with loam cover	Ivy	0.70809	0.00001	European beech	0.70827	0.00001	--	--	+

The Lay of Land - Supplement 1: Vegetation samples

Locality		GPS coordinates & altitude			Geology and sediment cover			Ground vegetation			Tree leaves			Suitability		
No.	Site	Lat.	Long.	Alt.	System	Serie	Bedrock and sediment cover	Species	$^{87}Sr/^{86}Sr$	± 2 SD	Species	$^{87}Sr/^{86}Sr$	± 2 SD	AC	PA	WP
BG 35	Frenkendorf	47.49940	7.67630	660	Jurassic	Malm (Upper Jurassic)	Limestone with thin humus cover	*Galium odoratum*	0.70854	0.00001	European beech	*0.70960*	*0.00001*	--	--	+
BG 36	Liestal	47.49298	7.70175	425	Jurassic	Dogger (Middle Jurassic)	Limestone debris with humus cover	Fern	0.70788	0.00001	European beech	0.70781	0.00001	--	--	+
BG 37	Gempen	47.49440	7.66335	660	Quarternary	Holocene	Thick, deeply weathered loam on limestone (Dogger; Middle Jurassic)	Grass	0.70859	0.00001	European beech	0.70850	0.00001	++	++	+
BG 38	Sissach	47.46958	7.79823	360	Quarternary	Late Pleistocene	Lower terrace deposits (calcareous Ergolz gravel)	Grass	0.70830	0.00001	Hazel	0.70832	0.00001	--	--	+
BG 39	Böckten	47.46840	7.83950	480	Jurassic	Dogger (Middle Jurassic)	Loamy limestone debris with humus cover	Ivy	0.70864	0.00001	European beech	0.70841	0.00001	--	--	o
BG 40	Nunningen	47.38375	7.61357	870	Jurassic	Dogger (Middle Jurassic)	Limestone (Hauptrogenstein) with humus cover	Grass	0.70788	0.00001	European beech	0.70801	0.00001	+	++	+
BG 41	Waldenburg	47.38112	7.76098	775	Jurassic	Dogger (Middle Jurassic)	Limestone (Hauptrogenstein) with humus cover	Grass	0.70780	0.00001	European beech	0.70776	0.00001	-	o	+
BG 42	Möhlin	47.57452	7.87747	340	Quarternary	Early Pleistocene	Moraine with thin loess loam cover	Small Balsam (*Impatiens parviflora*)	0.70989	0.00001	European hornbeam	0.71062	0.00001	--	--	+
BG 43	Herten	47.55813	7.72515	380	Triassic	Muschelkalk (Upper Triassic)	Dolomitic limestone with loess loam cover	Young Oak	0.70910	0.00001	Linden	0.70877	0.00001	++	++	+
BG 44	Degerfelden	47.57410	7.74803	395	Triassic	Middle Buntsandstein (Early Triassic)	Quartz rich sandstone	Fern	0.71538	0.00001	European beech	0.71638	0.00002	--	-	+
BG 45	Liestal	47.47883	7.70188	500	Quarternary	Holocene	Thick, deeply weathered loam on limestone (Dogger; Middle Jurassic)	*Galium odoratum*	0.70940	0.00001	European beech	0.70942	0.00002	o	o	+
BG 46	Inzlingen	47.60575	7.70625	490	Triassic	Keuper (Middle Triassic)	Marl with loam cover	Grass	0.71412	0.00001	European beech	0.71409	0.00001	--	++	+
BG 47	Brombach	47.63652	7.70888	360	Triassic	Muschelkalk (Upper Triassic)	Dolomitic limestone with loess loam cover	Fern	0.70987	0.00001	European beech	0.70906	0.00001	-	o	+
BG 48	Oberwil	47.50640	7.53922	350	Quarternary	Late Pleistocene	Loess loam, probably eroded (Ap-C profile) with underlying calcareous Birs gravel	Grass	0.70874	0.00001	European hornbeam	0.70888	0.00001	-	o	+
BG 49	Thann	47.81447	7.10315	370	Devonian / Carbonif.		Volcanic psephite with humus cover	Grass	0.71146	0.00001	European ash	0.71210	0.00001	--	--	+
BG 50	Kandern	47.71472	7.67602	405	Devonian / Carbonif.		Granite and gneiss	Fern	0.71662	0.00001	European beech	0.71794	0.00001	--	--	+

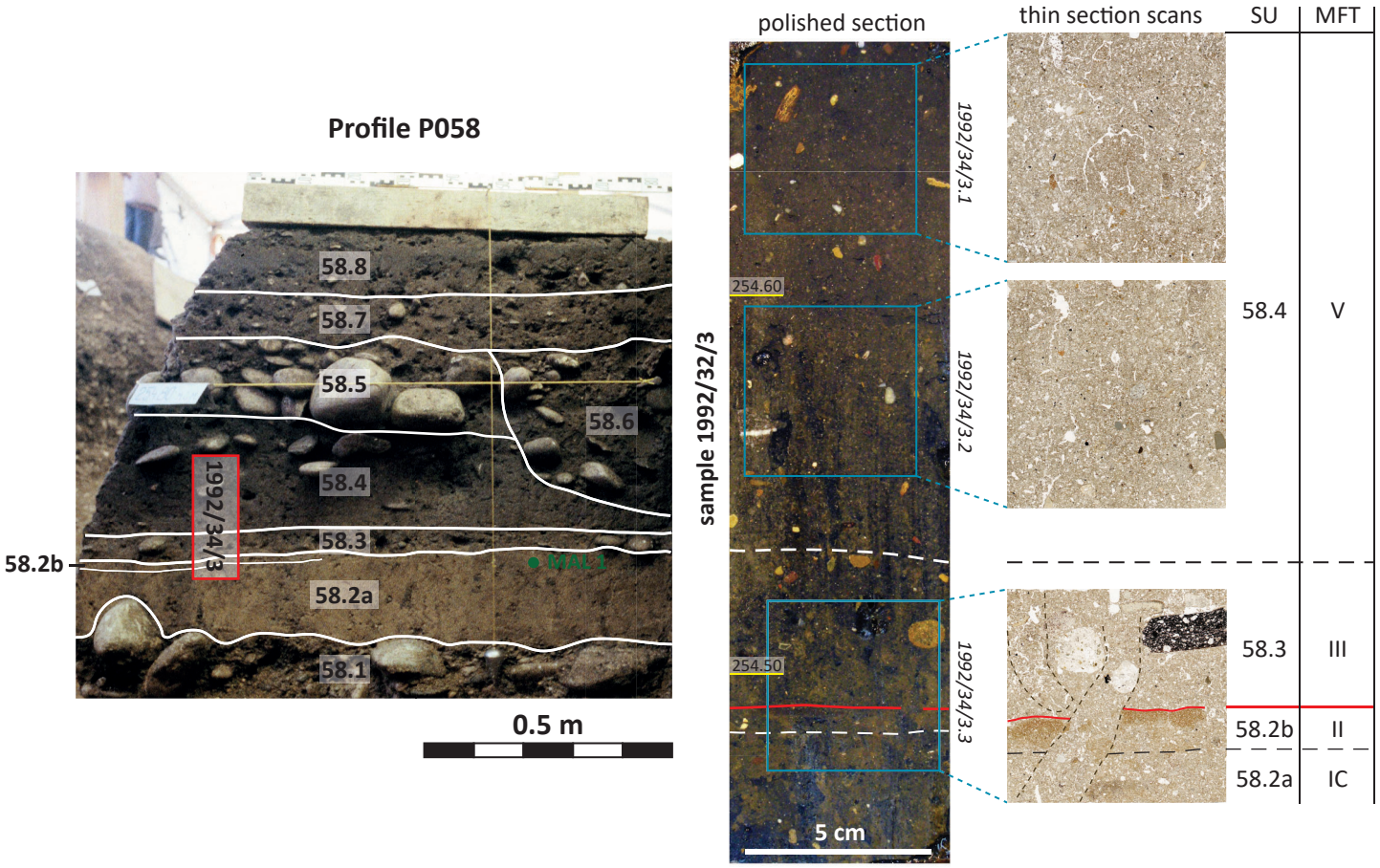
All coordinates in WGS84

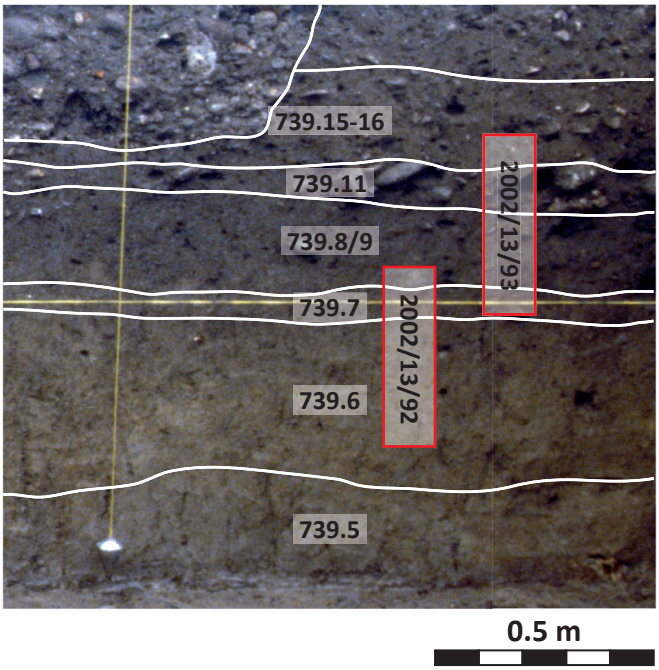
AC	agriculture
PA	pasture
WP	woodland pasture

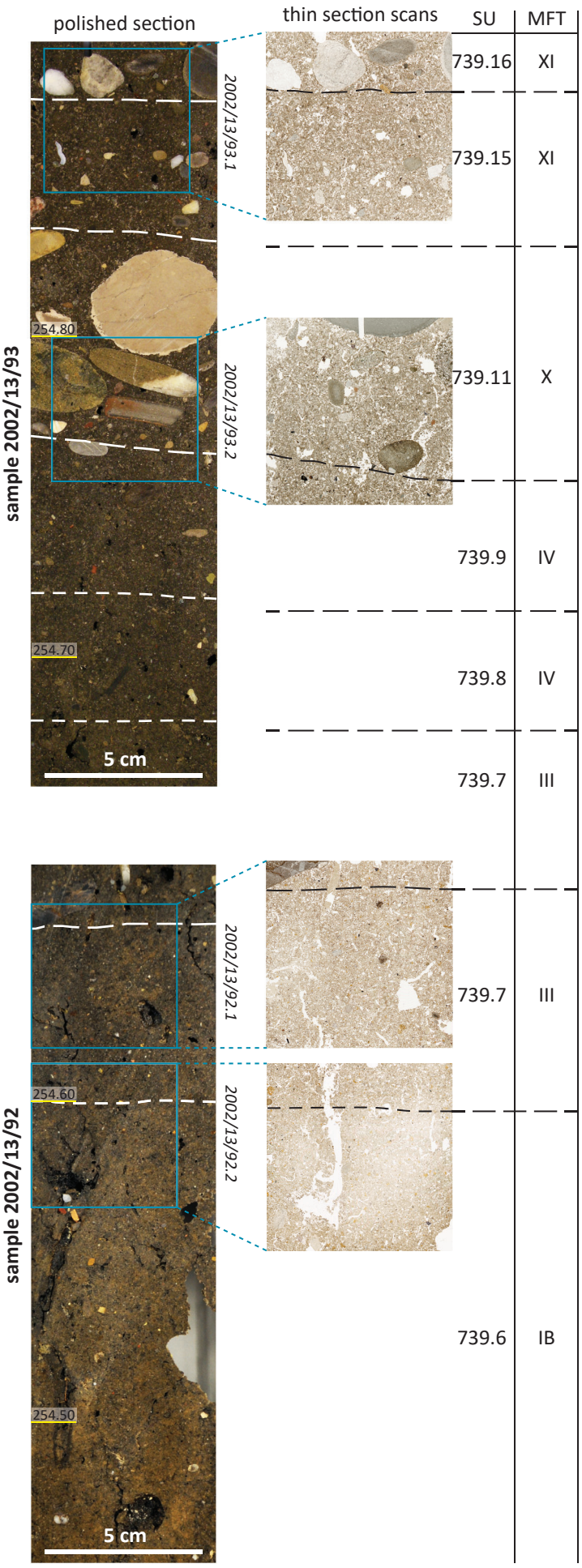
++	well suitable
+	suitable
o	moderately suitable
-	unsuitable
--	not possible

The Lay of Land - Supplement 2: Water data literature

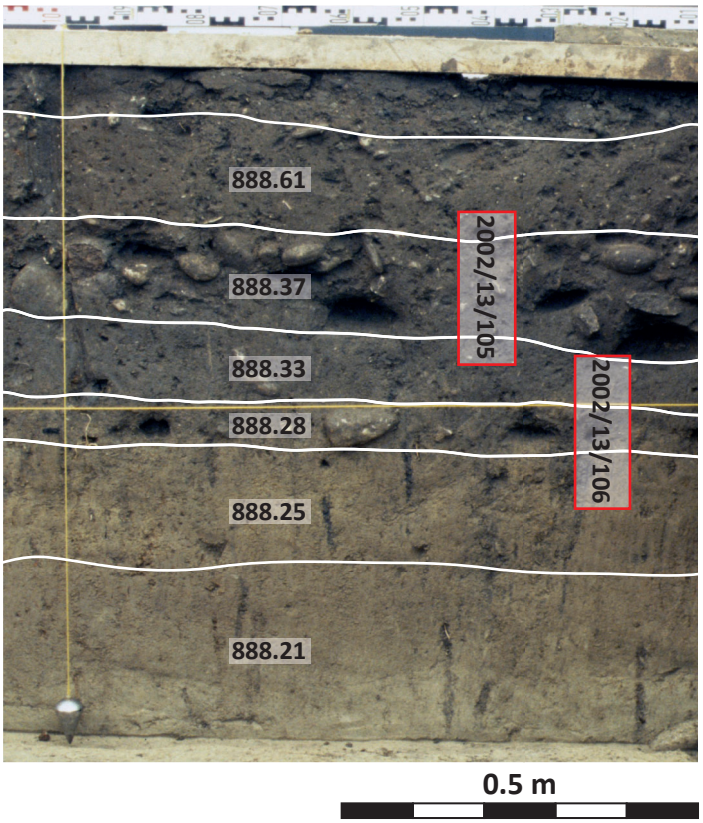
Body of Water	Site	landscape	$^{87}Sr/^{86}Sr$	Reference
Lake Constance	Rohrspitz	High Rhine	0.70850	Buhl et al. 1991
Lake Constance	Konstanz	High Rhine	0.70847	Buhl et al. 1991
Rhine	Close to Reckingen	High Rhine	0.70856	Buhl et al. 1991
Rhine	Rheinfelden	High Rhine	0.70846	Buhl et al. 1991
Rhine		Upper Rhine Rift	0.70843	Eikenberg et al. 2001
Rhine		Upper Rhine Rift	0.70848	Eikenberg et al. 2001
Rhine	Istein	Upper Rhine Rift	0.70844	Buhl et al. 1991
Rhine	Steinenstadt	Upper Rhine Rift	0.70848	Buhl et al. 1991
Rhine	Niederimsigen	Upper Rhine Rift	0.70848	Buhl et al. 1991
Rhine	Burkheim	Upper Rhine Rift	0.70873	Buhl et al. 1991
Rhine	Weisweil	Upper Rhine Rift	0.70867	Buhl et al. 1991
Rhine	Wittenweier	Upper Rhine Rift	0.70874	Buhl et al. 1991
Quarry pond	Sierentz	Upper Rhine Rift	0.70862	Kloppmann 2003
Sauruntz		Upper Rhine Rift	0.70875	Kloppmann 2003
Muehlbach	Koetzingue	Upper Rhine Rift	0.70880	Kloppmann 2003
Niedermattgraben		Upper Rhine Rift	0.70867	Kloppmann 2003
Muehlbach	Habsheim	Upper Rhine Rift	0.70903	Kloppmann 2003
Rhein-Rhône-Channel		Upper Rhine Rift	0.70841	Kloppmann 2003
Alte-Bach	Source	Upper Rhine Rift	0.70849	Kloppmann 2013
Alte-Bach		Upper Rhine Rift	0.70862	Kloppmann 2013
Groundwater	Colmar	Upper Rhine Rift	0.70875	Eikenberg et al. 2001
Groundwater	Colmar	Upper Rhine Rift	0.70878	Eikenberg et al. 2001
Groundwater	Colmar	Upper Rhine Rift	0.70866	Eikenberg et al. 2001
Groundwater	Colmar	Upper Rhine Rift	0.70875	Eikenberg et al. 2001
Thur		Upper Rhine Rift	0.70983	Eikenberg et al. 2001
Thur		Upper Rhine Rift	0.70977	Eikenberg et al. 2001
Ill		Upper Rhine Rift	0.70874	Buhl et al. 1991
Ill		Upper Rhine Rift	0.70888	Eikenberg et al. 2001
Ill		Upper Rhine Rift	0.70905	Eikenberg et al. 2001
Ill		Upper Rhine Rift	0.70878	Eikenberg et al. 2001
Ill		Upper Rhine Rift	0.70889	Eikenberg et al. 2001
Ill		Upper Rhine Rift	0.70905	Eikenberg et al. 2001
Ill		Upper Rhine Rift	0.70930	Eikenberg et al. 2001
Lauch		Upper Rhine Rift	0.70992	Eikenberg et al. 2001
Lauch		Upper Rhine Rift	0.71002	Eikenberg et al. 2001
Lauch		Upper Rhine Rift	0.70906	Eikenberg et al. 2001
Thur		Vosges	0.71390	Eikenberg et al. 2001
Fecht		Vosges	0.71340	Eikenberg et al. 2001
Cleurie		Vosges	0.71733	Eikenberg et al. 2001
Cleurie		Vosges	0.71798	Eikenberg et al. 2001
Muesbach		Vosges	0.71707	Eikenberg et al. 2001
Adelsbach		Vosges	0.71594	Eikenberg et al. 2001
Adelsbach		Vosges	0.71693	Eikenberg et al. 2001
Ibach		Vosges	0.71515	Eikenberg et al. 2001
Bergbach		Vosges	0.71661	Eikenberg et al. 2001
Strengbach	Source range (n=3)	Vosges	0.72104-0.72504	Eikenberg et al. 2001
Strengbach	range (n=7)	Vosges	0.72494-0.72250	Probst et al. 2000

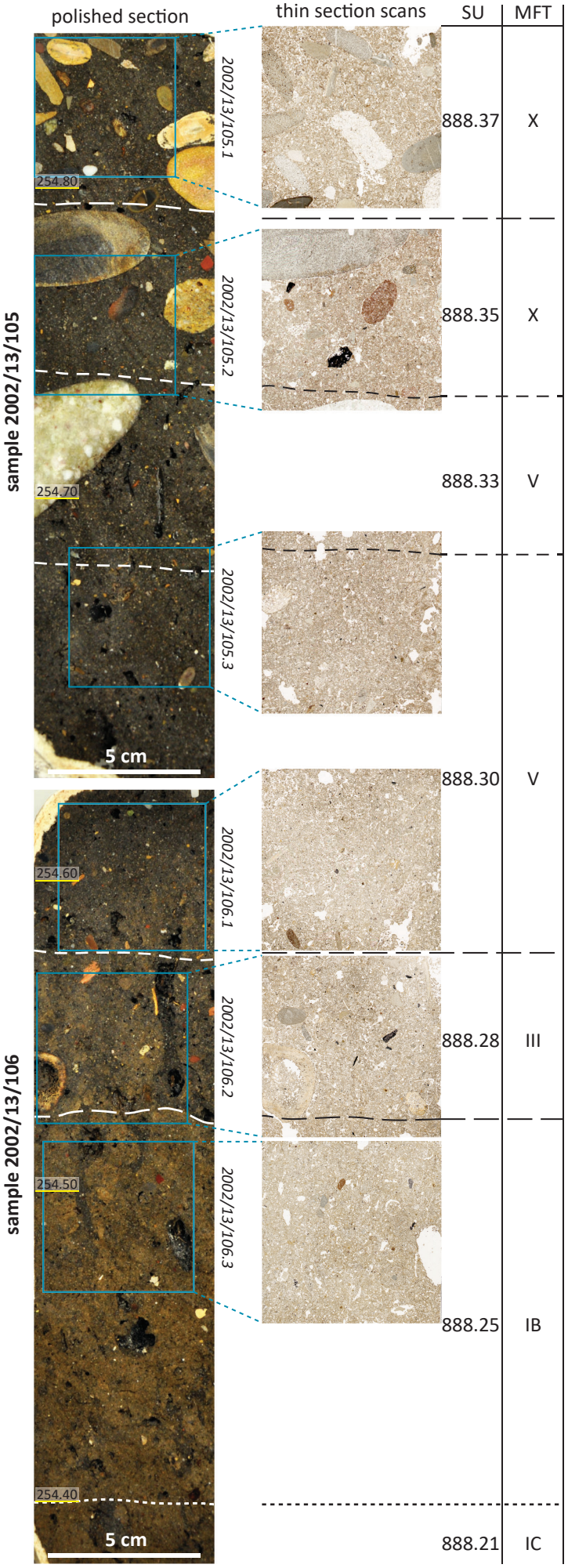

Profile P058
58.8
58.7
58.5
58.6
58.4
58.3
58.2a
58.1
58.2b
1992/34/3
MAL 1
0.5 m
polished section
thin section scans
SU
MFT
sample 1992/32/3
254.60
254.50
1992/34/3.1
1992/34/3.2
1992/34/3.3
5 cm
58.4
V
58.3
III
58.2b
II
58.2a
IC

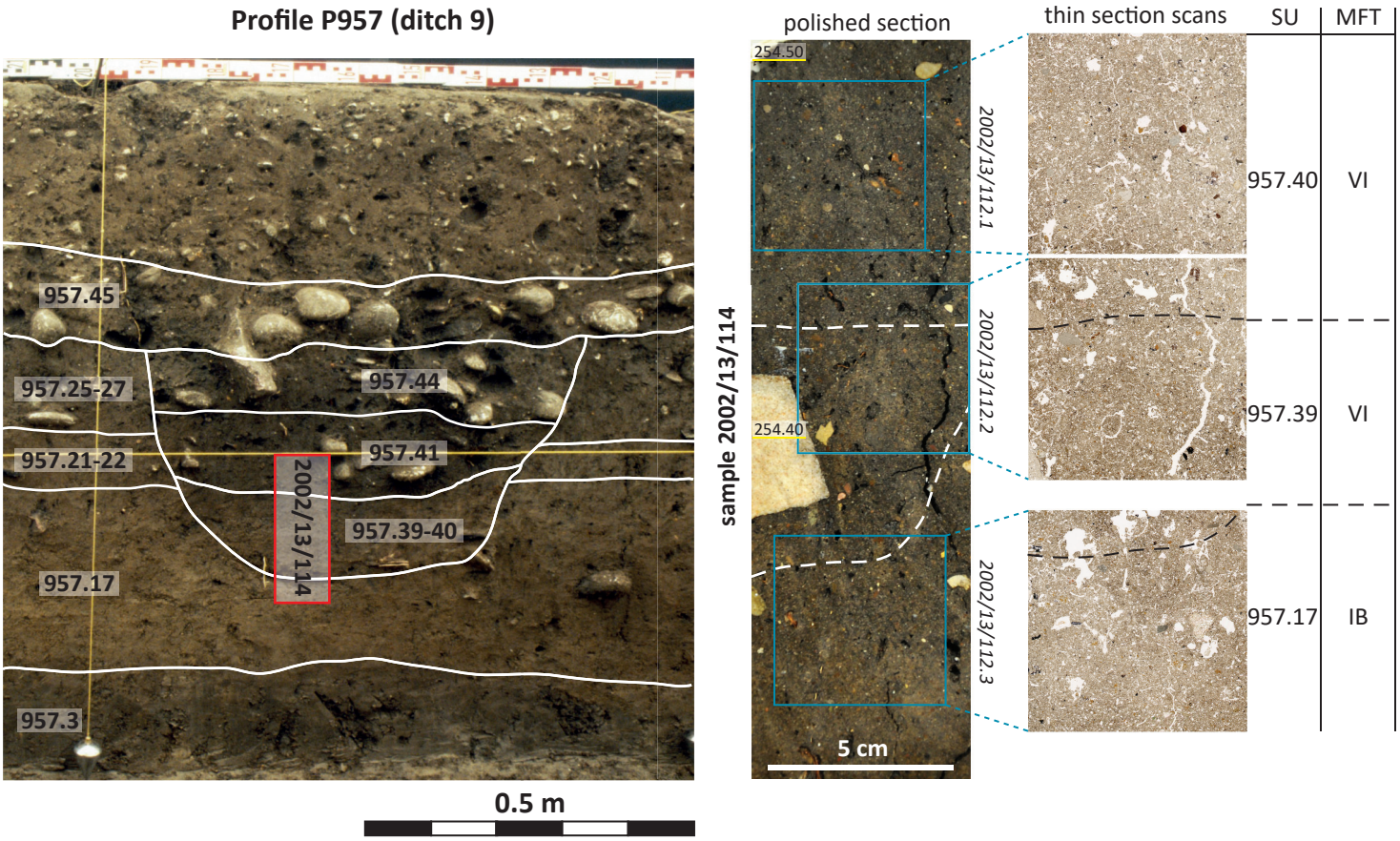

Profile P379
739.15-16
739.11
739.8/9
739.7
739.6
739.5
2002/13/93
2002/13/92
0.5 m


polished section
thin section scans
SU
MFT
sample 2002/13/93
2002/13/93.1
2002/13/93.2
254.80
254.70
5 cm
739.16
XI
739.15
XI
739.11
X
739.9
IV
739.8
IV
739.7
III
sample 2002/13/92
2002/13/92.1
2002/13/92.2
254.60
254.50
5 cm
739.7
III
739.6
IB

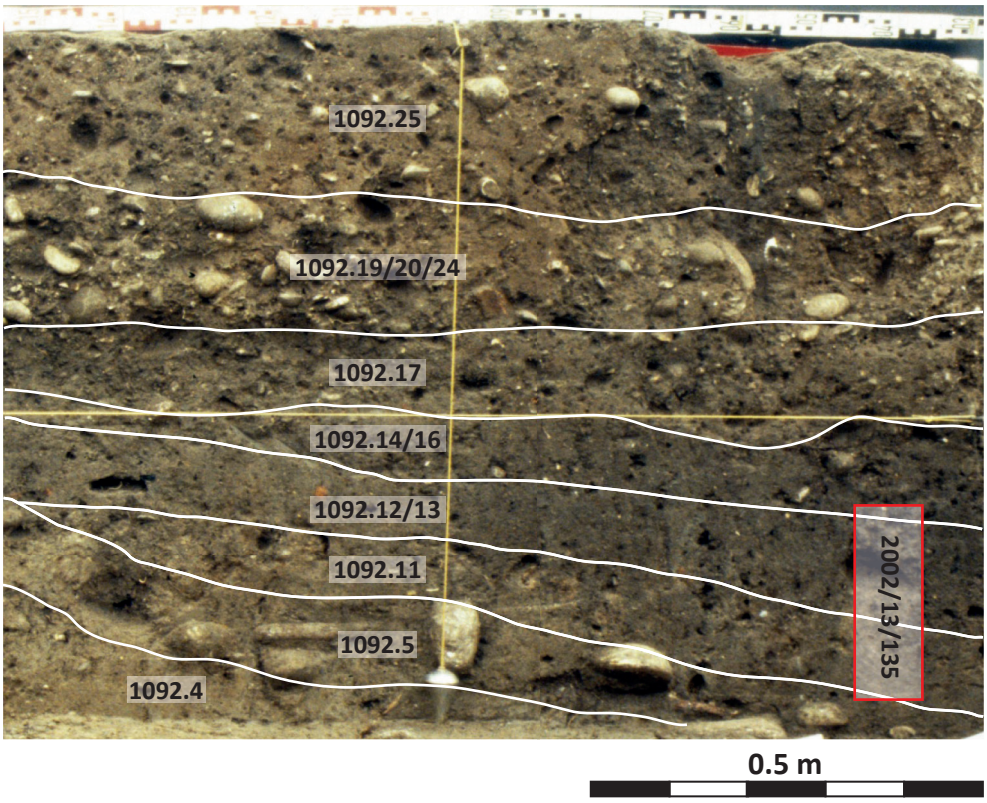
Profile P888

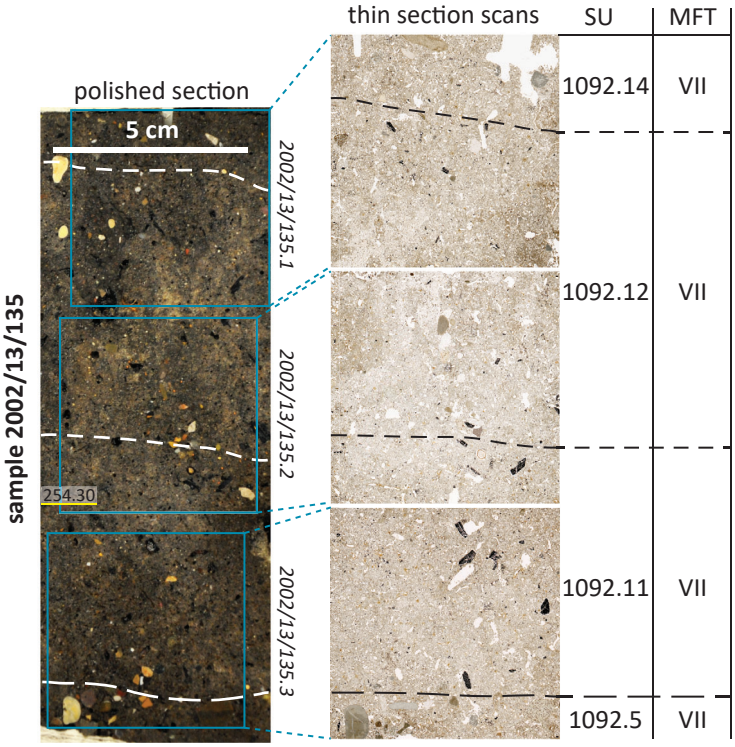




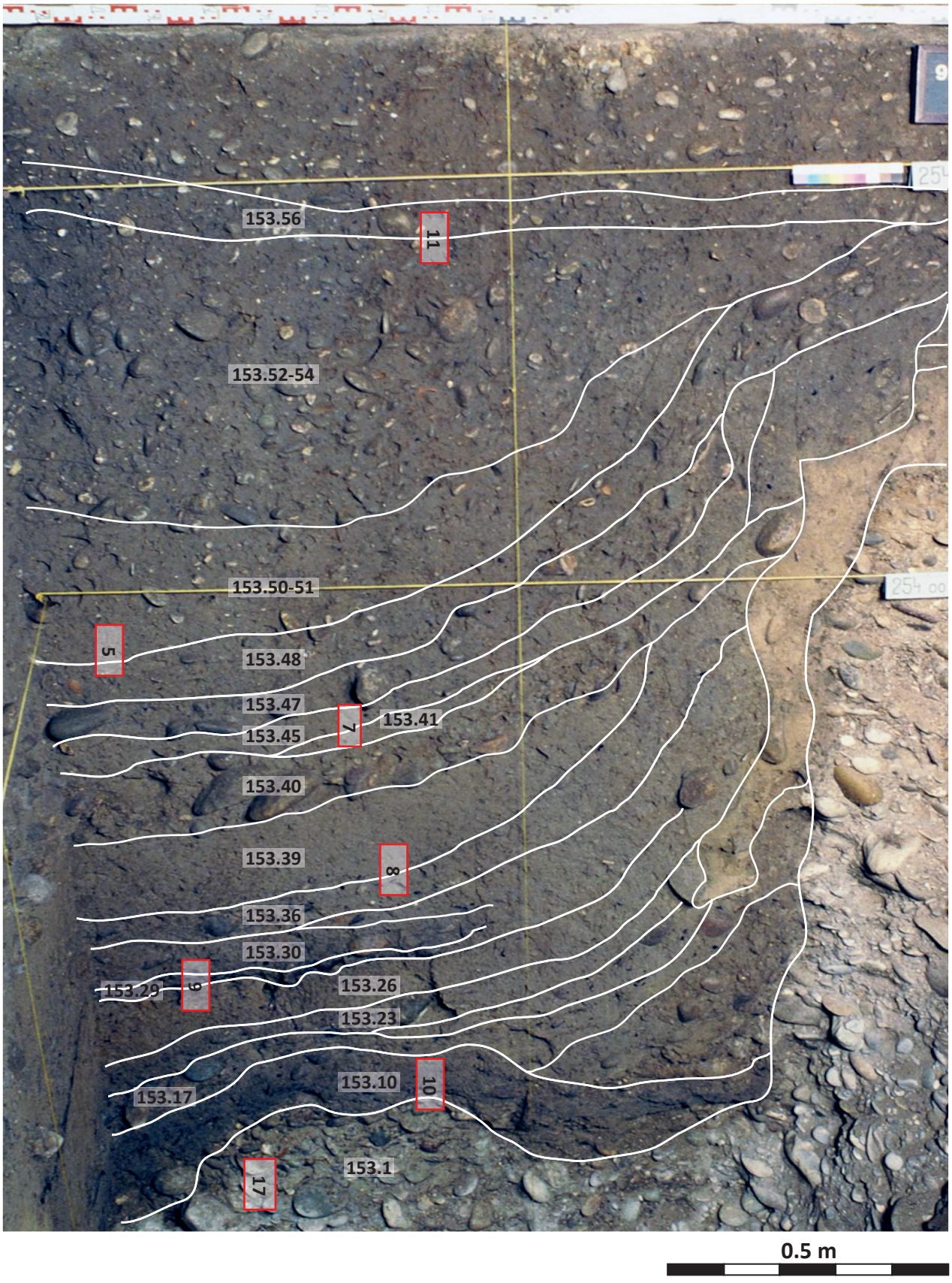

Profile P957 (ditch 9)
957.45
957.25-27
957.44
957.21-22
957.41
2002/13/114
957.39-40
957.17
957.3
0.5 m
polished section
thin section scans
SU
MFT
sample 2002/13/114
254.50
254.40
2002/13/112.1
2002/13/112.2
2002/13/112.3
5 cm
957.40
VI
957.39
VI
957.17
IB

Profile P1092 (ditch 4)

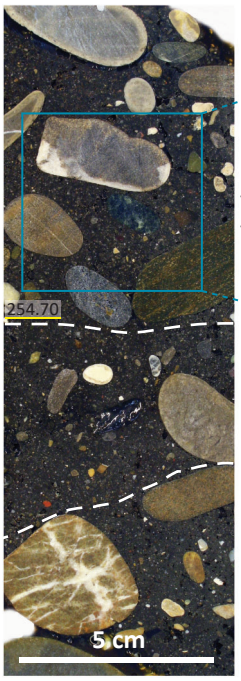


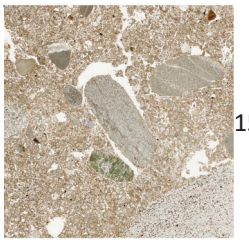


Profile P153 (pit 302)



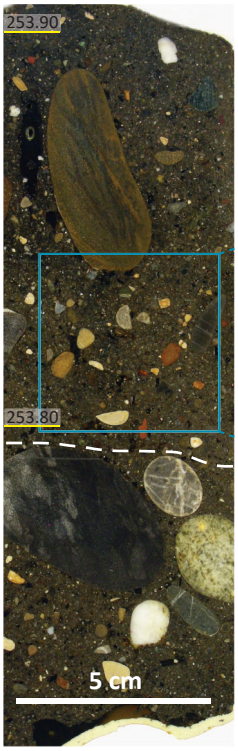
sample 1992/32/11

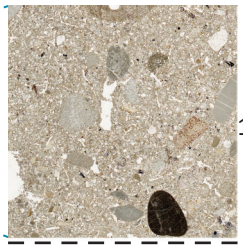




SU	MFT
153.56	XI
153.54	IX
153.53	IX

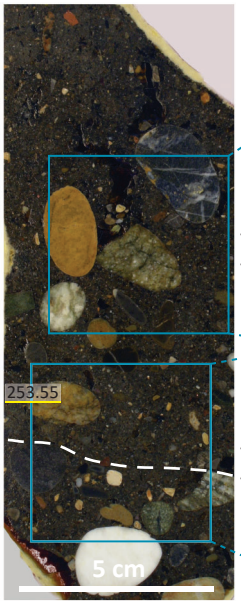
sample 1992/32/5

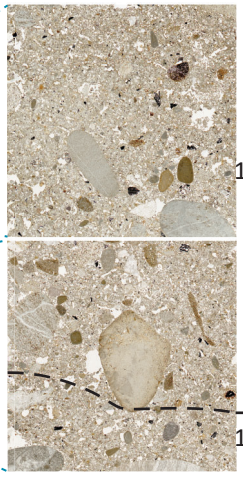




SU	MFT
153.50	IX
153.48	IX

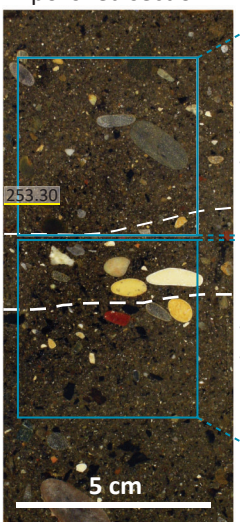
sample 1992/32/7

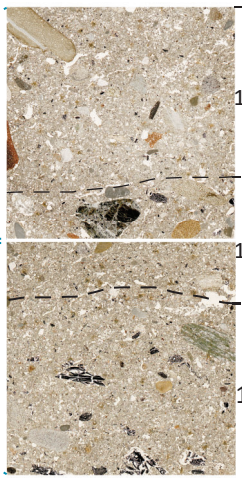




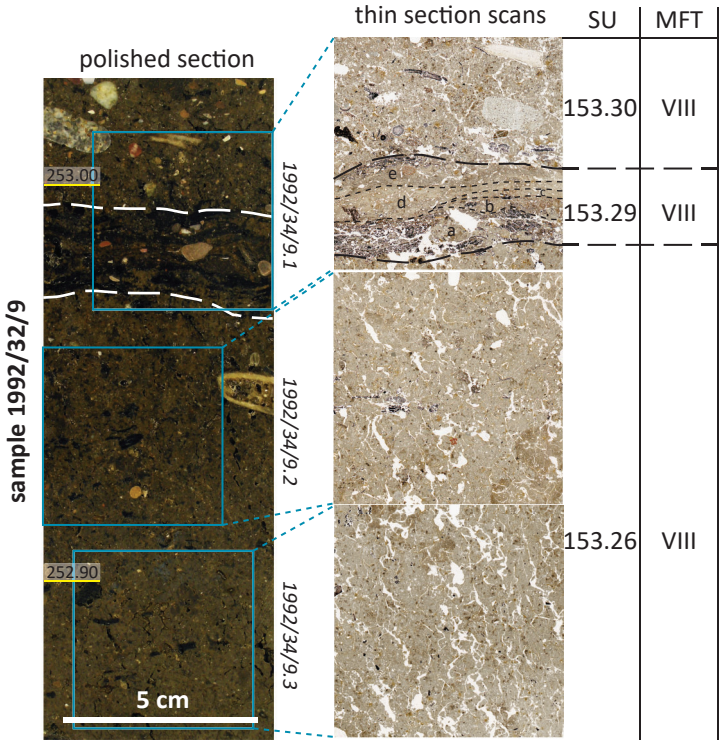
SU	MFT
153.45	IX
153.41	IX

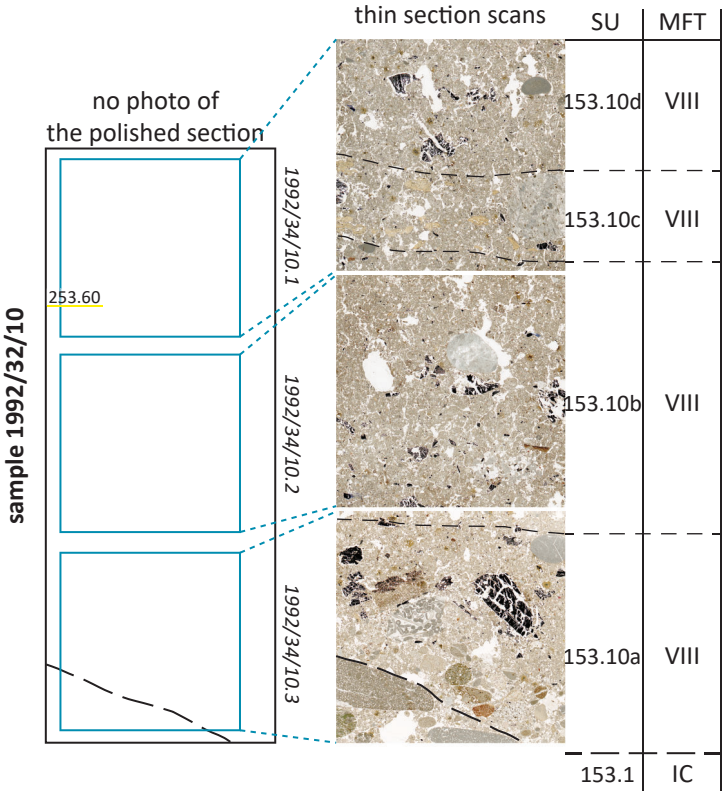
sample 1992/32/8

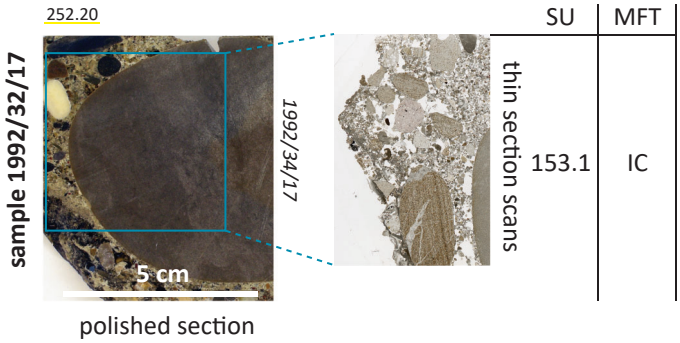




SU	MFT
153.39b	IX
153.39a	IX
153.36	IX


sample 1992/32/9
polished section
253.00
252.90
5 cm
1992/34/9.1
1992/34/9.2
1992/34/9.3
thin section scans
a
b
d
e
SU
MFT
153.30
VIII
153.29
VIII
153.26
VIII


sample 1992/32/10
no photo of
the polished section
253.60
1992/34/10.1
1992/34/10.2
1992/34/10.3
thin section scans
SU
MFT
153.10d
VIII
153.10c
VIII
153.10b
VIII
153.10a
VIII
153.1
IC


sample 1992/32/17
252.20
5 cm
1992/34/17
polished section
thin section scans
SU
MFT
153.1
IC

The Hidden Midden - Supplement 2: Micromorphological results

sample no.	stratigrahic unit	altitude	thickness [cm]	context	microfacies type	layering	microstructure	Porosity	clay content	silt content	sand content	gravel content	reddening (gravels)	organic content	bioturbation	earthworm granules	mollusc shells	quera	sclerotia	Fe/Mn precipitations	Ca-precipitations	P-precipitations	vivianite
1990/42/10.1	**3.2**	254.58	18	occupation layer	5	unlayered	channel and chamber structure	20%	5%	35%	37%	3%	none; clear	0%	4	2	0	0	0	1	0	4	3
1990/42/10.2	**3.1**	254.46	2	initial trampling horizon	3	weak horizontal orientation	channel and chamber structure	15%	5%	45%	33%	2%	none	0%	4	0	0	0	1	1	0	3	0
1990/42/10.2	**2**	254.44	11	natural overbank deposit	1C	unlayered	massive structure	5%	5%	55%	35%	0%		0%	5	3	0	2	0	6	1	6	0
1990/42/10/1	**3.3**	254.70	10	occupation layer	4	unlayered	channel and chamber structure	20%	5%	30%	35%	10%	none; weak	0%	4	1	0	0	0	1	0	3	1
1990/42/10/1	**3.2**	254.58	18	occupation layer	5	unlayered	channel and chamber structure	20%	5%	40%	32%	3%	none; clear	0%	4	0	0	0	0	0	0	3	2
1990/42/10/2	**3.1**	254.46	2	initial trampling horizon	3	weak horizontal orientation	channel and chamber structure	15%	5%	45%	33%	2%	none	0%	4	0	0	0	0	1	0	3	0
1990/42/10/2	**3.2**	254.58	18	occupation layer	5	unlayered	channel and chamber structure	20%	5%	35%	37%	3%	none	0%	4	0	1	0	0	1	0	3	0
1990/42/10/2	**2**	254.44	11	natural overbank deposit	1C	unlayered	channel and chamber structure	20%	5%	45%	30%	0%		0%	3	0	0	0	0	1	2	6	0
1990/42/11	**3**	254.64	22	initial trampling horizon	3	weak horizontal orientation	chamber structure	15%	10%	40%	35%	0%		0%	4	0	0	0	0	3	0	1	0
1990/42/11	**2.1**	254.46	22	natural overbank deposit	1C	unlayered	channel and chamber structure	15%	5%	45%	35%	0%		0%	4	0	0	0	0	2	0	0	0
1990/42/11	**2.2**	254.47	1	rammed earth floor	2	unlayered	complexe structure	2%	5%	50%	43%	0%		0%	4	0	0	0	0	4	0	1	1
1990/42/12	**8**	253.88		pit 287	8	laminated	vughy structure	25%	0%	65%	10%	0%		0%	3	0	0	0	0	2	0	0	0
1990/42/13	**4.2**	254.65	1	occupation layer	5	unlayered	channel and chamber structure	20%	5%	35%	28%	10%		2%	4	2	0	0	0	3	0	1	0
1990/42/13	**4.3**	254.69	4	occupation layer	5	unlayered	channel and chamber structure	20%	5%	38%	33%	2%	none	2%	4	2	1	1	0	2	0	1	0
1990/42/14	**3**	254.54	3	initial trampling horizon	3	unlayered	channel and chamber structure	20%	5%	43%	30%	2%	none	0%	4	0	0	3	0	3	0	3	1
1990/42/14	**2**	254.52	36	natural overbank deposit	1C	unlayered	channel and chamber structure	10%	10%	40%	40%	0%		0%	4	2	0	0	0	4	0	2	0
1990/42/14; 1990/42/13	**4.1**	254.64	10	occupation layer	5	unlayered	channel and chamber structure	20%	5%	38%	33%	2%	weak; burnt lime	2%	4	2	2	0	1	3	0	2	1

The Hidden Midden - Supplement 2: Micromorphological results

sample no.	stratigrahic unit	prop. Leucophosphite	horizontal orientation	compaction	loam chunks	dusty coatings	slaking crusts	agricutans	runoff-sediments	charcoals	micro-charcoals	charred org. remains	ashes	phytolith slags	melted quarz grains	bone frgm	bone chip	fish bone	teeth	egg shell frgm	ceramic frgm	burned loam	daub	daub preservation	iron grains	slags	flint	glass	phytoliths	coprolites	prop. Producer	dung	dung spherolites	phytolith layers	guano	avian uric acid spheres	parasite eggs
1990/42/10.1	**3.2**	0	0	0	0	2	2	3	0	0	2	0	0	0	0	2	1	0	0	0	0	1	0		0	0	0	0	0	0		1	1	0	1	2	0
1990/42/10.2	**3.1**	0	2	2	2	1	1	0	0	0	1	0	0	0	0	0	1	0	0	0	0	0	0		0	1	0	0	0	0		0	0	0	0	0	0
1990/42/10.2	**2**	0	0	3	1	0	0	0	0	0	6	0	0	0	0	0	6	0	0	0	0	0	0		0	0	0	0	0	0		0	0	0	0	0	0
1990/42/10/1	**3.3**	0	2	3	3	2	2	3	0	1	2	0	0	0	0	1	1	0	0	0	1	2	0		0	0	0	0	0	1	indet	0	0	0	0	0	0
1990/42/10/1	**3.2**	0	0	0	0	2	2	3	0	0	2	0	0	0	0	0	6	0	0	0	0	1	0		0	0	0	0	0	0		0	0	0	0	0	0
1990/42/10/2	**3.1**	0	3	2	3	0	1	0	0	0	1	0	0	0	0	0	0	0	0	0	0	1	0		0	0	0	0	0	0		0	0	0	0	0	0
1990/42/10/2	**3.2**	0	0	0	0	1	1	0	0	0	2	0	0	0	0	0	1	0	0	0	0	0	0		0	0	0	0	0	0		0	0	0	0	0	0
1990/42/10/2	**2**	0	0	2	0	0	0	0	0	0	6	0	0	0	0	0	0	0	0	0	0	0	0		0	0	0	0	0	0		0	0	0	0	0	0
1990/42/11	**3**	0	1	2	2	3	0	0	0	0	6	0	0	0	0	0	0	0	0	0	0	0	0		0	0	0	0	0	0		0	0	0	0	0	0
1990/42/11	**2.1**	0	0	0	0	2	0	0	0	0	6	0	0	0	0	0	0	0	0	0	0	0	0		0	0	0	0	0	0		0	0	0	0	0	0
1990/42/11	**2.2**	0	0	5	0	1	0	0	0	0	0	0	0	0	0	0	0	0	0	0	0	0	0		0	0	0	0	0	0		0	0	0	0	0	0
1990/42/12	**8**	0	4	0	4	0	0	0	0	3	1	0	5	3	4	0	0	0	0	0	0	4	0		0	0	0	0	3	0		0	0	0	0	0	0
1990/42/13	**4.2**	0	3	0	0	2	0	0	0	0	2	0	0	0	0	0	2	0	0	0	0	0	0		0	0	0	0	0	0		0	0	0	0	0	0
1990/42/13	**4.3**	0	1	0	0	2	0	0	0	0	7	0	0	0	0	0	7	0	0	0	0	0	0		0	0	0	0	0	0		0	0	0	0	0	0
1990/42/14	**3**	0	4	1	2	2	1	0	0	0	2	0	0	0	0	3	2	0	0	0	0	0	0		0	0	0	0	0	0		0	0	0	0	0	0
1990/42/14	**2**	0	0	3	0	3	0	0	0	0	7	0	0	0	0	0	6	0	0	0	0	0	0		0	0	0	0	0	0		0	0	0	0	0	0
1990/42/14; 1990/42/13	**4.1**	0	2	0	1	2	0	0	0	0	2	0	0	0	0	0	1	0	0	1	0	0	0		6	0	0	0	0	0		0	0	0	0	0	0

sample no.	stratigrahic unit	altitude	thickness [cm]	context	microfacies type	layering	microstructure	Porosity	clay content	silt content	sand content	gravel content	reddening (gravels)	organic content	bioturbation	earthworm granules	mollusc shells	quera	sclerotia	Fe/Mn precipitations	Ca-precipitations	P-precipitations	vivianite
1990/42/15	**5**	254.40	27	ditch 7	6	unlayered	channel and chamber structure	30%	2%	30%	35%	3%	clear	0%	5	1	0	3	0	4	0	2	0
1990/42/16.1	**19**	254.40	12	pit 287	9	unlayered	channel and chamber structure	20%	5%	35%	30%	10%		0%	4	0	1	0	0	3	1	3	2
1990/42/16.2	**17**	254.30	39	pit 287	9	unlayered	channel and chamber structure	20%	5%	35%	35%	5%	none	0%	4	2	1	0	0	3	0	2	1
1990/42/16.2	**3**	254.40	24	pit 287	1B	unlayered	channel and chamber structure	25%	10%	37%	28%	0%		0%	3	0	0	0	0	2	0	1	0
1990/42/18	**20**	253.80	12	pit 287	8	layered	channel and chamber structure	25%	0%	50%	25%	0%		0%	3	1	0	0	0	2	0	0	0
1990/42/20	**6**	253.62	2	pit 287	8	unlayered	channel and chamber structure	15%	0%	80%	5%	0%		0%	3	0	0	0	0	0	2	0	0
1992/34/1; 1992/34/1bis	**15**	254.70	10	pit hole	6	layered	channel and chamber structure	10%	10%	35%	40%	5%	weak	0%	4	1	0	4	0	2	0	0	0
1992/34/1; 1992/34/1bis	**16**	254.76	6	pit hole	9	layered	channel and chamber structure	15%	5%	30%	45%	5%	none	0%	4	0	0	4	0	2	0	0	0
1992/34/10.3	**10.1**	252.57	3	pit 302	8	horizontal orientation	channel and chamber structure	15%	0%	50%	25%	10%	strong; physical stress	0%	3	0	6	0	0	1	2	3	3
1992/34/10.3	**1**	252.54		natural rhine gravel	1C	unlayered	channel and chamber structure	15%	0%	25%	20%	40%	none	0%	3	0	0	0	0	0	0	3	3
1992/34/10.3; 1992/34/10.2; 1992/34/10.1	**10.2**	252.61	4	pit 302	8	horizontal orientation	channel and chamber structure	15%	0%	s	25%	2%	strong; physical stress	0%	3	2	2	0	0	1	1	2	2
1992/34/10.3; 1992/34/10.2; 1992/34/10.1	**10.3**	252.62	1	pit 302	8	horizontal orientation	channel and chamber structure	15%	0%	58%	25%	2%	strong; burnt lime; melted quarz grains; physical stress	0%	4	0	2	0	0	2	2	3	3
1992/34/10.3; 1992/34/10.2; 1992/34/10.1	**10.4**	252.66	4	pit 302	8	horizontal orientation	channel and chamber structure	15%	0%	58%	25%	2%	strong; physical stress	0%	4	0	2	0	0	2	1	3	3
1992/34/11	**56**	254.78	8	pit 302	9	unlayered	channel structure	15%	10%	20%	30%	25%	weak	0%	4	3	0	0	0	4	0	2	0
1992/34/14.2; 1992/34/14.1	**2**	254.35	13	natural overbank deposit	1C	unlayered	channel and chamber structure	15%	5%	45%	35%	0%		0%	4	0	0	2	1	0	0	6	6
1992/34/14.2; 1992/34/14.3	**1**	254.14		natural rhine gravel	1C	unlayered	complexe structure	15%	5%	10%	10%	60%	none	0%	3	0	0	0	0	0	0	0	0

sample no.	stratigrahic unit	prop. Leucophosphite	horizontal orientation	compaction	loam chunks	dusty coatings	slaking crusts	agricutans	runoff-sediments	charcoals	micro-charcoals	charred org. remains	ashes	phytolith slags	melted quarz grains	bone frgm	bone chip	fish bone	teeth	egg shell frgm	ceramic frgm	burned loam	daub	daub preservation	iron grains	slags	flint	glass	phytoliths	coprolites	prop. Producer	dung	dung spherolites	phytolith layers	guano	avian uric acid spheres	parasite eggs
1990/42/15	**5**	0	0	0	0	3	0	0	1	0	8	0	0	0	0	0	7	0	0	0	6	0	0		0	0	0	0	0	0		0	0	0	0	0	0
1990/42/16.1	**19**	0	0	0	0	1	2	0	0	1	2	1	1	0	0	1	6	0	0	0	1	3	0		0	0	0	0	0	0		0	0	0	0	0	0
1990/42/16.2	**17**	0	0	0	0	1	0	0	0	0	2	0	0	0	0	1	1	0	0	0	0	1	0		0	0	0	0	0	0		0	0	0	0	0	0
1990/42/16.2	**3**	0	0	0	0	1	0	0	0	0	7	0	0	0	0	0	7	0	0	0	0	0	0		0	0	0	0	0	0		0	0	0	0	0	0
1990/42/18	**20**	0	4	0	0	0	0	0	0	3	1	2	5	3	3	3	2	0	1	0	0	2	0		0	0	0	0	0	0		0	0	0	0	0	0
1990/42/20	**6**	0	0	0	0	0	0	0	0	0	1	2	5	2	2	0	1	0	0	0	0	0	0		0	0	0	0	2	1	indet	0	0	0	0	0	0
1992/34/1; 1992/34/1bis	**15**	0	3	0	0	4	3	0	0	0	1	1	1	0	0	2	1	0	0	0	0	1	2	burned	0	0	0	0	0	0		0	0	0	0	0	0
1992/34/1; 1992/34/1bis	**16**	0	0	0	0	0	3	0	0	0	2	0	0	0	0	0	0	0	0	0	0	0	5	burned	0	0	0	0	1	0		0	0	0	0	0	0
1992/34/10.3	**10.1**	4	3	1	0	0	0	0	0	3	4	1	5	2	3	0	6	0	0	6	0	2	0		0	0	0	0	4	6	prop. human	0	7	0	0	0	0
1992/34/10.3	**1**	0	0	0	0	0	0	0	0	0	3	0	3	0	0	0	0	0	0	0	0	0	0		0	0	0	0	2	0		0	0	0	0	0	0
1992/34/10.3; 1992/34/10.2; 1992/34/10.1	**10.2**	4	4	1	0	0	0	0	0	3	4	1	5	2	3	0	1	0	0	0	1	2	0		1	1	0	0	4	7	prop. human	0	7	0	0	0	0
1992/34/10.3; 1992/34/10.2; 1992/34/10.1	**10.3**	4	4	1	0	0	0	0	0	3	4	1	5	3	3	0	1	0	0	0	0	2	0		0	0	0	0	4	5	prop. human	0	7	0	0	0	1
1992/34/10.3; 1992/34/10.2; 1992/34/10.1	**10.4**	4	4	1	0	0	0	0	0	3	4	1	5	3	3	0	1	0	0	0	0	2	0		0	0	0	0	4	6	prop. human	0	7	0	0	0	0
1992/34/11	**56**	0	0	0	0	1	0	0	0	0	2	0	0	0	0	0	1	0	0	0	0	0	0		3	0	0	0	0	6	indet	0	0	0	0	0	0
1992/34/14.2; 1992/34/14.1	**2**	0	0	0	0	1	0	0	0	0	6	0	0	0	0	0	6	0	0	0	0	0	0		0	0	0	0	0	0		0	0	0	0	0	0
1992/34/14.2; 1992/34/14.3	**1**	0	0	0	0	0	0	0	0	0	6	0	0	0	0	0	6	0	6	0	0	0	0		0	0	0	0	0	0		0	0	0	0	0	0

sample no.	stratigrahic unit	altitude	thickness [cm]	context	microfacies type	layering	microstructure	Porosity	clay content	silt content	sand content	gravel content	reddening (gravels)	organic content	bioturbation	earthworm granules	mollusc shells	quera	sclerotia	Fe/Mn precipitations	Ca-precipitations	P-precipitations	vivianite
1992/34/15	**2**	254.44	23	natural overbank deposit	1C	unlayered	channel and chamber structure	15%	10%	35%	40%	0%		0%	4	1	0	0	0	3	0	1	0
1992/34/16a; 1992/34/16b	**37**	252.95	3	pit 302	8	laminated	complexe structure	20%	0%	55%	5%	0%		20%	3	0	0	0	0	2	2	2	2
1992/34/16b	**27.2**	253.89	2	pit 302	8	horizontal orientation	channel and chamber structure	10%	0%	55%	5%	30%	clear; physical stress	0%	3	1	0	0	0	2	0	3	3
1992/34/16b	**27.3**	253.92	3	pit 302	8	horizontal orientation	channel and chamber structure	10%	0%	80%	10%	0%		0%	3	2	2	0	1	2	0	4	4
1992/34/17	**1**	252.24		natural rhine gravel	1C	unlayered	bridged grain structure	30%	0%	10%	25%	35%	none	0%	3	0	0	0	0	0	5	0	0
1992/34/2	**8**	253.09		pit 302		laminated	channel and chamber structure	8%	5%	45%	40%	2%	none	0%	3	0	0	0	0	1	0	2	2
1992/34/28	**4**	254.55	6	initial trampling horizon	3	unlayered	channel and chamber structure	15%	10%	40%	25%	6%	none	4%	4	3	0	0	0	3	0	4	0
1992/34/3.2; 1992/34/3.1	**4**	254.63	12	occupation layer	5	weak horizontal orientation	channel and chamber structure	15%	5%	40%	35%	5%		0%	4	1	0	2	2	3	0	4	3
1992/34/3.3	**3.2**	254.51	3	initial trampling horizon	3	horizontal orientation	channel and chamber structure	15%	5%	35%	35%	10%		0%	4	0	0	3	0	2	0	1	0
1992/34/3.3	**3.1**	254.48	1	initial trampling horizon	3	unlayered	channel and chamber structure	15%	5%	45%	35%	0%		0%	4	0	1	2	3	1	1	1	0
1992/34/3.3	**2.1**	254.46	17	natural overbank deposit	1C	unlayered	channel and chamber structure	15%	5%	45%	35%	0%		0%	3	0	0	0	0	2	0	0	0
1992/34/3.3	**2.2**	254.47	1	rammed earth floor	2	unlayered	complexe structure	2%	5%	50%	43%	0%		0%	3	0	1	0	0	4	0	0	0
1992/34/30	**18**	253.72		pit 302	8	horizontal orientation	channel and chamber structure	10%	0%	80%	10%	0%		0%	3	0	1	0	0	1	0	3	3
1992/34/4	**4.2**	254.53	2	initial trampling horizon	3	horizontal orientation	channel and chamber structure	15%	5%	35%	35%	10%		0%	4	0	0	2	0	2	0	1	0
1992/34/4	**6**	254.64	16	occupation layer	5	weak horizontal orientation	channel and chamber structure	15%	5%	40%	35%	5%		0%	4	0	0	2	0	2	0	3	2
1992/34/4	**4.1**	254.50	2	initial trampling horizon	3	unlayered	channel and chamber structure	10%	5%	45%	40%	0%		0%	4	0	0	3	0	1	0	1	0
1992/34/5	**50**	253.91	11	pit 302	9	unlayered	channel and chamber structure	15%	5%	40%	25%	15%	weak; clear; strong; physical stress	0%	4	2	0	1	0	3	0	3	0

The Hidden Midden - Supplement 2: Micromorphological results

sample no.	stratigrahic unit	prop. Leucophosphite	horizontal orientation	compaction	loam chunks	dusty coatings	slaking crusts	agricutans	runoff-sediments	charcoals	micro-charcoals	charred org. remains	ashes	phytolith slags	melted quarz grains	bone frgm	bone chip	fish bone	teeth	egg shell frgm	ceramic frgm	burned loam	daub	daub preservation	iron grains	slags	flint	glass	phytoliths	coprolites	prop. Producer	dung	dung spherolites	phytolith layers	guano	avian uric acid spheres	parasite eggs
1992/34/15	**2**	0	0	0	0	1	0	0	0	0	6	0	0	0	0	0	6	0	0	0	0	0	0		0	0	0	0	0	0		0	0	0	0	0	0
1992/34/16a; 1992/34/16b	**37**	2	4	3	2	0	0	0	0	3	4	3	4	3	3	0	2	0	0	0	0	3	3	burned	0	0	0	0	4	0		5	5	4	0	0	1
1992/34/16b	**27.2**	3	5	3	0	0	0	0	0	2	4	0	5	3	3	6	1	0	0	0	6	0	0		0	6	0	0	4	0		5	5	1	0	0	3
1992/34/16b	**27.3**	4	5	3	0	0	0	0	0	2	4	1	5	3	3	6	1	0	0	0	1	0	0		0	0	1	0	4	0		5	5	1	0	0	3
1992/34/17	**1**	0	0	0	0	0	0	0	0	0	6	0	0	0	0	0	0	0	0	0	0	0	0		0	0	0	0	0	0		0	0	0	0	0	0
1992/34/2	**8**	0	0	5	0	0	0	0	0	0	6	0	1	0	0	0	0	0	0	0	0	0	0		1	0	0	0	0	0		0	0	0	0	0	0
1992/34/28	**4**	0	1	0	0	1	0	0	0	2	3	1	2	0	1	0	1	0	0	0	6	0	0		0	0	0	0	0	1	indet	0	0	0	0	0	1
1992/34/3.2; 1992/34/3.1	**4**	0	1	0	0	3	3	0	0	1	3	0	0	0	0	2	6	0	0	0	1	0	6		6	0	0	0	0	1	indet		1	0	0	0	1
1992/34/3.3	**3.2**	0	5	0	1	1	0	0	0	0	1	0	0	0	0	3	1	0	0	0	1	0	0		0	1	0	0	0	0		0	0	0	0	0	0
1992/34/3.3	**3.1**	0	0	0	0	1	0	0	0	0	7	0	0	0	0	0	7	0	0	0	0	0	0		0	0	0	0	0	0		0	0	0	0	0	0
1992/34/3.3	**2.1**	0	0	0	0	1	0	0	0	0	6	0	0	0	0	6	0	0	0	0	0	6	0		0	0	0	0	0	0		0	0	0	0	0	0
1992/34/3.3	**2.2**	0	0	5	0	0	0	0	0	0	0	0	0	0	0	0	0	0	0	0	0	0	0		0	0	0	0	0	0		0	0	0	0	0	0
1992/34/30	**18**	3		2	0	0	0	0	0	2	4	1	5	3	3	0	0	0	0	0	0	2	0		0	0	0	0	4	6	indet	5	5	2	0	0	0
1992/34/4	**4.2**	0	5	0	0	1	0	0	0	0	1	0	0	0	0	0	0	0	0	0	1	0	0		0	0	0	0	0	0		0	0	0	0	0	0
1992/34/4	**6**	0	1	0	0	3	3	0	0	2	2	1	0	0	0	0	6	0	0	0	0	0	0		0	0	0	0	0	0			0	0	0	0	0
1992/34/4	**4.1**	0	0	0	0	1	0	0	0	0	7	0	0	0	0	0	0	0	0	0	0	0	0		0	0	0	0	0	0		0	0	0	0	0	0
1992/34/5	**50**	0	0	0	0	2	0	0	0	2	3	0	0	0	0	2	1	0	0	6	6	6	0		1	0	0	0	2	6	indet	0	0	0	0	0	0

sample no.	stratigrahic unit	altitude	thickness [cm]	context	microfacies type	layering	microstructure	Porosity	clay content	silt content	sand content	gravel content	reddening (gravels)	organic content	bioturbation	earthworm granules	mollusc shells	quera	sclerotia	Fe/Mn precipitations	Ca-precipitations	P-precipitations	vivianite
1992/34/6.1; 1992/34/6.2	**21**	254.25		pit 302		unlayered	channel and chamber structure	15%	0%	55%	30%	0%		0%	4	2	0	0	0	2	2	2	1
1992/34/6.1; 1992/34/6.2	**19**	254.25		pit 302		unlayered	channel and chamber structure	15%	0%	45%	15%	25%	weak	0%	4	2	0	0	0	2	2	2	1
1992/34/7.2	**41**	253.54	5	pit 302	9	unlayered	channel and chamber structure	15%	5%	25%	25%	30%	clear; strong; physical stress	0%	4	0	1	0	1	2	0	3	1
1992/34/7.2; 1992/34/7.1	**45**	253.70	16	pit 302	9	unlayered	channel and chamber structure	15%	5%	35%	35%	10%	clear; strong; physical stress	0%	4	3	0	0	0	2	1	3	1
1992/34/8.1	**39.2**	253.46	17	pit 302	9	unlayered	channel and chamber structure	15%	5%	45%	25%	10%	none; clear; strong; physical stress	0%	4	0	0	0	0	2	0	3	3
1992/34/8.2	**36**	253.27	10	pit 302	9	unlayered	channel and chamber structure	15%	5%	45%	25%	10%	none; clear; physical stress	0%	4	2	0	0	2	2	0	3	3
1992/34/8.2; 1992/34/8.1	**39.1**	253.29	2	pit 302	9	unlayered	channel and chamber structure	15%	5%	35%	20%	25%	none; clear; strong; physical stress	0%	4	0	0	0	0	2	0	2	2
1992/34/9.1	**29**	252.99	2	pit 302	8	laminated	chamber structure	10%	0%	60%	10%	0%		20%	3	1	0	0	0	2	3	2	2
1992/34/9.1	**30**	253.03	4	pit 302	8	horizontal orientation	channel and chamber structure	15%	0%	55%	18%	10%	clear; strong; physical stress	2%	4	0	6	0	2	3	2	3	2
1992/34/9.3; 1992/34/9.2; 1992/34/9.1	**26**	252.97	20	pit 302	8	horizontal orientation	channel and chamber structure	10%	0%	80%	10%	0%		0%	4	2	0	0	0	2	0	4	4
2001/25/3.1	**17**	254.77	10	ditch	6	layered	channel and chamber structure	15%	10%	20%	30%	25%	none; physical stress	0%	4	3	0	0	1	3	0	0	0
2001/25/3.3; 2001/25/3.2	**16**	254.67	12	ditch	6	layered	channel and chamber structure	15%	10%	20%	30%	25%	none	0%	4	2	0	0	1	2	0	0	0
2001/25/4.1	**27/29**	254.55	6	ditch	6	horizontal orientation	channel and chamber structure	15%	5%	30%	25%	25%	none; weak; physical stress	0%	4	1	6	0	0	3	1	0	0
2001/25/4.2	**10**	254.46	12	pit 386	9	weak horizontal orientation	channel and chamber structure	20%	3%	45%	25%	7%	none; clear; strong; physical stress	0%	5	0	0	0	0	2	0	2	0
2001/25/4.2; 2001/25/4.1	**12**	254.49	3	pit 386	9	weak horizontal orientation	channel and chamber structure	15%	5%	35%	20%	25%	none; weak; clear; physical stress	0%	5	1	0	0	0	3	0	1	0
2002/13/105.1	**37**	254.86	7	gravel layer	10	horizontal orientation	channel and chamber structure	15%	5%	35%	25%	20%	none; weak; physical stress	0%	4	1	0	0	2	3	0	1	0
2002/13/105.2	**35**	254.79	5	gravel layer	10	horizontal orientation	channel and chamber structure	15%	5%	35%	30%	15%	none; weak; physical stress	0%	4	2	0	0	2	3	1	2	0

The Hidden Midden - Supplement 2: Micromorphological results

sample no.	stratigrahic unit	prop. Leucophosphite	horizontal orientation	compaction	loam chunks	dusty coatings	slaking crusts	agricutans	runoff-sediments	charcoals	micro-charcoals	charred org. remains	ashes	phytolith slags	melted quarz grains	bone frgm	bone chip	fish bone	teeth	egg shell frgm	ceramic frgm	burned loam	daub	daub preservation	iron grains	slags	flint	glass	phytoliths	coprolites	prop. Producer	dung	dung spherolites	phytolith layers	guano	avian uric acid spheres	parasite eggs
1992/34/6.1; 1992/34/6.2	**21**	0	0	0	0	2	0	0	0	0	6	0	0	0	0	0	6	0	0	0	6	0	0		0	0	0	0	0	6	indet	0	0	0	0	0	0
1992/34/6.1; 1992/34/6.2	**19**	0	0	0	0	2	0	0	0	0	6	0	0	0	0	0	6	0	0	0	0	0	0		0	0	0	0	0	0		0	0	0	0	0	0
1992/34/7.2	**41**	1	0	0	0	2	0	0	0	1	2	0	0	0	0	0	1	0	0	0	0	0	0		0	0	0	0	0	6	indet	0	0	0	0	0	0
1992/34/7.2; 1992/34/7.1	**45**	0	0	0	0	3	0	0	0	2	2	0	0	0	0	0	2	0	0	0	6	6	0		1	0	6	0	0	6	indet	0	0	0	0	0	0
1992/34/8.1	**39.2**	1	0	0	0	0	0	0	0	2	3	0	3	0	2	0	2	0	0	0	2	0	0		1	0	0	0	2	1	indet	0	0	0	0	0	0
1992/34/8.2	**36**	0	0	0	0	0	0	0	0	3	3	1	3	1	2	0	2	0	0	0	2	2	0		1	0	0	0	2	6	indet	0	0	0	0	0	0
1992/34/8.2; 1992/34/8.1	**39.1**	0	3	0	0	0	0	0	0	1	3	0	3	0	2	0	2	0	6	1	2	0	0		6	0	6	0	2	1	indet	0	0	0	0	0	0
1992/34/9.1	**29**	3	4	4	4	0	0	0	0	3	2	3	5	4	3	0	1	0	0	0	0	3	0		0	0	0	0	5	0		5	5	4	0	0	0
1992/34/9.1	**30**	3	4	2	0	0	0	0	0	3	4	1	5	2	2	1	7	0	0	0	0	2	0		0	0	1	0	3	6	indet	3	3	0	0	0	0
1992/34/9.3; 1992/34/9.2; 1992/34/9.1	**26**	4	5	2	0	0	0	0	0	2	4	1	5	3	3	1	6	1	0	0	6	3	0		0	0	0	0	4	0		5	5	2	0	0	1
2001/25/3.1	**17**	0	0	0	0	3	0	0	3	0	1	0	0	0	0	0	1	0	0	0	0	0	0		1	0	0	0	0	0		0	0	0	0	0	0
2001/25/3.3; 2001/25/3.2	**16**	0	0	0	0	2	0	0	3	0	1	0	0	0	0	0	2	0	0	0	1	0	0		1	0	0	0	0	0		0	0	0	0	0	0
2001/25/4.1	**27/29**	0	3	0	0	4	3	0	3	1	3	1	3	0	0	2	2	0	1	0	1	0	0		0	0	0	0	0	0		0	0	0	0	0	0
2001/25/4.2	**10**	0	2	0	0	0	0	0	0	3	4	2	3	0	0	1	3	0	0	0	0	1	0		0	0	0	0	0	0		0	0	0	0	0	1
2001/25/4.2; 2001/25/4.1	**12**	0	4	1	0	2	2	0	0	1	4	1	3	0	0	2	3	0	1	0	1	1	2	burned	0	0	0	0	0	0		0	0	0	0	0	0
2002/13/105.1	**37**	0	3	0	0	2	0	0	0	1	2	0	0	0	0	3	1	0	0	0	0	0	0		1	0	0	0	0	0		0	0	0	0	0	0
2002/13/105.2	**35**	2	3	0	0	3	0	0	0	1	2	0	0	0	0	1	1	0	0	0	1	1	0		2	1	0	0	0	0		0	0	0	0	0	0

sample no.	stratigrahic unit	altitude	thickness [cm]	context	microfacies type	layering	microstructure	Porosity	clay content	silt content	sand content	gravel content	reddening (gravels)	organic content	bioturbation	earthworm granules	mollusc shells	quera	sclerotia	Fe/Mn precipitations	Ca-precipitations	P-precipitations	vivianite
2002/13/105.3	**33**	254.70	6	occupation layer	5	unlayered	complexe structure	15%	5%	40%	30%	10%	none; weak; physical stress	0%	4	4	0	0	1	3	0	3	0
2002/13/106.1	**30**	254.64	6	occupation layer	5	unlayered	complexe structure	20%	5%	40%	30%	5%	none; clear; physical stress	0%	5	2	0	0	3	3	0	4	0
2002/13/106.2	**28**	254.58	6	initial trampling horizon	3	horizontal orientation	complexe structure	15%	5%	35%	30%	15%	none; weak; clear; physical stress	0%	4	3	0	0	1	3	0	3	0
2002/13/106.3; 2002/13/106.2	**25**	254.52	6	natural overbank deposit	1B	unlayered	channel and chamber structure	20%	10%	40%	28%	2%	none	0%	4	2	0	0	0	2	0	4	0
2002/13/111.1	**21**	254.47	7	initial trampling horizon	3	weak horizontal orientation	channel and chamber structure	20%	5%	40%	33%	2%	none	0%	4	3	0	0	1	3	0	3	2
2002/13/111.1	**18**	254.40	10	natural overbank deposit	1B	unlayered	channel and chamber structure	15%	10%	45%	28%	2%	none	0%	4	2	0	0	2	3	0	4	2
2002/13/112.2; 2002/13/112.1	**40**	254.50	7	ditch 9	6	weak horizontal orientation	channel and chamber structure	20%	5%	40%	30%	5%	none; weak; clear; physical stress	0%	4	3	1	3	2	5	0	4	3
2002/13/112.3	**17**	254.40	10	natural overbank deposit	1B	unlayered	complexe structure	20%	10%	35%	33%	2%	none	0%	5	2	0	0	2	3	0	4	2
2002/13/112.3; 2002/13/112.2	**39**	254.43	3	ditch 9	6	layered	channel and chamber structure	20%	5%	45%	25%	5%	none	0%	4	3	2	2	2	5	0	4	2
2002/13/114.1	**22.2**	254.64	6	initial trampling horizon	3	unlayered	complexe structure	20%	5%	35%	30%	10%	none; weak	0%	5	3	0	0	2	3	0	3	2
2002/13/114.2; 2202/13/114.1	**22.1**	254.58	4	initial trampling horizon	3	weak horizontal orientation	channel and chamber structure	15%	5%	40%	30%	10%	none; weak; clear	0%	4	3	0	0	1	4	0	4	2
2002/13/114.3; 2002/13/114.2	**8; 10**	254.54	11	natural overbank deposit	1B	unlayered	channel and chamber structure	20%	10%	40%	30%	0%		0%	4	3	1	0	3	3	0	4	2
2002/13/115.1	**6**	254.55	4	initial trampling horizon	3	weak horizontal orientation	complexe structure	20%	5%	30%	30%	15%	none; weak; physical stress	0%	5	3	0	0	0	3	0	4	0
2002/13/116.1	**15**	254.64	9	occupation layer	5	unlayered	channel and chamber structure	20%	5%	40%	30%	5%	none; clear; strong; physical stress	0%	5	2	0	0	0	2	0	3	0
2002/13/116.1; 2002/13/116.2	**7**	254.55	3	initial trampling horizon	3	weak horizontal orientation	complexe structure	20%	5%	30%	30%	15%	physical stress	0%	5	3	0	0	0	3	0	4	0
2002/13/116.2	**5.1**	254.51	7	natural overbank deposit	1B	unlayered	channel and chamber structure	20%	10%	40%	25%	5%	none; physical stress	0%	4	1	1	0	0	2	1	4	0
2002/13/116.2	**5.2**	254.52	1	natural overbank deposit	1B	unlayered	channel and chamber structure	5%	10%	45%	35%	5%	none; physical stress	0%	4	0	0	0	0	2	0	4	0

The Hidden Midden - Supplement 2: Micromorphological results

sample no.	stratigrahic unit	prop. Leucophosphite	horizontal orientation	compaction	loam chunks	dusty coatings	slaking crusts	agricutans	runoff-sediments	charcoals	micro-charcoals	charred org. remains	ashes	phytolith slags	melted quarz grains	bone frgm	bone chip	fish bone	teeth	egg shell frgm	ceramic frgm	burned loam	daub	daub preservation	iron grains	slags	flint	glass	phytoliths	coprolites	prop. Producer	dung	dung spherolites	phytolith layers	guano	avian uric acid spheres	parasite eggs
2002/13/105.3	**33**	0	0	0	0	3	0	4	0	2	3	0	1	0	0	1	1	0	0	0	0	0	1	burned	3	1	0	0	0	1	omn/carn	0	0	0	0	0	1
2002/13/106.1	**30**	0	0	0	0	3	0	3	0	2	3	0	2	0	0	1	1	0	0	0	6	7	6	burned	1	0	0	0	0	1	omn/carn	0	0	0	0	0	0
2002/13/106.2	**28**	1	4	0	0	3	0	0	0	1	3	0	1	0	0	3	2	0	0	0	0	7	0		3	0	0	0	0	1	carnivor	0	0	0	0	0	0
2002/13/106.3; 2002/13/106.2	**25**	3	0	0	0	4	3	0	0	0	6	0	0	0	0	0	6	0	0	0	6	0	0		0	0	0	0	0	0		0	0	0	0	0	0
2002/13/111.1	**21**	0	3	0	1	3	3	0	0	2	3	1	1	0	0	0	6	1	0	0	6	7	0		2	0	0	0	0	6	omn/carn	0	0	0	0	0	0
2002/13/111.1	**18**	0	0	0	0	4	0	0	0	6	8	0	0	0	0	0	6	0	0	0	6	0	0		7	0	0	0	0	0		0	0	0	0	0	0
2002/13/112.2; 2002/13/112.1	**40**	0	3	0	0	2	0	0	2	3	4	1	3	0	1	2	3	0	0	0	0	2	0		2	1	0	1	2	0		0	0	0	1	0	0
2002/13/112.3	**17**	0	0	0	0	5	0	0	0	7	8	0	0	0	0	7	6	0	0	0	6	6	0		7	0	0	0	0	6	omn/carn	0	0	0	0	0	0
2002/13/112.3; 2002/13/112.2	**39**	0	3	0	0	3	0	0	2	2	3	1	2	0	0	0	3	0	0	0	1	6	0		2	0	0	0	2	0		0	0	0	0	0	0
2002/13/114.1	**22.2**	1	2	2	0	3	0	0	0	2	2	0	0	0	1	2	3	0	0	0	1	0	0		2	0	0	0	0	1	omn/carn	0	0	0	0	0	0
2002/13/114.2; 2202/13/114.1	**22.1**	0	3	0	0	3	0	2	0	1	3	0	6	0	0	3	2	0	0	0	0	7	0		3	0	0	0	0	0		6	0	0	0	0	0
2002/13/114.3; 2002/13/114.2	**8; 10**	1	0	0	0	3	0	0	0	6	7	0	6	0	0	0	8	0	0	0	6	0	0		7	0	0	0	0	0		0	0	0	0	0	0
2002/13/115.1	**6**	0	4	0	0	3	0	0	0	1	3	0	0	0	0	3	2	0	0	0	3	7	0		0	0	0	0	0	0		0	0	0	0	0	0
2002/13/116.1	**15**	0	2	0	0	2	0	0	0	1	3	0	0	0	0	2	1	0	0	0	0	0	0		0	0	0	0	0	0		0	0	0	0	0	0
2002/13/116.1; 2002/13/116.2	**7**	0	3	0	0	3	0	0	0	1	3	0	0	0	0	2	1	0	0	0	1	7	0		0	0	0	0	0	0		0	0	0	0	0	0
2002/13/116.2	**5.1**	0	0	0	0	3	0	0	0	0	6	0	0	0	0	0	6	0	0	0	0	0	0		6	0	0	0	0	0		0	0	0	0	0	0
2002/13/116.2	**5.2**	0	0	4	0	4	3	0	0	0	6	0	0	0	0	0	6	0	0	0	0	0	0		0	0	0	0	0	0		0	0	0	0	0	0

sample no.	stratigrahic unit	altitude	thickness [cm]	context	microfacies type	layering	microstructure	Porosity	clay content	silt content	sand content	gravel content	reddening (gravels)	organic content	bioturbation	earthworm granules	mollusc shells	quera	sclerotia	Fe/Mn precipitations	Ca-precipitations	P-precipitations	vivianite
2002/13/118.1	**8**	254.60	5	occupation layer	5	unlayered	channel and chamber structure	15%	5%	40%	35%	5%	none	0%	5	0	0	0	1	3	0	3	3
2002/13/118.1	**6**	254.55	5	initial trampling horizon	3	weak horizontal orientation	complexe structure	20%	5%	30%	30%	15%	physical stress	0%	5	3	0	0	1	4	0	3	2
2002/13/118.2	**4**	254.50	6	natural overbank deposit	1B	unlayered	channel and chamber structure	20%	10%	45%	25%	0%		0%	4	0	0	0	0	4	1	3	2
2002/13/119.1	**5**	254.54	7	initial trampling horizon	3	unlayered	channel and chamber structure	15%	5%	35%	30%	15%	clear; physical stress	0%	5	2	0	1	2	4	0	4	0
2002/13/120.1	**6**	254.56	8	initial trampling horizon	3	unlayered	channel and chamber structure	15%	5%	35%	30%	15%	clear; physical stress	0%	5	2	0	0	2	4	0	4	4
2002/13/134.1	**20**	254.52	9	ditch 4	7	unlayered	bridged grain structure	15%	0%	20%	40%	25%	none; weak	0%	4	2	0	2	0	0	2	3	0
2002/13/134.1	**19**	254.43	5	ditch 4	7	layered	single grain structure	30%	0%	0%	65%	5%	none; weak	0%	3	2	0	0	0	0	0	0	0
2002/13/135.1	**14**	254.44	5	ditch 4	7	unlayered	bridged grain structure	20%	0%	20%	50%	10%	none; weak	0%	4	2	0	0	0	2	1	3	2
2002/13/135.2; 2002/13/135.1	**12**	254.39	7	ditch 4	7	layered	single grain structure	30%	0%	0%	70%	5%	none; weak	0%	4	2	0	0	0	3	0	3	2
2002/13/135.3	**5**	254.26	8	ditch 4	7	unlayered	channel and chamber structure	15%	0%	25%	35%	25%	none; weak; physical stress	0%	4	0	0	3	0	0	0	3	1
2002/13/135.3; 2002/13/135.2	**11**	254.32	6	ditch 4	7	layered	channel and chamber structure	20%	0%	35%	45%	0%		0%	4	2	0	2	0	3	1	4	2
2002/13/136.1	**60**			pit 400	8	laminated	channel and chamber structure													0			
2002/13/140.1	**56**			pit 400	8	laminated	channel and chamber structure													0			
2002/13/140.1	**64**			pit 400	8	laminated	channel and chamber structure													0			
2002/13/141.1	**59**			pit 400	8	laminated	channel and chamber structure													0			
2002/13/141.2; 2002/13/141.1	**58**			pit 400	8	laminated	channel and chamber structure													2			
2002/13/143.1	**40**			pit 400	8	laminated	channel and chamber structure													0			

The Hidden Midden - Supplement 2: Micromorphological results

sample no.	stratigrahic unit	prop. Leucophosphite	horizontal orientation	compaction	loam chunks	dusty coatings	slaking crusts	agricutans	runoff-sediments	charcoals	micro-charcoals	charred org. remains	ashes	phytolith slags	melted quarz grains	bone frgm	bone chip	fish bone	teeth	egg shell frgm	ceramic frgm	burned loam	daub	daub preservation	iron grains	slags	flint	glass	phytoliths	coprolites	prop. Producer	dung	dung spherolites	phytolith layers	guano	avian uric acid spheres	parasite eggs
2002/13/118.1	8	0	2	0	0	1	0	0	0	0	3	0	0	0	0	0	1	0	0	0	6	0	0		6	0	0	0	0	0		0	0	0	0	0	0
2002/13/118.1	6	0	4	0	0	2	0	0	0	1	3	0	1	0	0	6	7	0	0	0	0	0	0		0	0	0	0	0	0		0	0	0	0	0	0
2002/13/118.2	4	0	0	0	0	2	0	0	0	6	7	0	0	0	0	6	6	0	0	0	0	0	0		0	0	0	0	0	6	indet	0	0	0	0	0	0
2002/13/119.1	5	0	3	0	0	2	0	0	0	1	3	0	0	0	0	2	1	0	0	0	6	1	0		6	0	0	0	0	0		0	0	0	0	0	0
2002/13/120.1	6	0	3	0	0	2	0	0	0	1	3	0	0	0	0	0	6	0	0	0	0	0	0		0	0	1	0	0	0		0	0	0	0	0	0
2002/13/134.1	20	0	3	0	0	5	0	0	0	2	2	0	0	0	0	0	1	0	0	0	0	0	0		2	0	0	0	0	6	omn/carn	0	0	0	0	0	0
2002/13/134.1	19	0	0	2	0	0	0	0	0	7	7	0	0	0	0	6	7	0	0	0	6	6	0		0	0	0	0	0	0		0	0	0	0	0	0
2002/13/135.1	14	0	3	0	0	5	0	0	0	2	2	0	0	0	0	0	1	0	0	0	0	0	0		0	0	0	0	0	6	omn/carn	0	0	0	0	0	0
2002/13/135.2; 2002/13/135.1	12	0	0	0	0	4	0	0	0	8	2	0	7	0	0	6	2	0	0	0	0	0	0		6	6	0	0	0	7	omn/carn	0	0	0	0	0	0
2002/13/135.3	5	0	3	0	0	3	0	0	0	7	2	0	0	0	0	0	1	0	0	0	0	0	0		0	0	0	0	0	0		0	0	0	0	0	0
2002/13/135.3; 2002/13/135.2	11	0	0	0	0	3	0	0	0	7	2	0	0	0	0	0	2	0	0	0	0	1	0		0	0	0	0	0	7	omn/carn	0	0	0	0	0	0
2002/13/136.1	60					0	0			3	4	1	5			0	3	0	0			0	0		0	0				0	omn/carn	0	0		0	0	
2002/13/140.1	56					1	0			3	4	2	5			1	3	0	0			0	0		1	0				0	omn/carn	0	0		0	0	
2002/13/140.1	64					1	0			3	3	1	5			0	2	0	0			1	0		0	0				0	omn/carn	0	0		0	0	
2002/13/141.1	59					0	0			3	4	1	5			2	3	0	0			2	0		0	0		3		0		0	0		4	2	
2002/13/141.2; 2002/13/141.1	58					0	0			3	4	1	5			3	3	0	2			2	1		0	0		3		0	omn/carn	0	0		2	2	
2002/13/143.1	40					0	0			4	4	1	5			4	3	0	0			3	0		1	0		2		0		0	0		4	3	

The Hidden Midden - Supplement 2: Micromorphological results

sample no.	stratigrahic unit	altitude	thickness [cm]	context	microfacies type	layering	microstructure	Porosity	clay content	silt content	sand content	gravel content	reddening (gravels)	organic content	bioturbation	earthworm granules	mollusc shells	quera	sclerotia	Fe/Mn precipitations	Ca-precipitations	P-precipitations	vivianite
2002/13/143.2	**25a**			pit 400	8	laminated	channel and chamber structure													0			
2002/13/144.2; 2002/13/144.1	**19**			pit 400	8	laminated	channel and chamber structure													0			
2002/13/76.1	**9**	254.66	6	initial trampling horizon	3	horizontal orientation	complexe structure	20%	5%	35%	30%	10%	none; weak; clear; physical stress	0%	4	2	1	0	1	4	0	3	0
2002/13/76.2; 2002/13/76.1	**6**	254.61	6	natural overbank deposit	1B	unlayered	channel and chamber structure	20%	10%	40%	28%	2%	none	0%	4	2	0	0	1	3	0	3	2
2002/13/77.1	**25**			modern plough horizon	11	unlayered	channel and chamber structure	20%	5%	35%	30%	10%	none	0%	5	0	0	0	2	4	0	1	0
2002/13/77.2	**23.1**	254.78	3	occupation layer	4	unlayered	complexe structure	20%	5%	35%	30%	10%	none; clear; physical stress	0%	5	1	0	0	1	3	0	2	0
2002/13/77.2	**23.2**	254.81	3	occupation layer	4	unlayered	complexe structure	20%	5%	30%	30%	15%	none; clear; physical stress	0%	5	3	1	0	3	3	0	2	0
2002/13/77.2; 2002/13/77.1	**24**	254.87	6	gravel layer	10	horizontal orientation	channel and chamber structure	20%	5%	30%	25%	20%	none; weak; physical stress	0%	5	3	0	0	3	3	1	1	0
2002/13/77.3	**12**	254.75	9	occupation layer	4	unlayered	complexe structure	20%	5%	40%	30%	5%	none; clear; physical stress	0%	5	3	0	0	3	3	0	3	0
2002/13/92.2	**7**	254.67	7	initial trampling horizon	3	weak horizontal orientation	channel and chamber structure	20%	5%	35%	38%	2%	none; weak; clear; physical stress	0%	4	3	0	1	2	4	0	4	1
2002/13/92.2	**8**	254.72	5	occupation layer	4	weak horizontal orientation	channel and chamber structure	20%	5%	30%	35%	10%	none; weak; clear; physical stress	0%	4	3	0	0	1	4	0	4	1
2002/13/92.2	**6**	254.60	5	natural overbank deposit	1B	unlayered	channel and chamber structure	20%	10%	40%	28%	2%	none	0%	4	3	0	2	1	3	0	4	0
2002/13/93.1	**15**	254.87	4	occupation layer	4	weak horizontal orientation	complexe structure	20%	5%	35%	30%	10%	none	0%	5	3	0	1	3	4	0	1	1
2002/13/93.1	**16**			occupation layer	4	weak horizontal orientation	complexe structure	20%	5%	25%	25%	25%	none	0%	5	2	0	0	3	3	0	1	0
2002/13/93.2	**11**	254.83	6	gravel layer	10	horizontal orientation	complexe structure	20%	5%	25%	20%	30%	none; physical stress	0%	5	3	0	1	2	4	0	2	2
2002/13/93.2	**9**	254.77	5	occupation layer	4	weak horizontal orientation	complexe structure	20%	5%	35%	38%	2%	none; weak; clear	0%	5	2	0	0	0	4	1	3	2

sample no.	stratigrahic unit	prop. Leucophosphite	horizontal orientation	compaction	loam chunks	dusty coatings	slaking crusts	agricutans	runoff-sediments	charcoals	micro-charcoals	charred org. remains	ashes	phytolith slags	melted quarz grains	bone frgm	bone chip	fish bone	teeth	egg shell frgm	ceramic frgm	burned loam	daub	daub preservation	iron grains	slags	flint	glass	phytoliths	coprolites	prop. Producer	dung	dung spherolites	phytolith layers	guano	avian uric acid spheres	parasite eggs
2002/13/143.2	**25a**					0	0			4	4	2	5			3	3	0	0			1	0		0	0		0		0		0			0	2	
2002/13/144.2; 2002/13/144.1	**19**					0	0			3	4	1	5			3	3	0	0			1	0		0	0		3		0		0	0		2	4	
2002/13/76.1	**9**	0	3	0	0	3	0	0	0	1	2	0	0	0	0	1	3	0	0	0	1	7	0		2	0	0	0	0	1	carnivor	0	0	0	0	0	0
2002/13/76.2; 2002/13/76.1	**6**	0	0	0	0	3	0	0	0	6	7	0	0	0	0	0	6	0	0	0	6	0	0		7	8	0	0	0	6	omn/carn	0	0	0	0	0	0
2002/13/77.1	**25**	0	0	0	0	0	0	0	0	0	1	0	0	0	0	0	6	0	0	0	0	6	0		0	0	0	0	0	0		0	0	0	0	0	0
2002/13/77.2	**23.1**	2	3	0	1	3	2	3	0	2	2	0	0	0	0	1	1	0	0	0	0	6	0		2	0	0	0	0	0		0	0	0	0	0	0
2002/13/77.2	**23.2**	0	4	0	1	3	1	3	0	2	2	0	0	0	0	2	2	0	0	0	0	6	0		3	0	0	0	0	0		0	0	0	0	0	0
2002/13/77.2; 2002/13/77.1	**24**	0	4	0	0	2	0	0	0	1	2	0	0	0	0	1	1	0	0	0	2	6	0		2	0	0	0	0	0		0	0	0	0	0	0
2002/13/77.3	**12**	0	2	0	1	3	0	3	0	2	2	0	0	0	0	1	2	0	0	0	6	8	0		2	0	0	0	0	0		0	0	0	0	0	1
2002/13/92.2	**7**	0	2	0	0	3	0	0	0	1	2	0	0	0	0	0	2	0	0	0	0	7	0		2	0	0	0	0	0		0	0	0	0	0	0
2002/13/92.2	**8**	0	3	0	0	2	0	0	0	1	2	0	0	0	0	1	1	0	0	0	0	7	0		2	0	0	0	0	0		0	0	0	0	0	0
2002/13/92.2	**6**	0	0	0	0	3	0	0	0	0	7	0	0	0	0	0	6	0	0	0	0	0	0		6	0	0	0	0	0		0	0	0	0	0	0
2002/13/93.1	**15**	0	3	0	0	3	0	0	0	1	1	0	0	0	0	0	8	0	6	0	6	0	0		2	0	0	0	0	0		0	0	0	0	0	0
2002/13/93.1	**16**	0	3	0	0	2	0	0	0	1	1	0	0	0	0	0	1	0	0	0	0	0	0		1	0	0	0	0	0		0	0	0	0	0	0
2002/13/93.2	**11**	0	4	0	0	3	0	0	0	1	2	0	0	0	0	0	7	0	0	0	7	0	0		1	0	0	0	0	0		0	0	0	0	0	0
2002/13/93.2	**9**	0	2	0	0	3	0	0	0	1	2	0	0	0	0	0	7	0	0	0	6	0	0		0	0	0	0	0	0		0	0	0	0	0	0

The Hidden Midden - Supplement 2: Micromorphological results

Quantity		Quality	
0	absent	0	none
1	single	1	poorly
2	few	2	weak
3	frequent	3	clear
4	numerous	4	strong
5	dominant	5	intense

Contextualising the Dead - Supplement 1: Histotaphonomic data

sample no. (italic) / thin section no.	excavation	structure ID	sample size	sample type	archaeological feature	sediment type	sediment components	$CaCO_3$ content	WTI	BAI	CAI	CRI	COI	HEI
1990/32/2.1	1990/32	pit 283	small frgm.	prob. animal	pit	TSM	CH; AS	+++	5	5	5	4	2	0
1990/32/2.1	1990/32	pit 283	bone chip	prob. animal	pit	TSM	CH; AS	+++	4	3	5	5	3	1
1990/32/2.1	1990/32	pit 283	bone chip	prob. animal	pit	TSM	CH; AS	+++	4	5	5	5	1	2.5
1990/32/2.1	1990/32	pit 283	small frgm.	Tooth	pit	TSM	CH; AS	+++	5	3	5	5	3	-
1990/32/3.1	1990/32	pit 283	small frgm.	prob. animal	pit	TSM	CH	++	4	5	5	4	3	1
1990/32/3.1	1990/32	pit 283	small frgm.	Tooth	pit	TSM	CH	++	5	5	5	5	1	2
1990/32/4.1	1990/32	pit 283	small frgm.	prob. animal	pit	TSM	CH	++	5	5	5	4	3	1
1990/32/5.1	1990/32	pit 283	small frgm.	prob. animal	pit	TSM	CH	++	4	2	5	5	4	0
1990/32/5.2	1990/32	pit 283	bone chip	prob. animal	pit	TSM	CH; AS	+++	5	5	5	4	4	1
1990/32/5.2	1990/32	pit 283	small frgm.	prob. animal	pit	TSM	CH; AS	+++	5	5	5	5	3	1
1990/32/5.2	1990/32	pit 283	bone chip	prob. animal	pit	TSM	CH; AS	+++	4	5	5	4	2	1.5
1990/32/9.1	1990/32	pit 283	bone chip	prob. animal	pit	TSM	CH; AS	+++	4	5	5	4	3	1
1990/32/9.2	1990/32	pit 283	small frgm.	prob. animal	pit	TSM	CH; AS	+++	5	2	5	3	-	1
1990/42/10.1	1990/42	layer 010.3	bone chip	prob. animal	trampled surface	LC	FMC	++	5	4	5	4	2	0
1990/42/10.1a	1990/42	layer 010.3	small frgm.	prob. animal	trampled surface	LC	FMC	++	5	1	5	4	2	0.5
1990/42/14	1990/42	layer 211.3	small frgm.	prob. animal	trampled surface	LC	FMC	++	2	4	5	5	4	0
1990/42/16.2	1990/42	pit 287	small frgm.	prob. animal	pit	TSM	CH	++	4	5	5	3	3	2
1990/42/18	1990/42	pit 287	small frgm.	prob. animal	pit	TSM	AS	+++	5	5	5	4	3	2
1990/42/18	1990/42	pit 287	small frgm.	prob. animal	pit	TSM	AS	+++	5	5	5	3	1	2.5
1992/34/1	1992/34	layer 013.15	big frgm.	prob. animal	post hole	TSM	FMC	-	4	1	5	5	2	1
1992/34/16a	1992/34	pit 302	bone chip	prob. animal	pit	TSM	AS	+++	3	5	5	5	4	0
1992/34/16a	1992/34	pit 302	bone chip	prob. animal	pit	TSM	AS	+++	5	5	5	4	1	2
1992/34/3.2	1992/34	layer 058.4	small frgm.	prob. animal	trampled surface	LC	FMC	++	3	4	5	5	4	0
1992/34/3.2	1992/34	layer 058.4	small frgm.	prob. animal	trampled surface	LC	FMC	++	4	5	5	4	3	0.5
1992/34/3.2	1992/34	layer 058.4	small frgm.	prob. animal	trampled surface	LC	FMC	++	4	5	5	5	2	1
1992/34/3.2	1992/34	layer 058.4	small frgm.	prob. animal	trampled surface	LC	FMC	++	5	5	5	4	3	2
1992/34/3.3	1992/34	layer 058.3	small frgm.	prob. animal	trampled surface	LC	FMC	++	3	5	5	5	2	0.5
1992/34/5	1992/34	pit 302	bone chip	prob. animal	pit	TSM	CH	++	5	5	5	5	5	0
1992/34/5	1992/34	pit 302	small frgm.	prob. animal	pit	TSM	CH	++	5	5	5	3	3	0.5
1992/34/7.2	1992/34	pit 302	bone chip	prob. animal	pit	TSM	CH	++	5	5	5	5	5	0.5
1992/34/7.2	1992/34	pit 302	bone chip	prob. animal	pit	TSM	CH	++	4	5	5	4	1	1.5
1992/34/8.1	1992/34	pit 302	small frgm.	prob. animal	pit	TSM	CH; AS	+++	5	5	4	5	1	0.5
1992/34/8.1	1992/34	pit 302	small frgm.	prob. animal	pit	TSM	CH; AS	+++	5	5	5	3	1	0.5
1992/34/9.1	1992/34	pit 302	small frgm.	prob. animal	pit	TSM	AS	+++	5	5	5	5	3	0.5
1993/13/1.1	1993/13	pit 305	bone chip	prob. animal	pit	TSM	CH; AS	+++	4	5	5	5	3	1
1993/13/1.1	1993/13	pit 305	small frgm.	prob. animal	pit	TSM	CH; AS	+++	4	5	3	2	2	2
1993/13/1.2	1993/13	pit 305	bone chip	prob. animal	pit	TSM	CH; AS	+++	5	5	5	5	2	1.5
1993/13/1.3	1993/13	pit 305	small frgm.	prob. animal	pit	TSM	CH; AS	+++	5	5	5	5	4	0
1993/13/1.3	1993/13	pit 305	bone chip	prob. animal	pit	TSM	CH; AS	+++	5	5	5	4	3	1
1993/13/2.1	1993/13	pit 305	small frgm.	prob. animal	pit	TSM	CH; AS	+++	5	1	5	5	3	0
1993/13/3.4	1993/13	pit 305	bone chip	prob. animal	pit	TSM	CH; AS	+++	4	5	5	5	4	1
1996/01/1	1996/01	pit 321	small frgm.	prob. animal	pit	TSM	CH	+	5	0	5	5	2	0
1996/01/1	1996/01	pit 321	small frgm.	prob. animal	pit	TSM	CH	+	3	3	5	5	1	0
1996/01/2.0	1996/01	pit 321	small frgm.	prob. animal	pit	TSM	CH	+	5	5	5	4	4	1
1996/01/2.1	1996/01	pit 321	small frgm.	prob. animal	pit	TSM	CH	+	4	5	5	5	3	0.5
1996/01/3.1	1996/01	pit 321	small frgm.	Tooth	pit	TSM	CH	++	5	5	5	5	-	0
1996/01/3.1	1996/01	pit 321	small frgm.	prob. animal	pit	TSM	CH	++	4	4	5	4	3	0.5
1996/01/3.2	1996/01	pit 321	small frgm.	prob. animal	pit	TSM	CH	++	5	5	5	5	1	2
1996/01/3.3	1996/01	pit 321	small frgm.	prob. animal	pit	TSM	CH	++	5	5	5	5	4	0.5
1996/01/3.3	1996/01	pit 321	bone chip	prob. animal	pit	TSM	CH	++	5	2	5	5	1	0.5
1996/01/3.3	1996/01	pit 321	small frgm.	prob. animal	pit	TSM	CH	++	5	5	5	5	4	1
1996/01/3.3	1996/01	pit 321	bone chip	prob. animal	pit	TSM	CH	++	5	5	3	5	-	2
1996/01/5.1	1996/01	pit 321	bone chip	prob. animal	pit	TSM	CH	+	4	5	5	5	3	1
1996/01/7.2	1996/01	pit 321	bone chip	prob. animal	pit	TSM	CH	++	5	5	5	5	2	2.5
2001/25/3.2	2001/25	ditch 1	small frgm.	prob. animal	ditch	LC	FMC	++	5	5	5	5	5	0
2001/25/3.2	2001/25	ditch 1	bone chip	prob. animal	ditch	LC	FMC	++	5	5	5	5	5	0
2001/25/3.3	2001/25	ditch 1	bone chip	prob. animal	ditch	LC	FMC	++	5	5	5	5	5	0
2001/25/4.1	2001/25	pit 386	small frgm.	prob. animal	pit	TSM	CH; AS	++	5	1	5	5	5	0
2001/25/4.1	2001/25	pit 386	bone chip	prob. animal	pit	TSM	CH; AS	++	5	5	5	4	3	0
2001/25/4.1	2001/25	ditch 1	small frgm.	Tooth	ditch	TSM	FMC	++	4	5	5	3	3	0.5
2001/25/4.1	2001/25	ditch 1	bone chip	prob. animal	ditch	TSM	FMC	++	5	5	5	5	2	2
2001/25/4.1	2001/25	pit 386	bone chip	prob. animal	pit	TSM	CH; AS	++	5	5	5	4	1	2
2001/25/4.1	2001/25	ditch 1	bone chip	prob. animal	ditch	TSM	FMC	++	4	5	5	5	3	3
2001/25/4.2	2001/25	pit 386	small frgm.	prob. animal	pit	TSM	CH; AS	+++	5	1	5	5	5	0
2001/25/4.2	2001/25	pit 386	bone chip	prob. animal	pit	TSM	CH; AS	+++	5	5	5	4	3	0.5
2001/25/4.2	2001/25	pit 386	small frgm.	prob. animal	pit	TSM	CH; AS	+++	5	5	3	5	3	1
2001/25/4.2	2001/25	pit 386	small frgm.	Tooth	pit	TSM	CH; AS	+++	5	5	5	5	2	1.5
2001/25/4.2	2001/25	pit 386	big frgm.	prob. animal	pit	TSM	CH; AS	+++	5	5	5	4	1	3
2002/13/10.1	2002/13	layer 205.28	small frgm.	prob. animal	trampled surface	LB	FMC	-	5	1	5	5	4	0
2002/13/10.3	2002/13	layer 205.24	bone chip	prob. animal	bedrock bioturbated	LC		-	5	2	5	5	3	0
2002/13/105.1	2002/13	layer 888.37	small frgm.	prob. animal	trampled surface	LB	FMC	-	5	3	5	5	3	0
2002/13/105.1	2002/13	layer 888.37	small frgm.	prob. animal	trampled surface	LB	FMC	-	5	2	5	5	3	0
2002/13/105.1	2002/13	layer 888.37	bone chip	prob. animal	trampled surface	LB	FMC	-	3	5	5	4	2	0
2002/13/105.2	2002/13	layer 888.35	bone chip	prob. animal	trampled surface	LB	FMC	-	0	5	5	5	2	0
2002/13/105.3	2002/13	layer 888.33	small frgm.	prob. animal	trampled surface	LB	FMC	+	5	5	5	3	2	0.5
2002/13/105.3	2002/13	layer 888.33	bone chip	prob. animal	trampled surface	LB	FMC	+	5	5	5	3	2	1.5
2002/13/106.1	2002/13	layer 888.30	bone chip	prob. animal	trampled surface	LB	FMC	+	5	5	5	4	4	0
2002/13/106.1	2002/13	layer 888.30	small frgm.	prob. animal	trampled surface	LB	FMC	+	2	4	5	5	3	0
2002/13/106.1	2002/13	layer 888.30	bone chip	prob. animal	trampled surface	LB	FMC	+	0	5	5	4	1	0
2002/13/106.2	2002/13	layer 888.28	bone chip	prob. animal	trampled surface	LB	FMC	+	4	5	5	5	4	0
2002/13/106.2	2002/13	layer 888.28	big frgm.	prob. animal	trampled surface	LB	FMC	+	2	3	5	5	2	0
2002/13/106.2	2002/13	layer 888.28	bone chip	prob. animal	trampled surface	coprolite	coprolite	-	5	5	5	4	2	0
2002/13/106.2	2002/13	layer 888.28	big frgm.	prob. animal	trampled surface	LB	FMC	+	5	2	5	5	1	0
2002/13/106.2	2002/13	layer 888.28	small frgm.	prob. animal	trampled surface	LB	FMC	+	5	5	4	4	1	0
2002/13/11.1	2002/13	layer 205.35	small frgm.	prob. animal	trampled surface	LB	FMC	-	3	5	5	5	1	0.5
2002/13/11.2	2002/13	layer 205.23	small frgm.	prob. animal	trampled surface	LB	FMC	-	4	5	5	5	2	2
2002/13/111.1	2002/13	layer 957.21	big frgm.	prob. animal	trampled surface	LB	FMC	-	3	5	5	5	2	0.5
2002/13/112.1	2002/13	ditch 9	small frgm.	prob. animal	ditch	TSM	FMC	+	5	5	4	4	2	0
2002/13/112.1	2002/13	ditch 9	bone chip	prob. animal	ditch	TSM	FMC	+	5	4	5	4	3	0.5
2002/13/112.1	2002/13	ditch 9	bone chip	prob. animal	ditch	TSM	FMC	+	5	5	5	3	3	0.5
2002/13/112.1	2002/13	ditch 9	small frgm.	prob. animal	ditch	TSM	FMC	+	4	5	5	5	2	0.5
2002/13/112.2	2002/13	ditch 9	bone chip	prob. animal	ditch	TSM	FMC	+	5	5	5	4	4	0
2002/13/112.3	2002/13	ditch 9	small frgm.	prob. animal	ditch	TSM	FMC	+	4	5	5	5	4	0
2002/13/112.3	2002/13	ditch 9	bone chip	prob. animal	ditch	TSM	FMC	+	0	5	5	5	3	0
2002/13/112.3	2002/13	ditch 9	bone chip	prob. animal	ditch	TSM	FMC	+	3	5	5	4	3	0.5
2002/13/112.3	2002/13	ditch 9	bone chip	prob. animal	ditch	TSM	FMC	+	2	5	5	5	1	2.5
2002/13/114.1	2002/13	layer 868.22	small frgm.	prob. animal	trampled surface	LB	FMC	+	4	5	5	4	3	0.5
2002/13/114.1	2002/13	layer 868.22	big frgm.	prob. animal	trampled surface	LB	FMC	+	4	5	5	5	2	0.5
2002/13/114.2	2002/13	layer 868.22	bone chip	prob. animal	trampled surface	LB	FMC	+	5	5	5	5	1	1
2002/13/114.3	2002/13	layer 868.10	bone chip	prob. animal	trampled surface	LB	FMC	-	1	4	5	5	2	0
2002/13/115.1	2002/13	layer 1007.6	small frgm.	prob. animal	trampled surface	LB	FMC	-	2	3	5	5	2	0
2002/13/115.1	2002/13	layer 1007.6	small frgm.	prob. animal	trampled surface	LB	FMC	-	3	4	5	4	1	0
2002/13/116.1	2002/13	layer 1007.15	small frgm.	prob. animal	trampled surface	LB	FMC	-	2	4	5	5	2	0.5
2002/13/116.1	2002/13	layer 1007.15	small frgm.	prob. animal	trampled surface	LB	FMC	-	5	5	5	3	2	0.5
2002/13/118.2	2002/13	layer 1025.4	small frgm.	prob. animal	trampled surface	LB	FMC	-	3	5	5	4	2	2
2002/13/119.1	2002/13	layer 895.5	big frgm.	prob. animal	trampled surface	LB	FMC	+	3	5	5	3	3	0
2002/13/119.1	2002/13	layer 895.5	small frgm.	prob. animal	trampled surface	LB	FMC	+	5	2	5	4	1	0.5
2002/13/123.1	2002/13	layer 1024.5	small frgm.	prob. animal	trampled surface	LB	FMC	-	2	5	5	5	3	0
2002/13/123.1	2002/13	layer 1024.5	big frgm.	prob. animal	trampled surface	LB	FMC	-	4	5	5	5	2	1.5
2002/13/123.1	2002/13	layer 1024.5	small frgm.	prob. animal	trampled surface	LB	FMC	-	5	5	5	5	1	3

Contextualising the Dead - Supplement 1: Histotaphonomic data

2002/13/126.1	2002/13	pit 394	small frgm.	prob. animal	pit	TSM	CH	++	5	5	5	5	4	0
2002/13/126.1	2002/13	pit 394	small frgm.	prob. animal	pit	TSM	CH	++	4	5	5	3	1	2
2002/13/126.2	2002/13	pit 394	big frgm.	prob. animal	pit	TSM	CH	++	5	5	4	5	4	0.5
2002/13/129.1	2002/13	pit 394	small frgm.	prob. animal	pit	TSM	CH	++	5	5	5	5	5	0
2002/13/132.1	2002/13	pit 394	big frgm.	prob. animal	pit	TSM	CH	++	5	5	4	5	3	1.5
2002/13/132.1	2002/13	pit 394	small frgm.	prob. animal	pit	TSM	CH	++	5	5	5	4	2	1.5
2002/13/132.1	2002/13	pit 394	big frgm.	prob. animal	pit	TSM	CH	++	4	5	5	3	1	2
2002/13/135.1	2002/13	ditch 4	bone chip	prob. animal	ditch	TSM	FMC	+	3	5	5	4	3	0
2002/13/135.1	2002/13	ditch 4	bone chip	prob. animal	ditch	TSM	FMC	+	4	5	5	5	3	0.5
2002/13/14.3	2002/13	layer 213.32	small frgm.	prob. animal	trampled surface	LB	FMC	-	3	5	5	3	2	0.5
2002/13/14.3	2002/13	layer 213.32	small frgm.	prob. animal	trampled surface	LB	FMC	-	5	5	5	5	3	2.5
2002/13/141.1	2002/13	pit 400	bone chip	prob. animal	pit	TSM	CH	++	4	5	5	5	4	0.5
2002/13/141.2	2002/13	pit 400	big frgm.	prob. animal	pit	TSM	CH	++	5	5	5	4	4	0
2002/13/141.2	2002/13	pit 400	big frgm.	prob. animal	pit	TSM	CH	++	4	5	5	5	3	1
2002/13/143.1	2002/13	pit 400	small frgm.	prob. animal	pit	TSM	CH	++	5	5	5	4	4	0.5
2002/13/143.1	2002/13	pit 400	small frgm.	prob. animal	pit	TSM	CH	++	5	5	5	5	2	1
2002/13/143.1	2002/13	pit 400	small frgm.	prob. animal	pit	TSM	CH	++	4	5	5	4	3	2
2002/13/143.1	2002/13	pit 400	small frgm.	prob. animal	pit	TSM	CH	++	5	5	5	4	2	2.5
2002/13/143.2	2002/13	pit 400	small frgm.	prob. animal	pit	TSM	CH	++	5	5	5	5	4	0.5
2002/13/143.2	2002/13	pit 400	small frgm.	prob. animal	pit	TSM	CH	++	5	5	5	5	3	0.5
2002/13/143.2	2002/13	pit 400	small frgm.	prob. animal	pit	TSM	CH	++	5	5	5	3	1	2
2002/13/20.1	2002/13	layer 199.32	small frgm.	prob. animal	trampled surface	LB	FMC	-	3	0	5	5	4	0
2002/13/20.1	2002/13	layer 199.32	bone chip	prob. animal	trampled surface	LB	FMC	-	5	5	5	2	1	2.5
2002/13/20.3	2002/13	layer 199.25	big frgm.	prob. animal	trampled surface	LB	FMC	-	3	5	5	5	5	1
2002/13/24.2	2002/13		small frgm.	prob. animal	bedrock bioturbated	LB		-	5	3	5	5	5	0
2002/13/26.4	2002/13	layer 256.7	big frgm.	prob. animal	trampled surface	LB	FMC	-	3	5	4	5	2	1.5
2002/13/26.4	2002/13	layer 256.7	small frgm.	prob. animal	trampled surface	LB	FMC	-	3	5	5	3	2	1.5
2002/13/26.5	2002/13	layer 256.6	big frgm.	prob. animal	trampled surface	LB	FMC	-	2	3	5	5	2	0
2002/13/26.5	2002/13	layer 256.6	big frgm.	prob. animal	trampled surface	LB	FMC	-	2	4	5	4	2	1.5
2002/13/32.1	2002/13	depression 1	bone chip	prob. animal	shallow pit	TSM	CH; AS	+++	5	5	5	5	5	0
2002/13/32.1	2002/13	depression 1	bone chip	prob. animal	shallow pit	TSM	CH; AS	+++	5	0	5	5	4	0
2002/13/32.1	2002/13	depression 1	bone chip	prob. animal	shallow pit	TSM	CH; AS	+++	5	2	5	5	3	0.5
2002/13/32.1	2002/13	depression 1	bone chip	prob. animal	shallow pit	TSM	CH; AS	+++	5	5	5	3	4	1
2002/13/32.1	2002/13	depression 1	small frgm.	prob. animal	shallow pit	TSM	CH; AS	+++	5	5	5	5	3	1
2002/13/32.1	2002/13	depression 1	small frgm.	prob. animal	shallow pit	TSM	CH; AS	+++	4	5	5	4	3	2
2002/13/32.1	2002/13	depression 1	bone chip	prob. animal	shallow pit	TSM	CH; AS	+++	5	5	5	5	1	3
2002/13/32.2	2002/13	depression 1	bone chip	prob. animal	shallow pit	TSM	CH; AS	+++	5	5	5	5	5	0
2002/13/32.2	2002/13	depression 1	bone chip	prob. animal	shallow pit	TSM	CH; AS	+++	5	5	5	5	5	0
2002/13/32.2	2002/13	depression 1	bone chip	prob. animal	shallow pit	TSM	CH; AS	+++	5	5	4	4	2	1
2002/13/32.2	2002/13	depression 1	bone chip	prob. animal	shallow pit	TSM	CH; AS	+++	5	5	5	5	1	1
2002/13/32.2	2002/13	depression 1	small frgm.	prob. animal	shallow pit	TSM	CH; AS	+++	5	1	5	4	3	1.5
2002/13/32.3	2002/13	depression 1	bone chip	prob. animal	shallow pit	TSM	CH; AS	+++	5	5	5	5	5	0
2002/13/32.3	2002/13	depression 1	small frgm.	prob. animal	shallow pit	TSM	CH; AS	+++	5	5	5	5	5	0
2002/13/46.1	2002/13	pit 396	small frgm.	prob. animal	pit	TSM	CH	++	5	5	4	4	4	0
2002/13/46.1	2002/13	pit 396	small frgm.	prob. animal	pit	TSM	CH	++	4	5	5	3	4	0.5
2002/13/46.1	2002/13	pit 396	small frgm.	prob. animal	pit	TSM	CH	++	4	5	5	4	2	0.5
2002/13/47.1	2002/13	pit 396	small frgm.	prob. animal	pit	TSM	CH	++	5	5	5	3	3	0
2002/13/55.1	2002/13	layer 468.7	bone chip	prob. animal	trampled surface	LB	FMC	-	3	5	5	5	3	0.5
2002/13/55.1	2002/13	layer 468.7	small frgm.	prob. animal	trampled surface	LB	FMC	-	3	5	5	5	3	0.5
2002/13/55.1	2002/13	layer 468.7	big frgm.	prob. animal	trampled surface	LB	FMC	-	3	3	5	4	2	0.5
2002/13/66.1	2002/13	layer 560.4	small frgm.	prob. animal	trampled surface	LB	FMC	-	4	5	3	4	4	0
2002/13/67.1	2002/13	layer 560.26	small frgm.	prob. animal	trampled surface	LB	FMC	-	4	1	5	5	2	0
2002/13/67.1	2002/13	layer 560.26	small frgm.	prob. animal	trampled surface	LB	FMC	-	5	3	5	4	2	0
2002/13/67.1	2002/13	layer 560.26	small frgm.	prob. animal	trampled surface	LB	FMC	-	4	2	5	4	1	0
2002/13/76.1	2002/13	layer 710.9	bone chip	prob. animal	trampled surface	LB	FMC	-	5	5	5	4	4	0
2002/13/76.1	2002/13	layer 710.9	bone chip	prob. animal	trampled surface	LB	FMC	-	3	5	5	4	4	0
2002/13/76.1	2002/13	layer 710.9	small frgm.	prob. animal	trampled surface	LB	FMC	-	4	5	5	5	3	0
2002/13/77.2	2002/13	layer 710.23	big frgm.	prob. animal	trampled surface	LB	FMC	-	3	5	5	5	4	0
2002/13/77.2	2002/13	layer 710.23	bone chip	prob. animal	trampled surface	LB	FMC	-	0	5	5	5	1	0
2002/13/77.2	2002/13	layer 710.23	small frgm.	prob. animal	trampled surface	LB	FMC	+	5	5	5	2	2	0.5
2002/13/77.2	2002/13	layer 710.23	small frgm.	prob. animal	trampled surface	LB	FMC	-	4	5	5	5	1	2
2002/13/77.2	2002/13	layer 710.23	bone chip	prob. animal	trampled surface	LB	FMC	-	5	5	5	5	1	2.5
2002/13/77.3	2002/13	layer 710.12	small frgm.	prob. animal	trampled surface	LB	FMC	+	3	2	5	4	4	0
2002/13/77.3	2002/13	layer 710.12	small frgm.	prob. animal	trampled surface	LB	FMC	+	4	5	5	3	4	0.5
2002/13/77.3	2002/13	layer 710.12	bone chip	prob. animal	trampled surface	LB	FMC	+	4	5	5	4	2	0.5
2002/13/77.3	2002/13	layer 710.12	bone chip	prob. animal	trampled surface	LB	FMC	+	5	5	5	4	3	1
2002/13/82.2	2002/13	pit 392	small frgm.	prob. animal	pit	TSM	CH	++	5	4	5	3	3	0
2002/13/9.2	2002/13	layer 205.34	small frgm.	prob. animal	trampled surface	LB	FMC	-	0	5	5	5	3	0
2003/08/13.1	2003/08	layer 478.16	bone chip	prob. animal	trampled surface	LC	FMC	++	4	5	5	5	3	0
2003/08/13.2	2003/08	layer 478.16	small frgm.	prob. animal	trampled surface	LC	FMC	++	4	5	5	5	4	0
2003/08/8.1	2003/08	layer 424.7	bone chip	prob. animal	trampled surface	LC	FMC	++	5	5	5	3	2	0
2003/08/8.1	2003/08	layer 424.7	bone chip	prob. animal	trampled surface	LC	FMC	++	2	5	5	5	3	0.5
2003/08/8.1	2003/08	layer 424.7	big frgm.	prob. animal	trampled surface	LC	FMC	++	1	5	5	5	3	0.5
BGA 18-1	2006/41	burial pit 18	bone section	human (hum.)	burial pit	LG		-	5	0	5	4	3	-
BGA 18-2	2006/41	burial pit 18	bone section	human (fem.)	burial pit	LG		-	4	0	5	3	3	0.5
BGB 10-1	2005/09	burial pit 10	bone section	human (hum.)	burial pit	LG		+	4	0	-	5	-	-
BGB 10-2	2005/09	burial pit 10	bone section	human (fem.)	burial pit	LG		+	4	0	-	5	2	-
BGB 13-1	2005/09	burial pit 13	bone section	human (fem.)	burial pit	LG		-	4	0	5	5	4	0
BGB 13-1	2005/09	burial pit 13	bone section	human (hum.)	burial pit	LG		-	5	0	5	5	4	0.5
BGB 9-1	2005/09	burial pit 9	bone section	human (hum.)	burial pit	LG		-	4	0	5	-	1	-
BGB 9-2	2005/09	burial pit 9	bone section	human (fem.)	burial pit	LG		-	4	0	5	5	3	0.5
BGS 21	2003/08	depression 2	bone section	human (hum.)	shallow pit	LC	FMC	++	3	5	5	3	5	0.5
BGS 22	2004/06	ditch area 6	bone section	human (hum.)	ditch	-	-	-	4	0	-	4	3	0.5
BGS 25	1963/30	pit 194	bone section	human (hum.)	pit	TSM	CH	++	-	0	-	-	1	-
BGS 26	2004/18	ditch area 29	bone section	human (hum.)	ditch	-	-	-	-	0	-	4	1	-
BGS 27	2001/25	pit 387	bone section	human (hum.)	pit	-	-	-	4	1	5	3	4	0.5
BGS 29	1990/42	pit 286	bone section	human (hum.)	pit	TSM	CH	++	4	0	5	5	3	0.5
BGS 30	2002/03	depression 3	bone section	human (hum.)	shallow pit	-	-	-	5	0	5	3	4	-
BGS 33	2000/13	ditch area 11	bone section	human (hum.)	ditch	LB	FMC	-	5	0	-	5	2	-
BGS 34	1975/40	pit 236	bone section	human (hum.)	pit	-	-	-	5	0	-	4	1	0.5
BGS 35	2002/03	ditch area 32	bone section	human (hum.)	ditch	-	-	-	4	1	5	5	3	0.5
BGS 51	1999/12	pit 341	bone section	human (fem.)	pit	-	-	-	4	0	-	5	2	-
BGS 52	1999/12	pit 348	bone section	human (fem.)	pit	-	-	-	4	2	5	4	4	0.5
BGS 53	2003/08	depression 2	bone section	human (fem.)	shallow pit	LC	FMC	++	1	3	5	3	3	0
BGS 54	2004/18	ditch area 45	bone section	human (fem.)	ditch	-	-	-	-	0	-	4	1	-
BGS 55	2004/36	pit	bone section	human (fem.)	pit	TSM	CH	++	4	0	-	5	1	0.5
BGS 6-1	1996/01	pit 321	bone section	human (hum.)	pit	TSM	CH	++	5	0	5	3	1	0.5
BGS 6-2	1996/01	pit 321	bone section	human (fem.)	pit	TSM	CH	++	4	0	5	4	1	0.5

sample size		sediment types		sediment components		evaluation	
bone chip	< 2 mm	LG	loamy gravel	FMC	few (micro-) charcoal	-	no information
small fragm.	2-10 mm	LC	loam (C horizon)	CH	charcoal-rich		
big fragm.	> 10 mm	LB	loam (B horizon)	AS	ash-rich		uncertain
bone section		TSM	topsoil-material				

Contextualising the Dead - Supplement 2: Archaeoanthropological data

sample no.	excavation	context	structure	inventory no.	skeletal element	sex	age
BGA 18-1	2006/41	cemetery A	grave-pit 18	43.2	humerus dx	m?	30-50
BGA 18-2	2006/41	cemetery A	grave-pit 18	43.59	femur sn	m?	30-50
BGB 9-1	2005/09	cemetery B	grave-pit 9	80.21	humerus sn	m?	30-50
BGB 9-2	2005/09	cemetery B	grave-pit 9	80.28	femur dx	m?	30-50
BGB 10-1	2005/09	cemetery B	grave-pit 10	75.18	humerus sn	f	18-24
BGB 10-2	2005/09	cemetery B	grave-pit 10	75.21	femur dx	f	18-24
BGB 13-1	2005/09	cemetery B	grave-pit 13	89.33	humerus dx	f	40-60
BGB 13-2	2005/09	cemetery B	grave-pit 13	89.41	femur sn	f	40-60
BGS 6-1	1996/01	settlement	depression 2	233.1	humerus sn	m	30-35
BGS 6-1	1996/01	settlement	ditch area 6	239.1	femur dx	m	30-35
BGS 21	2003/08	settlement	pit 194	514	humerus dx	indet	30-50
BGS 22	2004/06	settlement	ditch area 29	18	humerus dx	m?	30-50
BGS 25	1963/30	settlement	pit 387	2410/7	humerus dx	m	40-60
BGS 26	2004/18	settlement	pit 286	38	humerus dx	indet	> 40
BGS 27	2001/25	settlement	depression 3	13257	humerus dx	indet	40-60
BGS 29	1990/42	settlement	ditch area 11	9978	humerus dx	indet	30-50
BGS 30	2002/03	settlement	pit 236	3891	humerus sn	f?	> 50
BGS 33	2000/13	settlement	ditch area 32	3134	humerus dx	f	> 50
BGS 34	1975/40	settlement	pit 341	Rec 101	humerus dx	f	30-50
BGS 35	2002/03	settlement	pit 348	3893	humerus dx	indet	20-40
BGS 51	1999/12	settlement	depression 2	22102	femur dx	m?	30-50
BGS 52	1999/12	settlement	ditch area 45	22098	femur dx	f?	40
BGS 53	2003/08	settlement	pit	519	femur dx	m	40-60
BGS 54	2004/18	settlement	pit 321	54	femur dx	m	> 60
BGS 55	2004/36	settlement	pit 321	8469	femur dx	m?	30-50

Bacterial attack (BAI) and supposed fungal attack (Wedl tunnels; WTI) in relation to sediment type
Burnt and unburnt animal bone fragments (n = 180)

	BAI						FAI					
	LB		LC		TSM		LB		LC		TSM	
index	num.	%	num.	%	num.	%	num.	%	num.	%	num.	%
5	41	68	12	75	87	84	19	32	7	44	70	67
4	5	8	3	19	3	3	12	20	4	25	28	27
3	6	10	0	0	3	3	17	28	2	13	4	4
2	5	8	0	0	4	4	7	12	2	13	1	1
1	2	3	1	6	5	5	1	2	1	6	0	0
0	1	2	0	0	2	2	4	7	0	0	1	1
indet	*0*	*0*	*0*	*0*	*0*	*0*	*0*	*0*	*0*	*0*	*0*	*0*
total	60	100	16	100	104	100	60	100	16	100	104	100
	180						**180**					

LB loamy sediment; decalcified

LC loamy sediment; calcareous

TSM Topsoil material; microcharcoals, ashes, faeces etc.

Bacterial attack (BAI) and supposed fungal attack (Wedl tunnels; WTI) in relation to sediment type
Unburnt animal bone fragments (n = 113)

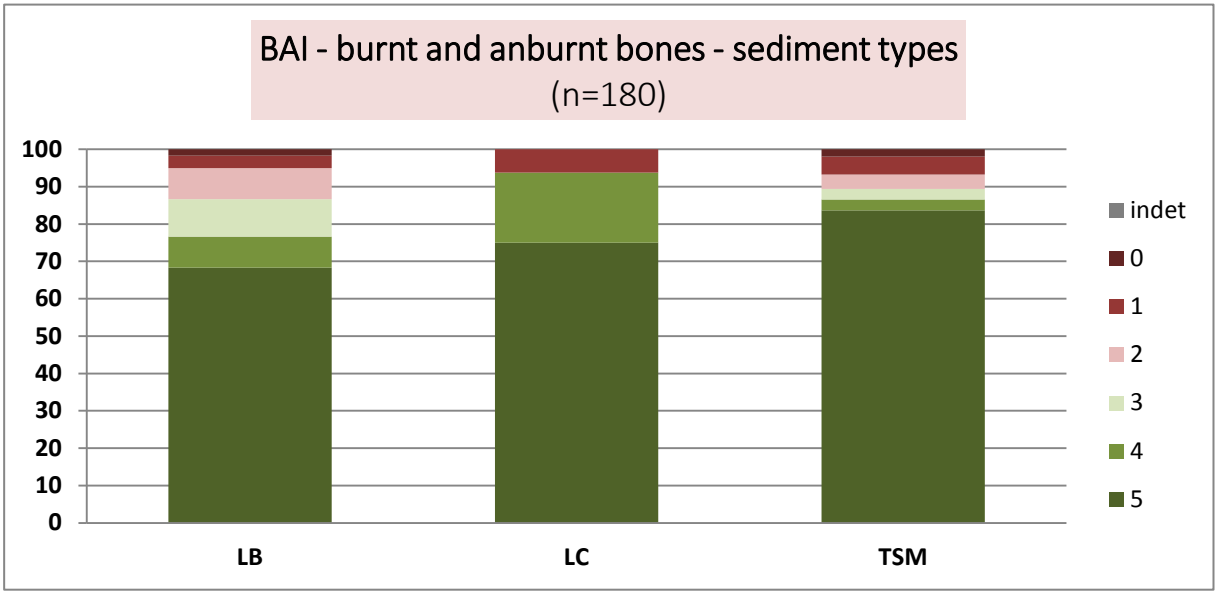
	BAI						FAI					
	LB		LC		TSM		LB		LC		TSM	
index	num.	%	num.	%	num.	%	num.	%	num.	%	num.	%
5	27	59	10	71	41	77	13	28	6	43	38	72
4	4	9	3	21	3	6	9	20	3	21	10	19
3	7	15	0	0	1	2	13	28	2	14	4	8
2	5	11	0	0	3	6	6	13	2	14	0	0
1	2	4	1	7	3	6	1	2	1	7	0	0
0	1	2	0	0	2	4	4	9	0	0	1	2
indet	*0*	*0*	*0*	*0*	*0*	*0*	*0*	*0*	*0*	*0*	*0*	*0*
total	46	100	14	100	53	100	46	100	14	100	53	100
	113						**113**					

LB loamy sediment; decalcified

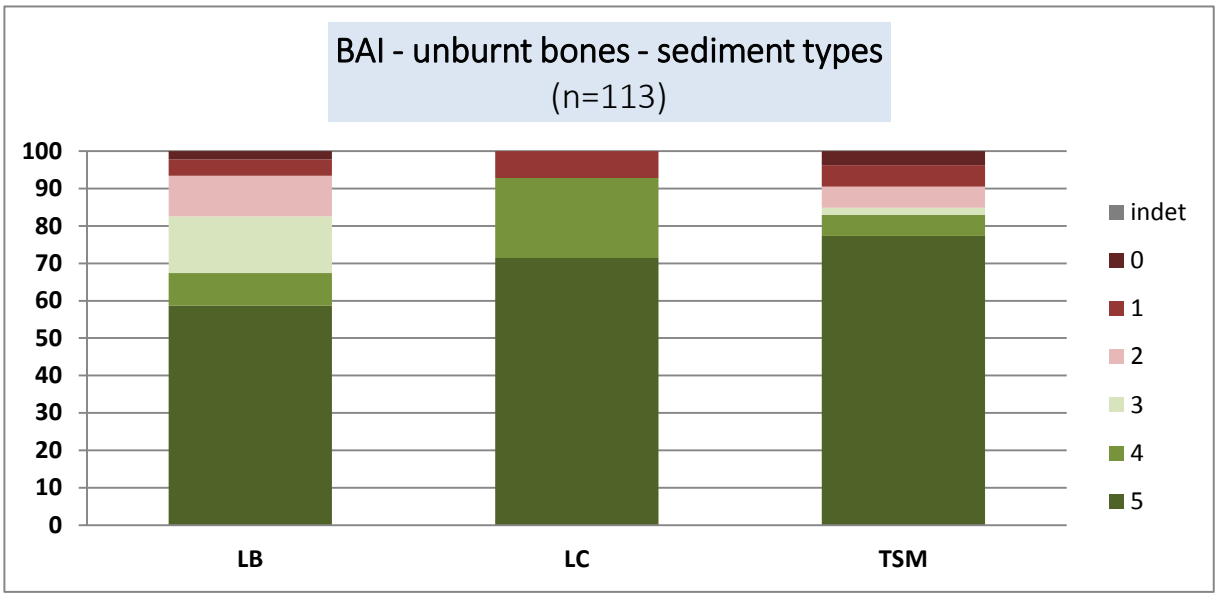
LC loamy sediment; calcareous

TSM Topsoil material; microcharcoals, ashes, faeces etc.

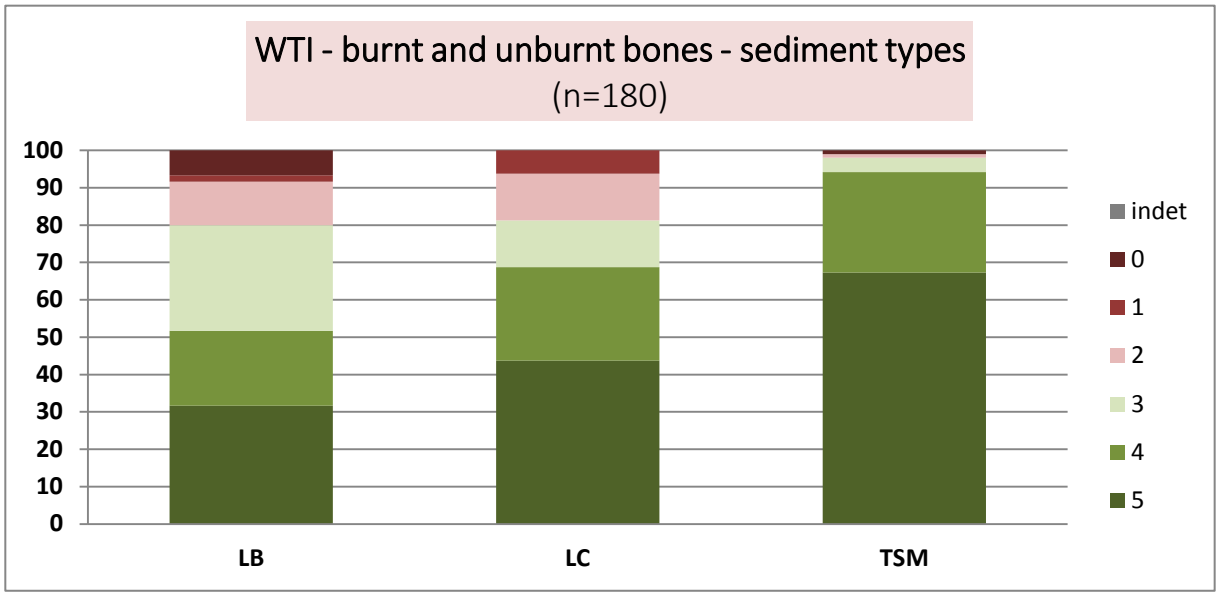
Bacterial attack (BAI) and supposed fungal attack (Wedl tunnels; WTI) in relation to sediment type
Burnt and unburnt animal bone fragments (n = 180)



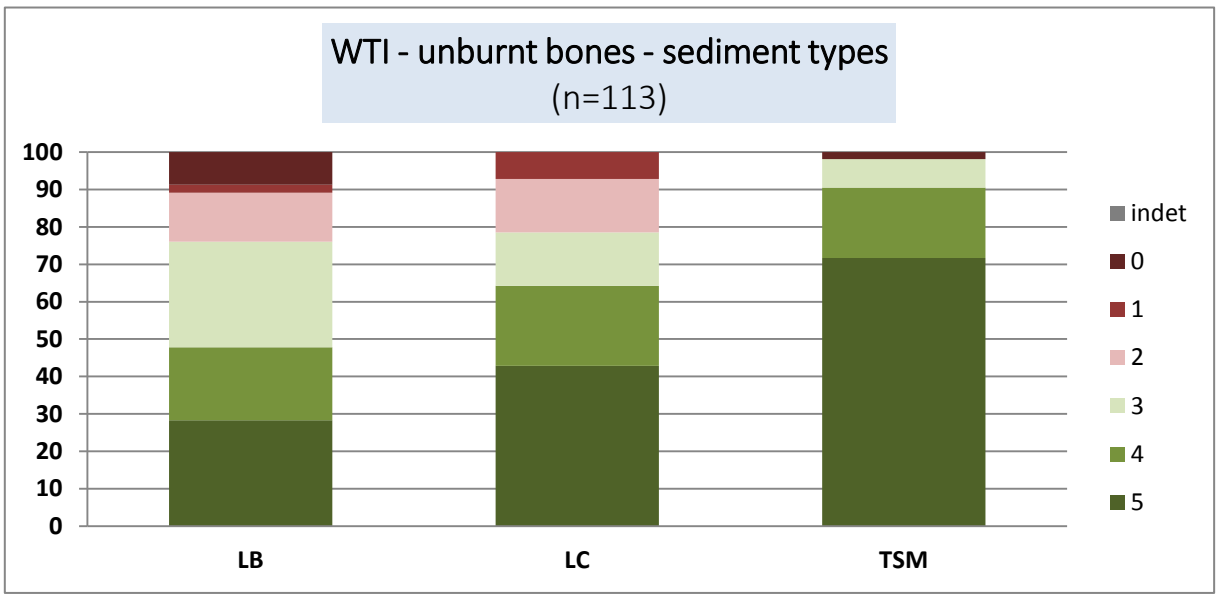
Bacterial attack (BAI) and supposed fungal attack (Wedl tunnels; WTI) in relation to sediment type
Unburnt animal bone fragments (n = 113)



Bacterial attack (BAI) and supposed fungal attack (Wedl tunnels; WTI) in relation to sediment type
Burnt and unburnt animal bone fragments (n = 180)



Bacterial attack (BAI) and supposed fungal attack (Wedl tunnels; WTI) in relation to sediment type
Unburnt animal bone fragments (n = 113)



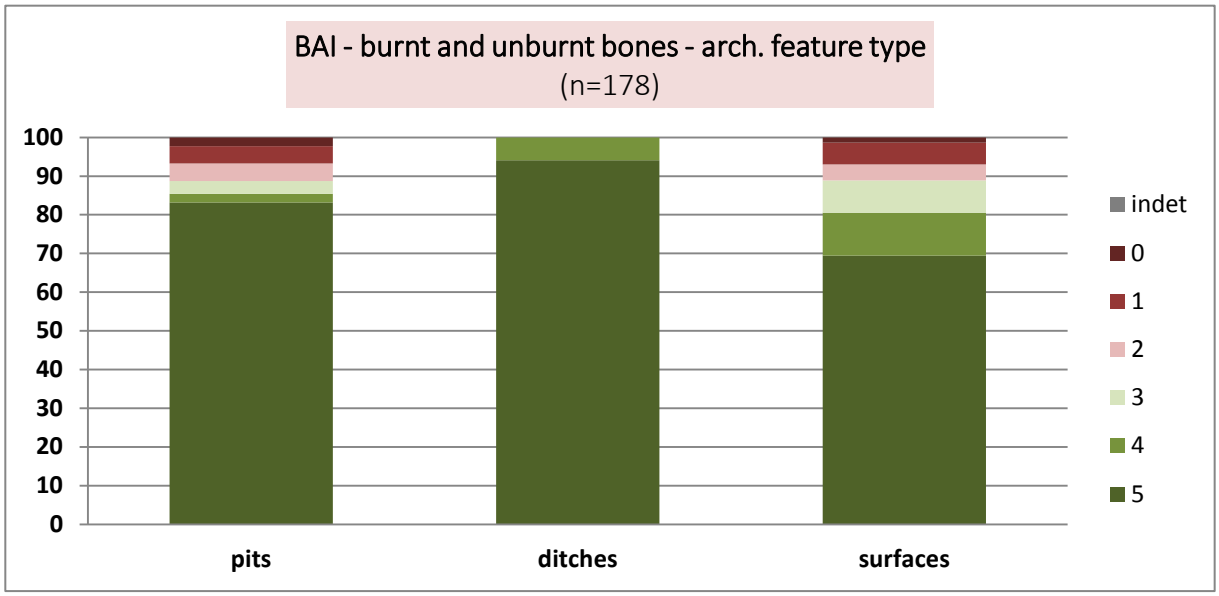
Bacterial attack (BAI) and supposed fungal attack (Wedl tunnels; WTI) in relation to feature types
Burnt and unburnt animal bone fragments (n = 178)

	BAI						FAI					
	pits		ditches		surfaces		pits		ditches		surfaces	
index	num.	%	num.	%	num.	%	num.	%	num.	%	num.	%
5	74	83	16	94	50	69	65	73	8	47	22	31
4	2	2	1	6	8	11	22	25	5	29	17	24
3	3	3	0	0	6	8	2	2	2	12	18	25
2	4	4	0	0	3	4	0	0	1	6	9	13
1	4	4	0	0	4	6	0	0	0	0	2	3
0	2	2	0	0	1	1	0	0	1	6	4	6
indet	*0*	*0*	*0*	*0*	*0*	*0*	*0*	*0*	*0*	*0*	*0*	*0*
total	89	100	17	100	72	100	89	100	17	100	72	100
	178						**178**					

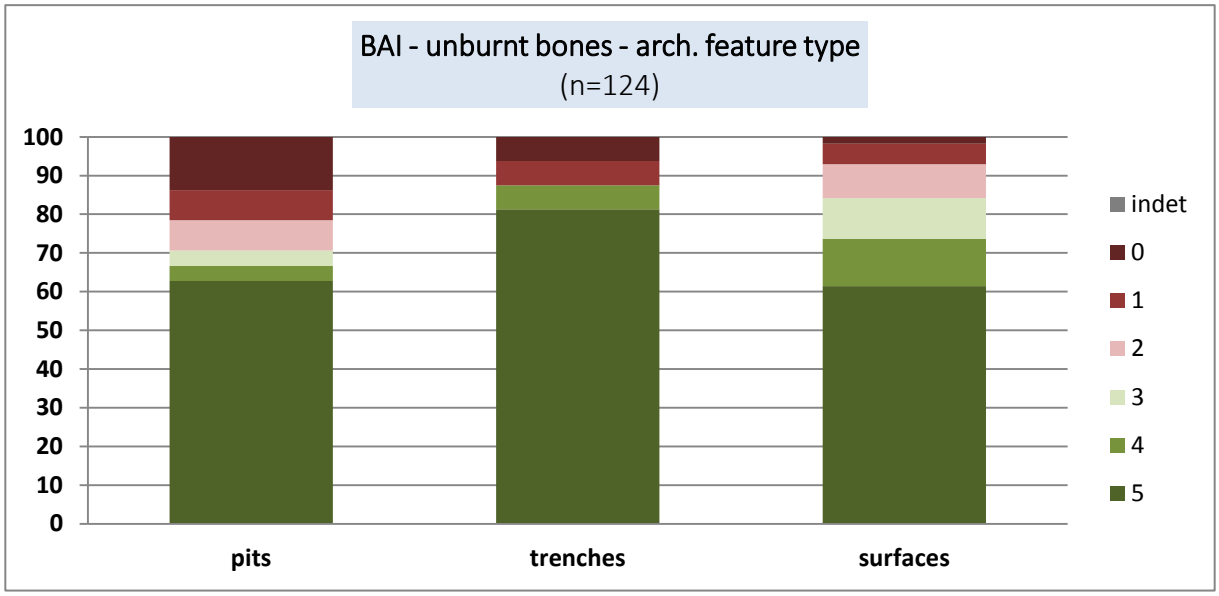
Bacterial attack (BAI) and supposed fungal attack (Wedl tunnels; WTI) in relation to feature types
Unburnt animal bone fragments (n = 124)

	BAI						FAI					
	pits		trenches		surfaces		pits		trenches		surfaces	
index	num.	%	num.	%	num.	%	num.	%	num.	%	num.	%
5	32	63	13	81	35	61	36	71	7	44	16	28
4	2	4	1	6	7	12	10	20	6	38	12	21
3	2	4	0	0	6	11	4	8	2	13	15	26
2	4	8	0	0	5	9	0	0	0	0	8	14
1	4	8	1	6	3	5	1	2	0	0	2	4
0	7	14	1	6	1	2	0	0	1	6	4	7
indet	*0*	*0*	*0*	*0*	*0*	*0*	*0*	*0*	*0*	*0*	*0*	*0*
total	51	100	16	100	57	100	51	100	16	100	57	100
	124						**124**					

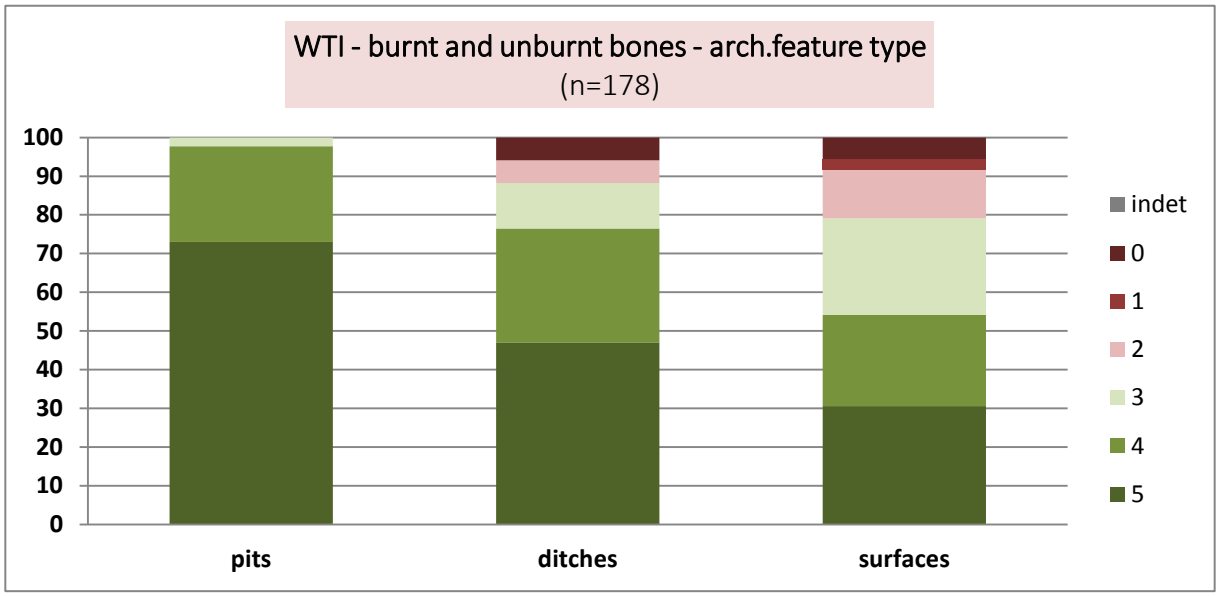
Bacterial attack (BAI) and supposed fungal attack (Wedl tunnels; WTI) in relation to feature types
Burnt and unburnt animal bone fragments (n = 178)



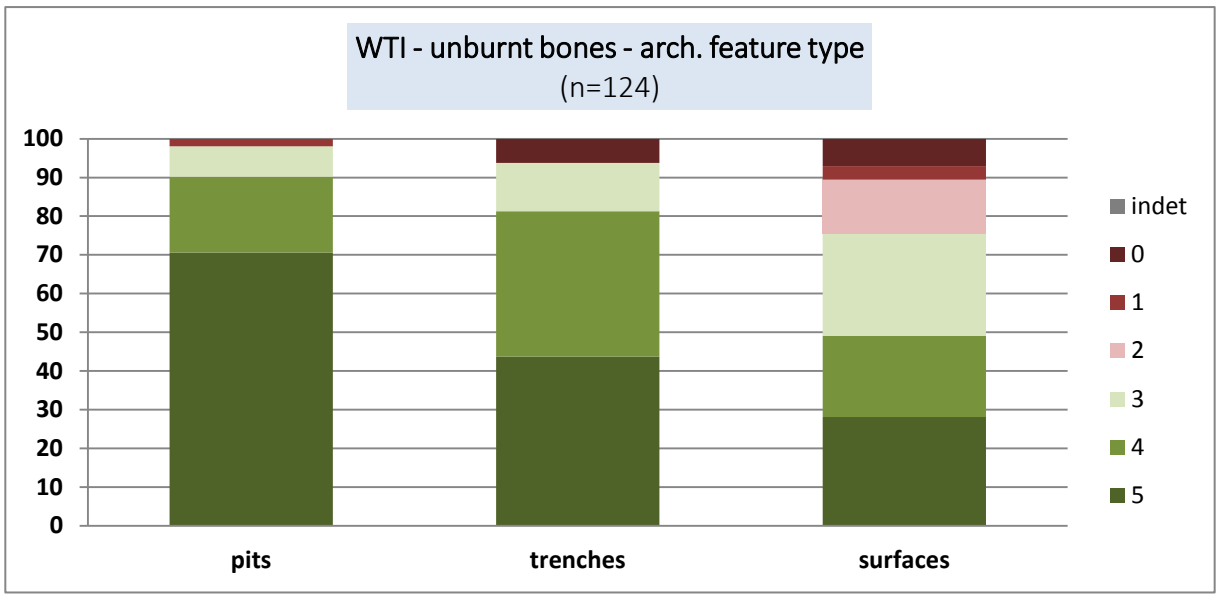
Bacterial attack (BAI) and supposed fungal attack (Wedl tunnels; WTI) in relation to feature types
Unburnt animal bone fragments (n = 124)



Bacterial attack (BAI) and supposed fungal attack (Wedl tunnels; WTI) in relation to feature types
Burnt and unburnt animal bone fragments (n = 178)



Bacterial attack (BAI) and supposed fungal attack (Wedl tunnels; WTI) in relation to feature types
Unburnt animal bone fragments (n = 124)



David Brönnimann
Breisacherstrasse 20
4057 Basel
david.broennimann@unibas.ch

Basel, 31.08.2020

Curriculum vitae

David Simon Brönnimann
Geboren am 24. März 1984 in Binningen
Nationalität: Schweiz
Heimatort: Gurzelen (BE)

Schulische & universitäre Ausbildung

1991-1996	Primarschule in Frenkendorf
1996-2000	Progymnasium in Frenkendorf
2000-2003	Gymnasium in Liestal (Matur im Dez. 2003 mit Schwerpunkt „Angewandte Mathematik und Physik“)
Herbst 2004-	Studium „Prähistorische und naturwissenschaftliche Archäologie“ an der Universität
Januar 2011	Basel
FS 2006-HS 2009	Studierendenvertretung der PNA & Vertretung in der Unterrichtskommission
2007-2009	Hilfswissenschafter Abteilung Geoarchäologie (Werkstatt- und Laborarbeiten)

Beruflicher Werdegang

20. Januar 2011	Master-Abschluss „Science in Prehistory and Archaeological Science” an der Universität Basel.
Seit Januar 2011	Wissenschaftlicher Mitarbeiter am IPNA der Universität Basel in der Forschungsgruppe Geoarchäologie (Leitung: PD Dr. Ph. Rentzel). Geoarchäologische Auswertungen verschiedener Fundstellen in der Schweiz.
Januar 2011-	Mitarbeit beim SNF-Projekt „Über die Toten zu den Lebenden:
Juni 2014	Menschliche Überreste vom spätlatènezeitlichen Fundplatz Basel-Gasfabrik und ihre kulturgeschichtlichen Deutungen“.
März 2015-	Dissertation an der Universität Basel mit dem Titel „Geoarchäologische
Oktober 2018	Untersuchungen zum Abfall- und Ressourcen-Management in der jüngerlatènezeitlichen Siedlung Basel Gasfabrik“; Gutachter: PD Dr. Philippe Rentzel und Prof. Dr. Brigitte Röder; Fakultätsverantwortlicher: Prof. Dr. Jörg Schibler
14. November 2018	Abschluss Dissertation (Doktoratsexamen) an der Universität Basel.
Seit November 2018	PostDoc und Projekt-Koordination des interdisziplinären Auswertungsprojektes „MAGIA“ (Mittelbronzezeit im Aargau: Interdisziplinär Ausgewertet) an der Universität Basel.
Seit Januar 2019	Koordination interdisziplinäre Publikation zum SNF-Forschungsprojekt „Über die Toten zu den Lebenden: Menschliche Überreste vom spätlatènezeitlichen Fundplatz Basel-Gasfabrik und ihre kulturgeschichtlichen Deutungen“ an der Archäologischen Bodenforschung Basel-Stadt.

Lehrerfahrung

HS 2012, 2014, 2016	Jeweils 1 Lektion zur geomagnetischen Prospektion in der Lehrveranstaltung „Einführung in die Archäometrie: Naturwissenschaftliche Methoden zur Material- und Fundplatzanalyse“ (Dr. Sandra Pichler) (LV 25932-01).
HS 2014, 2018	2 Lektionen der Vorlesung „Geoarchäologie 1: Einführung“ (PD Dr. Philippe Rentzel) (LV 10340-01).
HS 2014	Befristeter Lehrauftrag an der Philosophisch-Historischen Fakultät: Seminar „Häuser, Haushalte und Aktivitätszonen: Siedlungsbefunde zu Alltagspraktiken aus (geo)archäologischer Sicht“, zusammen mit Prof. Dr. Brigitte Röder (LV 38096-01); Betreuung von einer Seminararbeit.
HS 2016	Befristeter Lehrauftrag an der Philosophisch-Historischen Fakultät: Seminar „Integrative Analyse von Kleinräumen: Ansätze und Fallbeispiele“, zusammen mit Prof. Dr. Brigitte Röder (LV 44864).
HS 2017	Betreuung einer Praktikumsarbeit (Master-Stufe Ur- und Frühgeschichte).
HS 2018	Mitarbeit Seminar „Ausgewählte Themen zur naturwissenschaftlichen Archäologie: Rohstoffe und ihre Verarbeitung“ (PD Dr. Sabine Deschler-Erb, PD Dr. Philippe Rentzel) (LV 52073-01)

Weiterbildungen an der Universität Basel

HS 2016	Weiterbildung „Effizient Wissenschaftlich Schreiben: Der Weg zum Text“
HS 2017	Didaktik-Kurs „Lehrmethoden für lernförderliche Seminare, Workshops, Blockkurse“
HS 2017	Didaktik-Kurs „Vorlesungen lernförderlich gestalten“
2017-2018	4-teiliger Didaktik-Kurs „Meine erste Lehrveranstaltung“
FS 2018	Weiterbildung „Projektmanagement I Basis“
HS 2019	Weiterbildung „Grundlagen Führung“
FS 2019	Weiterbildung „Gruppen erfolgreich führen“
HS 2019	Weiterbildung „Begleiten und Bewerten von Abschluss- und Seminararbeiten“

Diverses

September 2013	Mitorganisation des internationalen Geoarchäologie-Workshops WASM (International Workshop on Archaeological Soil Micromorphology) und der internationalen Geoarchäologie-Konferenz DIG (Developing International Geoarchaeology) in Basel
Januar 2017	Mit-Organisation der Doktorandentagung „TriKanDok“ in Zürich
Seit 2017	Gruppierungsvertreter Gruppierung III im Departement Umweltwissenschaften
2019	Mitorganisation des internationalen Geoarchäologie-Workshops WASM (International Workshop on Archaeological Soil Micromorphology) in Basel (September 2019)
2019	Organisation einer Session (#81 “From micro- to macroscale: It’s all a matter of perspective”) an der “25th Annual Meeting of the European Association of Archaeologists” in Bern (September 2019).

Publikationen

Brönnimann, David; Rentzel, Philippe (2020): Geoarchäologische Einblicke in den Boden. In: Ramstein, Marianne; Cornelissen, Marcel; Schimmelpfennig, Dirk; Rentzel, Philippe (Eds.): Der Dolmen von Oberbipp, Steingasse. Archäologische und naturwissenschaftliche Untersuchung eines spätneolithischen Megalithgrabes. Archäologie Bern 2019 (Bern), 109–118.

Brönnimann, David; Wimmer, Johannes; Müller-Kissing, Milena; Stopp, Barbara; Rissanen, Hannele; Spichtig, Norbert (2020): One man's trash is another man's treasure. Interdisciplinary examination of taphonomic aspects of ceramic sherds, animal bones and sediments from the La Tène period settlement at Basel-Gasfabrik. PLoS ONE 15 (7), 1–28. DOI: 10.1371/journal.pone.0236272.

Brönnimann, David; Rentzel, Philippe; Röder, Brigitte; Spichtig, Norbert; Rissanen, Hannele; Lassau, Guido (2020): The hidden midden – Geoarchaeological investigation of sedimentation processes, waste disposal practices and resource management at the Latène settlement Basel-Gasfabrik (Switzerland). Geoarchaeology: An International Journal 35, 522-544. DOI: 10.1002/gea.21787.

Joray, Sophia; **Brönnimann, David**; Kühn, Marlu; Maise, Christian; Matter, Georg; Rentzel, Philippe; Röder, Brigitte (2020): Die Mittelbronzezeit im Fokus: das interdisziplinäre Forschungsprojekt MAGIA. Archäologie Schweiz 43 (1), 16–23.

Brönnimann, David (2019): Schichtgenese und Landschaftsgeschichte – die geoarchäologischen Untersuchungen. In: Horisberger, Beat (Eds.): Keltische und römische Eliten im zürcherischen Furttal. Gräber, Strassen und Siedlungen von der Frühbronzezeit bis in die Neuzeit: Ergebnisse der Rettungsgrabungen 2009–2014 in Regensdorf-Geissberg/Gubrist. Monographien der Kantonsarchäologie Zürich 53 (Zürich, Egg), 30-43.

Brönnimann, David; Portmann, Cordula; Rissanen, Hannele (2018): Betrachtungen auf der "Mikro-Ebene" – Erste Resultate interdisziplinärer Auswertungen von archäologischen, geoarchäologischen und archäoanthropologischen Untersuchungen der latènezeitlichen Gräberfelder von Basel-Gasfabrik (Schweiz). In: Wendling, Holger; Augstein, Melanie; Fries-Knoblach, Janine; Ludwig, Katrin; Schumann, Robert; Tappert, Claudia; Trebsche, Peter; Wiethold, Julian (Eds.): Übergangswelten - Todesriten. Forschungen zur Bestattungskultur der europäischen Eisenzeit (Langenweissbach), 181–189.

Brönnimann, David; Portmann, Cordula; Pichler, Sandra L.; Booth, Thomas J.; Röder, Brigitte; Vach, Werner; Schibler, Jörg; Rentzel, Philippe (2018): Contextualising the dead – Combining geoarchaeology and osteo-anthropology in a new multi-focus approach for bone histotaphonomy. Journal of Archaeological Science 98, 45-58.

Brönnimann, David; Rissanen, Hannele (2018): Vivre et mourir sur le site La Tène de Bâle-Gasfabrik (Suisse) – l'étude interdisciplinaire de structures d'habitat choisies et de deux nécropoles donne un aperçu de la société à la fin de l'âge du Fer. In: Cannot, Anna; Le Cozanet, Thibault; Remy, Julie; Wilczek, Josef (Eds.): Interdisciplinarity and New Approaches in the Research of the Iron Age. International Doctoral Conference 2015. Bibracte (France), 2015 (Brno), 93-97.

Brönnimann, David; Rentzel, Philippe (2018): Die Bodenbeschaffenheit zur Zeit des Frühneolithikums. In: Altorfer, Kurt; Hartmann, Chantal (Eds.): Frühe Bauern im Klettgau - Der alt- und mittelneolithische Siedlungsplatz Gächlingen-Goldäcker. Schaffhauser Archäologie 10 (Schaffhausen), 50-52.

Brönnimann, David; Knipper, Corina; Pichler, Sandra L.; Röder, Brigitte; Rissanen, Hannele; Stopp, Barbara et al. (2018): The lay of land: Strontium isotope variability in the dietary catchment of the Late Iron Age proto-urban settlement of Basel-Gasfabrik, Switzerland. Journal of Archaeological Science: Reports 17, 279-292.

Knipper, Corina; Pichler, Sandra L.; **Brönnimann, David**; Rissanen, Hannele; Rosner, Martin; Spichtig, Norbert et al. (2018): A knot in a network: Residential mobility at the Late Iron Age proto-urban centre of Basel-Gasfabrik (Switzerland) revealed by isotope analyses. Journal of Archaeological Science: Reports 17, 735-753.

Brönnimann, David; Rentzel, Philippe; Wick, Lucia (2017): Late glacial environmental history and early soil formation in Northwest Switzerland. In: Dorota Wojtczak, Mustafa Al Najjar, Reto Jagher, Hani Elsuede, Fabio Wegmüller, Marcel Otte (Eds.): Vocation Préhistoire. Hommage à Jean-Marie Le Tensorer. ERAUL 148, 57-68.

Brönnimann, David; Pümpin, Christine; Ismail-Meyer, Kristin; Rentzel, Philippe; Egüez, Natàlia (2017): Excrements of omnivores and carnivores. In Cristiano Nicosia, Georges Stoops (Eds.): Archaeological soil and sediment micromorphology (Hoboken), 67-81.

Brönnimann, David; Ismail-Meyer, Kristin; Rentzel, Philippe; Pümpin, Christine; Lisá, Lenka (2017): Excrements of herbivores. In Cristiano Nicosia, Georges Stoops (Eds.): Archaeological soil and sediment micromorphology (Hoboken), 55-65.

Pichler, Sandra L.; Röder, Brigitte; **Brönnimann, David**; Knipper, Corina; Kühn, Marlu; Rentzel, Philippe et al. (2017): The Basel-Gasfabrik research project: Addressing complex topics by an integrative approach. In Vyacheslav I. Molodin, Svend Hansen (Eds.): Multidisciplinary approach to archaeology: Recent achievements and prospects. Proceedings of the international symposium "Multidisciplinary Approach to Archaeology: Recent achievements and prospects" (Novosibirsk), 240-247.

Rentzel, Philippe; Nicosia, Cristiano; Gebhardt, Anne; **Brönnimann, David**; Pümpin, Christine; Ismail-Meyer, Kristin (2017): Trampling, poaching and the effect of traffic. In Cristiano Nicosia, Georges Stoops (Eds.): Archaeological soil and sediment micromorphology (Hoboken), 281-297.

Rentzel, Philippe; Pümpin, Christine; **Brönnimann, David** (2015): Geoarchäologischer Report: Eine kurze Geschichte des Rheins. Geologische und archäologische Impressionen aus Basel. Jahresbericht der Archäologischen Bodenforschung des Kantons Basel-Stadt 2014, 108-135.

Rentzel, Philippe; Pümpin, Christine; **Brönnimann, David** (2015): Am Anfang war … der Rhein! Geschichte einer Landschaft. Archäologie Schweiz 38 (2), 28-29.

Knipper, Corina; Pichler, Sandra L.; **Brönnimann, David**; Alt, Kurt W. (2015): Über den Tellerrand geschaut: High-Tech lässt alte Knochen sprechen. Archäologie Schweiz 38 (2), 60-61.

Guélat, Michel; **Brönnimann, David**; Pümpin, Christine (2015): Etude sédimentologique et micromorphologique. In Bastien Jakob, Christian Falquet (Eds.): Onnens-Praz Berthoud (canton de Vaud, Suisse). Contexte, environnement et occupations du Mésolithique au début du Néolithique (Fouilles de l'autoroute A5•2). Cahiers d'archéologie romande, 152, 35-48.

Brönnimann, David; Rentzel, Philippe; Sedlmeier, Jürg; Wick, Lucia (2015): Karstspalte Schachlete. Ein Archiv der spätglazialen und holozänen Landschafts- und Klimageschichte. With assistance of Bruno Baur, Trudi Meier. In Jürg Sedlmeier (Ed.): Die letzten Wildbeuter der Eiszeit. Neue Forschungen zum Spätpaläolithikum im Kanton Basel-Landschaft. Schriften der Archäologie Baselland, 51, 210-241.

Brönnimann, David; Rentzel, Philippe (2014): Naturraum und Geologie. In: Oppler, Dominique: Ausflug in die Vergangenheit. Archäologische Streifzüge durchs Baselbiet (Hochwald) 17-24.

Auf der Maur, Christian; Cornelissen, Marcel; unter Mitarbeit von **Brönnimann, David** (2014): Die spätmesolithische und bronzezeitliche Fundstelle Hospental-Moos. Ein Einblick in das urgeschichtliche Urserntal. Historisches Neujahrsblatt 2013, Neue Folge, 68. Band, 1. Reihe, 103. Heft (Altdorf) 37-83.

Pichler, Sandra; Pümpin, Christine; **Brönnimann, David**; Rentzel, Philippe (2014): Life in the Proto-Urban Style: The identification of parasite eggs in micromorphological thin sections from the Swiss Basel-Gasfabrik late Iron Age settlement. Journal of Archaeological Science 43: 55-65.

Wegmüller, Fabio; **Brönnimann, David**; Schindler, Martin P. (2013): Der Abri Unterkobel in Oberriet (SG) – Neue Einblicke in die Geschichte des Alpenrheintals. Archäologie Schweiz 36/1, 16-23.

Nagy, Patrick; Schwarz, Peter Andrew (2013): Archäologische Prospektion im Kanton Obwalden. Vorbericht zur Kampagne 2012. Unter Mitarbeit von Rahel C. Ackermann, **David Brönnimann**, José Diaz Tabernero, Tina Lander, Katrin Schäppi, Thomas Scherer und Daniel Schuhmann. Jahrbuch Archäologie Schweiz 96, 152-164.

Rissanen, Hannele; Spichtig, Norbert; Alt, Kurt W.; **Brönnimann, David**; Knipper, Corina; Kühn, Marlu; Rentzel, Philippe; Röder, Brigitte; Schibler, Jörg; Stopp, Barbara; Vach, Werner; Warnberg; Ole; Lassau, Guido (2013): "Wenn Kinder sterben …" - Säuglinge und Kleinkinder vom latènezeitlichen Fundplatz Basel-Gasfabrik (Kanton Basel-Stadt, Schweiz). In: Wefers, Stefanie; Esther-Fries, Jana; Fries-Knoblach, Janine; Later, Christiana; Rambuscheck, Ulrike; Trebsche, Peter; Wiethold, Julian (Hrsg.): Bilder - Räume - Rollen. Beiträge zur gemeinsamen Sitzung der AG Eisenzeit und der AG Geschlechterforschung während des 7. Deutschen Archäologenkongresses in Bremen 2011. Sonderdruck aus: Beiträge zur Ur- und Frühgeschichte Mitteleuropas 72, 127-142.

Brönnimann, David; Rentzel, Philippe (2011): Mikromorphologie. In: Altorfer, Kurt; Affolter, Jehanne; Schaffhauser Silex-Vorkommen und Nutzung. Wirtschaftsarchäologische Untersuchungen an den Silices der jungneolithischen Stationen Büttenhardt-Zelg, Schaffhausen (Herblingen)-Grüthalde und Lohn-Setzi. Beiträge zur Schaffhauser Archäologie 5, 9-30.